Halogenated Heterocycles for Drug Discovery

WILSON, IAN

A Thesis Entitled

Halogenated Heterocycles for Drug Discovery

Submitted by

Ian Wilson MChem (Hons) Dunelm

College of St. Hild and St. Bede

Department of Chemistry

A Candidate for the Degree of Doctor of Philosophy 2011

Declaration

The work presented within this thesis was carried out at Durham University between October 2006 and December 2009. This thesis is the work of the author, except where acknowledged by reference and has not been submitted for any other degree. The copyright of this thesis lies solely with the author, no quotation from it should be published without prior written consent, and information derived from it should be acknowledged.

Part of this work has been the subject of the following:

- Matthew W. Cartwright, Emma L. Parks, Graham Pattison, Rachel Slater, Graham Sandford, Ian Wilson, Dmitrii S. Yufit, Judith A.K. Howard, John A. Christopher, David D. Miller, *Tetrahedron*, 2010, **66**, 3222

and has been presented at:

- 9th RSC Fluorine Subject Group Postgraduate Meeting, Southampton, September 2009

Statement of Copyright

Acknowledgements

Firstly, I would like to thank my supervisor, Professor Graham Sandford, I do not think it would have been possible for me to have had a better boss over the last few years. I would also like to thank my industrial supervisor, Dr. John Christopher, for all his help and encouragement, particularly while I was in Stevenage. I am very grateful for the advice I have received from Professor Dick Chambers and Dr. David Miller over many meetings.

My thanks are due to all the analytical staff at Durham, many of whom have gone out of their way to provide me with the data I have needed, and have been extremely tolerant of my questions and requests.

I would like to thank all those I met at GSK Stevenage, who made me very welcome and helped me out tirelessly during my placement there, I enjoyed myself greatly. Thanks go to GSK and EPSRC for funding this work.

Thanks to all those who have come and gone through 115 in my time there, too many to list here, but you know who you are. I've had some good times.

Finally, I would like to thank Tamsin Lilley for her astonishing patience, among many other things.

Abbreviations

Å	Ångstrom
Ac	Acetyl
Bn	Benzyl
Boc	*t*-Butyloxycarbonyl
BINAP	Binaphthalene
DCM	Dichloromethane
DDQ	2,3-Dichloro-5,6-dicyano-1,4-benzoquinone
DIPEA	Di*iso*propylethylamine
DMF	Dimethylformamide
DMSO	Dimethylsulfoxide
E	Electrophile
EtOAc	Ethyl Acetate
GCMS	Gas Chromatography Mass Spectrometry
h	Hours
HPLC	High Performance Liquid Chromatography
IR	Infrared
IPA	*Iso*propyl Alcohol
J	Coupling Constant / Hz
LCMS	Liquid Chromatography Mass Spectrometry
LDA	Lithium Di*iso*propylamide
LiTMP	Lithium Tetramethylpiperidine
MDAP	Mass Directed Automated Purification
mol	Moles
mp	Melting Point
MW	Microwave
NaHMDS	Sodium Hexamethyldisilazide
NFSI	N-Fluorobenzenesulfonimide
NMP	N-Methylpyrrolidone

NMR	Nuclear Magnetic Resonance
nOe	Nuclear Overhauser Effect
Nuc	Nucleophile
PCC	Pyridinium Chlorochromate
ppm	Parts Per Million
Rf	Retention Factor
TBAF	Tetra-*n*-butylammonium Fluoride
THF	Tetrahydrofuran
TFA	Trifluoroacetic Acid
TMEDA	Tetramethylethylenediamine
TMSA	Trimethylsilylacetylene
TMSCl	Trimethylsilyl Chloride
TLC	Thin Layer Chromatography
TTF	Tetrathiafulvalene
δ	Chemical Shift / ppm

Contents

Abstract

Within a number of industries, and particularly within the pharmaceutical industry, there is a desire for reliable, high yielding routes towards large numbers of valuable small molecules that allow a wide range of products to be synthesised.

Heterocyclic compounds are particularly sought after as useful compounds, with an estimated 70% of pharmaceutical products being based on heterocyclic structures. A drawback of many traditional routes towards heterocyclic compounds is that the range of substituents that may be placed around the ring is limited. This is especially limiting if ring substituents have to be placed early in a synthesis, reducing the opportunities for elaboration at a late stage.

Our approach is to take highly halogenated heterocyclic systems and use them as scaffolds for the synthesis of novel compounds by the sequential replacement of halogen atoms with other functionalities.

This approach has led to the generation of a number of novel highly substituted heterocyclic species.

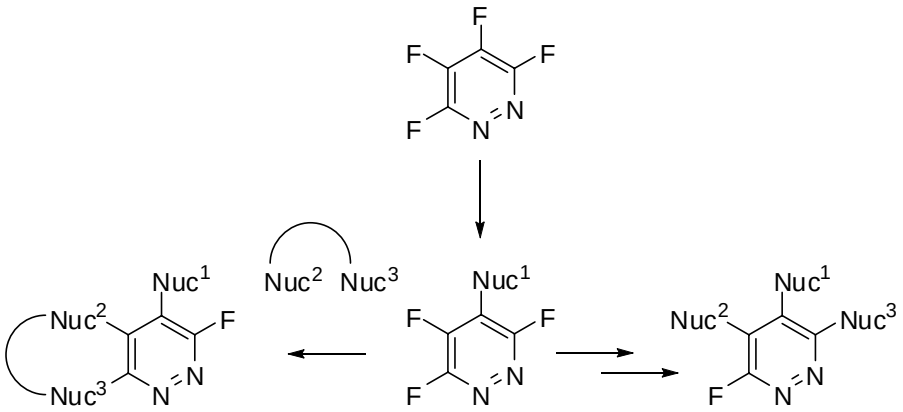

Chapter 1

Introduction

1.1 The Pharmaceutical Industry

Historically, the birth of the pharmaceutical industry can be seen as being closely related to the growth of the synthetic dye industry, both of them being lent impetus by the burgeoning state of research into coal tar derivatives towards the end of the nineteenth century. Much of this research flowed from Liebig, lauded in Germany as the father of organic chemistry, and his seminal chemistry school at Giessen,[1] through which passed such famous names as Erlenmeyer, Fehling, and Kekule.

At the time, the great demand for quinine, and its resultant high cost, had led to attempts to produce it synthetically. Liebig had unsuccessfully turned his hand to the artificial generation of quinine,[2] and this, coupled with the increasing recognition of the similarities between coal tar bases and the decomposition products of plant alkaloids, led Hofmann, himself a leading researcher of coal tar derivatives and a former pupil of Liebig, to consider the possibility of forming quinine via the introduction of the amine functionality to naphthalene. The proposed synthesis was unsuccessful, but research carried out by one of Hofmann's students resulted in the discovery of mauveine, the first synthetic dye. An offshoot of the new chemical dye industry was the application of its products to biology. The existence of "chemoreceptors" in living systems was suggested by the medical student Paul Ehrlich, based upon the observation that dyes demonstrated selective affinities for biological tissues.[3] It was argued that the chemoreceptors of certain parasites and microbes would differ from those found in the host and, as such, could be targeted. Ehrlich expressed this concept as the search for "magic bullets" that would specifically target the organisms at which they were aimed, and it forms the basis of modern chemotherapy.[4]

1.2 Modern Drug Discovery

As far as drug discovery is concerned, until recently many lead structures were found by screening microbial broths, plant extracts, and existing compound collections.[5] This changed with the advent of combinatorial chemistry, coupled with high throughput screening (HTS), whereby vast libraries of compounds were synthesised simultaneously, and then all screened to determine useful bioactivity and find 'hits'.[6]

While at first it was envisaged that these techniques would lead to a huge increase in the number of hit compounds found, it is coming to be acknowledged that investment in this technology has not provided the rewards imagined. To give some idea of the success rate of standard HTS, it has been suggested that in a screen for even a relatively "easy" target, typically one high quality lead compound may be found out of 100,000 molecules tested.[7]

One explanation for this is that while combinatorial chemistry undoubtedly produces large numbers of compounds, the very fact that syntheses have been designed to give as much structural variety as possible means that a large proportion of the compounds produced for screening are not "drug-like", and are therefore unlikely to possess the bioactivity necessary to be useful lead compounds.

The primary problem in drug development is that a large proportion of hit compounds must be abandoned during clinical development because of unsuitable pharmacokinetic properties. Consequently, steps are being taken to recognise the properties that make a molecule drug-like, and to increase the drug-likeness during the lead optimisation process.[8]

A major advance in this area was the publication of Lipinski's "rules of five",[9] a set of guidelines which stated that orally available drug-like molecules: have a molecular weight less than or equal to 500; have a log P (where P is a partition coefficient) that is less than or equal to 5; have 5 or fewer H-bond donors (NH and OH); and have 10 or fewer H-bond acceptors (N and O). The rules do not apply to substrates of transporters and natural

products. It has been found that the rule of five is associated with 90% of orally active drugs that have achieved phase II status.[10] More recent extensions to the rules include the observations that the polar surface area should be less than 140 $Å^2$ (or that the sum of H-bond donors and acceptors should be less than or equal to 12) and that there should be no more than 10 rotatable bonds.[11]

As these concepts of drug-likeness are becoming understood and acted upon, a corresponding reduction in the attrition rate of new chemical entities (NCEs) during clinical development is being observed.[12] Between 1991 and 2000 the percentage of projects involving NCEs failing due to bioavailability and pharmacokinetic reasons fell from 40% to 10%,[13] demonstrating the utility of drug-likeness considerations.

1.3 Properties of Heterocyclic Systems

Bearing in mind the points outlined above, it can be seen that appropriately functionalised low molecular weight heteroaromatic species may be excellent candidates exhibiting drug-like properties. In fact, it has been estimated that 70% of pharmaceutical products are based upon heterocyclic structures.[14] One of the major useful attributes of heterocyclic systems is the ability to hold given substituents in well-defined positions in three dimensional space, allowing far fewer degrees of conformational freedom than would be afforded by acyclic structures.[15] In addition to this, the presence of heteroatoms gives greater scope for electronic interactions, potentially altering absorption, distribution, metabolism and excretion (ADME) properties.

This thesis is concerned with the chemistry of highly halogenated pyridazines and thiophenes, two sub-classes of heterocyclic systems, and as such it seems appropriate to first give an overview of the typical chemistries of these heterocycles, followed by more detailed explorations of the idiosyncrasies of the aforementioned halogenated species.

1.4 Pyridazines in Medicinal Chemistry

The relatively recent identification of the pyridazine moiety in Nature (hexahydropyridazines were first observed in natural products in 1971,[16] and it was many more years before the first aromatic pyridazine was described[17]) has resulted in there traditionally being less interest in pyridazines than in the other diazines, however, with the freedom for generation of new intellectual property given by the previously sparse covering of the area, extensive expansion seems likely.

A number of pharmaceuticals contain the pyridazine moiety, including, but by no means limited to, the antibacterials Cefozopran, Cinoxacin, Sulfamethoxypyridazine, and Nifurprazine, the antidepressant Minaprine, and the anti-inflammatory and analgesic Emorfazone (Figure 1.1).[18-20]

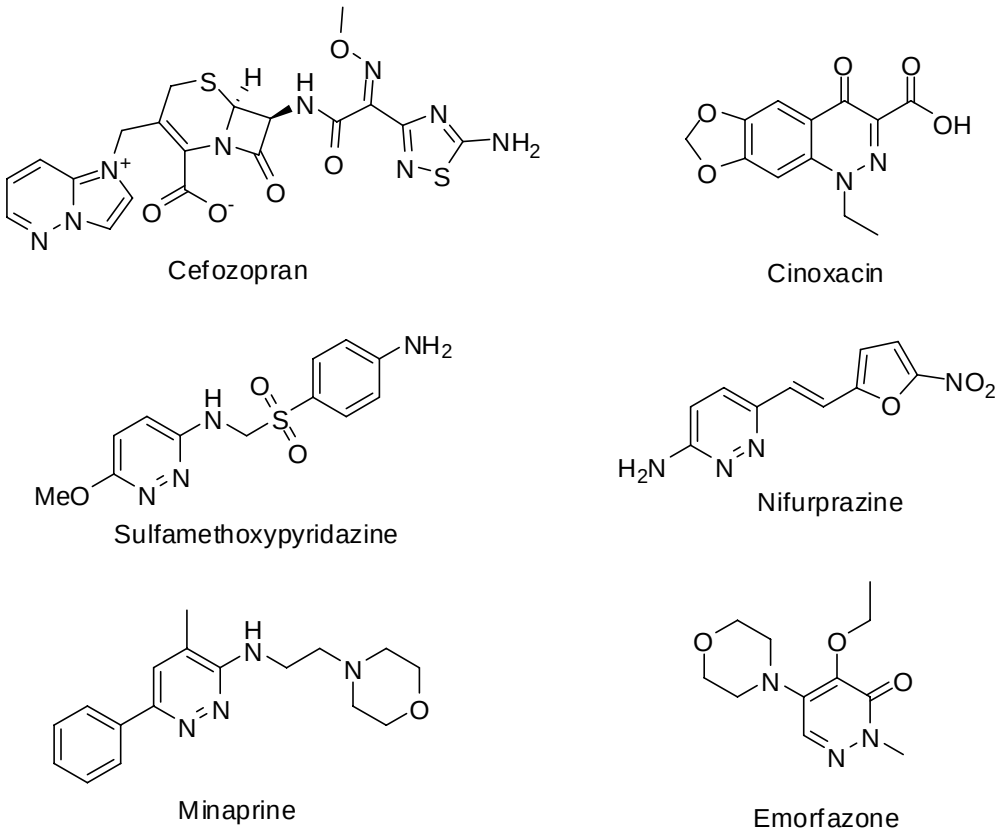

Figure 1.1

1.5 Syntheses of Pyridazines

1.5.1 By Formation of One Bond

A well known method for the construction of pyridazine rings by formation of the inter-heteroatom bond is the intramolecular oxidative coupling of two amino groups, an illustration of which is given below (Scheme 1.1).[21]

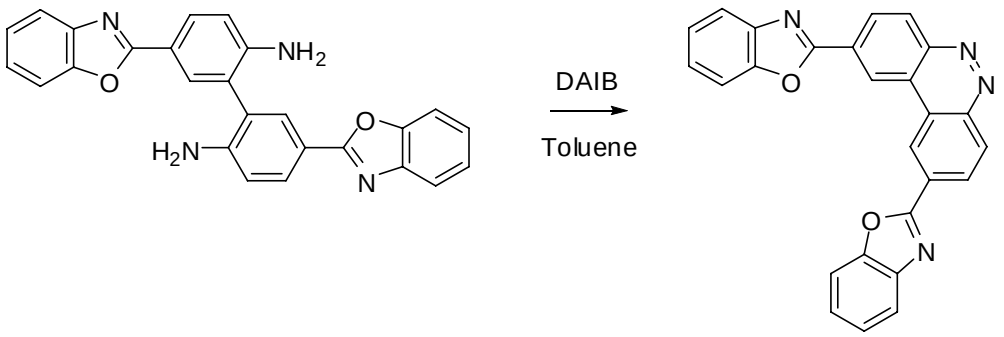

Scheme 1.1

A similar process involves the trapping of a nitroso intermediate by a nucleophilic heterocycle, leading to the formation of ring fused polyheterocycles, such as the pyrrolocinnolineone system shown (Scheme 1.2).[22]

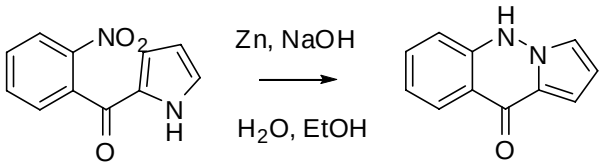

Scheme 1.2

An alternative class of ring closure reactions, one particularly useful for the synthesis of cinnolines, is that involving bond formation adjacent to one of the heteroatoms.

In the case of benzo-fused pyridazines, this bond forming reaction may be between the heteroatom and the benzene ring, or between the heteroatom and a carbon atom α- or β- to the ring. An example of the first scenario is the synthesis of cinnolin-3-ylio oxides by intramolecular nucleophilic aromatic substitution (Scheme 1.3).[23] In the first stage, hydrazine is introduced to an acid chloride, and the resulting amine may be reacted with the aromatic ring, replacing the activated halogen.

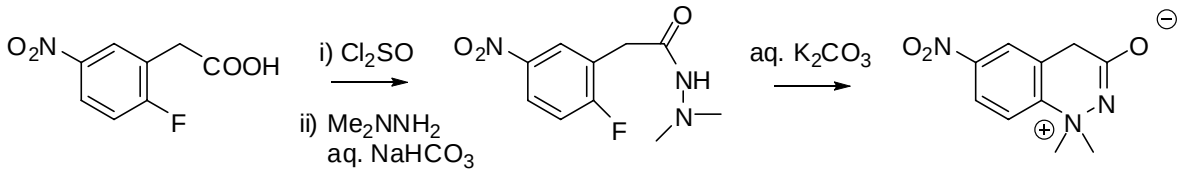

Scheme 1.3

An electrophilic carbon atom α- to the ring is utilised in the synthesis of pyrido[3,4-*d*]pyridazine derivatives (Scheme 1.4) via an addition-elimination reaction yielding the fused heterocycle and hydrazine from the dicarboxhydrazide.[24]

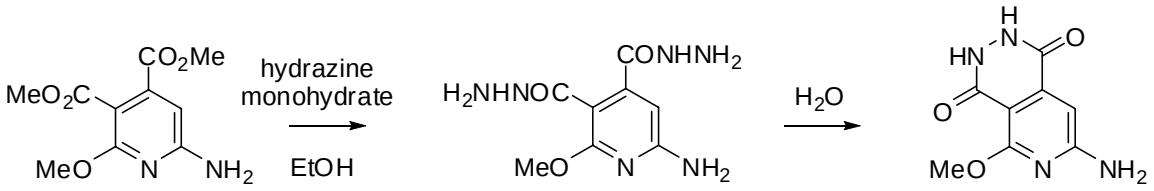

Scheme 1.4

Finally, the new bond may be formed between nitrogen and a carbon atom β- to the ring, often part of an alkynyl benzene parent system, as in the Richter cinnoline synthesis (Scheme 1.5).[25]

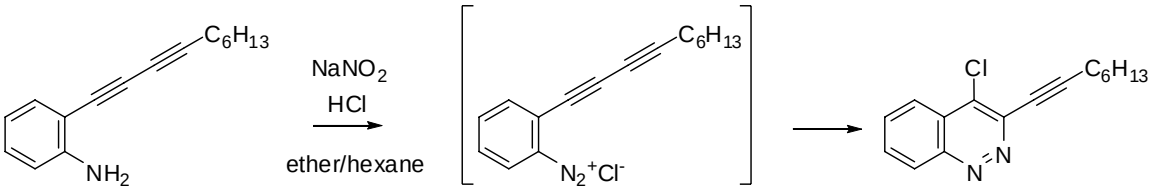

Scheme 1.5

This approach has been extended to allow solid-supported chemistry to be performed.[26] In this case (Scheme 1.6), treatment of the supported diazo compound with acid allows cleavage and cyclisation.

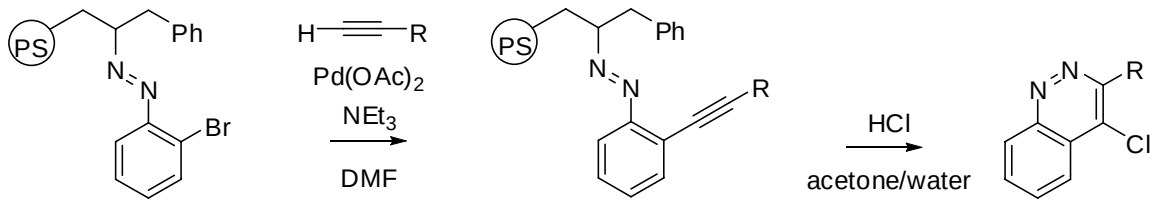

Scheme 1.6

The remaining one bond forming step leading to pyridazines involves creation of a bond γ- to a heteroatom. One approach has been the base-induced cyclisation of *ortho*-trifluoromethyl phenylhydrazides (Scheme 1.7), whereby initial deprotonation gives a quinine methide intermediate which cyclises to the difluoropyridazine, and then reacts further with the base to form the final amino pyridazine.[27]

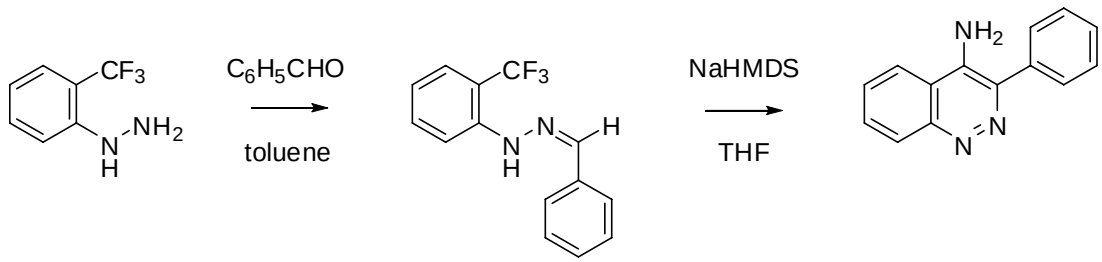

Scheme 1.7

A similar method was employed for the syntheses of 3-aroylcinnolines, in which the hydrazones were protonated to give a reactive intermediate susceptible to electrocyclisation, affording the target compounds after dehydration (Scheme 1.8).[28]

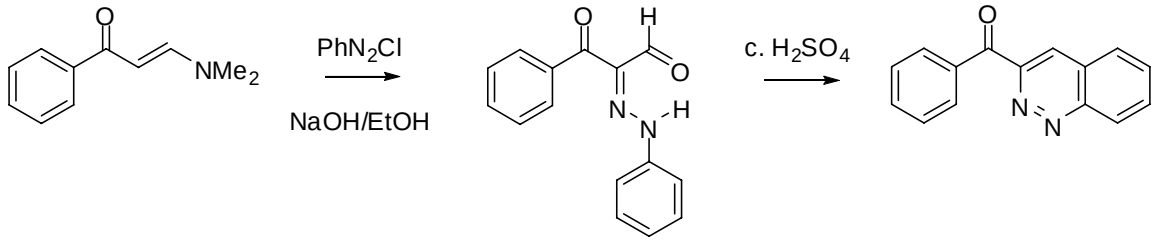

Scheme 1.8

Cyclisation may also be effected by an intramolecular reaction between a carbon nucleophile and a sufficiently activated electrophilic site, as in the synthesis of a range of tricyclic quinolones known to possess considerable antibacterial activity (Scheme 1.9).[29]

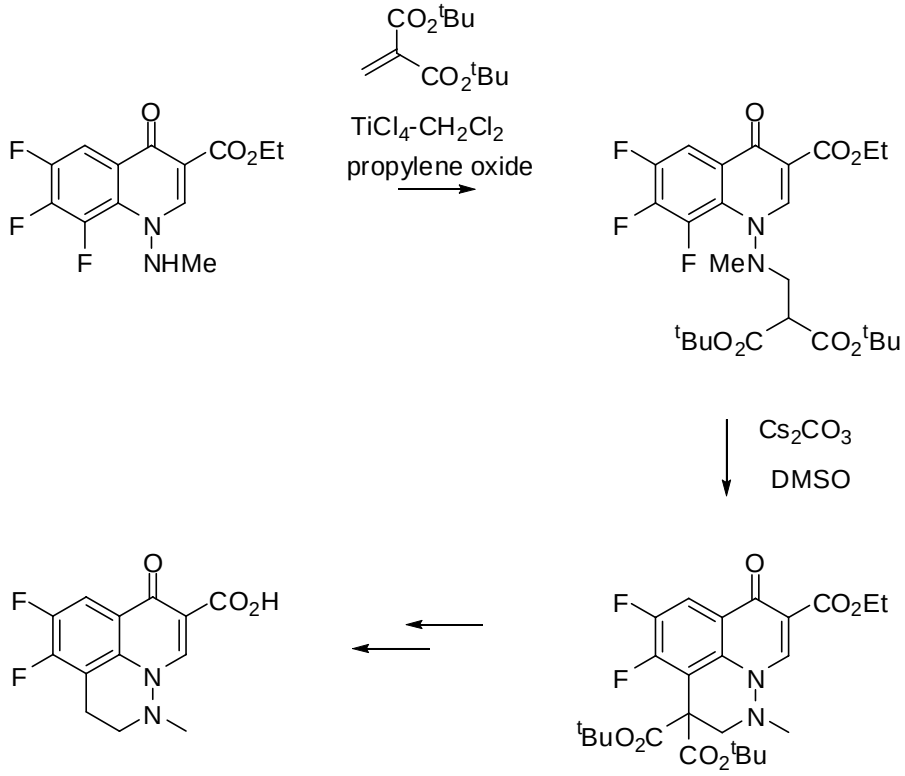

Scheme 1.9

1.5.2 By Formation of Two Bonds

Of the various two bond disconnections leading to fragments of four and two ring atoms, the most commonly applied is that which corresponds to the reaction between a four carbon motif with a dinitrogen compound, and the most straightforward subclasses of this category are the reactions of 1,4-dicarbonyl compounds with hydrazine.

An example of this approach is shown in the synthesis of the kinase inhibitor FR180204, in which a pyrazolo-pyridazine motif is constructed by initial formation of a pyridazine-containing intermediate (Scheme 1.10).[30]

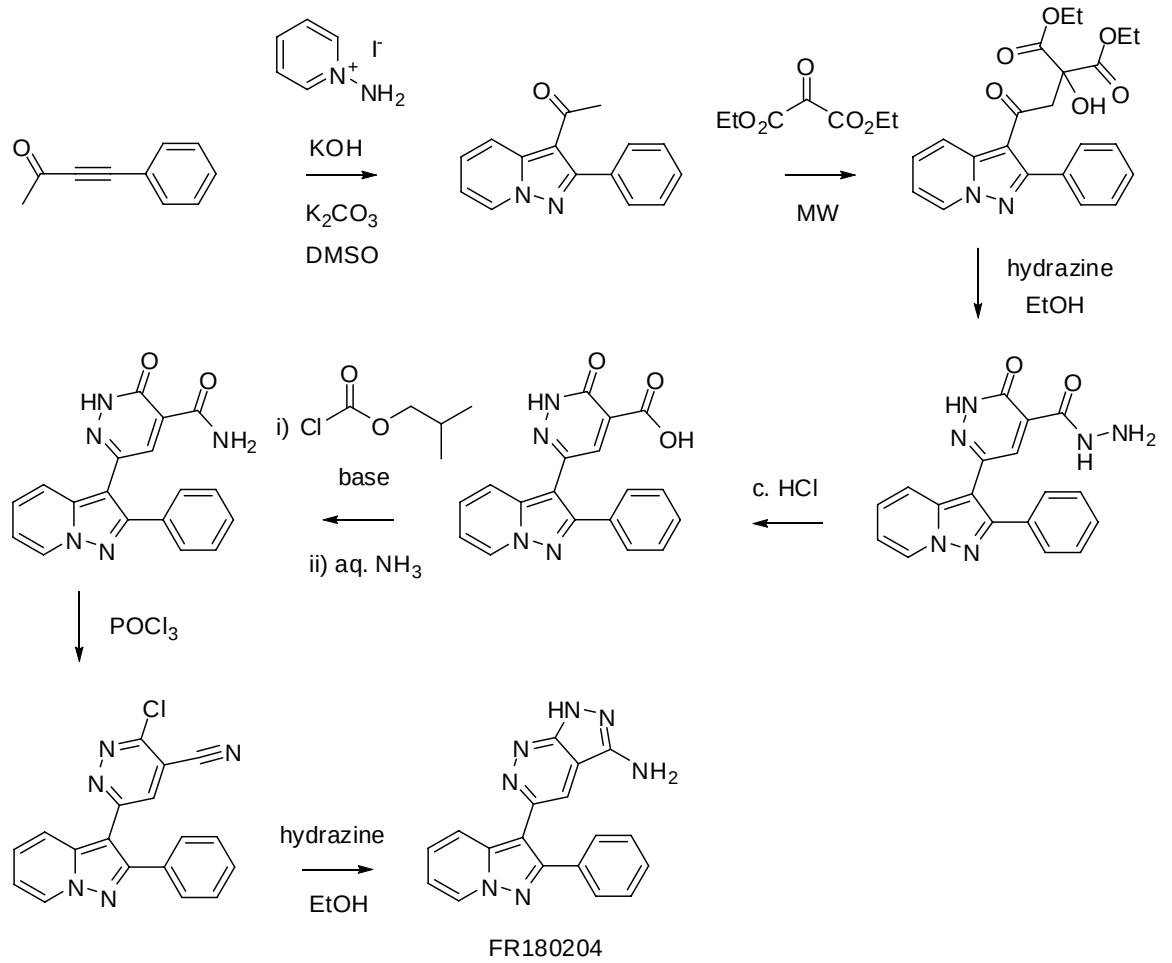

Scheme 1.10

Examples are also known where a nitrile functionality replaces the carbonyl group, leading to a 3-aminopyridazine type compound (Scheme 1.11).[31]

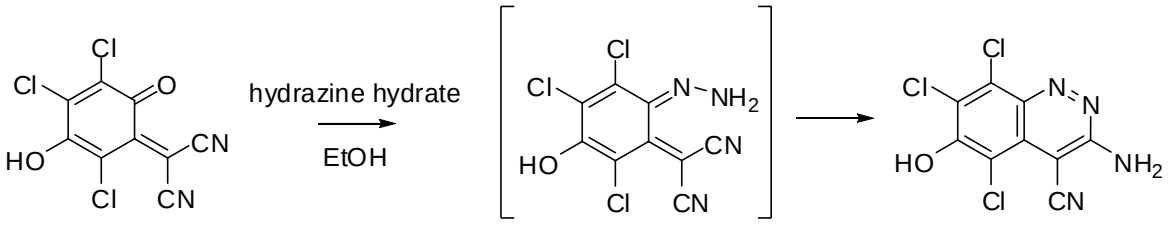

Scheme 1.11

The alternative approach involving simultaneous formation of two bonds is the Diels-Alder type [4+2] cycloaddition, the most well-known example being the Carboni-Lindsey reaction, which involves reaction of a 1,2,4,5-tetrazine with either an alkene or alkyne (Scheme 1.12). The use of alkenes initially yields 1,4-dihydropyridazines, which must then be oxidised to pyridazines. Pyridazines are directly afforded through the reaction of alkynes, the utility of which are, however, lessened by their decreased reactivity and propensity to give lower yields.[32]

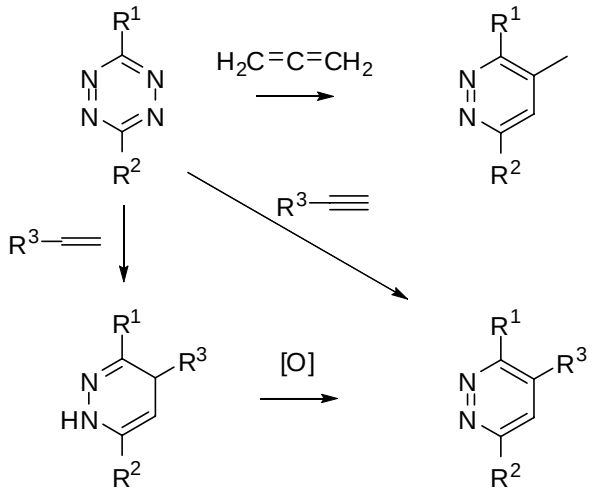

Scheme 1.12

The less common type of [4+2] cycloaddition simply involves reaction of an azo dienophile with a conjugated diene. This method is especially appropriate for the synthesis of 1,2,3,6-tetrahydropyridazines, as shown in the example below (Scheme 1.13).[33]

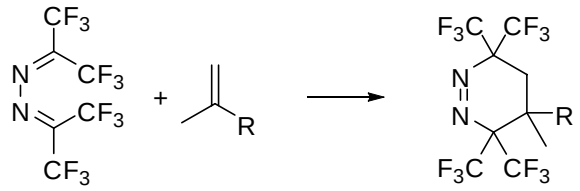

Scheme 1.13

The final class of cycloaddition syntheses are the [3+3] cycloadditions. Cyclopropenes may be made to react with diazo compounds to give cycloadducts that upon rearrangement yield pyridazines (Scheme 1.14).[34]

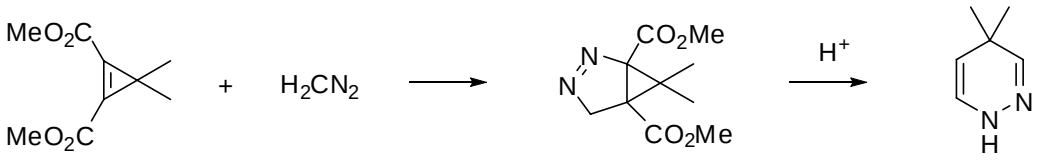

Scheme 1.14

Finally, a number of ring expansions that convert 5-membered heterocycles into pyridazines have been reported, including those of furans, thiophenes, 1-aminopyrrolidines, pyrrolidinediones and isoxazolines.[35] The most important of these are probably the reactions of hydrazine with furans, in a process similar to the condensations between hydrazine and 1,4-dicarbonyls outlined above.

1.6 Functionalisation of Pyridazines

A simple and versatile approach to substituted pyridazines is deprotonation of the parent heterocycle and subsequent trapping with an electrophile. The first factor to be taken into account for this method is the relative acidity of the protons in the starting material. A selection of informative examples whose pK_a's (in DMSO) have been recently calculated is shown below (Figure 1.2).[36]

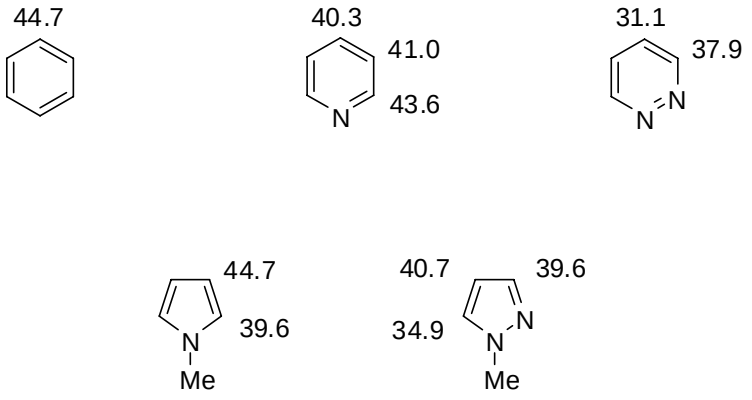

Figure 1.2

It can be seen that upon the change from benzene to pyridine, the acidity of the ring protons is increased as degree of conjugation in the pi system decreases. The 4-position of pyridine is the most susceptible to deprotonation, being furthest from the electronegative heteroatom. Addition of a second nitrogen atom increases acidity, and produces two acidic domains separated by a pK_a difference of approximately 7 units. It is worth noting that the trend in acidities round the 6-membered heterocycles differs from that seen in the five-membered cousins; the decreased external bond angles in the 6-membered cycles increase the electron repulsion felt by adjacent electron clouds.

This difference in acidity has been exploited using a strong, non-metallic organic base (^{t}Bu-P4) to form the anion, followed by trapping with carbonyl compounds to give pyridazines substituted with a secondary or tertiary alcohol at the 4-position (Scheme 1.15).[37]

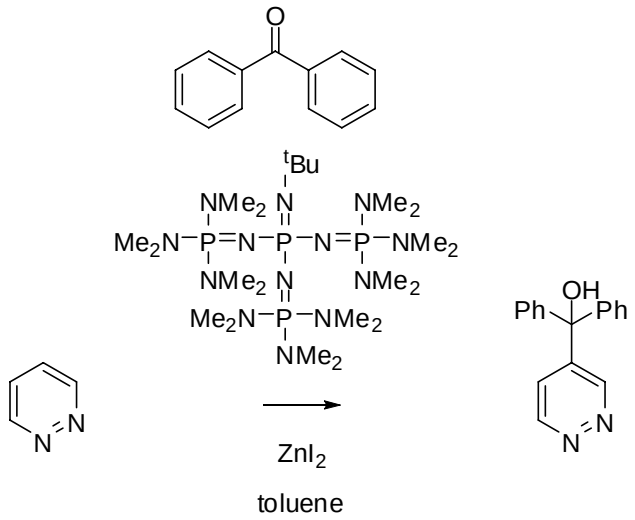

Scheme 1.15

Although reactions such as these appear simple enough, factors such as choice of base and the presence of ring substituents quickly complicate proceedings. The base employed in the previous example is fairly exotic, and the use of more common metallic bases changes the picture of reactivity. The electron deficient pyridazine ring, especially when one of the nitrogen atoms is coordinated to a cation, is susceptible to nucleophilic attack, meaning that commonly used strong bases such as butyllithium are unsuitable. More useful are hindered (and therefore less nucleophilic) lithium amide bases such as LDA or LiTMP, however, reactions can still tend towards oligomerisation as lithiated intermediates attack electrophilic pyridazines coordinated to metal. This can be alleviated to some extent by the formation of the anion using an excess of base and the trapping of the intermediate after a fairly short (minutes) reaction time (Scheme 1.16).[38]

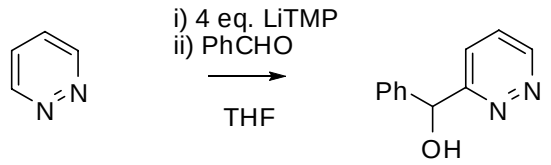

Scheme 1.16

It is interesting to note that in this case, the regioselectivity of the reaction is reversed, most probably due to the ring nitrogen atom interacting with the base and acting as a directing group.

A similar procedure using a more stable organometallic intermediate allows fairly regioselective iodination of pyridazine, once again showing a propensity for reaction at the 3-position (Scheme 1.17).[39]

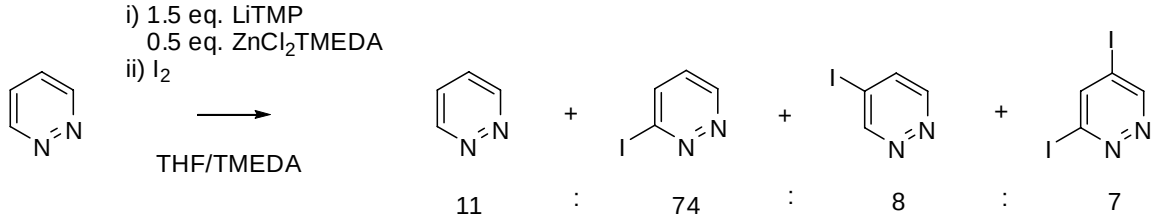

Scheme 1.17

Despite possessing an arguably attractive austerity, monosubstitutions of bare pyridazine are fairly removed from the desired goal of multifunctional heterocycles, and for further complexity to be achieved through deprotonation and trapping, the effects of other adornments around the ring must be taken into account. The use of directing groups in lithiation of pyridazine has a fairly short history, an early and facile example being the 4-substitution of 3,6-dimethoxypyridazine using LiTMP and a variety of electrophiles.[40]

A more useful reactivity is observed for pyridazine-3-carboxamide, where deprotonation occurs at the 4-position, *ortho*- to the directing group and away from the ring nitrogen

(Scheme 1.18). Trapping with carbonyls gives 3,4-disubstituted products, while trapping with iodine leads to the "wrong" 3,5- substitution pattern, a result of the intermediate undergoing a halogen dance reaction.[41]

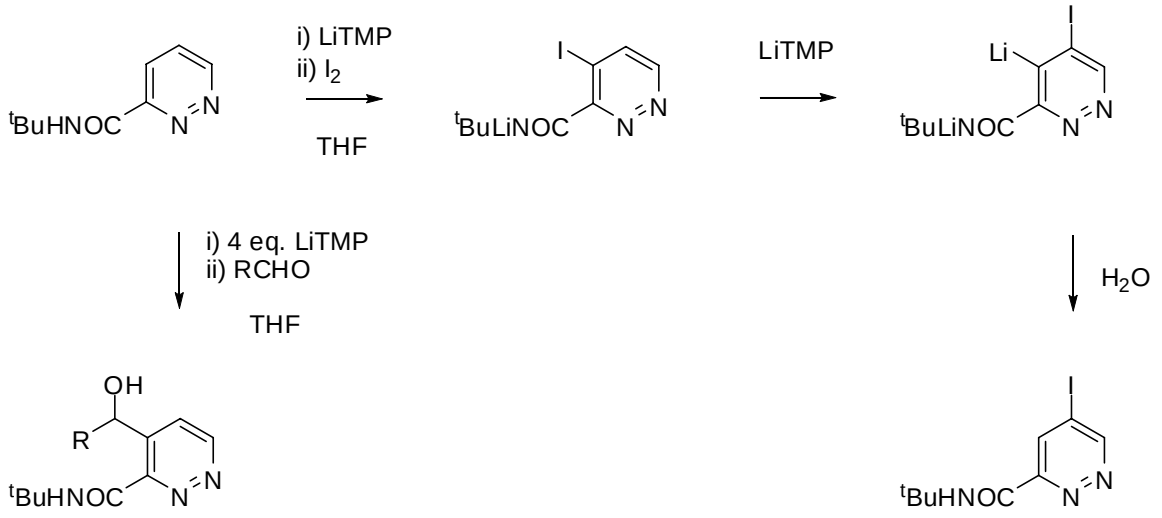

Scheme 1.18

The potential complexity increases further with the presence of multiple directing groups. In these cases competition between directing effects can lead to mixtures of products unless reaction conditions are carefully optimised.

An example of a starting material possessing such conflicting influences is 3-chloro-6-methoxypyridazine. Lithiations using standard dialkylamide bases followed by trapping with a range of electrophiles gave poor to moderate regioselectivities, while increasingly basic and hindered lithium amides gave selectivities approaching ninety nine percent in good yields (Scheme 1.19).[42]

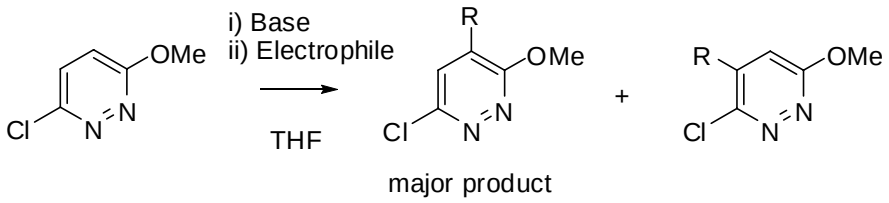

Scheme 1.19

The presence of a halogen atom in the previous example foreshadows the alternative common method for the regioselective functionalisation of pyridazine cores by metallation and then reaction with electrophiles: halogen-metal exchange.

Although the literature contains fewer examples of metalation by halogen exchange than it does those performed via simple deprotonation, a couple of reactions are notable. The first procedure was developed in order to circumvent the necessity of performing lithiations of diazines at low temperatures. As noted above, lithiated pyridazine derivatives are highly reactive, and very low reaction temperatures, often combined with short reaction times, are required to prevent unwanted side reactions such as oligomerisation. In contrast, functionalisation of polysubstituted iodinated pyridazines could be achieved by sonicating the heterocycle at room temperature in the presence of lithium metal and an electrophile, which immediately captures the intermediate carbanion species upon formation (Scheme 1.20).[43]

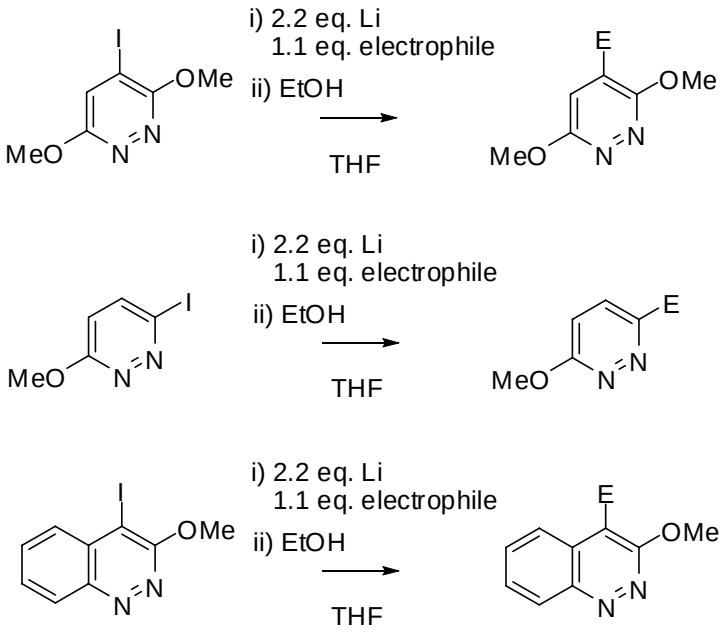

Scheme 1.20

An alternative option that allows use of metalated pyridazine derivatives at room temperature is to use magnesated rather than lithiated species (Scheme 1.21). Dibrominated and diiodinated pyridazines have been shown to undergo exchange reactions with alkyl magnesium chlorides at room temperature to give heteroaryl Grignard compounds that could be trapped using a variety of electrophiles, allowing the formation of polyfunctional pyridazines still bearing a reactive halogen handle.[44]

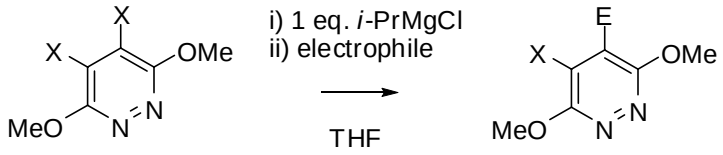

Scheme 1.21

Halogenated pyridazines may also be functionalised via transition metal mediated cross coupling reactions. A variety of methodologies have been demonstrated, but all are united by the common themes of oxidative addition, transmetalation, and reductive elimination.

One methodology that has been shown to be suitable for the selective reaction of symmetrically chlorinated pyridazines is the Negishi coupling. Reaction of 3,6-dichloropyridazine with phenyl- and benzyl-zinc bromides gave almost exclusively monosubstituted products in moderate yields (Scheme 1.22).[45]

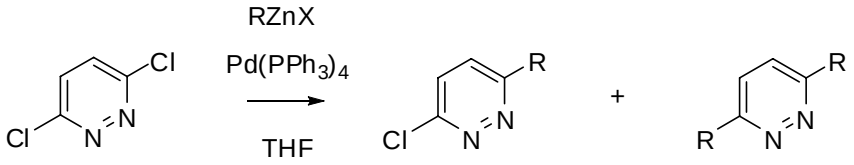

Scheme 1.22

The resulting monochloro derivatives could be reacted further at higher temperatures under similar conditions to give unsymmetrical 3,6-disubstituted products.

Suzuki reaction conditions applied to the same substrate give less satisfactory results, as some degree of disubstitution seems unavoidable (Scheme 1.23).[46, 47]

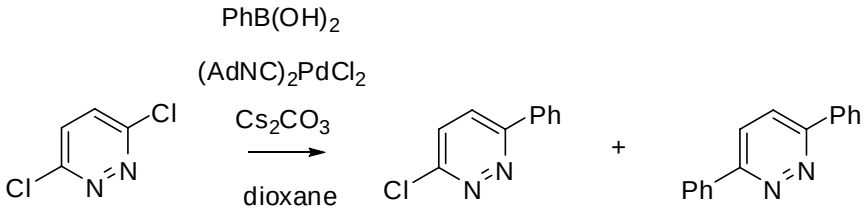

Scheme 1.23

The desired 3-chloro-6-aryl pyridazines could be accessed via Suzuki reaction if the molecule was first desymmetrised by selective replacement of a single chlorine atom by iodine, accomplished by warming the dichloro compound in hydroiodic acid and sodium iodide.[48] The change in halogen atom considerably lowers the energy barrier to oxidative addition and allows monosubstitution to be smoothly realised, as has also been demonstrated for Sonogashira couplings on the same substrate.

Exploitation of this difference in the susceptibility of aryl halogens to oxidative addition also allows synthesis of halogenated pyridazines bearing substituents at the 4- and 5-positions, as shown in the following synthesis of a potential antihypertensive agent (Scheme 1.24). The specific synthetic scheme shown is an improvement on the previously established route to the target molecule, giving an increase in overall yield from 20 to 43%, but the key step is the Suzuki coupling, which may be performed in two successive regioselective steps to allow differing aryl groups to be arranged on the pyridazine scaffold.[49]

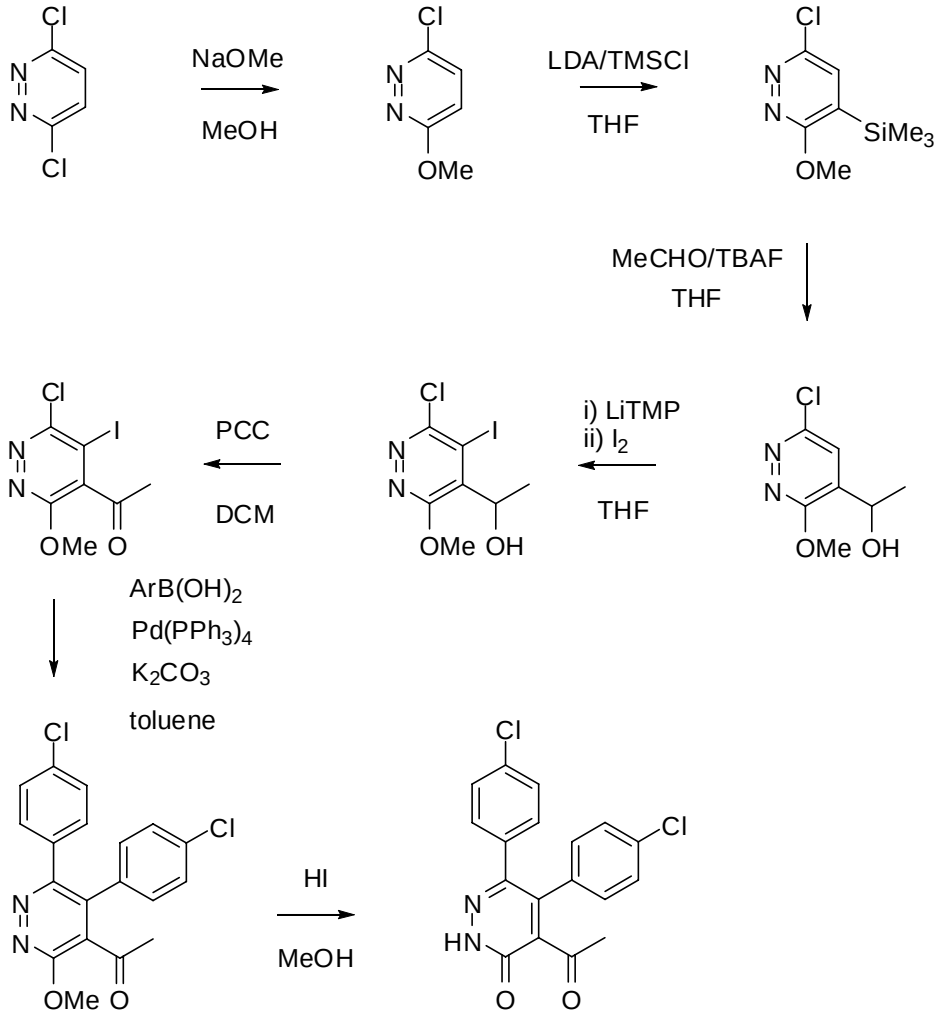

Scheme 1.24

Halopyridazinones have also been shown to react under Buchwald-Hartwig amination conditions, as in the example below (Scheme 1.25).[50] Formation of the biaryl ether analogue was possible using simple base-mediated nucleophilic aromatic substitution, but bromoaniline proved insufficiently reactive. Palladium catalysis gave straightforward access to the desired product.

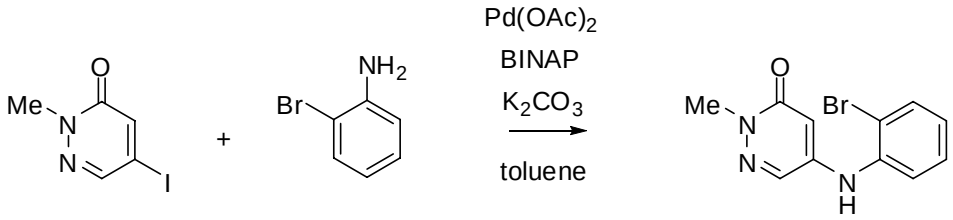

Scheme 1.25

The final major class of transformations that may be performed on halogenated pyridazines is that of nucleophilic aromatic substitution. This may in some way be considered as complementary to the functionalisations given above, as substitution generally requires chlorine, or even fluorine atoms to be present, as opposed to the metalations and cross coupling procedures which are better suited to the heavier halogens such as bromine and iodine.

One relatively recent use of chloropyridazine as an electrophilic coupling partner was in the synthesis of some phenyl heteroaryl ketones (Scheme 1.26), an intermediate in whose production was diarylacetonitrile.[51]

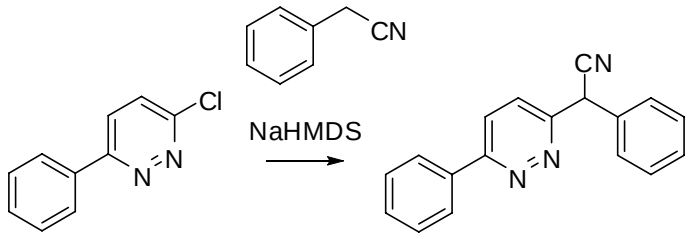

Scheme 1.26

Pyridazines bearing multiple electron withdrawing groups are known to be excellent electrophiles, and may be used to trap particularly recalcitrant nucleophiles, as shown in the examples below (Scheme 1.27).[52]

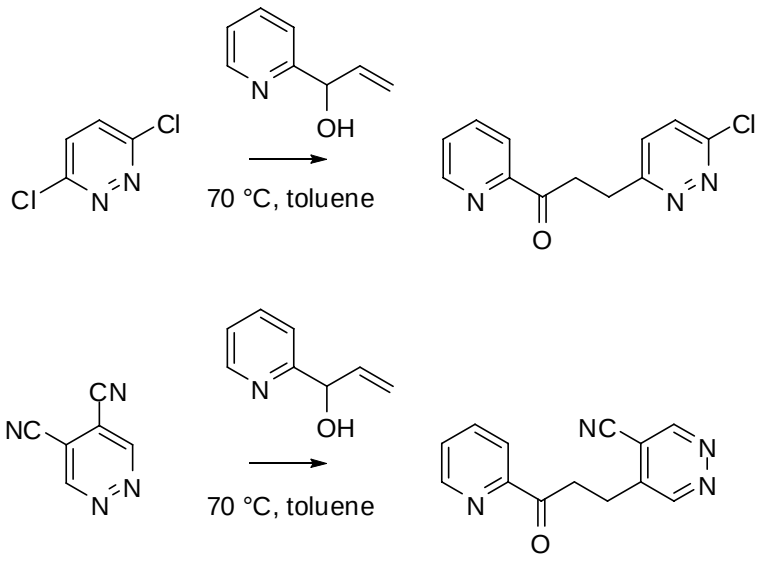

Scheme 1.27

1.7 Thiophenes in Medicinal Chemistry

Thiophene is widely represented in medicinal chemistry, appearing in molecules with such diverse uses as antihypertensives, opioids, CNS drugs and anti-cancer agents. A small sample of such compounds is shown below (Figure 1.3).[53-64]

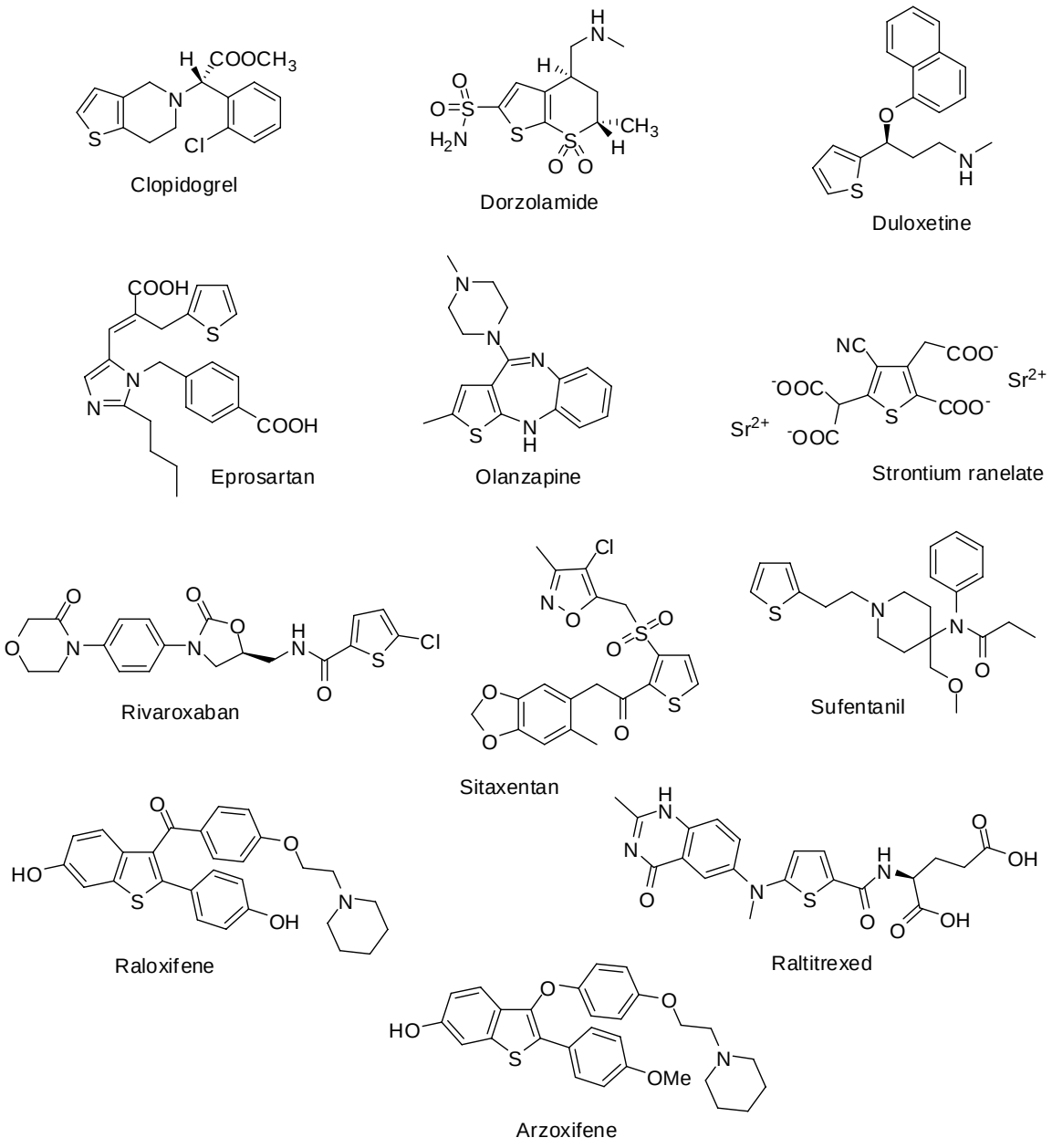
Clopidogrel
Dorzolamide
Duloxetine
Eprosartan
Olanzapine
Strontium ranelate
Rivaroxaban
Sitaxentan
Sufentanil
Raloxifene
Raltitrexed
Arzoxifene

Figure 1.3

1.8 Syntheses of Thiophenes

1.8.1 By Formation of One Bond

Ring closures α- to the heteroatom are fairly uncommon, generally involving sulfur as a nucleophile. One interesting application is the synthesis of 2,3,5-trisubstituted thiophenes from aryl ketones, propargyl bromide, morpholine, and sulfur (Scheme 1.28).[65] The first step is a Willgerodt-Kindler reaction giving the thiomorpholide, which can then be reacted with propargyl bromide in the presence of base. The resulting compound undergoes a Claisen rearrangement to give an allene, which is attacked intramolecularly by the sulfur atom to furnish the substituted thiophene.

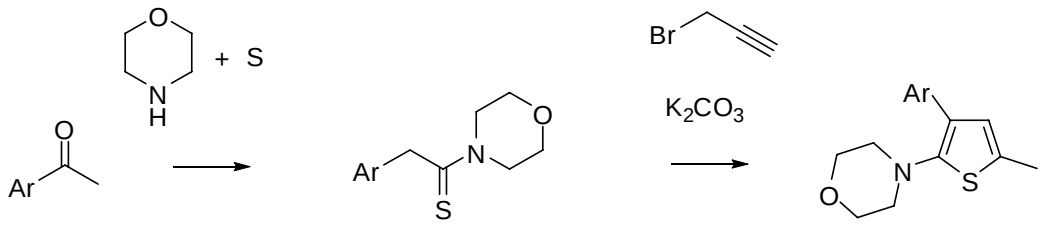

Scheme 1.28

Ring closures β- to the heteroatom may be subdivided into Knoevenagel and Thorpe Ziegler type, depending on whether the intramolecular cyclisation is onto a carbonyl or nitrile functionality, respectively. The Thorpe-Ziegler class yields 3-aminothiophenes, such as in the example below (Scheme 1.29).[66]

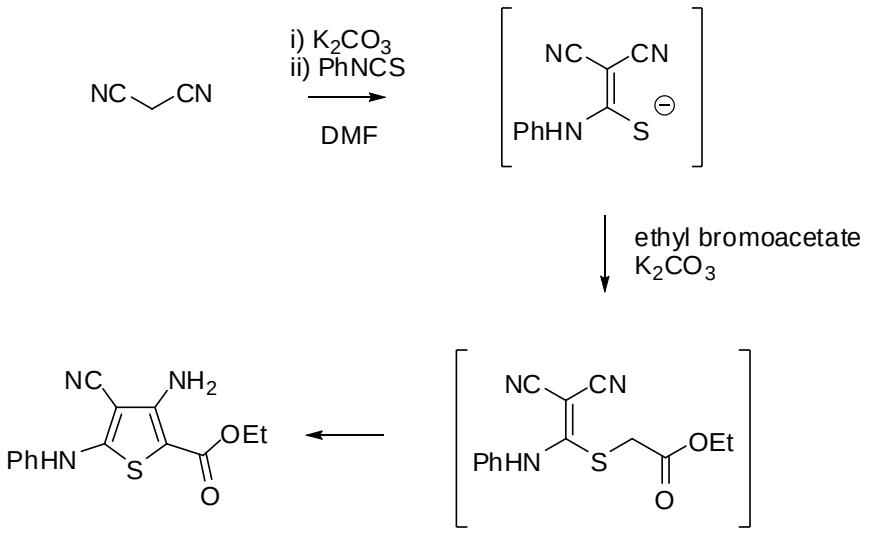

Scheme 1.29

The Knoevenagel type approach has been used for the synthesis of thienodolin, a natural product known to affect the growth of rice seedlings (Scheme 1.30).[67]

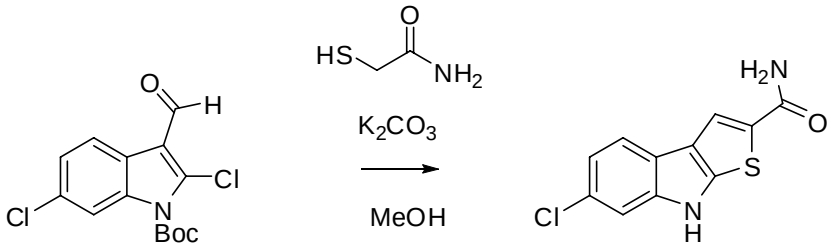

Scheme 1.30

Ring syntheses where the final step is bond formation γ- to the heteroatom are a less common class, although one approach worthy of mention is the Nakayama procedure, which involves the zinc and titanium tetrachloride mediated cyclisation of diketo sulfides (Scheme 1.31).[68] Symmetrically substituted sulfides may be prepared by the reaction between sodium sulfide and α-haloketones, while unsymmetrical compounds may be obtained from α-haloketones and α-mercaptoketones.[69]

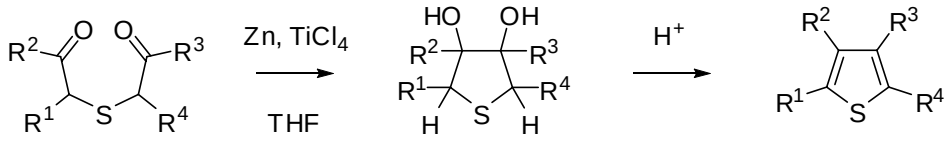

Scheme 1.31

1.8.2 By Formation of Two Bonds

One of the more traditional approaches to thiophene systems is via two bond forming reactions between a sulfur atom and a four carbon component. Reactions of this sort may be further subdivided into two major groups: Gewald syntheses and Paal-Knorr syntheses.

The Gewald reaction is a multi-component reaction, the first step of which is a Knoevenagel condensation between an α-cyanoester and an α-methylene carbonyl compound. Subsequent reaction with elemental sulfur leads to formation of 2-aminothiophenes.

This method has been employed for the production of polysubstituted thiophenes intended to act as templates for structural diversification and library synthesis.[70] The resulting thiophenes were subsequently diversified by functionalisation of the amine and sequential deprotection and reaction of the two ester groups (Scheme 1.32).

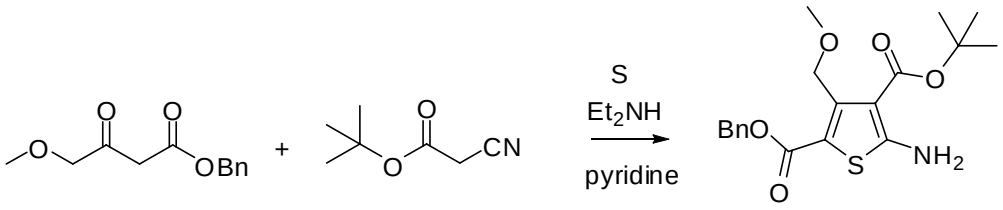

Scheme 1.32

The Gewald reaction has also been used in the construction of a key intermediate for the total synthesis of 3-deazathiamine.[71] Initial attempts to form the thiophene from the unhalogenated olefin led to a mixture of isomers, necessitating the synthesis of the chlorinated analogue, which could be cleanly cyclised to the desired intermediate (Scheme 1.33).

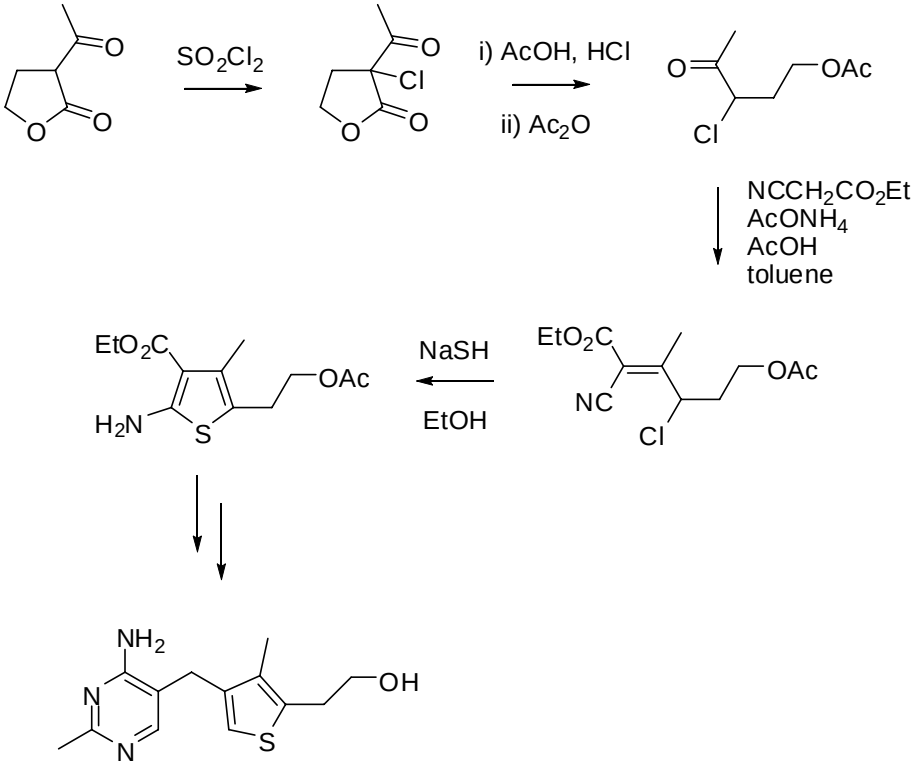

Scheme 1.33

The alternative [4C + S] approach is the Paal-Knorr synthesis (Scheme 1.34). This involves the condensation of a dicarbonyl compound using a sulfurising agent, such as Lawesson's reagent. These cyclisations may be performed quickly in the absence of solvent under microwave irradiation.[72]

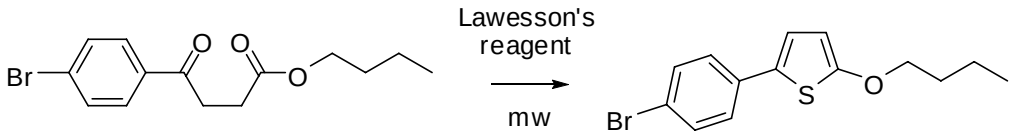

Scheme 1.34

One of the limitations on the utility of Lawesson's reagent is the ease with which it may be removed from the reaction mixture after use. A novel solution to this problem has been suggested in the form of fluorous technology (Scheme 1.35).[73]

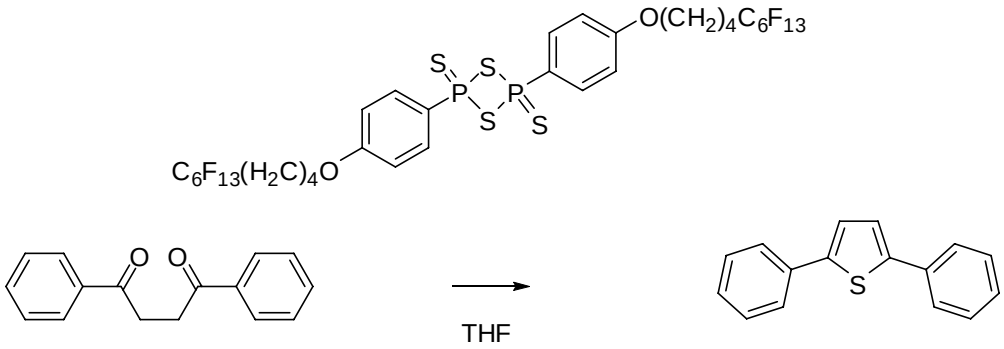

Scheme 1.35

The final class of important two bond forming reactions leading to thiophenes is that consisting of marriage between fragments of two and three atoms, the most important of which is the Hinsberg synthesis (Scheme 1.36), which gives 2,5-dicarboxylated thiophenes from thiodiacetates and α-diketones.[74]

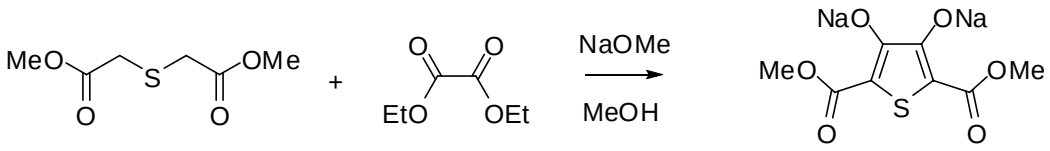

Scheme 1.36

1.9 Functionalisation of Thiophenes

Alkylation and acylation reactions of thiophenes are fairly few in number, largely due to the instability of thiophenes under traditional Friedel-Crafts reaction conditions. There are however, a handful of processes that allow these difficulties to be bypassed. For example, silica gel may be used in place of harsher Lewis acid catalysts such as aluminium trichloride. This methodology has been employed for the *tert*-butylation of the parent heterocycle (Scheme 1.37).[75]

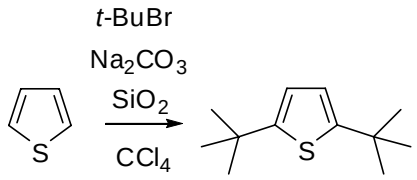

Scheme 1.37

Thiophene may also be alkylated via the Mannich reaction (Scheme 1.38), although the process is considerably slower than that seen for pyrrole or furan, and generally requires the use of alkoxy substituted starting materials.[76]

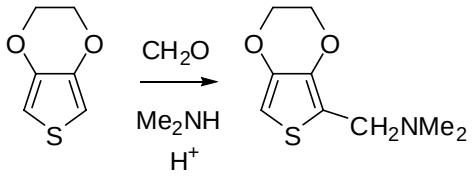

Scheme 1.38

In the above case, the two alkoxy substituents are tied back, reducing steric hindrance and increasing reactivity compared to similar non-cyclised dialkoxylated examples.[77]

Acylation reactions are also difficult. One alternative is lithiation of thiophene followed by trapping with DMF.[78] In the example shown below (Scheme 1.39), this approach is complementary to Vilsmeier formylation, which results in functionalisation of the pyrrole ring.

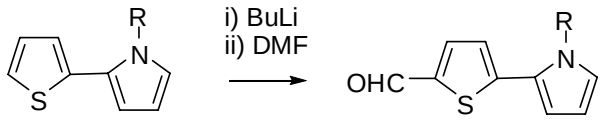

Scheme 1.39

One of the more versatile strategies for the functionalisation of the thiophene scaffold is the employment of transition metal catalysis. A wide variety of such processes have been performed, and a few recent examples are given below.

The Heck reaction is possibly the most straightforward approach of this type, as it enables direct C-H activation and corresponding increase in functionality. Although more traditional methods for the Heck coupling of unsubstituted thiophenes require harsh conditions,[79] the use of the Jeffery method allows regioselective functionalisation of activated thiophenes in a relatively mild fashion (Scheme 1.40).[80]

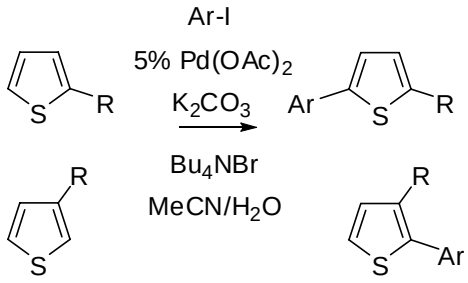

Scheme 1.40

R is an electron withdrawing group such as nitro, cyano, or aldehyde, which, along with the sulfur atom, directs the reaction. 3-Substituted thiophenes react regioselectively at the 2-position, although a competing reaction at the 5-position is observed, as well as some 2,5-disubstitution. In contrast, 2-substituted starting materials give exclusively the 5-substituted product. Unfortunately, the reactivity of these systems is lower. Isolated yields are in the region of 30 – 80%, with the best results being observed for reactions of 2-cyanothiophene (77 – 81%). This methodology has been extended to the synthesis of arylated benzo[*b*]thiophenes (Scheme 1.41).[81]

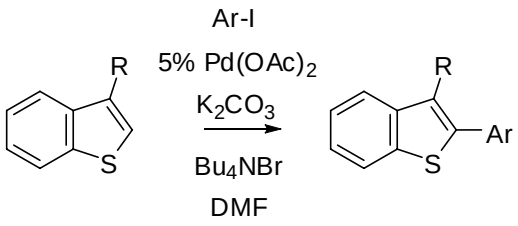

Scheme 1.41

Halogenated thiophenes are also useful coupling partners in palladium-mediated cross-coupling processes. An early example of this is the Negishi coupling between iodothiophene and alkynylzinc reagents (Scheme 1.42).[82]

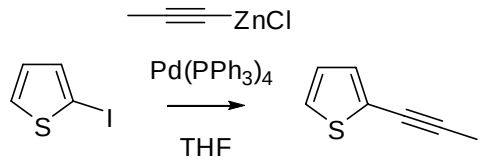

Scheme 1.42

Of more interest in the search for polysubstituted thiophenes is the regioselective reaction of multiply halogenated parent compounds.

Where thiophene is halogenated at two inequivalent positions, a degree of regioselectivity is made possible, but total selectivity may be hard to achieve. In the case of the Negishi coupling to 2,3-dibromothiophene (Scheme 1.43), clean reaction at the 2-position is found in good yield, allowing further functionalisation through the remaining bromine.[83]

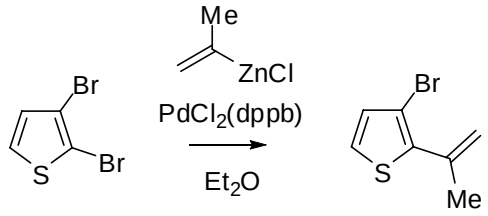

Scheme 1.43

The Suzuki reaction of 2,3-disubstituted thiophenes has also been observed to give preferential substitution at the 2-position, with excess boronic acid leading to both halogens being replaced.[84] In certain cases, mixtures of products may be obtained, as seen, for example, in the following step (Scheme 1.44) taken from a synthesis of a liquid crystal, where the desired 2-substituted product is produced in 83% yield alongside 2% of the undesired isomer.[85]

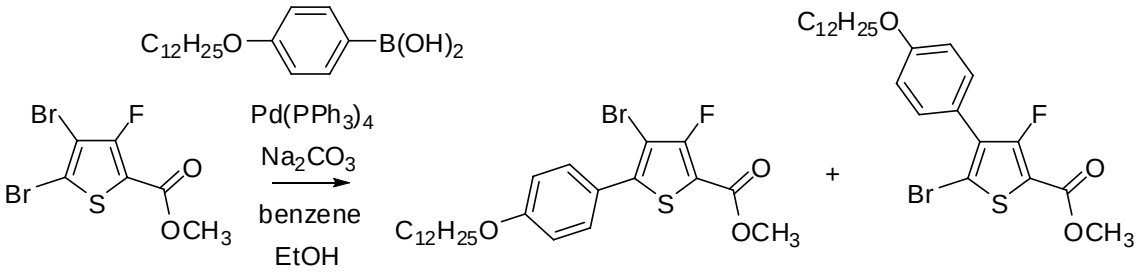

Scheme 1.44

The Stille coupling of 2,3-dibromothiophene has generally been found to lead to some degree of disubstitution, with the exact ratios depending on coupling partner and reaction conditions used (Scheme 1.45).[86] Performed under the modified Farina conditions ($AsPh_3$

as ligand in NMP)[87] the desired monosubstitution product was obtained in 17 – 70% yield, with 4 – 12% of the disubstituted product observed. Use of the modified Fu conditions (P^tBu as ligand, with CsF in dioxane)[88] – a more reactive system – gave yields of monosubstituted product that were in the same range, 25 – 72%, but increased the level of disubstitution to 11 – 71%.

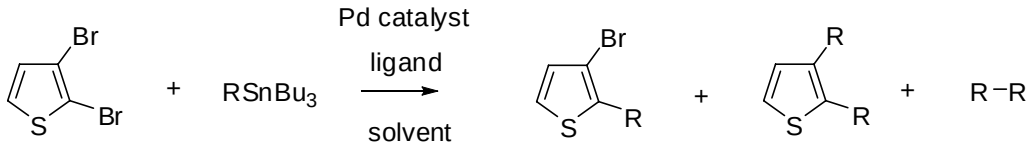

Scheme 1.45

Just as the difference in reactivity between the two halogenated sites in 2,3-dibrominated thiophenes may be exploited to give regioselective processes, so may similar differences in the 2,4-dibrominated substrate. 2,4-Dihalogenated thiophene was used as the precursor in the synthesis of thio-enyne containing natural products found in various plants of the *Anthemis* genus (Scheme 1.46).[89] The first step was conversion to 4-bromo-2-(1-propynyl)thiophene, achieved in 70% yield by simple Negishi coupling with propynylzinc chloride (although further differentiation of the two sites by initial transhalogenation to 4-bromo-2-iodo thiophene allows the coupling to be performed in 80% yield).

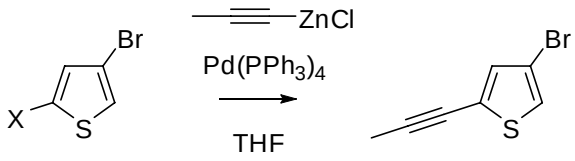

Scheme 1.46

This difference in reactivity was also exploited to allow an elegant synthesis of 3,4'-dibromo-2,2'-bithiophene, via two separate functionalisations of 3-bromothiophene followed by regioselective Stille coupling of the products (Scheme 1.47).[90]

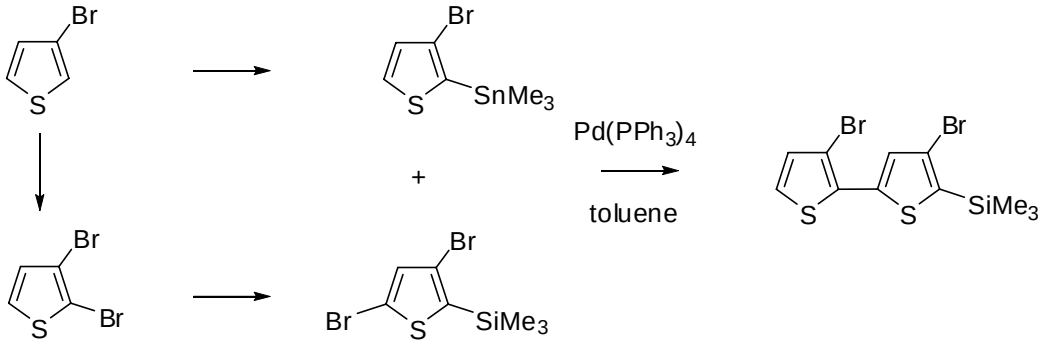

Scheme 1.47

When thiophene bears multiple halogen atoms in equally reactive positions, selective monosubstitution becomes difficult, for example, based purely on statistical considerations, reaction of a symmetrically dihalogenated substrate with an equimolar amount of coupling partner should result in a 1:2:1 ratio of starting material:monosubstituted product:disubstituted product. Despite this, other factors may allow for increased selectivity through either steric or electronic means.

In the case of 3,4-dihalogenated thiophenes, the most obvious effect is the former, as a sufficiently bulky substituent may interfere with the oxidative addition and transmetallation at the adjacent site. Reaction of 3,5-dibromothiophene with one equivalent of benzylzincbromide under palladium catalysis was shown to give 52% monosubstituted product along with 6% of the disubstituted species and 20% recovered starting material.[91]

Attempts to synthesise a range of diheteroarylated thiophenes gave further insight into the activity of these 3,4-dihalogenated systems.[92] Reaction of 3,4-dibromo-2,5-dimethylthiophene with an excess of heteroaryl boronic acid resulted in an approximately equimolar mixture of starting material and mono- and di-coupled products, while use of the more reactive 3,4-diiodo-2,5-dimethylthiophene allowed synthesis of the desired dicoupled products in reasonable yields. Attempts to perform a dicoupling between the

diiodothiophene and a trimethylstannylthiazole gave only the monosubstituted product in 16% yield, suggesting that the change from a boronic acid to an organo tin compound increased the steric demand involved in the reaction.

Polyhalogenated parent compounds are probably the most widely applicable route towards polyfunctionalised thiophenes. Halogenation of thiophene is straightforward, and multiple reactions are made possible. A simple example is subsequent replacement of halogen atoms by nucleophilic aromatic substitution (Scheme 1.48). This approach is often limited by the requirement of a nitro group to activate *ortho*- substituents to substitution.[93]

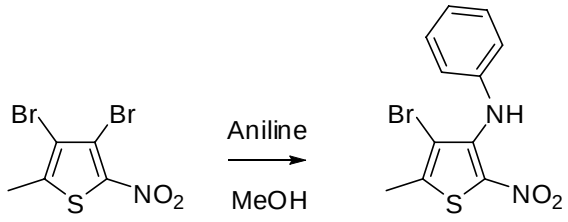

Scheme 1.48

Halogen atoms attached to the ring in the 3- or 4-positions may also undergo halogen metal exchange, allowing the generation of anions in positions other than those favoured by simple deprotonation (Scheme 1.49).[94] This allows trapping with electrophiles from positions not allowed by the methods outlined at the start of this section.

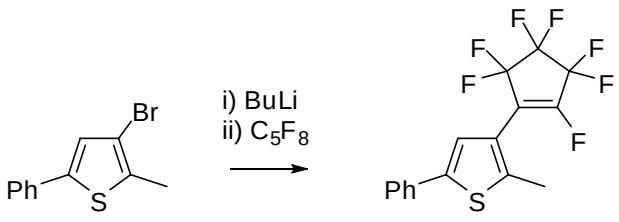

Scheme 1.49

1.10 Conclusions

The literature outlined above has demonstrated the need for methodology tailored to the reliable exploration of chemical space with particular regard to drug-like molecules containing heterocyclic motifs, namely pyridazine and thiophene. A variety of pyridazine- and thiophene- containing drug molecules has been exhibited, and currently favoured methods for the synthesis and functionalisation of these desired species have been briefly reviewed to provide an overview of the types of chemistry possible for the synthesis of functionalised pyridazine and thiophene derivatives. The majority of the rest of this work will examine approaches to the realisation of diverse ranges of these drug-like heterocyclic compounds.

1.11 References

1 W. H. Brock, 'Justus von Liebig', Cambridge University Press, 1997.
2 A. S. Travers, *Technol. Cult.*, 1990, **31**, 51.
3 J. Drews, *Science*, 2002, **287**, 1960.
4 'Nobel Lectures, Physiology or Medicine 1901 - 1921', Elsevier Publishing Company, 1967.
5 D. V. Patel and E. M. Gordon, *Drug Discov. Today*, 1996, **1**, 134.
6 D. Bailey and D. Brown, *Drug Discov. Today*, 2001, **6**, 57.
7 W. P. Walters, A. Murcko, and M. A. Murcko, *Curr. Opin. Chem. Biol.*, 1999, **3**, 384.
8 T. H. Keller, A. Pichota, and Z. Yin, *Curr. Opin. Chem. Biol.*, 2006, **10**, 357.
9 C. A. Lipinski, F. Lombardo, B. W. Dominy, and P. J. Feeny, *Adv. Drug Deliver. Rev.*, 1997, **23**, 3.
10 C. A. Lipinski, *Drug Discov. Today: Technologies*, 2004, **1**, 337.
11 D. F. Veber, S. R. Johnson, H. Y. Cheng, B. R. Smith, K. W. Ward, and K. D. Kopple, *J. Med. Chem.*, 2002, **45**, 2615.
12 Y. Sugiyama, *Drug Discov. Today*, 2005, **10**, 1577.
13 R. Frank and R. Hargreaves, *Nature Rev. Drug Discov.*, 2003, **2**, 566.
14 G. Sandford, R. Slater, D. S. Yufit, J. A. K. Howard, and A. Vong, *J. Org. Chem.*, 2005, **70**, 7208.
15 B. Beck, A. Picard, E. Herdtweck, and A. Domling, *Org. Lett.*, 2004, **6**, 39.
16 C. H. Hassall, R. B. Morton, Y. Ogihara, and D. A. S. Phillips, *J. Chem. Soc. (C)*, 1971, 526.
17 R. Grote, Y. Chen, A. Zeeck, Z. Chen, H. Zahner, P. Mischnick-Lubbecke, and W. A. Konig, *J. Antibiotic.*, 1988, **41**, 595.

[18] Y. Iizawa, K. Okonogi, R. Hayashi, T. Iwahi, T. Yamazaki, and A. Imada, *Antimicrob. Agents Ch.*, 1993, **37**, 100.

[19] A. R. Katritzky, M. A. Munawar, J. Kovacs, and L. Khelashvili, *Org. Biomol. Chem.*, 2009, **7**, 2359.

[20] J.-P. Kan, C. Mouget-Goniot, P. Worms, and K. Biziere, *Biochem. Pharmacol.*, 1986, **35**, 875.

[21] M. F. G. Stevens, D.-F. Shi, and A. Castro, *J. Chem. Soc., Perk. T. 1*, 1996, 83.

[22] A. Kimbaris and G. Varvounis, *Tetrahedron*, 2000, **56**, 9675.

[23] V. J. Aran, J. L. Asensio, J. Molina, P. Munoz, J. R. Ruiz, and M. Stud, *J. Chem. Soc., Perk. T. 1*, 1997, 2229.

[24] J. Cobo, A. Sanchez, M. Nogueras, and E. D. Clercq, *Tetrahedron*, 1997, **53**, 8225.

[25] O. V. Vinogradova, V. N. Sorokoumov, S. F. Vasilevsky, and I. A. Balova, *Tetrahedron Lett.*, 2007, **48**, 4907.

[26] S. Brase, S. Dahmen, and J. Heuts, *Tetrahedron Lett.*, 1999, **40**, 6201.

[27] A. S. Kiselyov and C. Dominguez, *Tetrahedron Lett.*, 1999, **40**, 5111.

[28] N. A. Al-Awadi, M. H. Elnagdi, Y. A. Ibrahim, K. Kaul, and A. Kumar, *Tetrahedron*, 2001, **57**, 1609.

[29] D. Barrett, H. Sasaki, H. Tsutsumi, M. Murata, T. Terasawa, and K. Sakane, *J. Org. Chem.*, 1995, **60**, 3928.

[30] S. Patnaik, H. C. Dietz, W. Zheng, C. Austin, and J. J. Marugan, *J. Org. Chem.*, 2009, **74**, 8870.

[31] M. A.-M. Gomaa, *Tetrahedron Lett.*, 2003, **44**, 3493.

[32] R. A. Carboni and R. V. Lindsey, *J. Am. Chem. Soc.*, 1959, **81**, 4342.

[33] S. E. Armstrong and A. E. Tipping, *J. Fluorine Chem.*, 1973, **3**, 119.

[34] M. Franck-Neumann and C. Buchecker, *Tetrahedron Lett.*, 1969, **31**, 2659.

[35] J. Parrick, C. J. G. Shaw, and L. K. Mehta, in 'Supplements to the 2nd Edition of Rodd's Chemistry of Carbon Compounds Volume IV Part I', ed. M. F. Ansell, Amsterdam, 1995.

[36] K. Shen, Y. Fu, J.-N. Li, L. Liu, and Q.-X. Guo, *Tetrahedron*, 2007, **63**, 1568.

[37] T. Imahori and Y. Kondo, *J. Am. Chem. Soc.*, 2003, **125**, 8082.

[38] N. Ple, A. Turck, K. Couture, and G. Queguiner, *J. Org. Chem.*, 1995, **60**, 3781.

[39] A. Seggio, F. Chevallier, M. Vaultier, and F. Mongin, *J. Org. Chem.*, 2007, **72**, 6602.

[40] R. J. Mattson and C. P. Sloan, *J. Org. Chem.*, 1990, **55**, 3410.

[41] C. Fruit, A. Turck, N. Ple, L. Mojovic, and G. Queguiner, *Tetrahedron*, 2002, **58**, 2743.

[42] L. Mojovic, A. Turck, N. Ple, M. Dorsy, B. Ndzi, and G. Queguiner, *Tetrahedron*, 1996, **52**, 10417.

[43] A. Lepetre, A. Turck, N. Ple, and G. Queguiner, *Tetrahedron*, 2000, **56**, 3709.

[44] A. Lepetre, A. Turck, N. Ple, P. Knochel, and G. Queguiner, *Tetrahedron*, 2000, **56**, 265.

[45] D. S. Chekmarev, A. E. Stepanov, and A. N. Kasatkin, *Tetrahedron Lett.*, 2005, **46**, 1303.

[46] A. Turck, N. Ple, L. Mojovic, and G. Queguiner, *B. Soc. Chim. Fr.*, 1993, **130**, 488.

[47] D. Villemin, A. Jullien, and N. Bar, *Tetrahedron Lett.*, 2007, **48**, 4191.

[48] A. J. Goodman, S. P. Stanforth, and B. Tarbit, *Tetrahedron*, 1999, **55**, 15067.

[49] F. Trecourt, A. Turck, N. Ple, A. Paris, and G. Queguiner, *J. Heterocyclic Chem.*, 1995, **32**, 1057.

[50] B. Dajka-Halasz, K. Monsieurs, O. Elias, L. Karolyhazy, P. Tapolcsanyi, B. U. W. Maes, Z. Riedl, G. Hajos, R. A. Dommisse, G. L. F. Lemiere, J. Kosmrlj, and P. Matyus, *Tetrahedron*, 2004, **60**, 2283.

[51] Z. Yin, Z. Zhang, J. F. Kadow, N. A. Meanwell, and T. Wang, *J. Org. Chem.*, 2004, **69**, 1364.

[52] D. Giomi, M. Piacenti, and A. Brandi, *Tetrahedron Lett.*, 2004, **45**, 2113.

[53] J.-M. Pereillo, M. Maftouh, A. Andrieu, M.-F. Uzabiaga, O. Fedeli, P. Savi, M. Pascal, J.-M. Herbert, J.-P. Maffrand, and C. Picard, *Drug Metab. Dispos.*, 2002, **30**, 1288.

[54] H. Kubinyi, *J. Recept. Signal Tr.*, 1999, **19**, 15.

[55] N. Carter and P. McCormack, *CNS Drugs*, 2009, **23**, 523.

[56] G. L. Plosker, *Drugs*, 2009, **69**, 2477.

[57] J. D. Croxtall and L. J. Scott, *CNS Drugs*, 2010, **24**, 245.

[58] R. Trivedi, A. Mithal, and N. Chattopadhyay, *Curr. Mol. Med.*, 2010, **10**, 14.

[59] E. Perzborn, S. Roehrig, A. Straub, D. Kubitza, W. Mueck, and V. Laux, *Arterioscl. Throm. Vas. Biol.*, 2010, **30**, 376.

[60] H. A. M. Mucke, *Clin. Med.: Therapeutics*, 2009, **1**, 111.

[61] J. Scholz, M. Steinfath, and M. Schulz, *Clin. Pharmacokinet.*, 1996, **31**, 275.

[62] B. L. Riggs and L. C. Hartmann, *New Engl. J. Med.*, 2003, **348**, 618.

[63] A. D. Palkowitz, A. L. Glasebrook, K. J. Thrasher, K. L. Hauser, L. L. Short, D. L. Phillips, B. S. Muehl, M. Sato, P. K. Shetler, G. J. Cullinan, T. R. Pell, and H. U. Bryant, *J. Med. Chem.*, 1997, **40**, 1407.

[64] E. D. Mattia and G. Toffoli, *Eur. J. Cancer*, 2009, **45**, 1333.

[65] F. M. Moghaddam and H. Zali-Boinee, *Tetrahedron Lett.*, 2003, **44**, 6253.

[66] G. Sommen, A. Comel, and G. Kirsch, *Tetrahedron*, 2003, **59**, 1557.

[67] R. Engqvist, A. Javaid, and J. Bergman, *European J. Org. Chem.*, 2004, 2589.

[68] J. Nakayama, H. Machida, R. Saito, and M. Hoshino, *Tetrahedron Lett.*, 1985, **26**, 1983.

[69] J. Nakayama, H. Machida, and M. Hoshino, *Tetrahedron Lett.*, 1985, **26**, 1981.

[70] B. P. McKibben, C. H. Cartwright, and A. L. Castelhano, *Tetrahedron Lett.*, 1999, **40**, 5471.

[71] D. Hawksley, D. A. Griffin, and F. J. Leeper, *J. Chem. Soc., Perk. T. 1*, 2001, 144.

[72] A. A. Kiryanov, P. Sampson, and A. J. Seed, *J. Org. Chem.*, 2001, **66**, 7925.

[73] Z. Kaleta, B. T. Makowski, T. Soos, and R. Dembinski, *Org. Lett.*, 2006, **8**, 1625.

[74] N. Agarwal, C.-H. Hung, and M. Ravikanth, *Tetrahedron*, 2004, **60**, 10671.

[75] Y. Kamitori, M. Hojo, R. Masuda, T. Izumi, and S. Tsukamoto, *J. Org. Chem.*, 1984, **49**, 4161.

[76] A. K. Mohanakrishnan, A. Hucke, M. A. Lyon, M. V. Lakshmikantham, and M. P. Cava, *Tetrahedron*, 1999, **55**, 11745.

[77] J. Halfpenny, P. B. Rooney, and Z. S. Sloman, *J. Chem. Soc., Perk. T. 1*, 2001, 2595.

[78] M. M. M. Raposo, A. M. R. C. Sousa, A. M. C. Fonseca, and G. Kirsch, *Tetrahedron*, 2006, **62**, 3493.
[79] M. Yamashita, M. Oda, K. Hayashi, I. Kawasaki, and S. Ohta, *Heterocycles*, 1998, **48**, 2543.
[80] C. Gozzi, L. Lavenot, K. Ilg, V. Penalva, and M. Lemaire, *Tetrahedron Lett.*, 1997, **38**, 8867.
[81] J. F. D. Chabert, C. Gozzi, and M. Lemaire, *Tetrahedron Lett.*, 2002, **43**, 1829.
[82] A. O. King, E.-I. Negishi, F. J. Villani, and A. Silveira, *J. Org. Chem.*, 1978, **43**, 358.
[83] K. Tamao, K. Nakamura, H. Ishii, S. Yamaguchi, and M. Shiro, *J. Am. Chem. Soc.*, 1996, **118**, 12469.
[84] J. C. Bussolari and D. C. Rehborn, *Org. Lett.*, 1999, **1**, 965.
[85] A. A. Kiryanov, A. J. Seed, and P. Sampson, *Tetrahedron Lett.*, 2001, **42**, 8797.
[86] R. Pereira, B. Iglesias, and A. R. d. Lera, *Tetrahedron*, 2001, **57**, 7871.
[87] V. Farina and G. P. Roth, *Tetrahedron Lett.*, 1991, **32**, 4243.
[88] A. F. Littke and G. C. Fu, *Angew. Chem., Int. Ed. Engl.*, 1999, **38**, 2411.
[89] J. O. Karlsson, S. Gronowitz, and T. Frejd, *J. Org. Chem.*, 1982, **47**, 374.
[90] L. Antolini, F. Goldoni, D. Iarossi, A. Mucci, and L. Schenetti, *J. Chem. Soc., Perk. T. 1*, 1997, 1957.
[91] A. Minato, K. Tamao, T. Hayashi, K. Suzuki, and M. Kumada, *Tetrahedron Lett.*, 1980, **21**, 845.
[92] S. Gronowitz and D. Peters, *Heterocycles*, 1990, **30**, 645.
[93] G. Consiglio, D. Spinelli, S. Gronowitz, A.-B. Hornfeldt, B. Maltesson, and R. Noto, *J. Chem. Soc., Perk. T. 2*, 1982, 625.
[94] A. Peters, C. Vitols, R. McDonald, and N. R. Branda, *Org. Lett.*, 2003, **5**, 1183.

Chapter 2

Nucleophilic Aromatic Substitution Reactions of Polyfluoropyridazines

2.1 Background

The aim of this thesis is to describe advances that have been made concerning the synthesis of new and diversely substituted heterocycles, namely pyridazine and thiophene. The bulk of the following work concerns transformations performed using tetrafluoropyridazine as a starting material.

As discussed in chapter 1, functionalised pyridazines are potentially valuable molecules possessing a range of desirable pharmaceutical properties. Routes towards these targets are numerous, including various ring-closing procedures, such as cycloadditions or condensations of dicarbonyls, and functionalisations of the parent heterocycle by such means as transition metal mediated reactions, metallations, and nucleophilic substitutions.

Our approach was to utilise the chemistry of perhalogenated heterocycles to allow us to produce a diverse range of desirable polyfunctional pyridazine and thiophene molecules. For our explorations of the reactions of pyridazine, we used the perfluorinated derivative as our starting material, the choice of which requires some explanation.

The chemistry of fluorocarbon systems differs notably from that of hydrocarbon systems due to the disparity in electronic properties between hydrogen and fluorine. While the C-H bond in aromatic systems is relatively non-polar, the extreme electronegativity of fluorine causes polarisation of the C-F bond, leading, in the case of polyfluorinated aromatic systems, to electron deficient rings susceptible to nucleophilic, rather than the more usual electrophilic, attack. Additionally, fluorine is able to act as a leaving group, as F^-, while hydrogen tends to be abstracted as H^+.[1]

For these reasons, perfluorinated aromatic systems exhibit reactivity that may be viewed as complementary to that of their hydrocarbon counterparts. While the chemistry of benzene is dominated by electrophilic aromatic substitution, proceeding via a Wheland intermediate, the reactions of hexafluorobenzene are predominantly nucleophilic aromatic substitution processes, which pass through a conceptually similar Meisenheimer intermediate, for the reasons outlined above (Scheme 2.1).[2, 3] This dichotomy leads some to describe the reactions of perfluorinated species as 'mirror image' chemistry with respect to the more familiar hydrocarbon behaviour.

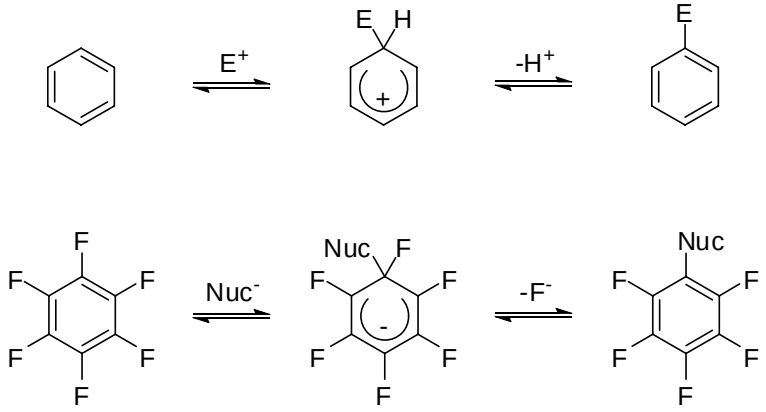

Scheme 2.1

This same reactivity holds true for perfluorinated heterocyclic compounds, and the insertion of electronegative nitrogen atoms into the ring system serves to activate the remaining ring carbon atoms, further facilitating substitution. Pentafluoropyridine has previously been used as a scaffold for drug discovery purposes, and a few words about its use as such appear appropriate here.

The first thing that becomes obvious when examining the nucleophilic aromatic substitution chemistry of pentafluoropyridine as opposed to hexafluorobenzene is that the molecule has become less symmetrical; six identical potential sites of attack have given

way to five sites, one of which is unique, and four of which are paired into two symmetrical domains. This situation leads in effect to three possible sites of attack, namely *ortho*-, *meta*-, and *para*- to ring nitrogen. Experimentally, nucleophilic substitution reactions of pentafluoropyridine generally proceed with replacement of the fluorine atom at the 4-position, giving 2,3,5,6-tetrafluorinated systems as products (Scheme 2.2).[4]

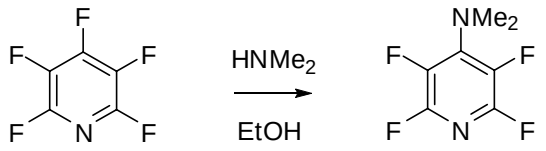

Scheme 2.2

To understand the regioselectivity of the reaction, it is necessary to examine the intermediates resultant from the potential sites of reaction (Scheme 2.3).

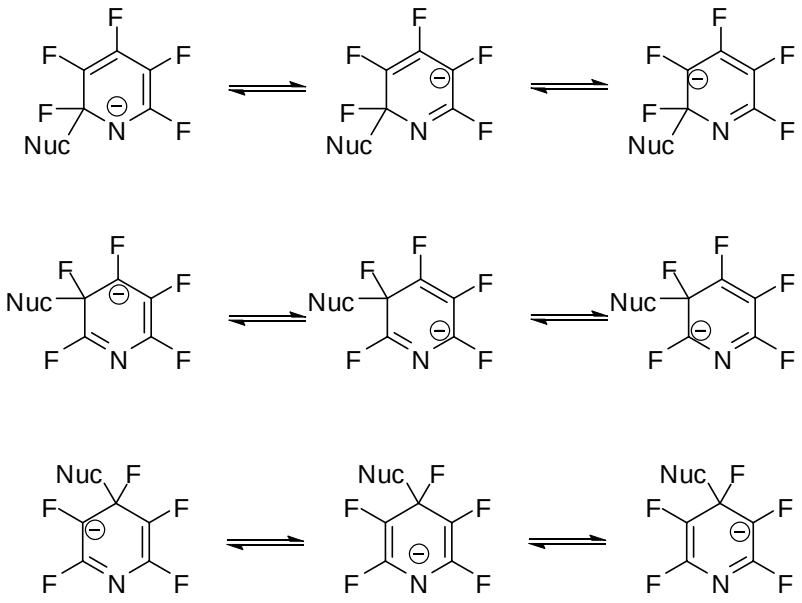

Scheme 2.3

It can be observed that in the case of nucleophilic attack *meta*- to the ring nitrogen, the negative charge is delocalised over three carbon atoms, each bearing a fluorine atom, while attack *ortho*- or *para*- to ring nitrogen allows one third of the resonance canonicals to involve delocalisation onto nitrogen. It is known that delocalisation onto electronegative nitrogen is preferable to delocalisation onto an sp^2 hybridised CF centre, as the latter case leads to unfavourable interactions between the charge and the lone pairs on fluorine, and as such *meta*- substitution should be disfavoured. This turns out to be the case, and pentafluoropyridine may be employed as an electrophile undergoing substitution at the 2-, 4-, and 6- positions.

This reactivity was exploited to allow the synthesis of a range of compounds showing potential as antithrombotic agents.[5] A representative synthesis is shown below (Scheme 2.4).

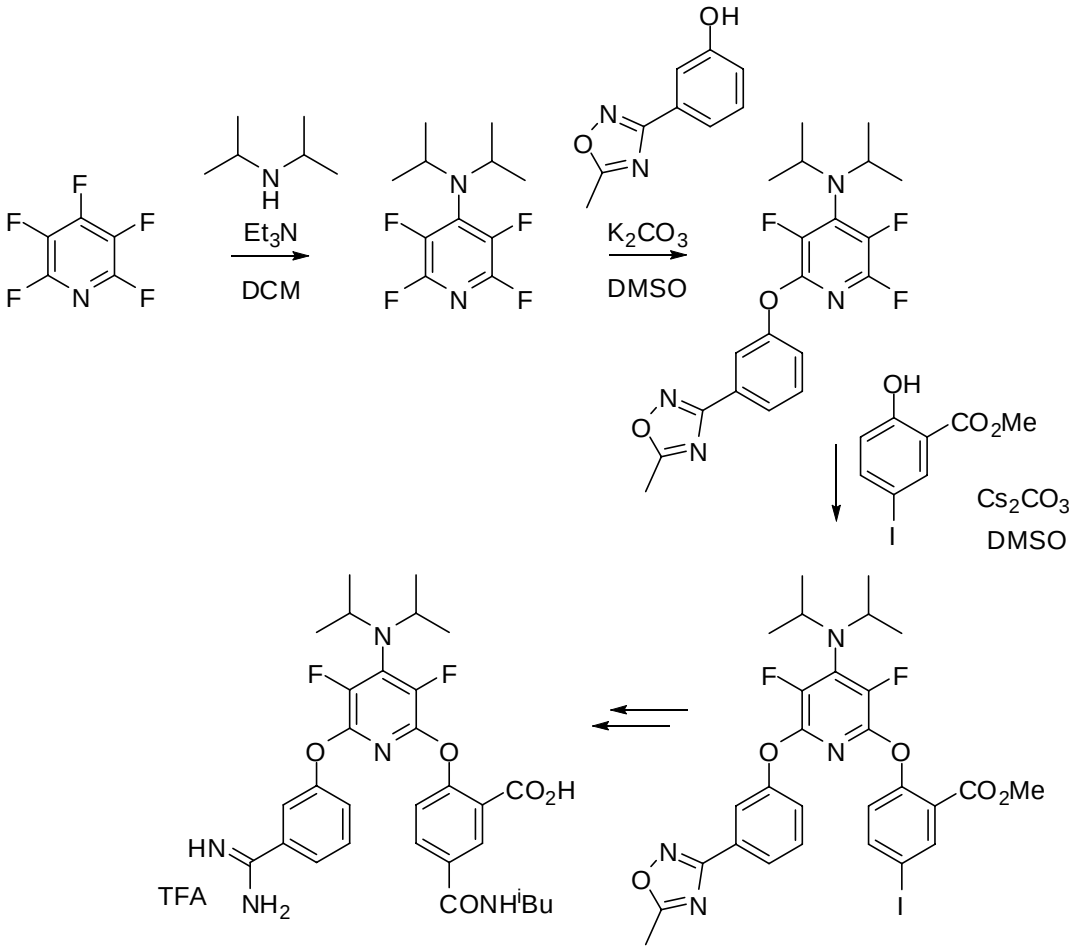

Scheme 2.4

Several similar syntheses utilising reactions of highly fluorinated pyridine scaffolds have been published by the Durham group, and it has been demonstrated that sequential reaction with a variety of nucleophiles produces novel compounds with good to excellent levels of regiocontrol, potentially making these processes suitable for use in diversity-oriented parallel synthesis targeted towards the discovery of new pharmaceutical agents.[6-8]

In light of this precedent, we have turned to investigating the merits of employing a similar approach to the diversification of other perhalogenated heterocyclic cores, and the following chapters will be concerned with our findings regarding the reactions of

tetrafluoropyridazine; consequently, a brief review of the chemistry of tetrafluoropyridazine follows.

Previous studies of the reactions of tetrafluoropyridazine have been limited and, as would be expected, have been in the main confined to its behaviour towards nucleophiles. The few nucleophilic species explored thus far have shown differing degrees of reactivity and regioselectivity.

Simple amines appear to be most easily controlled, with ammonia giving the 4-substituted product in good yield, while the more reactive potassium phthalimide gave a poor yield of the 4,5-disubstituted derivative.[9] Similarly, sodium thiophenoxide was found to be unsuitable for the purposes of selective substitution, with a single equivalent giving disubstitution, and three equivalents giving a mixture of di-, tri-, and tetra-substituted products.

Versatile routes to the synthesis of methyl ethers have been described, with the addition of successive equivalents of sodium methoxide leading sequentially to 4-, 4,5-, 4,5,6- and tetra-methoxy derivatives, while treatment of tetrafluoropyridazine with methanol and sulfuric acid gives substitution at the 3-position (Scheme 2.5).[10]

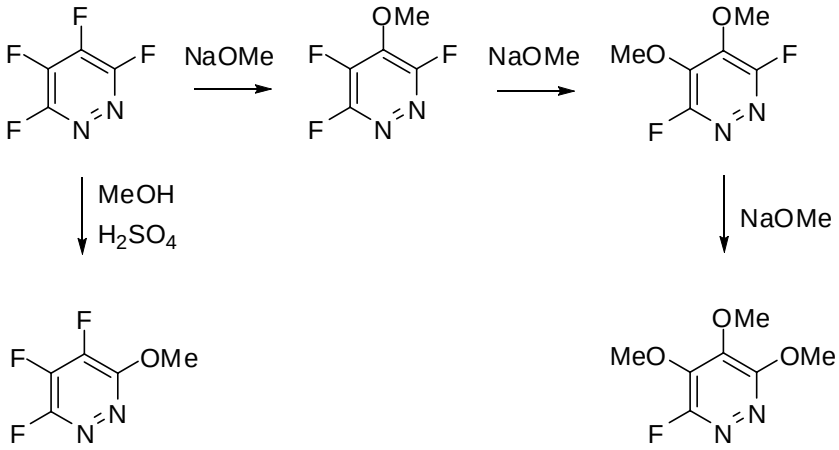

Scheme 2.5

Reaction with sulfuric acid in water leads to pyridazinone, while the action of hydrochloric acid converts tetrafluoropyridazine to the tetrachloro equivalent from which it is usually synthesised (Scheme 2.6).

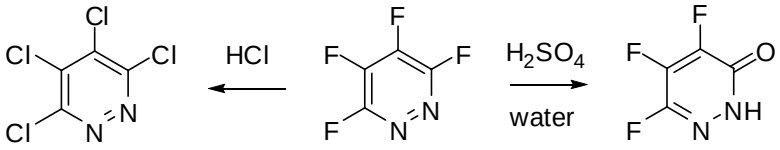

Scheme 2.6

Trifluoropyridazinone has been utilised as a potential scaffold for sequential nucleophilic aromatic substitution processes, with disubstituted products formed in variable selectivities and yields (Scheme 2.7).[11]

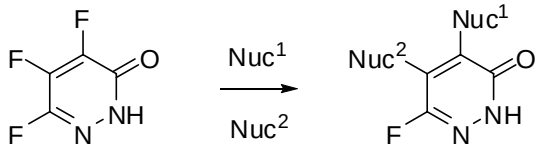

Scheme 2.7

Finally, a number of papers have described the reactions of tetrafluoropyridazine with various perfluorinated nucleophiles which, although of some interest due to their unusual electronic and steric properties, are of little importance in the pursuit of drug-like compounds.[12-15]

As can be seen, prior work has confirmed the suitability of the heterocycle as an electrophile, but fallen short of giving a picture of the degree of suitability for polyfunctionalisation by a series of selective, clean, and high yielding nucleophilic substitutions. What may be ascertained with certainty is that tetrafluoropyridazine readily undergoes substitution with a number of nucleophiles, and, at least in certain cases, shows a degree of regioselectivity. We chose to extend the known chemistry of this species in the hope that selective and clean routes could be found to exciting new chemical entities.

2.2 Aims and Approach

Given that previous studies had shown a bias towards reaction at the 4- and 5-positions, it was hoped that at least certain nucleophiles or conditions would lead to clean reaction at a single site. If this could be achieved, further selective reactions were desired, relying upon the properties imparted by existing substituents to guide subsequent reactions. It was envisaged that understanding the interplay between the electronic and steric properties of the electrophilic substrate and the incoming nucleophile could give ready access to a powerful methodology for the synthesis of a wide range of variously substituted heterocycles, as outlined in the following scheme (Scheme 2.8).

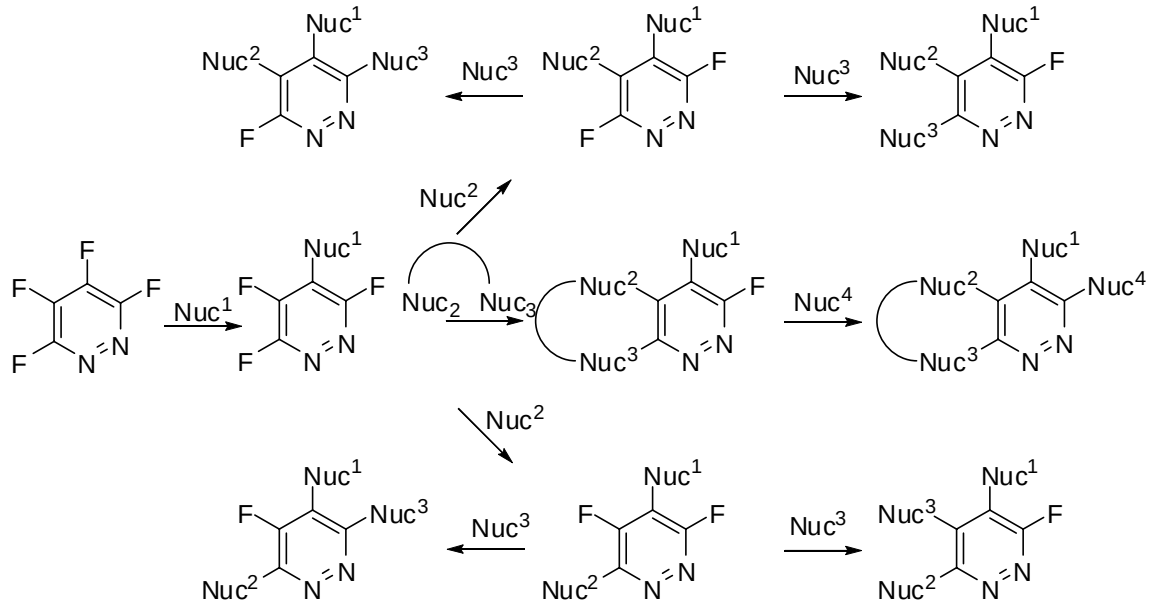

Scheme 2.8

2.3 Nucleophilic Aromatic Substitution Reactions of Tetrafluoropyridazine

Our first desire was to ascertain the applicability of the substitution reactions, so to this end, we decided to carry out a number of reactions between tetrafluoropyridazine and a variety of nucleophiles, hoping to observe clean, selective monosubstitutions and assess the scope of reactions of this species. To aid comparison, all reactions were carried out in the same solvent, and using a non-nucleophilic tertiary amine as base to neutralize the hydrofluoric acid liberated during the process of substitution. Reactions were performed between equimolar quantities of electrophile and nucleophile, and carried out at relatively low temperatures where feasible.

Nucleophilic species employed included amines, alcohols, thiols, and selected carbon nucleophiles, and the results of these experiments are outlined in the following sections. A range of steric and electronic properties was desired among the nucleophilic coupling partners, to allow observation of trends in reactivities and regioselectivities, to see if a

variety of reactants would be tolerated, and assess the suitability of this scaffold for parallel synthesis.

2.3.1 Reactions with Amines

Reactions of tetrafluoropyridazine with morpholine, diethylamine, N-methylallylamine, and aniline gave regioselective monosubstitution products in good yield upon stirring with DIPEA in THF for a few hours at 0 °C (Table 2.1). The products **1**, **2**, **3** and **4** were isolated and purified by means of column chromatography.

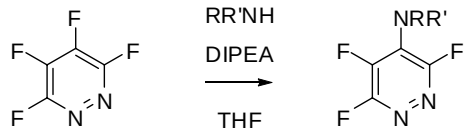

RR'NH	Product	^{o} C	Yield (%)
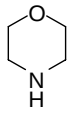	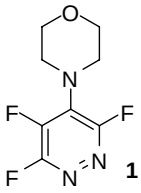 **1**	0	81
	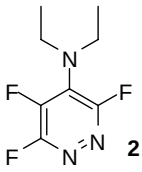 **2**	0	82
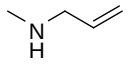	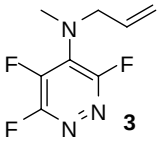 **3**	0	82
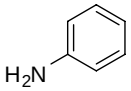	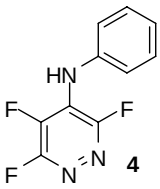 **4**	0	78
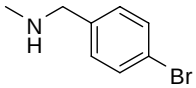	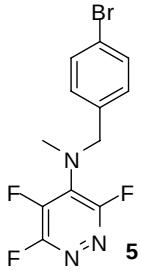 **5**	25[a]	65
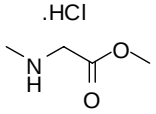	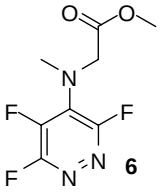 **6**	25[b]	50

[a] Reaction run overnight
[b] Reaction run for three days

Table 2.1

The orientation of substitution was determined by analysis of the NMR spectra obtained, a brief discussion of which will follow.

Proton NMR spectroscopy, as would be expected, gives little information about regiochemistry in these examples, as the hydrogen atoms in the molecules occupy sites on the nucleophile rather than around the ring.

A more useful structural probe is fluorine NMR spectroscopy, which may be analysed at various depths to interrogate the molecule. Tetrafluoropyridazine displays two signals, at -91 and -145 ppm relative to chlorotrifluoromethane in deuterated chloroform.[10] The more deshielded signal, at -91 ppm, corresponds to the fluorine atoms at the 3- and 6-positions, *ortho*- to ring nitrogen, while the less deshielded signal, at -145 ppm, corresponds to the remaining two fluorines, situated further from the electronegative nitrogen atoms.

A simple approach to structure confirmation consists of qualitative comparison between the spectrum of tetrafluoropyridazine and that of the entity in question. As an example, the product of reaction between tetrafluoropyridazine and diethylamine shows signals at -81, -101, and -147 ppm. Two of these shifts are close to the figure of -91 observed for fluorines adjacent to ring nitrogen in tetrafluoropyridazine, while only one is similar to the value of -145 seen for the fluorines in the 4- and 5-positions. This immediately suggests that substitution has taken place at the position *para*- to ring nitrogen.

A more rigorous approach involves consideration of the influence of substituents on nearby shifts to rationalise the spectrum. A simple example was alluded to earlier, while mentioning the deshielding effects of electronegative nitrogen on adjacent nuclei. It is obvious in the case of a perfluorinated system that replacing a fluorine atom with a different substituent will alter the resonance frequencies of the remaining fluorines to a greater or lesser extent. The degree of change for a few representative substituents seen in the context of pentafluorobenzene is illustrated below (Table 2.2).[16]

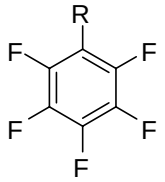

R	F-2/F-6	F-3/F-5	F-4
F	-162.9	-162.9	-162.9
H	-139.2	-162.7	-154.5
CH_3	-144.1	-164.4	-159.7
NH_2	-162.9	-165.5	-173.9
OH	-164.1	-164.3	-169.2
OCH_3	-158.4	-164.8	-164.8

Table 2.2

These values can be used to determine the shift differences that a given substituent causes at the *ortho*-, *meta*-, and *para*-positions. These substituent chemical shift (scs) differences are tabulated below (Table 2.3).

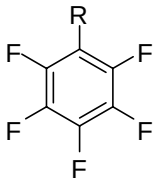

R	ortho	meta	para
H	+23.7	+0.2	+8.4
CH_3	+18.8	-1.5	+3.2
NH_2	0	-2.6	-11
OH	-1.2	-1.4	-6.3
OCH_3	+4.5	-1.9	-1.9

Table 2.3

It is possible to use these values to predict the NMR spectra of other compounds; for example, pentafluoroethylbenzene would be expected to have a very similar fluorine spectrum to pentafluoromethylbenzene. A slightly more profound use would be the combination of chemical shift differences to predict the spectra of disubstituted tetrafluorobenzenes in an additive fashion. For our purposes, it is necessary to apply these ideas to non-benzenoid species. A convenient stepping stone is the NMR behaviour of polyfluorinated pyridines, which has been studied in some depth.

The observed shifts of a number of substituted tetrafluoropyridines are shown below (Table 2.4). Of note is the fact that there are now two parameters changing – the relative position of the substituent with respect to the fluorine in question, and the position of the substituent on the pyridine ring.

Compound		F-2	F-3	F-4	F-5	F-6
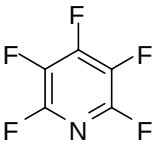	R	-87.6	-162.0	-134.1	-162.0	-87.6
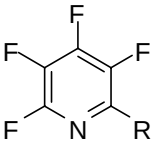	OCH_3	-	-164.5	-140.9	-171.9	-91.4
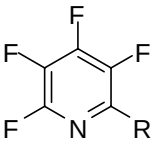	OH	-	-164.7	-141.3	-173.6	-91.6
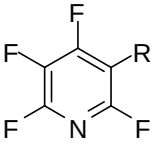	OH	-88.2	-	-133.8	-164.8	-96.6
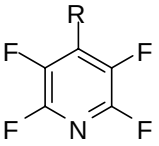	NH_2	-95.0	-165.0	-	-165.0	-95.0
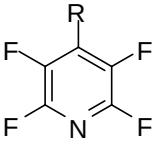	OH	-95.5	-164.6	-	-164.6	-95.5
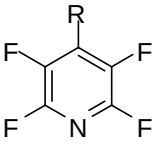	OCH_3	-92.9	-161.7	-	-161.7	-92.9

Table 2.4

With the shifts for each isomer of tetrafluorohydroxypyridine tabulated, it is possible to discern its effects on the fluorine nuclei from each position. When averaged, the chemical shift differences for the hydroxy substituent in pyridine are -1.1 to *ortho*- fluorines, -5.5 to

meta- fluorines, and -10.3 to *para*- fluorines. These values compare moderately well with the values observed in the fluorobenzene case, suggesting some commonality over different ring systems. Furthermore, despite limited data, amino- and methoxy- substituents demonstrate the same trends as seen in benzenoid examples.

It is now possible to apply these principles to our diethylamino substituted pyridazine. The *ortho*-, *meta*-, and *para*- shift differences elicited by the similar dimethylamino substituent in benzene have been reported as +9.69, -0.75, and -0.97 respectively.[17] By combining these values with the known shifts of tetrafluoropyridazine, as discussed above, it is possible to predict the expected spectra for both of the possible substitution products, which are as follows (Figure 2.1).

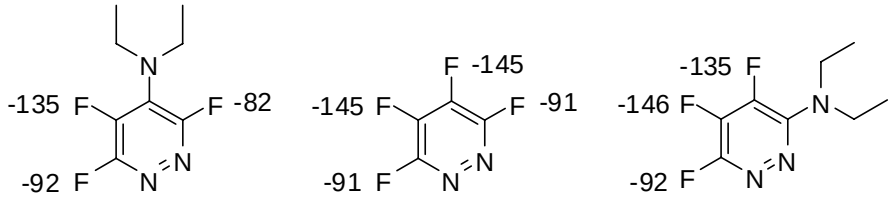

Figure 2.1

Clearly, the values predicted by the situation on the left hand side are considerably closer to the experimental values of -81, -110, and -147 ppm than those predicted by the alternative substitution, and also provide a distinction between the two more deshielded environments, something that was lacking in the previous crude analysis. Theoretical values are improved further by the use of chemical shift differences calculated for the diethylamino substituent on polyfluoropyridine,[18] which predicts the fluorine shifts in the 4-substituted isomer to be -87, -100, and -140 ppm. A similar approach was taken for the other products of reaction between tetrafluoropyridazine and amines, and all products were identified as being the result of substitution at the 4-position.

With the identity of the product confirmed, the necessity to explain the observed regioselectivity remains. This may be achieved by the same means used to rationalise the selectivity observed in reactions with pentafluoropyridine, with a few refinements. The addition of a second ring nitrogen reduces the number of possible sites of attack to two, each having a symmetrically identical counterpart. The two possible Meisenheimer intermediates are shown below (Scheme 2.9).

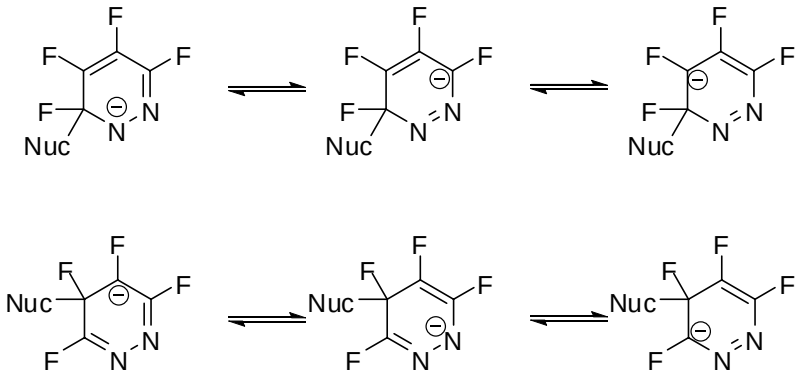

Scheme 2.9

It is immediately obvious that, unlike in the case of substitution in pentafluoropyridine, the two sets of resonance canonical forms are statistically the same, in that both contain one structure bearing the negative charge on ring nitrogen, and two structures bearing negative charges on fluorinated carbon. A further factor is required to account for the observed selectivity.

It has long been suggested that the three canonical forms involved in the intermediate are not of equal importance, as indicated by the preponderance of substitution *para*- rather than *ortho*- to the substituent in pentafluorobenzenes.[19] LCAO MO calculations performed to investigate the behaviour of aromatic systems undergoing reduction also imply that the charge density in the Meisenheimer intermediate will be greatest at the atom opposite the tetrahedral carbon, as shown below (Figure 2.2).[20]

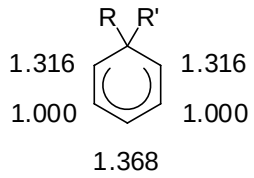

Figure 2.2

With this borne in mind, the observed selectivity of the reaction may be rationalised by considering that the negative charge present in the intermediate is better localised on the electronegative nitrogen atom, which is flanked by a further electronegative heteroatom and a sigma withdrawing C-F group, than on a carbon atom where it will be destabilised by unfavourable interactions with the non-bonding lone pairs on fluorine.

While the reactions of these first simple amines with tetrafluoropyridazine were complete within a matter of hours at 0 °C, giving good yields, a couple of other amines gave less satisfactory results. 1-(4-Bromophenyl)-N-methylmethanamine required stirring at room temperature overnight, due to its increased steric demand, while methyl 2-(methylamino)acetate, even after stirring at room temperature for several days, gave a disappointingly low yield of **6**. Part of this may be attributed to the poor solubility of the nucleophile in the reaction mixture.

Overall, it seems that the reactions of amines with tetrafluoropyridazine proceed with high regioselectivity in moderate to good yield, a promising first step towards selective polyfunctionalisation.

2.3.2 Reactions with Alcohols

After seeing encouraging results for the reactions of amines with tetrafluoropyridazine, we moved on to investigate the reactions of a selection of alcohols, a summary of which is shown below (Table 2.5).

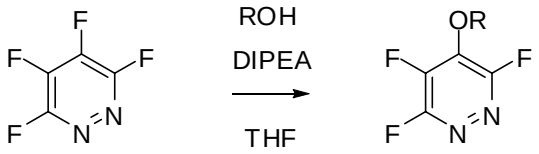

ROH	Product	T	Yield (%)
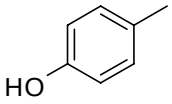	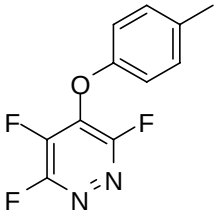 **7**	RT	61
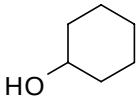	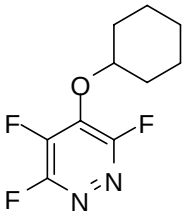 **8**	RT[a]	63
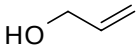	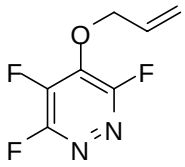 **9**	reflux	73
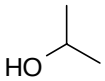	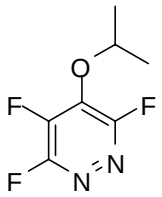 **10**	reflux	72

[a] Reaction run for six days

Table 2.5

The first example tested was *para*-cresol, which reacted fairly rapidly at room temperature to give the corresponding 4-substituted product **7**. The regioselectivity of the reaction was again confirmed by substituent chemical shift calculations. The separation of the product from traces of disubstituted material was not achieved using simple column chromatography, and HPLC was required to obtain analytically pure material.

The use of aliphatic alcohols resulted in a considerably reduced rate of reaction. This is probably best rationalised by comparing the acidities of the nucleophiles in question, which suggest that the aromatic alcohol is more likely to be deprotonated, and able to attack as a relatively reactive negatively charged species.

After the observation of the considerably increased reaction times necessary when using aliphatic alcohols, subsequent reactions with alcohols were performed at elevated temperature, allowing reactions to reach completion in good yield within a far more useful timescale. The regiochemistries of the reaction products were confirmed using NMR spectroscopy procedures as described above.

Once again, reactions of tetrafluoropyridazine with nucleophiles, in this case alcohols, have been shown to be high yielding and able to proceed with good regioselectivity.

2.3.3 Reactions with Carbon Nucleophiles

With successful substitution reactions involving nitrogen- and oxygen-centred nucleophiles in hand, we began to investigate reactions of tetrafluoropyridazine with a number of carbon nucleophiles. Firstly, in contrast to the nucleophiles already employed, phenylmagnesium bromide failed to give a clean and selective monosubstitution. Although the major product of the reaction was again monosubstitution at the 4- position, analysis of the reaction mixture by ^{19}F NMR spectroscopy also showed the presence of the 3-substituted product, along with traces of a disubstituted product (Scheme 2.10). The reaction of

phenylmagnesium bromide with a slight excess of tetrafluoropyridazine leads to 4-substitution, 3-substition, and a disubstituted isomer in an approximately 32:6:1 ratio by ^{19}F NMR spectral analysis of the reaction mixture. Increased quantities of nucleophile, while improving conversion, serve to bring about ever greater quantities of disubstituted material, whose removal by recrystallisation dramatically lowers the isolable yield of monosubstituted product.

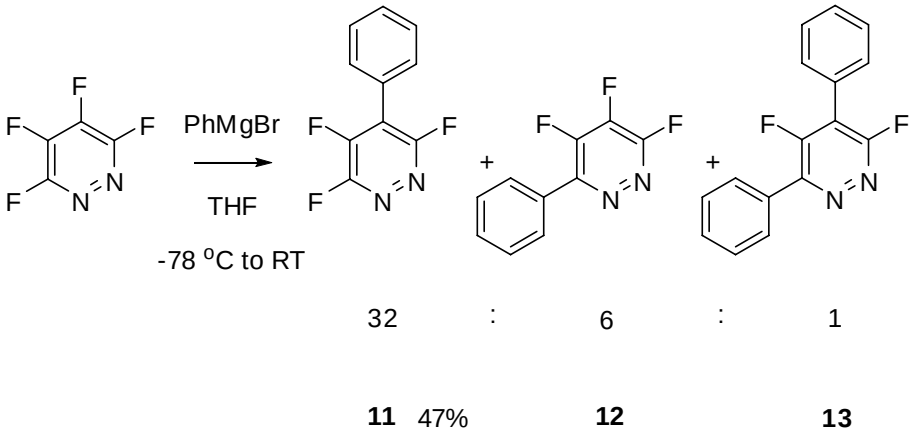

Scheme 2.10

The reason for this loss of selectivity may once again be explained by examination of the mechanism of reaction. As already outlined, nucleophilic substitution processes such as these proceed via a reactive intermediate, which then loses fluoride to give the final product. The substitution reaction can therefore be seen as a two-step reaction, the first step of which is rate determining, and dictates the regioselectivity of the reaction. Thus far, we have assumed that the regioselectivity is determined purely by the relative stabilities of the various intermediates possible, and this has, in all cases up to this point, been entirely in favour of substitution *para-* to ring nitrogen. Other factors, however, have been disregarded, the most relevant here being the initial electronic charge densities.

The free energy profile of the nucleophilic substitution reaction is represented schematically below (Figure 2.3), and shows the relative free energies of the starting

material, product, and the intermediate. It can be seen that upon forming the intermediate, the regioselectivity is already determined, and one can imagine a similar free energy profile for the reaction resulting in substitution *ortho*- to the ring nitrogen. The intermediate is higher in energy than the starting material, and as such we assume a late transition state for the first step of the reaction. With that in mind, we can describe the transition state as being similar to the intermediate, or at least more similar to the intermediate than to the starting material. This bears out our assertion that regioselectivity should be predictable by considering the various reactive intermediates possible and recognising which electronic configurations are most stabilised by the molecular structure of the ring.

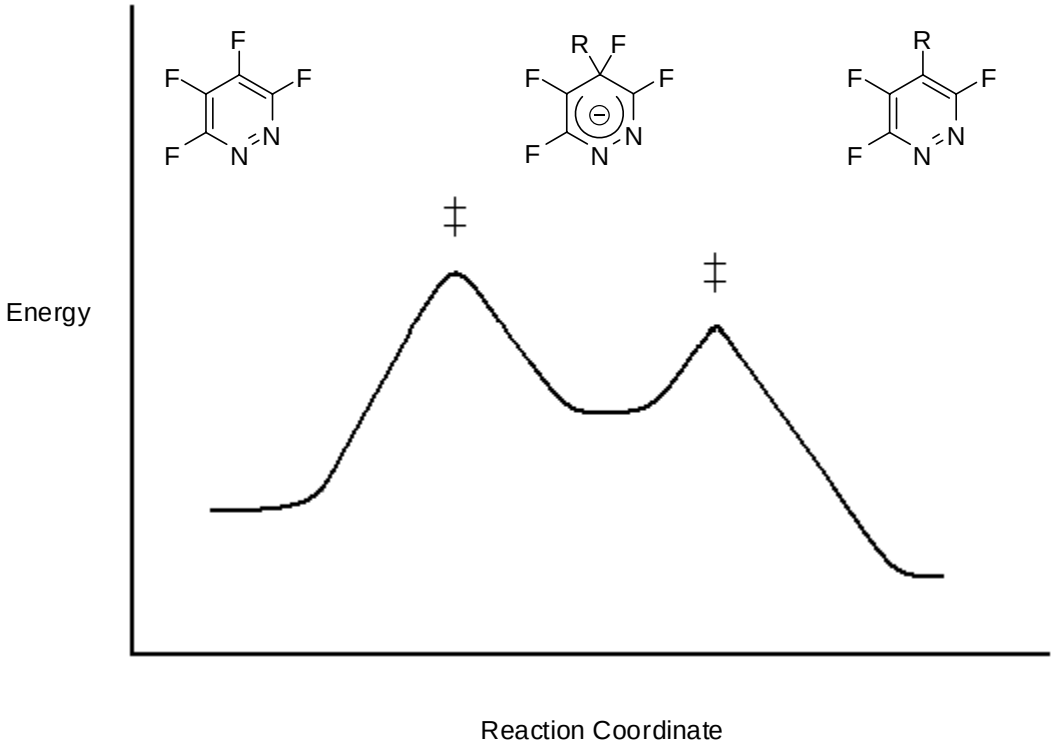

Figure 2.3

While this method has thus far adequately explained our findings, with the move to carbon nucleophiles we have observed products resulting from a competing pathway. This can be understood to be a result of the use of a far more reactive nucleophile than has been

employed up until this stage. While in former cases the transition state could be assumed to be late, with increasingly energetic starting materials the transition state will become earlier, and as such more like the starting material, so that regioselectivity is determined less by stabilising factors present in the intermediate, and more by factors present in the starting material, namely the electrophilicity of the various ring carbon atoms. These two considerations work in opposite directions for this reaction, with attack at the 3-position favoured by an early transition state, and attack at the 4-position favoured by a late transition state. As we increase the reactivity of the starting materials, we would expect to see an increase in 3-substitution, which is indeed observed.

The next carbon nucleophile to be employed was methylmagnesium bromide, which we expected to behave similarly to phenylmagnesium bromide, with possibly a slightly greater ratio of 3- to 4-substitution, due to the marginally higher instability of methyl, as opposed to phenyl carbanions. In fact, it was found that the reaction of tetrafluoropyridazine with methylmagnesium bromide leads to a complex mixture of products, consisting largely of intractable, tarry material. The marked contrast between this reaction and the relatively well behaved reaction with phenylmagnesium bromide is due to the presence, or absence, of an acidic proton in the initial product, which may be abstracted under the highly basic reaction conditions, leading to further nucleophilic substitution processes (Scheme 2.11).

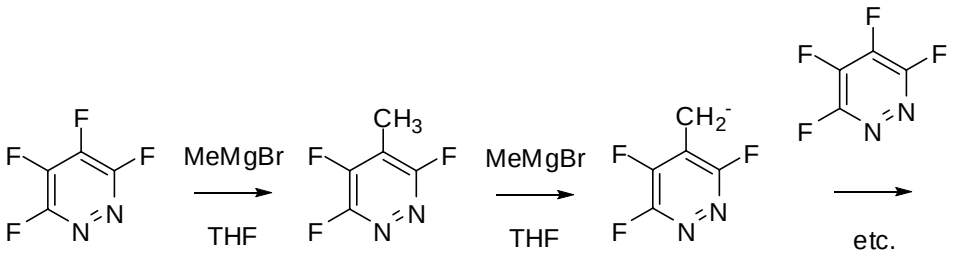

Scheme 2.11

Having established the unsuitability of strongly basic alkyl nucleophiles for use in the first functionalisation of tetrafluoropyridazine, we examined the use of a rather milder carbon

nucleophile. Ethyl acetoacetate may be deprotonated under fairly mild conditions, and as such we could avoid the harsh basic media inevitable during reactions with Grignard reagents. Initial experiments with ethyl acetoacetate, using a single equivalent of base, led to a mixture of fused compounds (Scheme 2.12), rather than the monosubstituted product that might have been expected. This would again appear to be due to the enhanced acidity of a proton alpha- to the fluorinated pyridazine ring system. While the methylene protons borne by the acetoacetate moiety are reasonably acidic, the remaining proton in that position subsequent to initial substitution is even more so, suggesting that ring closing reactions should start to occur even before complete consumption of starting material.

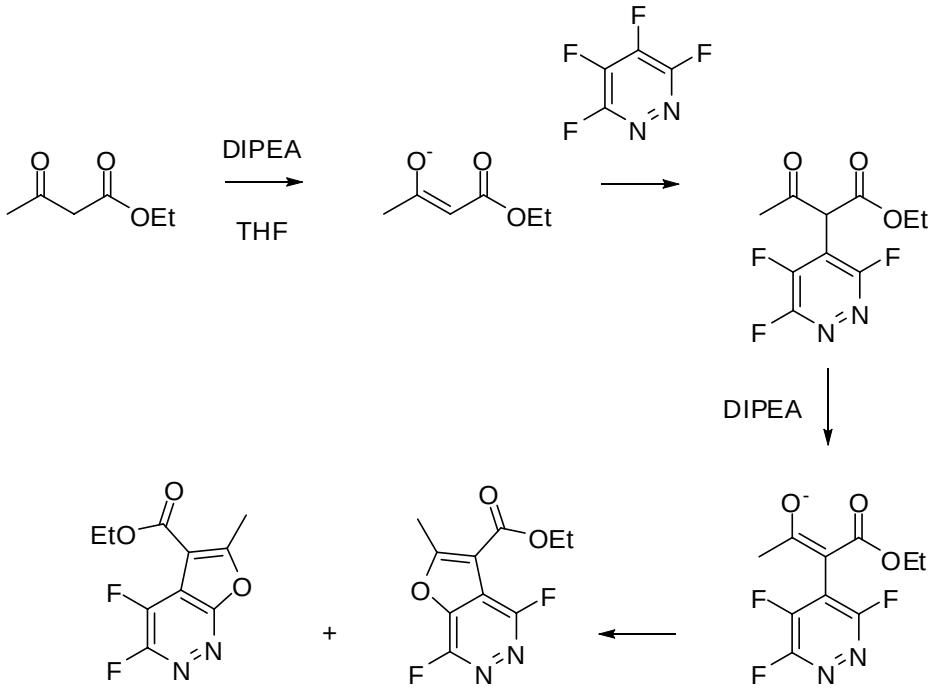

Scheme 2.12

Evidently, if using one equivalent each of base and nucleophile, all base will have been consumed by the time the reaction is halfway towards complete disubstitution. Beyond this point, base induced cyclisation is no longer driving the reaction, and substitution becomes promoted by the HF formed during conversion (Scheme 2.13).

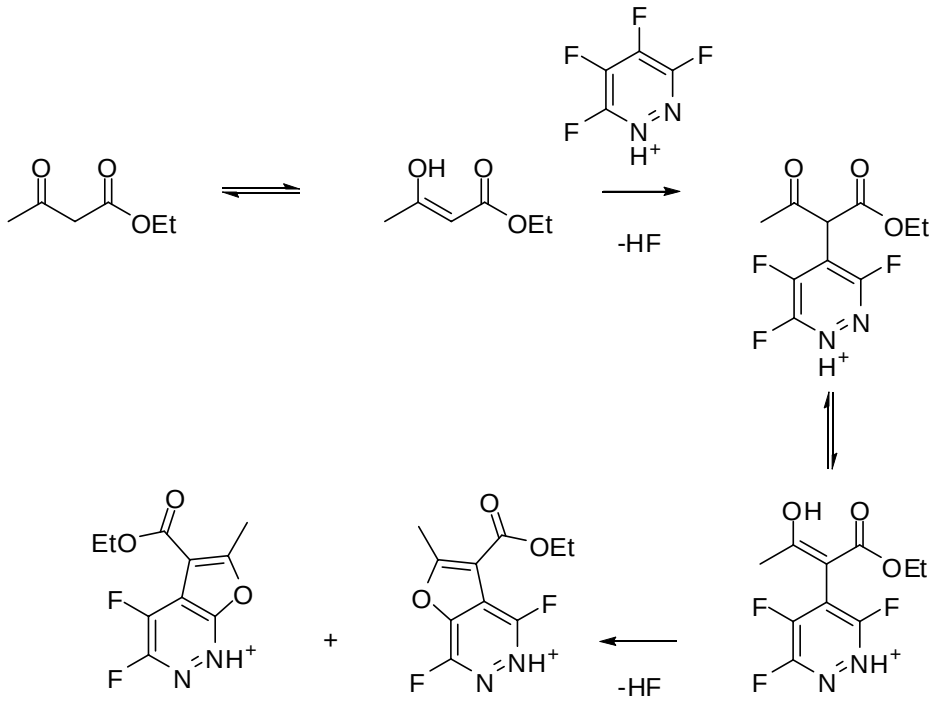

Scheme 2.13

Although reactions were performed in dry THF, this autocatalytic production of hydrofluoric acid was undesirable, not least because the presence of acid during and after aqueous work-up led to hydrolysis of the product, leading to further liberation of acid. Subsequently, reactions between tetrafluoropyridazine and ethyl acetoacetate were performed in the presence of an excess of base, leading not only to the cessation of the generation of hydrofluoric acid, but also noticeably cleaner reactions, with only one isomer of the ring fused system isolated (Scheme 2.14).

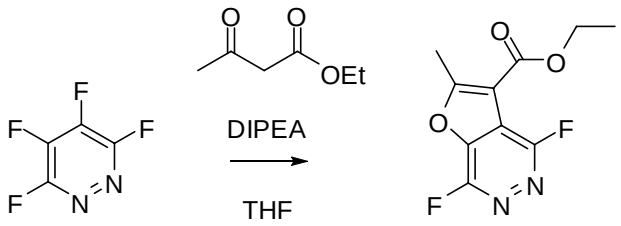

14 40%

Scheme 2.14

As far as confirmation of regiochemistry is concerned, it will be noticed that only two of four possible regioisomers are shown in the preceding two diagrams, both resulting from cyclisation through the ketone, rather than carboxyl, oxygen atom. Theoretically, four regioisomers are possible, and their structures are shown below (Figure 2.4).

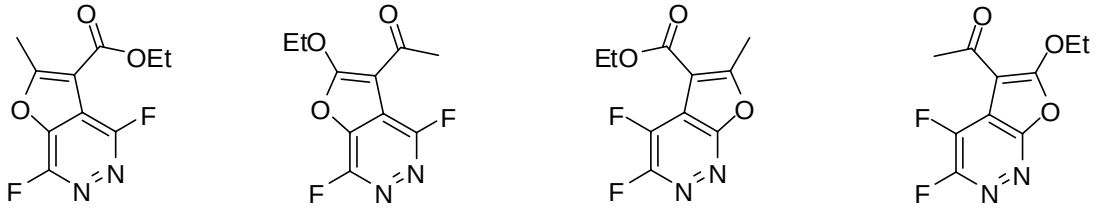

Figure 2.4

Although distinguishing between the first two structures and the second two is trivial with the aid of ^{19}F NMR spectroscopy, using processes similar to those described earlier in this chapter, it is not as straightforward to ascertain through which of the oxygen atoms cyclisation has occurred. Once analysis of the ^{19}F NMR spectrum has indicated to which side of the pyridazine ring the furan has been fused, consideration of proton and carbon NMR spectra give indications of the orientation of the substituents on the furan ring, with good evidence being provided by 2D NMR experiments.

In the case of the major product isolated from the reaction, ^{19}F NMR spectral shifts of -76.46 and -98.48 ppm suggest that the fluorine atoms are in the 3- and 6- positions, with both substitutions occurring *para*- to ring nitrogen, meaning that the product is one of the first two structures shown above. The two carbons, each bearing a fluorine atom, are easily located in the ^{13}C NMR spectrum, owing to their large $^{1}J_{CF}$ coupling constants. Equally, the other two carbons constituting the pyridazine ring may be readily identified by their splitting patterns. Proton NMR spectroscopy gives little information in isolation, but HSQC (Figure 2.5) allows assignment of the two methyl carbons by correlation with the readily assigned proton peaks. HMBC (Figure 2.6) shows connectivity between methylene protons and a carbon with a shift of 161 ppm, while the singlet methyl protons show connectivity to the carbon that was originally the methylene of ethyl acetoacetate, with a shift of 109 ppm, and another carbon nucleus resonating at 168 ppm, too low a value to be a ketone and therefore the β-carbon in the furan ring, suggesting that the resonance at 161 ppm is that of the ester carbon shown in the first of the four diagrams above.

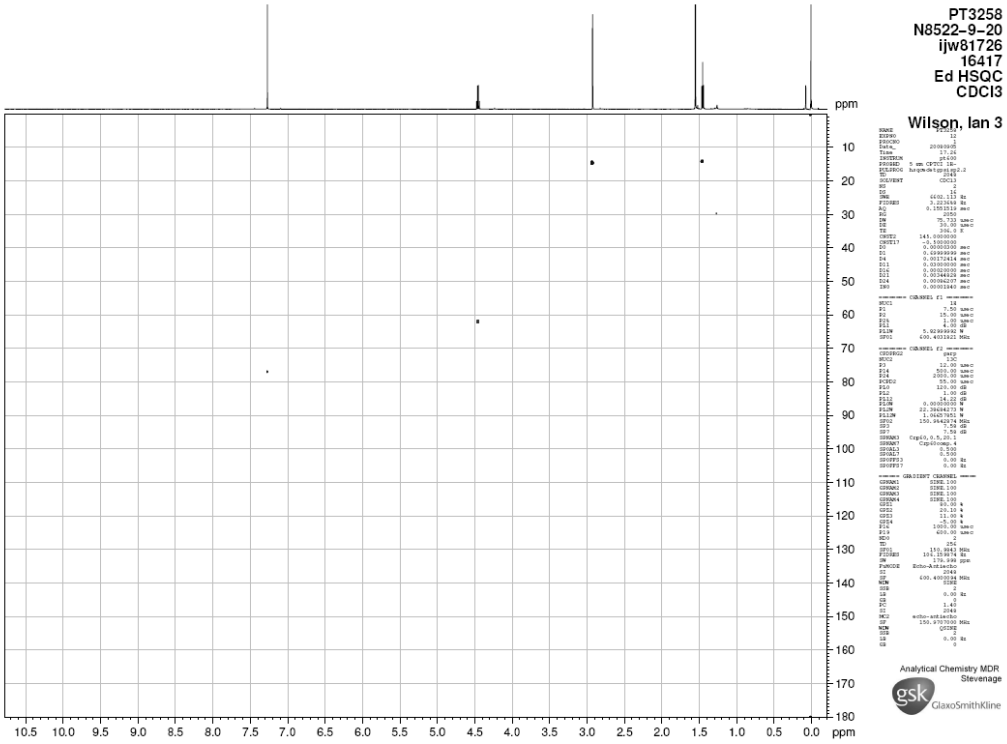
PT3258
N8522-9-20
ijw81726
16417
Ed HSQC
CDCl3
Wilson, Ian 3
Analytical Chemistry MDR
Stevenage
GlaxoSmithKline
ppm

Figure 2.5

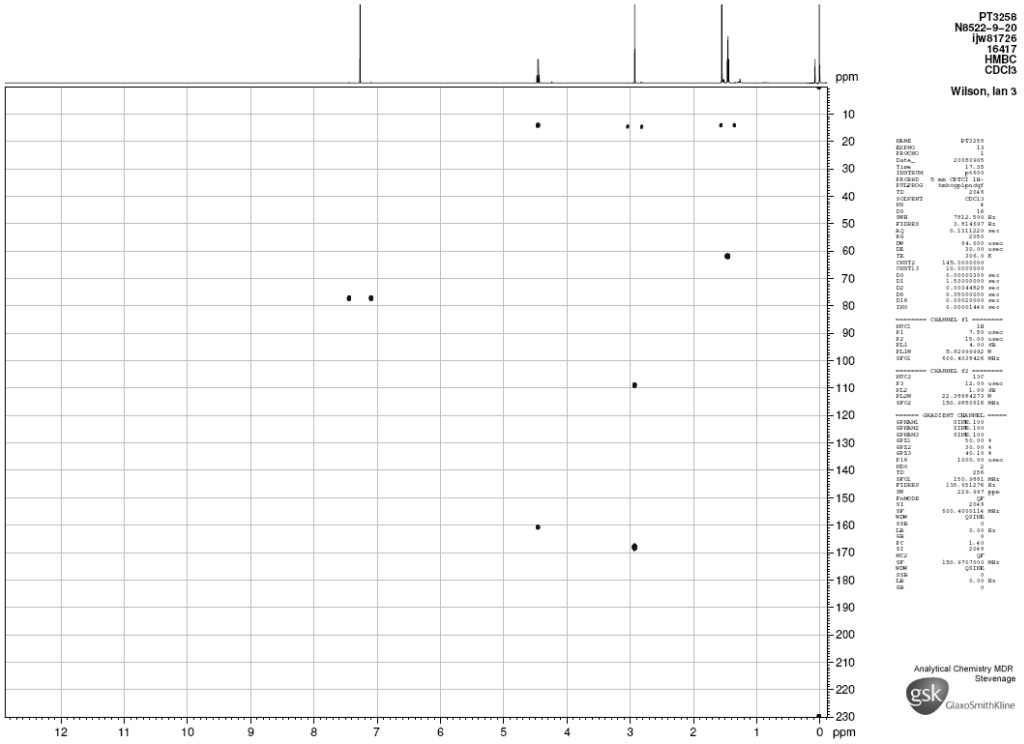

Figure 2.6

While the nucleophiles employed in previous sections of this chapter have behaved fairly predictably, the use of carbon nucleophiles has added some complicating factors. The presence of acidic protons in initial substitution products has been shown to lead to instability, and perhaps more interestingly the use of reactive nucleophiles has led to a decrease in the regioselectivity of the substitution process, with factors other than the stability of the Meisenheimer intermediate having to be considered.

2.3.4 Reactions with Thiols

The final set of reactions investigated for monosubstitution of tetrafluoropyridazine was that involving sulfur nucleophiles. The first nucleophile used was thiophenol, one

equivalent of which was found to give exclusively the disubstituted product **15**, with 50% conversion of starting material (Scheme 2.15).

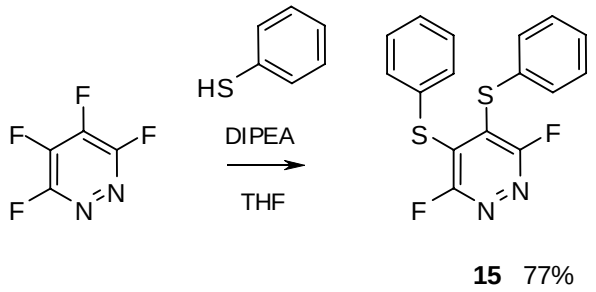

15 77%

Scheme 2.15

This observation may be explained by considering again the Meisenheimer intermediate involved in the reaction (Scheme 2.16). While the initial substitution reaction proceeds via the three resonance canonicals described earlier, the product of the initial substitution is able to undergo further reaction, in which the intermediate consists of four possible resonance canonicals, further stabilising the intermediate and making the product of initial substitution more reactive than the tetrafluorinated starting material, consistent with the known *para*- activating influence of thiophenolic substituents in reactions of polyfluorinated benzenes.[21]

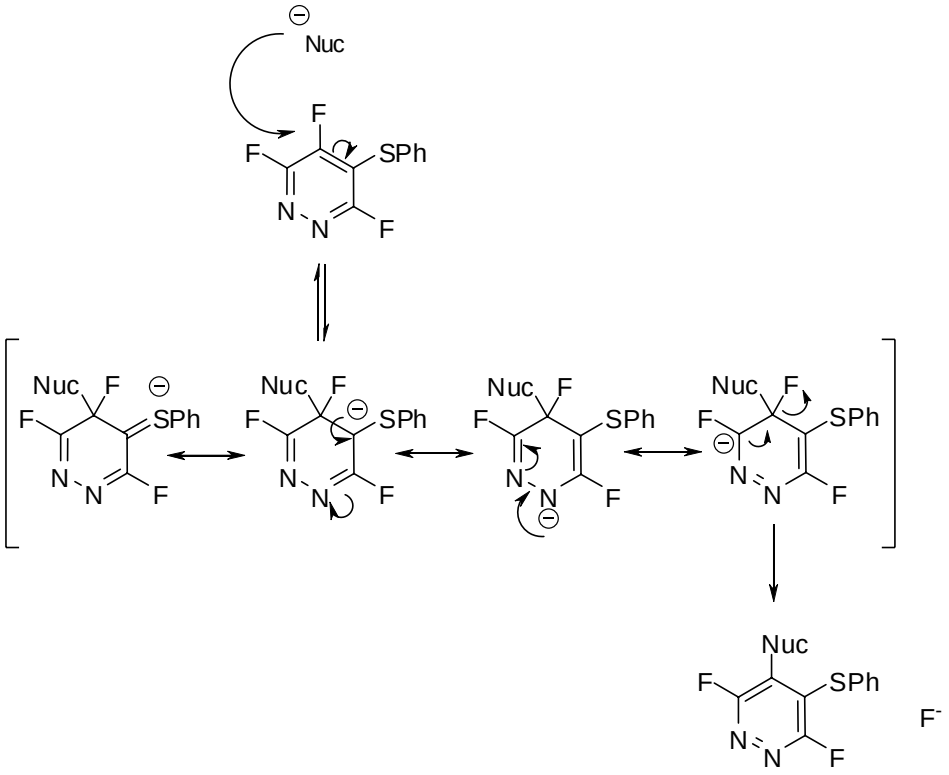

Scheme 2.16

Subsequently, alternative sulfur nucleophiles were employed in an attempt to ascertain whether monosubstitution was possible (Table 2.6). It was hoped that by altering the nucleophilicity, or the charge-stabilising properties of the thiol, the substitution could be halted after the first reaction, allowing synthesis of trifluorinated sulfur-substituted pyridazines.

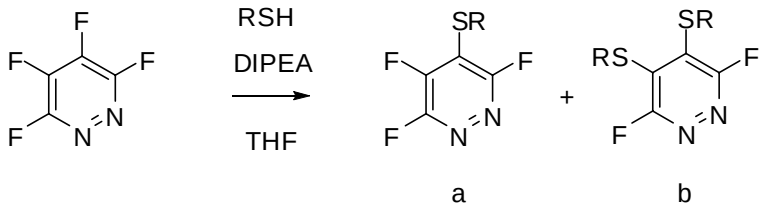

RSH	% a	% b
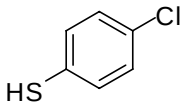	0	50
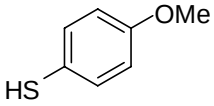	39	61
	100	0

Table 2.6

Two substituted thiophenols were investigated, one being the less nucleophilic 4-chlorothiophenol, the other the relatively electron rich 4-methoxythiophenol. While reaction with the chlorothiophenol again led to pure disubstitution in fifty percent conversion, reaction with one equivalent of 4-methoxythiophenol gave a reaction mixture containing approximately two parts disubstituted material for every one part of monofunctionalised product. We next increased the electron donating character of the nucleophile by moving to ethanethiol (Scheme 2.17).

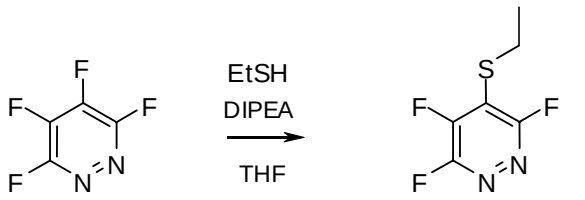

16 65%

Scheme 2.17

It was found that 4-ethylthio-2,3,5-trifluoropyridazine **16** could be obtained in good conversion from tetrafluoropyridazine, allowing selective monosubstitution with a sulfur centred nucleophile, and providing a further example of a substituted trifluorinated pyridazine on which to perform further investigative substitutions.

2.4 Nucleophilic Aromatic Substitution Reactions of Trifluoropyridazines

Having completed reactions of tetrafluoropyridazine with a number of nucleophiles, we observed that a range of nitrogen-, oxygen-, carbon-, and sulfur- centred substituents may be introduced to the pyridazine core by this method. In general, we have noted that the reactions give good selectivities and reasonable yields, and the instances where over-reaction has occurred give hope that further substitution of the trifluoropyridazine scaffold should be possible.

Our next suite of experiments was aimed at exploring the behaviour of a number of substituted trifluoropyridazines towards further nucleophilic attack. Of interest was not only the fact that our new electrophiles had four inequivalent sites of potential nucleophilic attack (displacement of any of the three fluorine atoms, or replacement of the substituent), but also that we expected to see some influence borne by the ring substituent already in place.

As we have already seen, simple consideration of the perhalogenated ring generally predicts substitution *para*- to the ring nitrogens, but there is room for complicating steric and electronic effects from substituents, with substituent *ortho*-, *meta*-, and *para*- directing effects, such as those observed for sulfur nucleophiles in the previous section, being of particular interest.

For the following experiments we took four representative products prepared in the previous sections, namely the products of reactions with morpholine (4-(3,5,6-trifluoro-pyridazin-4-yl)morpholine **1**), isopropyl alcohol (3,4,6-trifluoro-5-[(1-methylethyl)oxy]pyridazine **10**), phenylmagnesium bromide (3,4,6-trifluoro-5-phenylpyridazine **11**), and ethanethiol (4-(ethylthio)-3,5,6-trifluoropyridazine **16**), and reacted each with a further equivalent of a different nucleophile. In this fashion we hoped to explore the possibilities of a second nucleophilic substitution, the compatibility of existing substituents with incoming nucleophiles, and any unexpected trends in the behaviour of the reactions not discussed previously in the literature.

To aid comparability, all reactions were again performed under similar conditions with respect to solvents and concentrations as far as was reasonable.

2.4.1 Reactions with Amines and Thiols

The first nucleophiles to be applied were morpholine and thiophenol, and the results are summarised in the following table (Table 2.7).

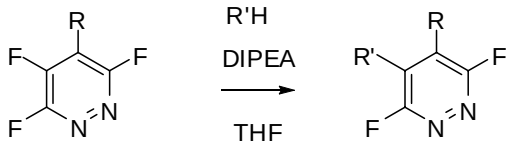

Substrate	R'H	Product	Yield (%)
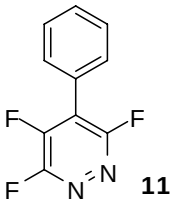 **11**	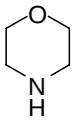	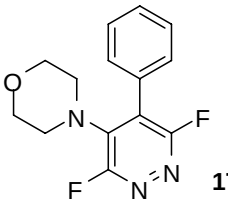 **17**	85
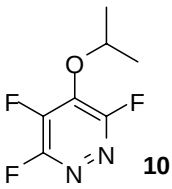 **10**	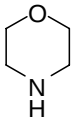	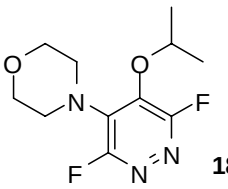 **18**	79
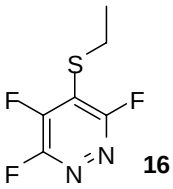 **16**	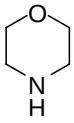	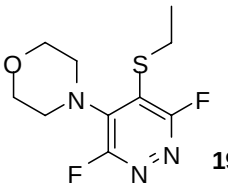 **19**	62
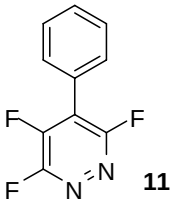 **11**	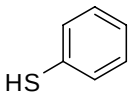	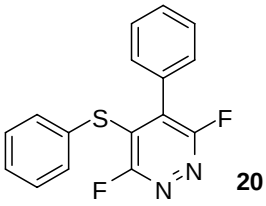 **20**	88
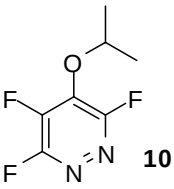 **10**	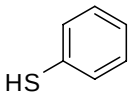	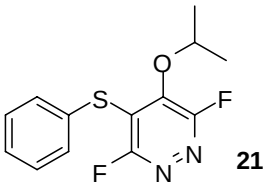 **21**	77
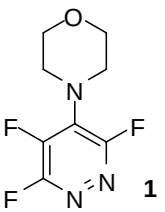 **1**	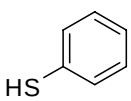	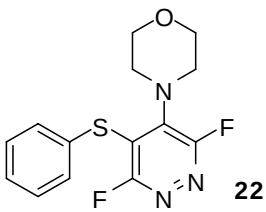 **22**	80

Table 2.7

Reactions of morpholine with trifluoropyridazines bearing phenyl, isopropoxy, and thioethoxy groups in the 4-position gave uniform good results, with clean monosubstitution occurring at the fluorinated position *para*- to ring nitrogen, as might have been expected from our earlier results. 4,5-Substitution was confirmed by the ^{19}F NMR spectra showing two peaks with shifts of around -85 ppm for each compound, consistent with fluorine *ortho*- to ring nitrogen. Reactions were noticeably slower for the trifluorinated materials than for the perfluorinated equivalent, with thioethoxy trifluoropyridazine taking a little over twenty four hours to react completely with morpholine at room temperature, and the phenyl and isopropoxy compounds taking several days at the same temperature.

Following these results, we next investigated the reactions of thiols with substituted trifluoropyridazines. Phenyl, isopropoxy, and morpholino substituted trifluoropyridazines were each reacted with a single equivalent of thiophenol. The high nucleophilicity of thiophenol is amply demonstrated in these examples, as the reactions all reached completion within one hour at 0 °C, a considerable reduction in reaction time compared to the reactions of morpholine with the same electrophiles.

Once again, all reactions went in good yield and gave, possibly surprisingly, clean monosubstitution at the remaining fluorinated position *para*- to ring nitrogen. In these examples, unlike the previously mentioned case of reaction of thiophenol with tetrafluoropyridazine, initial substitution did not then lead to preferential second substitution *ortho*- to the first sulfur substituent under the conditions employed. This may be rationalised by considering the uneven charge density in the intermediate, with differing importance attached to *ortho*- and *meta*- positions. The two cases are represented below (Figure 2.7).

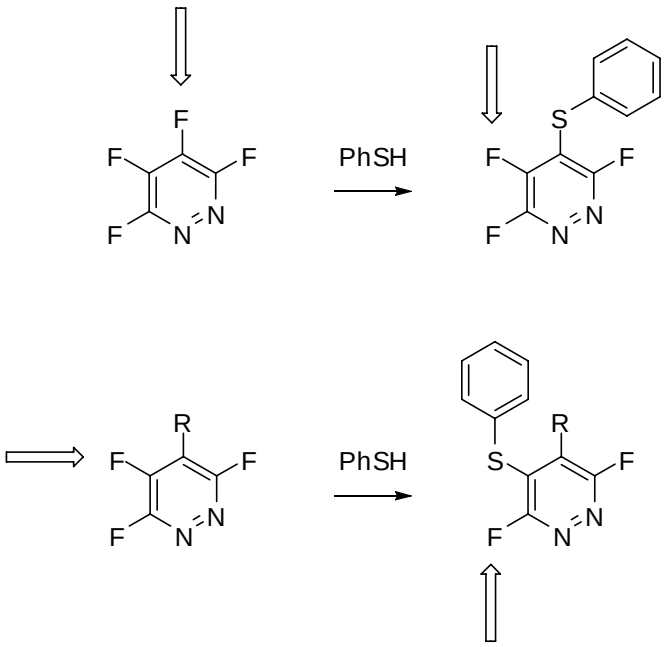

Figure 2.7

In the former reaction, as discussed earlier, initial substitution takes place at the arrowed 4-position, followed by rapid second substitution at the 5- position, arrowed on the right hand side of the diagram. The intermediate involved in the first reaction may be described as having the majority of the negative charge delocalised over two fluorine-bearing carbons and the ring nitrogen, with the greatest concentration on the heteroatom which, as noted before, is the preferred site for the charge, as it lacks the destabilising interactions found between charges on carbon and the fluorine lone pairs. Second substitution is more highly favoured still, as in this case the greatest component of the charge may still be located on a ring nitrogen, while a slightly destabilising interaction with fluorine is removed to be replaced by an electronegative but poorly overlapping sulfur atom, which also allows further delocalisation and therefore stabilisation of the charge.

In the latter reaction, initial substitution once again takes place *para*- to the available heteroatom, but further reaction *ortho*- to the thiophenol group requires substitution at the 3-position. While varying R groups will cause subtle differences, some general

observations can be made about the differences in the resulting intermediates. Both intermediates contain a ring nitrogen *meta*- to the position of substitution, while the other *meta*- position bears the R- group in the second step, as opposed to an inductively stabilising fluorine atom. The other factor opposing a second substitution is the interchange of the remaining heteroatom and C-F group – the first step involves an intermediate with *ortho*- C-F and *para*- nitrogen, while in the second step the positions are reversed, reducing stabilisation, and seemingly providing sufficient barrier to reaction to prevent oversubstitution.

In general, it appears that nucleophilic aromatic substitution reactions of functionalised trifluoropyridazines with amines and thiols may be performed to give good yields of difunctionalised difluorinated pyridazines with excellent levels of regioselectivity. The orientation of substitution is readily rationalised, and oversubstitution does not appear to be a problem when using activating sulfur nucleophiles.

2.4.2 Reactions with Alkoxides and Carbon Nucleophiles

Encouraged by our successful disubstitution reactions thus far, we moved on to assess reactions involving further classes of nucleophiles, namely oxygen- and carbon- centred species. The first to be employed was isopropyl alcohol. After four days at reflux, a mixture of 4-(3,5,6-trifluoro-4-pyridazinyl)morpholine **1**, isopropyl alcohol, and Hünig's base in tetrahydrofuran showed no conversion from starting material. As an extreme example, the theoretically most reactive trifluoropyridazine synthesised thus far, 4-(ethylthio)-3,5,6-trifluoropyridazine **16**, was dissolved in tetrahydrofuran with excess isopropyl alcohol and base, and microwave irradiated to a temperature of one hundred and eighty centigrade for ten minutes. Even under these forcing conditions, no conversion of the starting material was observed, so we moved to carry out reactions using the more reactive lithium isopropoxide. Our new nucleophile was reacted with phenyl-, morpholino-, and ethylthio-substituted trifluoropyridazines **11**, **1** and **16**, with addition of the nucleophile to the

reaction mixture occurring at -78 °C, followed by slow warming to room temperature (Table 2.8).

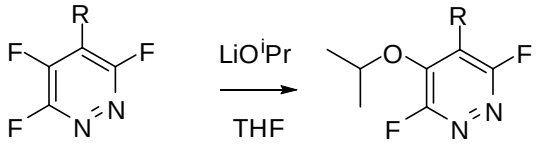

Electrophile	Product	Yield (%)
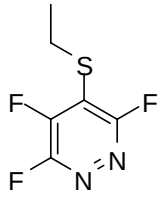	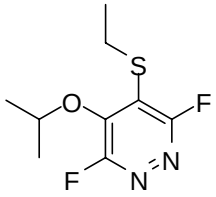	78
16	**23**	
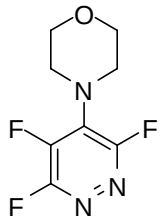	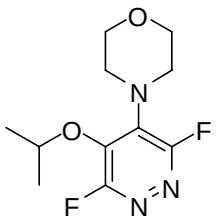	41
1	**18**	
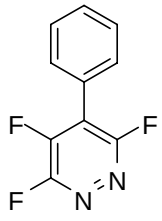	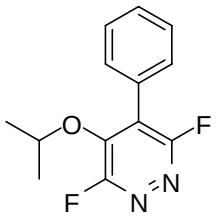	69[a]
11	**24**	

[a] Containing trace quantities of an inseparable isomer

Table 2.8

The reaction of 4-(ethylthio)-3,5,6-trifluoropyridazine **16** with lithium isopropoxide gave the expected 4,5-disubstituted product **23** in good yield, following the trend thus far established for second substitutions, with the regiochemistry of the product again confirmed by the methods discussed previously. Reaction of our nucleophile with the morpholino-substituted trifluoropyridazine **1**, however, gave traces of an isomeric byproduct, which proved difficult to separate from the major product, causing a significant reduction in isolated yield of **18**. This appears once again to be due to the use of a more reactive nucleophile reducing the importance of stabilisation of the intermediate, and pushing regioselectivity away from the expected site, although the consideration of steric effects gives further suggestion of disincentive to reaction at the 5-position. Reaction of lithium isopropoxide with the phenyl- substituted pyridazine **11** also leads to the formation of small amounts of byproducts, but in this case, we were unable to separate the regioisomeric byproducts from the major product **24**.

With regioselective reactions of trifluoropyridazines with nitrogen-, sulfur-, and oxygen-centred nucleophiles established, the final area we wanted to explore involved the behaviour of these electrophiles with carbon nucleophiles.

It is worth noting that the pyridazine ring is still highly electron deficient, and attempts to react methylmagnesium bromide with monosubstituted trifluoropyridazines still result in extensive decomposition and the formation of intractable product mixtures, as per previous explorations. As such, the carbon nucleophile we chose to employ was again phenylmagnesium bromide, for direct comparison with the previous results, and the desirable lack of α- hydrogen atoms. Reactions were performed with morpholino-, isopropoxy-, and thioethoxy- substituted trifluoropyridazines **1**, **10**, and **16**, with temperatures gradually being raised from -78 °C to room temperature over the course of the reaction (Table 2.9).

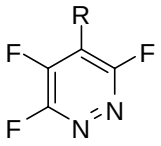

PhMgBr

THF

Products

Electrophile	Major product	Minor product
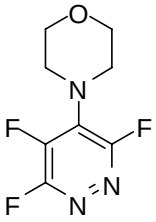 **1**	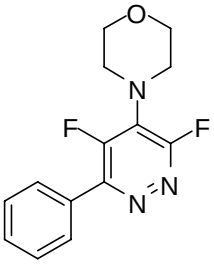 14 : 1 **25** 6%	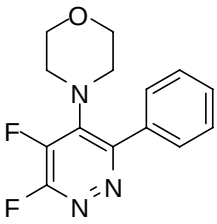 **26**
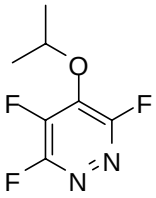 **10**	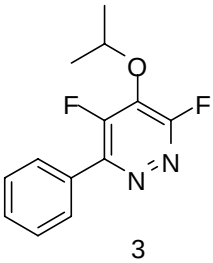 3 : 1 **27**	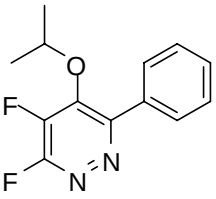 **28**
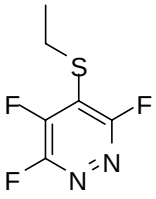 **16**	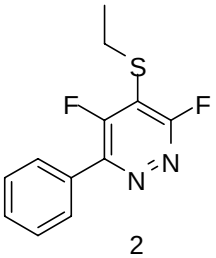 2 : 1 **29**	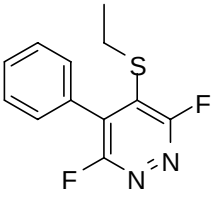 **30**

Table 2.9

The reaction of phenylmagnesium bromide with the morpholino- substituted trifluoropyridazine **1** provided two unusual results; not only was the major product the unexpected 6- substituted compound **25**, but a small quantity of the third possible substitution pathway was visible by ^{19}F NMR spectroscopy. Analysis of the spectral peaks suggested a pair of compounds each bearing a phenyl group *ortho*- to ring nitrogen, and each possessing one *ortho*- and one *para*- fluorine. Comparison with the previously acquired spectrum of the 4,5- difunctionalised compound **17** suggested that none of this expected isomer was present in the reaction mixture. Confirmation of the structure of the major product was provided by a ^{1}H-^{19}F heteronuclear nOe experiment (Figure 2.9), showing the proximity of the morpholine protons to the more deshielded fluorine nucleus.

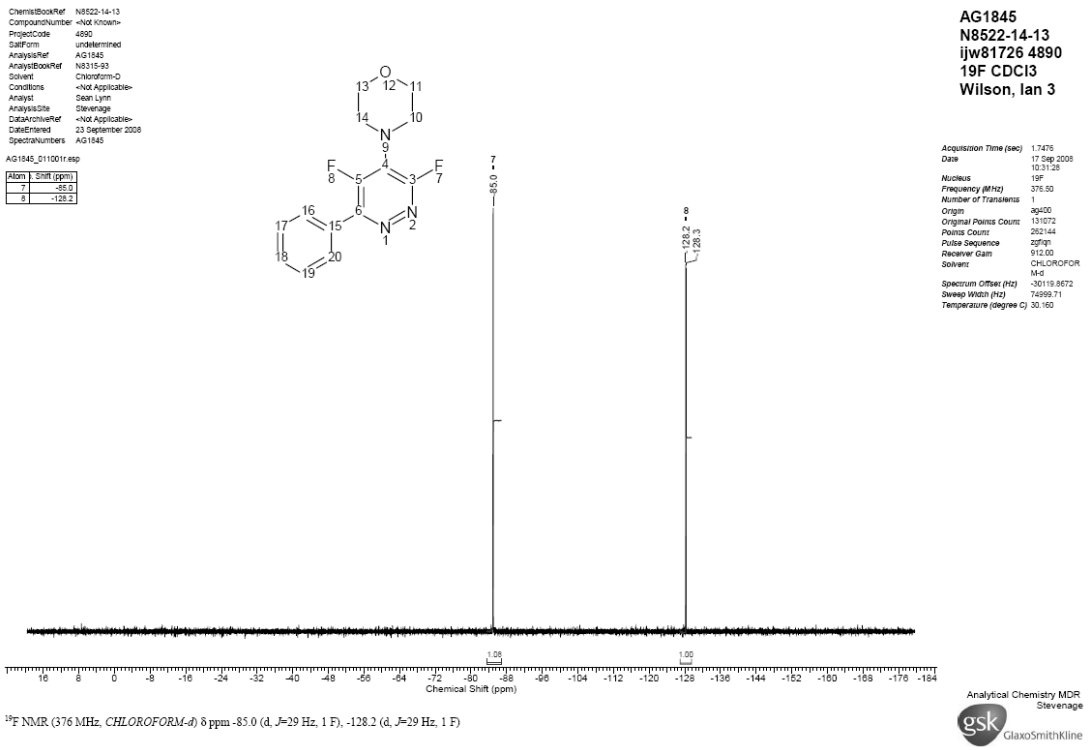

^{19}F NMR (376 MHz, *CHLOROFORM-d*) δ ppm -85.0 (d, *J*=29 Hz, 1 F), -128.2 (d, *J*=29 Hz, 1 F)

Figure 2.8

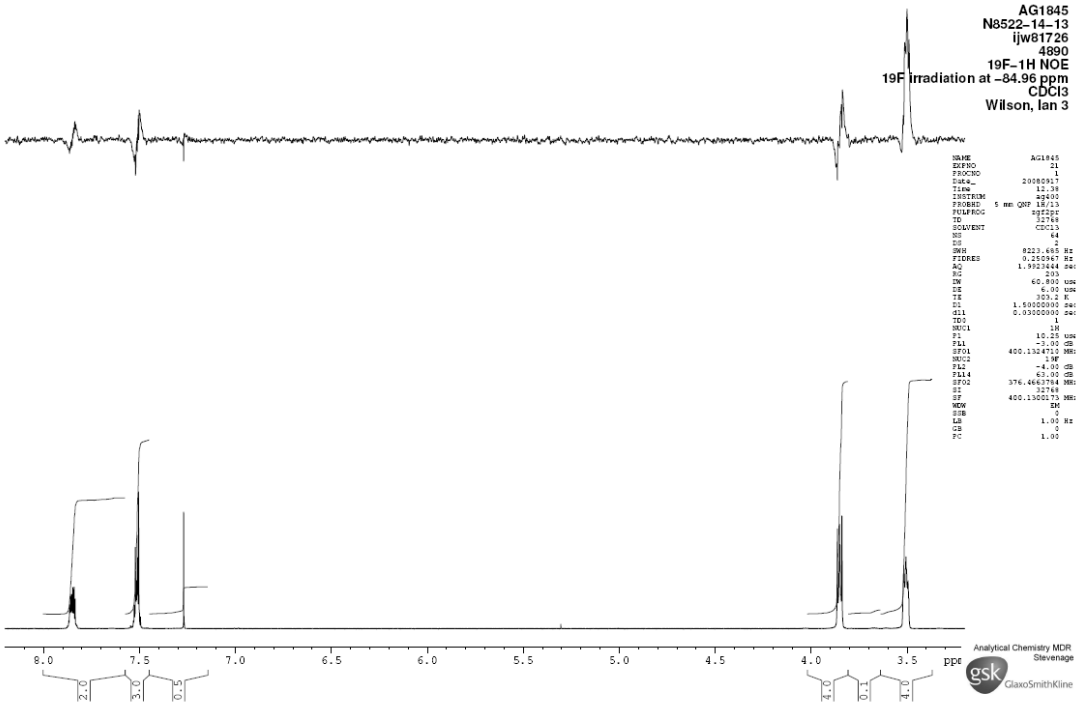

Figure 2.9

Reaction of the Grignard with the isopropoxy- substituted trifluoropyridazine **10** also showed a mixture of products, and although separation was not achieved, analysis of NMR spectra again suggested that the products were the result of reaction at the two sites adjacent to ring nitrogen.

Finally, reaction of the phenyl nucleophile with the 4-thioethoxy trifluoropyridazine **16** was performed. In this case, 4,5-disubstitution did appear to take place, but was the minor product of the reaction, with the majority of material produced again being the result of nucleophilic attack at one of the positions *ortho*- to ring nitrogen.

It is clear that the regioselectivity of reactions with phenylmagnesium bromide differs considerably from that seen in the reactions of amines and thiols. This can again be

attributed to the increased reactivity of the nucleophile and resultant alteration of the importances of electronic effects in the intermediate and initial state.

As far as the generation of polyfunctionalised pyridazine systems is concerned, the results discussed in this section indicate that the order of application of nucleophiles to the scaffold may be critical – for example, while alcohols are readily and regioselectively attached to the pyridazine core by reaction with tetrafluoropyridazine, reactions of alkoxide with 4-substituted 3,5,6-trifluoropyridazine systems seem to give rise to lower yielding and less regioselective processes.

2.5 Nucleophilic Aromatic Substitution Reactions of Difluoropyridazines

Having observed some examples of regioselective second substitutions, we wanted to ascertain whether or not a selective third substitution would be possible. Reasonable routes to 4,5-disubstituted difluorinated pyridazines having been found, the next functionalisation should lead to a trisubstituted pyridazine scaffold bearing a single fluorine atom *ortho*- to ring nitrogen. In going from reactions of the tetrafluorinated to the trifluorinated systems, we noted a distinct reduction in reactivity, which one would expect to be even greater over the transition from trifluorinated to difluorinated materials. Also, we observed that the major directing effect, among a number of contributory factors, up until this point has been a propensity for reaction *para*- to the ring nitrogens. With this influence removed, control of selectivity falls entirely to the properties of the two previously introduced substituents. With a view to maximising the disparity between reactivities at our fluorinated sites, the obvious choice of electrophile that we already had in hand was 4-(3,6-difluoro-5-(phenylthio)pyridazin-4-yl)morpholine **22**, bearing a thiophenoxy group, which we have already seen to be *ortho*- activating to some extent, and a morpholino group, which should be deactivating and therefore also somewhat *meta*- directing.

Reaction of our chosen electrophile with lithium isopropoxide gave moderate success, going to completion without the need for heating, and giving a five to one ratio of products by ^{19}F NMR spectroscopic analysis (Scheme 2.18).

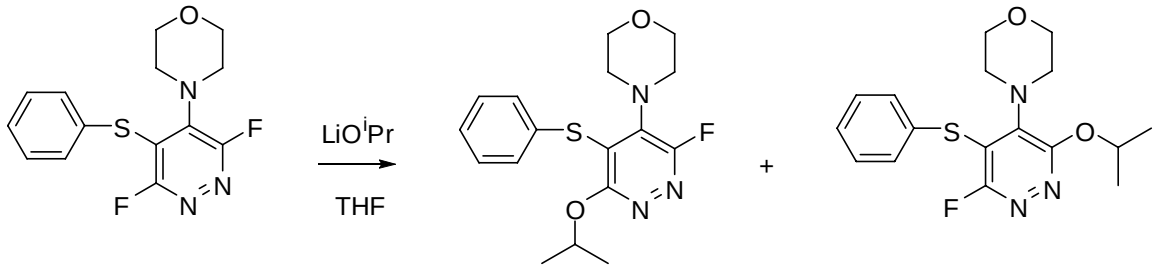

22 **31** **32**

Scheme 2.18

Unfortunately, these isomers proved resistant to separation, and we have been unable to characterise them individually.

It was hoped that the use of a less reactive nucleophile might allow for a cleaner product distribution, and enhanced ease of separation. With this intention, we performed the reaction between our chosen electrophile and morpholine. The reaction was sluggish, as might have been expected from past trends, but after microwave irradiation at 150 °C for 90 minutes, conversion of the starting material was complete, and ^{19}F NMR spectroscopy showed fairly clean transformation to a single major product **33** (Scheme 2.19).

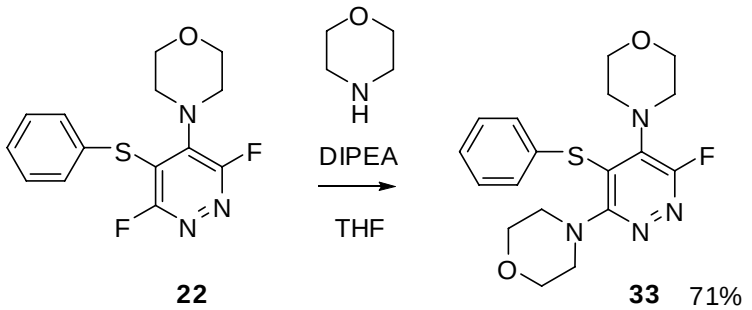

22 **33** 71%

Scheme 2.19

In this case, purification by column chromatography was fairly straightforward, and the trisubstituted fluoropyridazine could be isolated in 71% yield. X-ray crystallography determined the structure of the product as that shown (Figure 2.10).

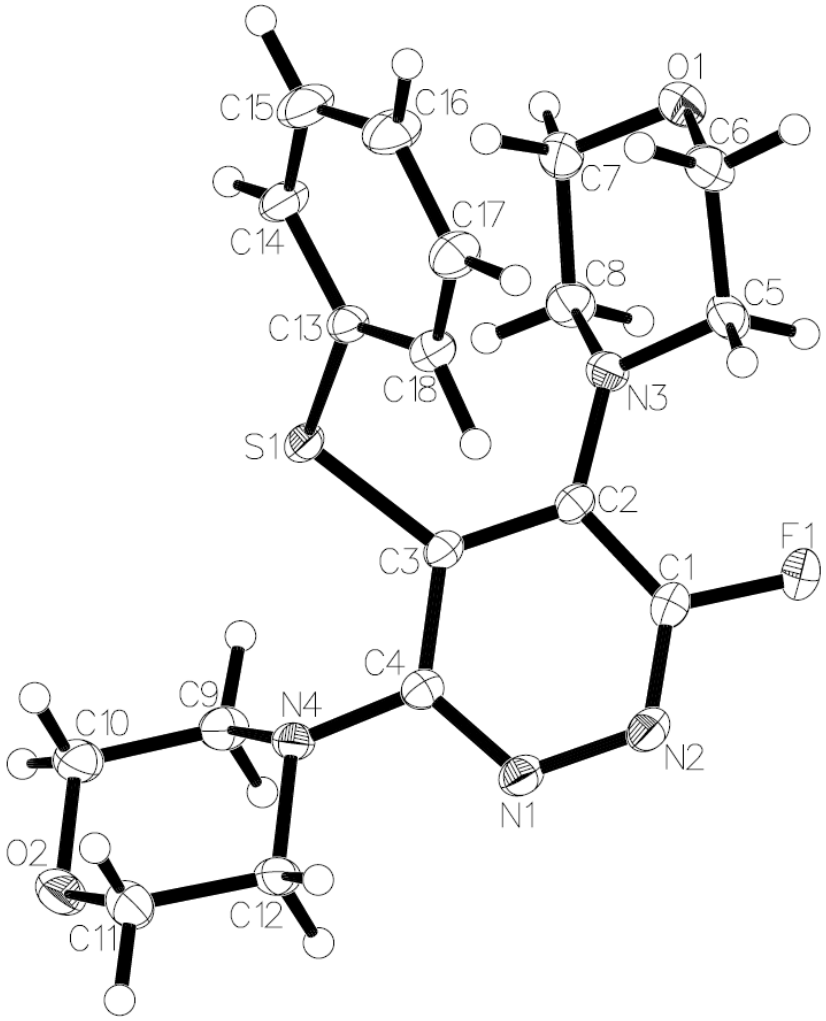

Figure 2.10

Confirmation of the structure demonstrates that a third regioselective substitution is possible, with the orientation determined by the directing effects of the previously introduced substituent.

2.6 Conclusions

The aims of this chapter were to explore the reactions of a number of variously fluorinated pyridazine systems with a range of nucleophilic species, with the intention of gaining a better understanding of the behaviour of electron deficient heterocyclic cores, and determine the suitability of tetrafluoropyridazine as a potential scaffold for the generation of multiply substituted new chemical entities. A number of routes towards highly functionalised pyridazine systems have been demonstrated, and several results of interest highlighted.

It has been shown that tetrafluoropyridazine will tolerate reaction with a wide variety of nucleophiles, giving encouraging yields of monosubstituted products, and that excellent selectivity for reaction at the 4- position is possible. It seems that the regioselectivity of substitution depends largely upon the ability of the reactive intermediate produced to stabilise the charge generated, but initial state considerations also bear non-negligible weight, with significant quantities of by-products formed when reactive nucleophiles are employed.

Second functionalisations showed a greater variety of selectivities; while amines and thiols behaved in a controlled fashion and reacted at the expected site to give good yields of difunctionalised products, more reactive nucleophiles gave less predictable results. Having established the unsuitability of alcohols for the second substitution, the use of alkoxides gave, in certain cases, mixtures of products, with the expected reaction pathway competing against substitution at the harder sites. The use of Grignard reagents pushes selectivity well away from that seen for amines and thiols, with considerable replacement of fluorine atoms *ortho*- to ring nitrogen. This variance in behaviour necessitates the careful sequencing of reactions in order to synthesise certain difunctionalised pyridazines, an illuminating example being the disparity in reaction products observed when reacting morpholine and

phenylmagnesium bromide with tetrafluoropyridazine, depending upon the order of application (Scheme 2.20).

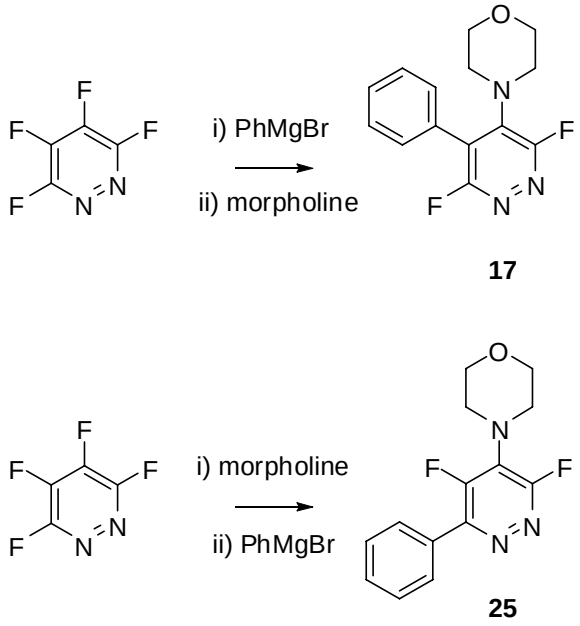

Scheme 2.20

By the third step, the reactivity of the electrophile is greatly reduced, and fairly forcing conditions are required. The directing effects available for differentiation of the two reactive sites are minimal, and even with optimal substituents for regioselectivity employed, selective substitutions are not guaranteed. While successful trifunctionalisation has been demonstrated, the example seems far from general.

2.7 References

1 R. D. Chambers, 'Fluorine in Organic Chemistry', Wiley, 1973.
2 G. A. Artamkina, M. P. Egorov, and I. P. Beletskaya, *Chem. Rev.*, 1982, **82**, 427.
3 H. Hasegawa, K. Mizuse, M. Hachiya, Y. Matsuda, N. Mikami, and A. Fujii, *Angew. Chem., Int. Ed.*, 2008, **47**, 6008.
4 R. E. Banks, J. E. Burgess, W. M. Cheng, and R. N. Haszeldine, *J. Chem. Soc.*, 1965, 575.

[5] J. T. Kohrt, K. J. Filipski, W. L. Cody, C. Cai, D. A. Dudley, C. A. V. Huis, J. A. Willardsen, L. S. Narasimhan, E. Zhang, S. T. Rapundalo, K. Saiya-Cork, R. J. Leadley, and J. J. Edmunds, *Bioorg. Med. Chem. Lett.*, 2006, **16**, 1060.

[6] G. Sandford, R. Slater, D. S. Yufit, J. A. K. Howard, and A. Vong, *J. Org. Chem.*, 2005, **70**, 7208.

[7] A. Baron, G. Sandford, R. Slater, D. S. Yufit, J. A. K. Howard, and A. Vong, *J. Org. Chem.*, 2005, **70**, 9377.

[8] M. W. Cartwright, G. Sandford, J. Bousbaa, D. S. Yufit, J. A. K. Howard, J. A. Christopher, and D. D. Miller, *Tetrahedron*, 2007, **63**, 7027.

[9] R. D. Chambers, J. A. H. MacBride, and W. K. R. Musgrave, *J. Chem. Soc. (C)*, 1968, 2116.

[10] R. D. Chambers, J. A. H. MacBride, and W. K. R. Musgrave, *J. Chem. Soc. (C)*, 1968, 2989.

[11] G. Pattison, G. Sandford, D. S. Yufit, J. A. K. Howard, J. A. Christopher, and D. D. Miller, *J. Org. Chem.*, 2009, **74**, 5533.

[12] R. D. Chambers, C. D. Hewitt, M. J. Silvester, and E. Klauke, *J. Fluorine Chem.*, 1986, **32**, 389.

[13] A. E. Bayliff and R. D. Chambers, *J. Chem. Soc., Perk. T. 1*, 1988, 201.

[14] W. Dmowski and A. Haas, *J. Chem. Soc., Perk. T. 1*, 1988, 1179.

[15] K. E. Peterman and W. Dmowski, *Org. Prep. Proced. Int.*, 1991, **23**, 760.

[16] S. Berger, S. Braun, and H.-O. Kalinowski, 'NMR Spectroscopy of the Non-Metallic Elements', Wiley-Blackwell, 1997.

[17] C. A. L. Mahaffy and J. R. Nanney, *J. Fluorine Chem.*, 1994, **67**, 67.

[18] R. D. Chambers, G. Sandford, and J. Trmcic, *J. Fluorine Chem.*, 2007, **128**, 1439.

[19] R. J. D. Pasquale and C. Tamborski, *J. Org. Chem.*, 1967, **32**, 3163.

[20] H. E. Zimmerman, *Tetrahedron*, 1961, **16**, 169.

[21] J. M. Birchall, M. Green, R. N. Haszeldine, and A. D. Pitts, *Chem. Commun.*, 1967, 338.

Chapter 3

Reactions of Trifluoropyridazines with Binucleophiles

3.1 Aims and Approach

While the preceding chapter concerned itself with the reactions of polyfluoropyridazine derivatives with monofunctional nucleophiles, we were also interested in the possibility of reacting polyfluoropyridazines with bifunctional nucleophiles. The most obvious reason for this interest is in the nature of the products obtained, which will be fused polycyclic systems similar to some of those seen in chapter 1, allowing what will hopefully be a general approach to a wide range of functionalised pyridazine ring fused systems in the manner shown below (Scheme 3.1).

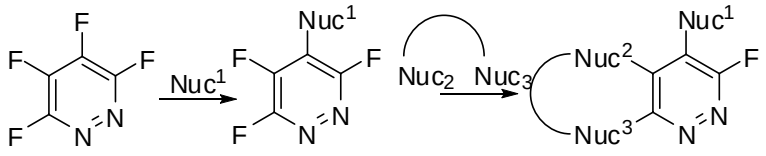

Scheme 3.1

Depending on the nature of the tether between the two ends of the binucleophile, a range of fused structures, including those containing the skeletal forms represented below (Figure 3.1), should be accessible. Frameworks such as these have been shown to be highly prevalent among pharmaceutical compounds, and as such similar structures might reasonably be expected to possess drug-like properties.[1]

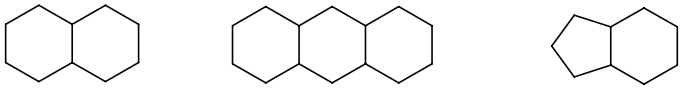

Figure 3.1

The other attractive possibility of reactions with binucleophiles is the level of regiocontrol that may be offered. As discussed at the end of the previous chapter, selective reactions of difluorinated pyridazines appear at present to be challenging. While some regiocontrol is possible, the major directing effect in reactions of tetra- and tri-fluoropyridazines, that of orientation with respect to ring nitrogens, will generally be absent in difluoropyridazines, with control of regiochemistry ceded to the rather more nebulous influences of the substituents. If, after introduction of the first substituent, a binucleophile is introduced to the fluoropyridazine, our prior results would indicate a reasonable likelihood of initial reaction *ortho*- to the first substituent, after which the tethered nature of binucleophile should direct subsequent attack to only one of the two available sites, encouraging clean generation of a single isomer of a functionalised, ring-fused pyridazine.

With these objectives in mind, the reactions described in this chapter will involve the combination of previously synthesised functionalised trifluoropyridazines with a number of binucleophiles. This should give an indication of the applicability of our general method to the generation of ring fused heterocyclic systems, and also establish the regioselectivity of reactions when employing asymmetrical binucleophiles.

3.2 Reactions of 4-(3,5,6-Trifluoropyridazin-4-yl)morpholine

For our initial experiments involving the reactions of functionalised fluorinated pyridazines with binucleophiles, we chose 4-(3,5,6-trifluoropyridazin-4-yl)morpholine as a model substrate, as it was relatively accessible and was expected to show chemistry representative of a number of our previously prepared compounds without possessing any functionality likely to interfere in subsequent nucleophilic aromatic substitution reactions.

The first reaction performed was between 4-(3,5,6-trifluoropyridazin-4-yl)morpholine **1** and N,N'-dimethylethylene diamine, a symmetrical binucleophile the reactivity of which has previously been demonstrated in its reactions with other polyfluorinated heterocycles.[2] While we were confident that initial nucleophilic attack would be successful, our previous experiments with sequential monosubstitutions suggested that the ring closure might be difficult. Happily, the desired fused product, 3-fluoro-5,8-dimethyl-4-morpholin-4-yl-5,6,7,8-tetrahydro-pyrazino[2,3-c]pyridazine **34**, was produced in good yield after stirring the reagents together in THF at room temperature (Scheme 3.2). The apparent ease of reaction in this case, in contrast to what might have been expected, can be attributed to the increase in reaction rate afforded by the fact that the final step is intramolecular, the rapidity of ring closing further emphasised by the good yield, and absence of ethylene diamine bridged bipyridazines.

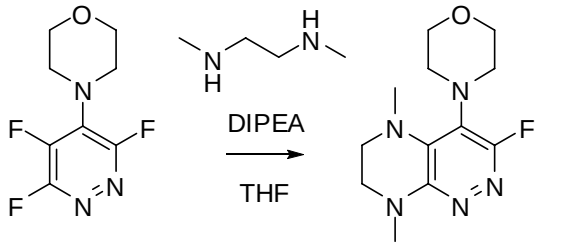

1 **34** 84%

Scheme 3.2

Encouraged by our successful reaction of a substituted trifluoropyridazine with a bifunctional nucleophile, we next investigated the use of some other dinitrogen nucleophiles, namely benzamidine and two aminopyridines. In these cases, the formation of the desired fused ring systems was not achieved, despite the use of vigorous conditions and strong bases such as alkyl lithiums and sodium hydride.

The final set of experiments performed on 4-(3,5,6-trifluoropyridazin-4-yl)morpholine **1** was that involving reaction with a range of asymmetrically disubstituted benzenes, the object of which was to produce a number of fused tricyclic systems.

The nucleophiles employed were 2-mercaptophenol, 2-aminophenol, and 2-aminobenzenethiol. Reaction with 2-mercaptophenol gave a tricyclic product after a few hours stirring at room temperature, the structure of which is presumed to be that shown below (Scheme 3.3), by analogy with the similar reactions outlined later in this chapter.

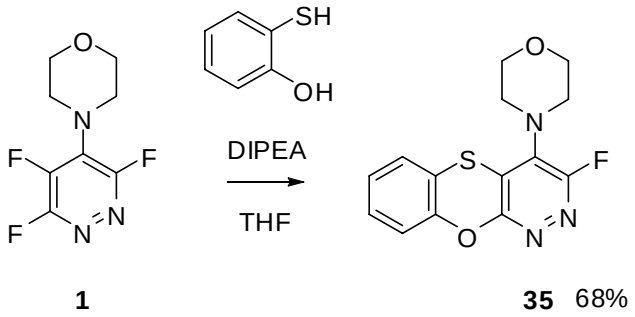

1 **35** 68%

Scheme 3.3

In contrast to the above, reactions with various aniline derivatives failed to effect the desired results, even after extended periods of heating, reflecting the difference in activating ability of sulfur- and nitrogen- centred substituents.

As we have already seen, a sulfur substituent activates the pyridazine ring to further attack, particularly *ortho*- and *para*- to itself, while a nitrogen substituent is deactivating, and should have a tendency to direct subsequent substitution to the *meta*- position (Figure 3.2). It is possible that a further factor is the presence of the hydrogen atom on the bridging nitrogen, which is potentially capable of hydrogen bonding to the second nucleophilic centre, orienting it away from the electrophilic diazine site.

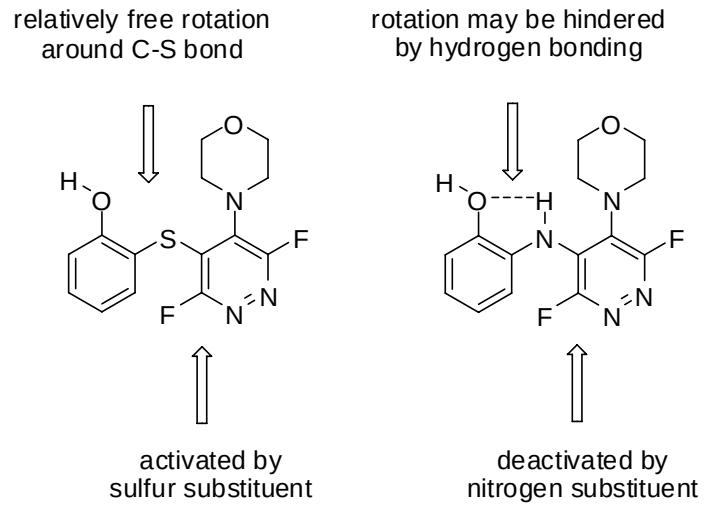

Figure 3.2

While a couple of syntheses of fused systems from 4-(3,5,6-trifluoropyridazin-4-yl)morpholine **1** have been demonstrated, it was disappointing that the procedure was not as general as might have been hoped, and we moved on to consider other monofunctionalised systems.

3.3 Reactions of 3,5,6-Trifluoropyridazin-4-amine

In our prior experiments, we observed the deactivating effect of a nitrogen substituent, and we were conscious that this effect may be a factor in the difficulties outlined in section 3.2. Another consideration is that the introduction of a secondary amine, while potentially useful as a route to increased diversity, is essentially irreversible and of little use for further synthetic transformations.

With this in mind, we turned to the investigation of the reactions of 4-amino-3,5,6-trifluoropyridazine **36**. It was hoped that this scaffold would present us with two valuable characteristics: of immediate interest was the possibility of reducing the deactivating influence of the nitrogen atom by oxidation to a nitro group, but we were also aware that

the amino group is in itself a useful synthetic handle, possibly allowing further functionalisation or even complete removal and replacement with a different group (Scheme 3.4).

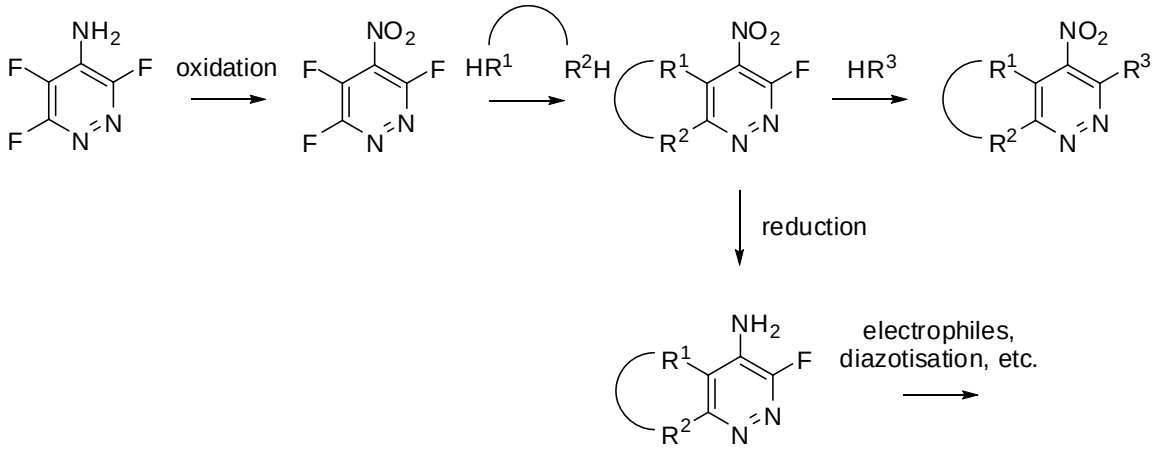

Scheme 3.4

The known[3] aminopyridazine was synthesised from tetrafluoropyridazine in moderate yield by straightforward reaction with ammonia (Scheme 3.5).

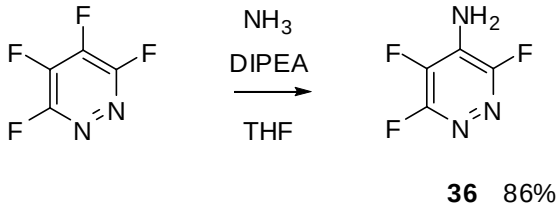

Scheme 3.5

Before any attempts were made to modify the amino group, we investigated the reactions of the amino pyridazine **36** with binucleophiles, to compare its behaviour with that of the morpholino- substituted pyridazine **1**.

Perhaps unsurprisingly, the reactivity of both substrates was found to be similar; reactions with aminopyridines again proved unsuccessful, while of the reactions attempted with disubstituted benzenes only that involving 2-mercaptophenol led to the isolation of a fused tricyclic product **37** (Scheme 3.6), most probably due to the reasons given above.

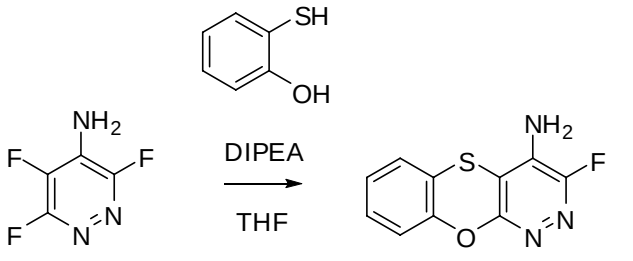

36 **37** 12%

Scheme 3.6

With the reactivity of the parent amine established, we looked towards methods of increasing reactivity by lessening the electron-donating properties of the amino group. Our first investigations in this area involved attempting to acylate the amino group, hopefully increasing the electrophilicity of the diazine (Scheme 3.7).

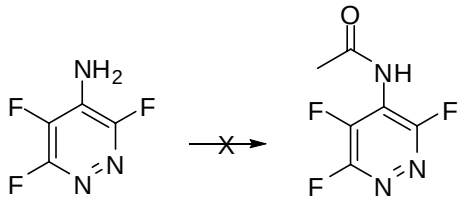

36

Scheme 3.7

Unfortunately, attempts to acylate our amine under various conditions failed to produce the desired product, demonstrating the very low nucleophilicity of the exocyclic nitrogen atom.

An alternative method of activation envisaged was the conversion of the amino group to a nitro functionality. The analogous reaction has previously been performed on 4-aminotetrafluoropyridine, using peroxytrifluoroacetic acid as the oxidising agent. Recent work at Durham has shown that the reaction may be performed more cleanly by using the powerful oxidising agent hypofluorous acid (Scheme 3.8).

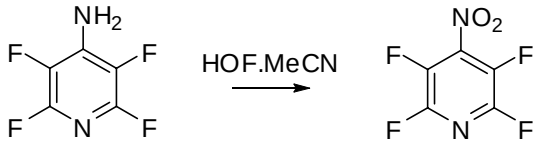

Scheme 3.8

Given the apparently low reactivity of our aminopyridazine and the ready availability of the necessary equipment for the generation and use of hypofluorous acid, we decided that the latter method was worth investigating. While reaction of 4-amino-3,5,6-trifluoropyridazine **36** with the oxidising agent showed gratifyingly high levels of conversion from the starting material, none of the desired trifluorinated nitro compound could be isolated from the reaction mixture. It seems likely that the initial product is highly unstable and rapidly undergoes further reaction, most probably with water, to form more stable species.

No further investigation of the reactions of the amino trifluoropyridazine was undertaken. It would appear that the scaffold is of limited use as a coupling partner for binucleophiles, and conversion to the nitro compound increases reactivity of the heterocycle to a point where storage and handling become very difficult.

3.4 Reactions of 4-(Ethylthio)-3,5,6-trifluoropyridazine

Having previously observed the activating effect of a sulfur substituent with respect to nucleophilic aromatic substitutions of polyfluoropyridazines, we hoped that such starting

materials would be the most likely to undergo successful reactions with binucleophiles to form the ring fused compounds we desired.

4-(Ethylthio)-3,5,6-trifluoropyridazine **16**, as synthesised in chapter 2, was chosen as the starting material for the following reactions in light of its ease of preparation and purification, and expected higher reactivity towards nucleophiles.

Reaction with N,N'-dimethylethylene diamine once again proceeded quickly and cleanly to give the expected fused bicyclic product **38** in good yield (Scheme 3.9).

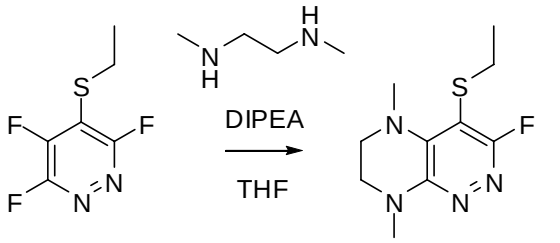

16 **38** 77%

Scheme 3.9

Reactions with the three disubstituted benzenes described above were then performed, in the hope that the increased reactivity towards nucleophiles bestowed on the heterocyclic ring by the thioethoxy group might allow all three adducts to be prepared. The first nucleophile employed was 2-mercaptophenol, which, unsurprisingly, reacted well to give the fused bicyclic product **39** (Scheme 3.10).

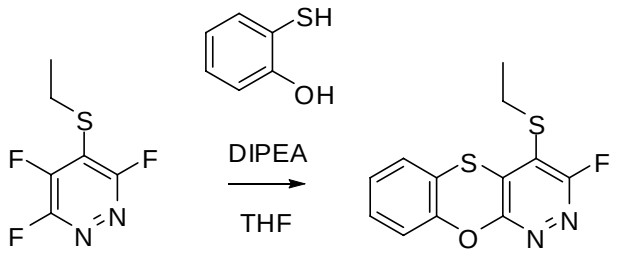

16 **39** 74%

Scheme 3.10

It was possible to grow crystals of the product that were suitable for analysis by X-ray crystallography, which confirmed the structure as shown below (Figure 3.3). It would appear that the initial attack is performed by the sulfur atom, further activating the intermediate to nucleophilic attack by the oxygen atom.

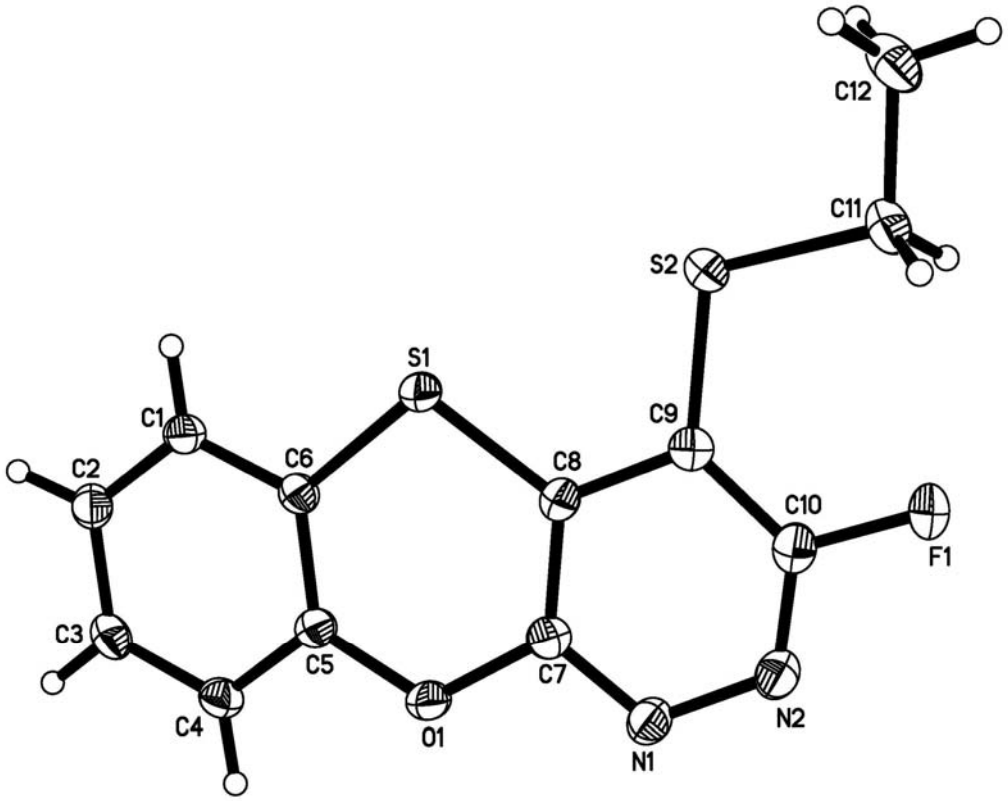

Figure 3.3

Reaction of 4-(ethylthio)-3,5,6-trifluoropyridazine **16** with 2-aminophenol at room temperature led to what appeared, by ^{19}F NMR spectroscopy, to be a difluorinated pyridazine, presumably the uncyclised intermediate. Microwave irradiation of the reaction mixture to an indicated temperature of 100 °C for a period of five minutes effected conversion to the tricyclic product **40** (Scheme 3.11).

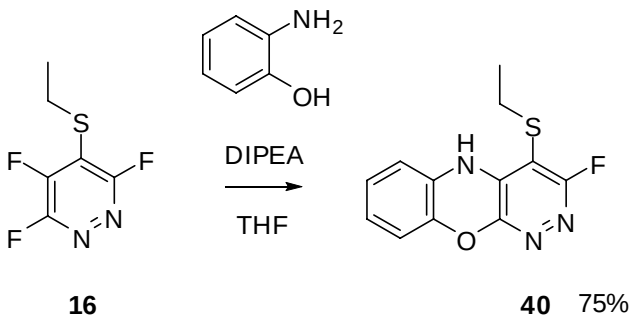

16 **40** 75%

Scheme 3.11

Once again it was possible to grow crystals suitable for X-ray crystallography, which demonstrated that the major product was 4-ethylsulfanyl-3-fluoro-10*H*-9-oxa-1,2,10-triaza-anthracene (Figure 3.4), formed via initial attack by nitrogen followed by cyclisation through oxygen, rather than the isomeric 4-ethylsulfanyl-3-fluoro-9*H*-10-oxa-1,2,9-triaza-anthracene.

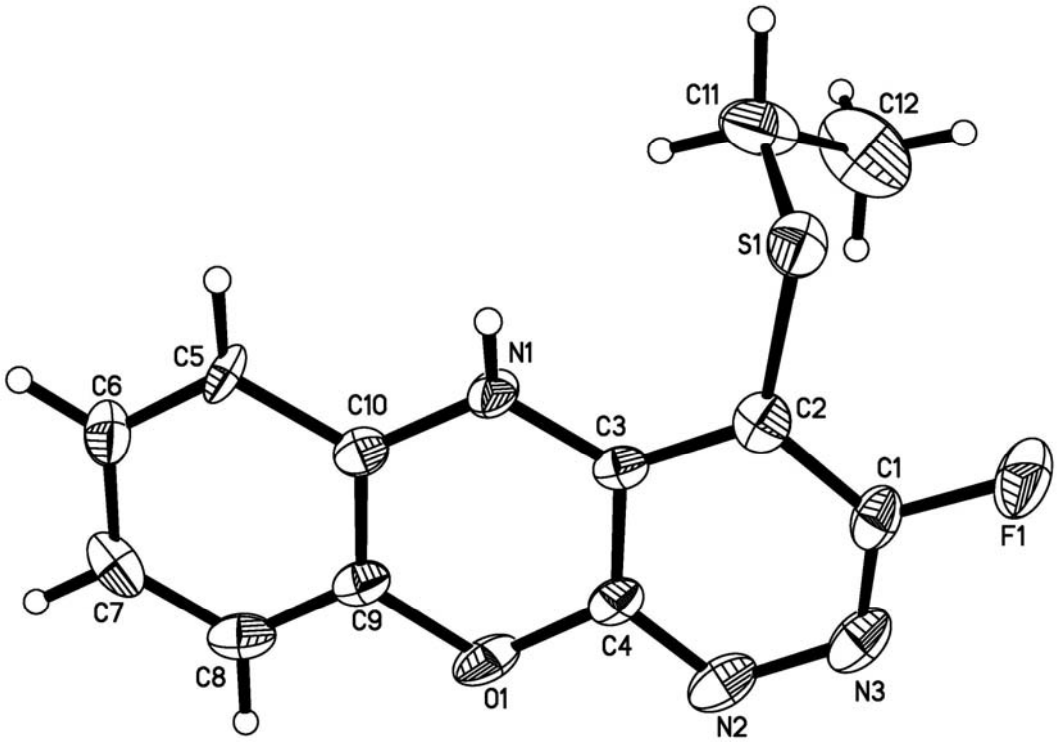

Figure 3.4

By comparing the structures of the two products above, it may be seen that the difference in reactivities may be rationalised by appreciating the differing effects of the substituents in the intermediate, as discussed in section 3.2. Also of note is the difference in reactivity between 4-(ethylthio)-3,5,6-trifluoropyridazine **16** and 4-(3,5,6-trifluoropyridazin-4-yl)morpholine **1**; while the former affords a ring fused product after reaction with 2-aminophenol, the deactivating character of the morpholino substituent in the latter made synthesis of the desired fused system impractical.

The third disubstituted benzene, 2-aminobenzenethiol, was also found to lead to the formation of a tricyclic product after microwave irradiation (Scheme 3.12). Although X-ray quality crystals could not be grown, analogy would suggest that the product is likely to be the result of initial attack by nitrogen, followed by cyclisation through sulfur, particularly

as initial attack by sulfur would be activating, giving reactivity similar to that seen for 2-mercaptophenol, and unlikely to require irradiation, as in the case of 2-aminophenol.

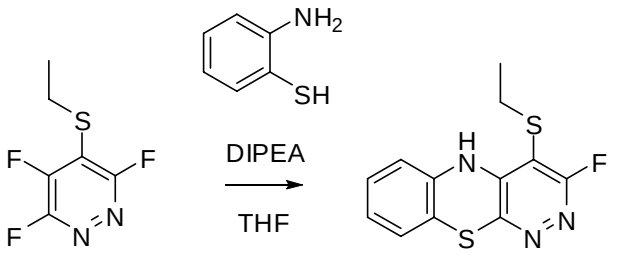

16 **41** 63%

Scheme 3.12

Encouraged by the increased reactivity shown by the thioethoxy- substituted trifluoropyridazine, we turned our attention back to the aminopyridines which had proved unsuitable for reaction with the nitrogen- substituted trifluoropyridazines.

Reaction of 4-(ethylthio)-3,5,6-trifluoropyridazine **16** with 2-aminopyridine, after microwave irradiation to an indicated temperature of 150 °C for thirty minutes, gave a moderate quantity of the aza-fluorene, assigned as 4-ethylsulfanyl-3-fluoro-1,2,4b,9-tetraaza-fluorene **42** as shown below (Scheme 3.13).

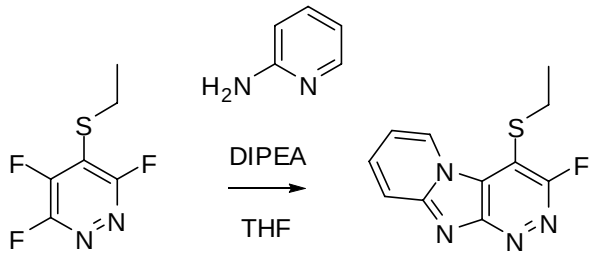

16 **42** 14%

Scheme 3.13

This regiochemistry is suggested by prior reactions between aminopyridines and perfluoropyridine derivatives, which have been shown to lead to products in which sp^3 hybridised nitrogen is attached to the site of initial nucleophilic attack.[4]

The slightly more nucleophilic 2-amino-3-picoline was also used, and in this case, although microwave irradiation proves useful in increasing the rate of reaction, complete conversion of starting material is observed after one week of stirring at room temperature (Scheme 3.14).

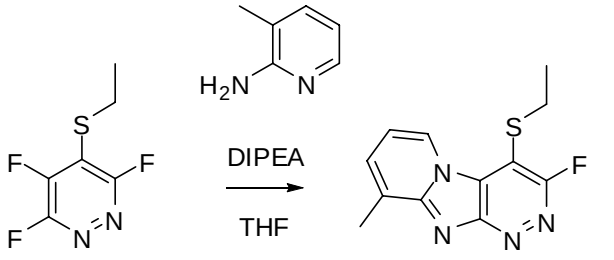

16 **43** 50%

Scheme 3.14

Recrystallisation of the product allowed elucidation of the structure by means of X-ray crystallography, confirming the geometry as shown (Figure 3.5).

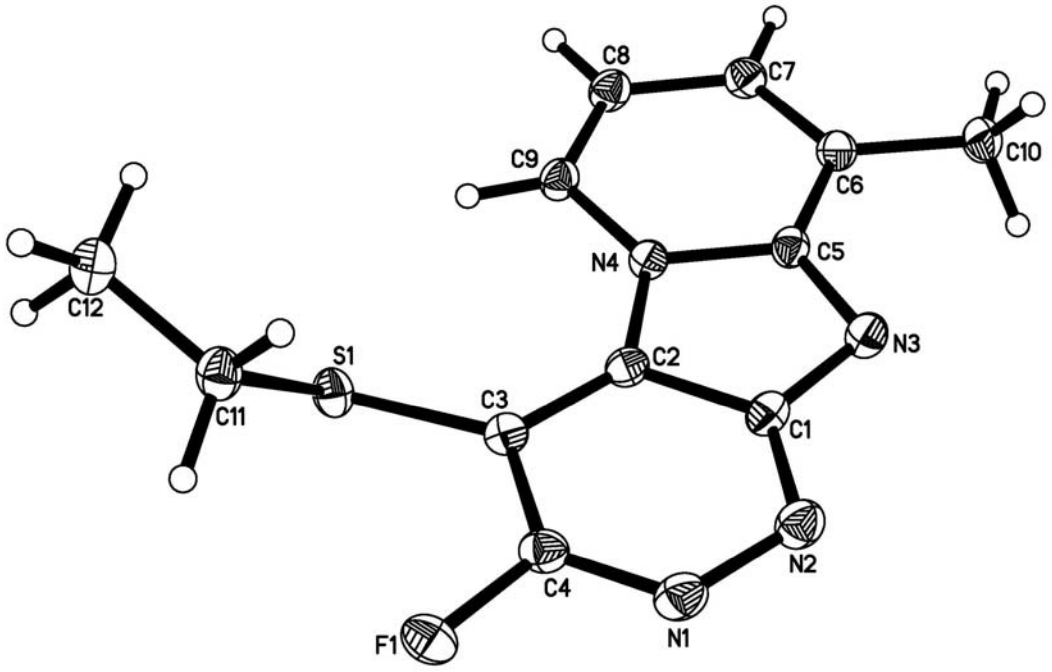

Figure 3.5

The final binucleophile employed was ethyl acetoacetate (Scheme 3.15). In contrast to its behaviour when combined with tetrafluoropyridazine, the reaction with 4-(ethylthio)-3,5,6-trifluoropyridazine **16** was very sluggish, requiring extended microwave irradiation to push the reaction to completion.

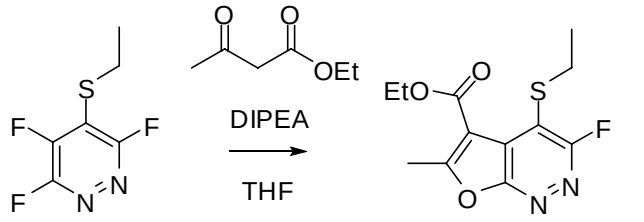

16 **44** 28%

Scheme 3.15

The structure of the product may be inferred by analogy with the behaviour observed when combining the nucleophile with tetrafluoropyridazine, as discussed in chapter 2, and from the known reactions of ethyl acetoacetate with similar polyfluorinated systems.[5]

3.5 Conclusions

In undertaking the work detailed in this chapter we set out to demonstrate the applicability of our synthetic approach to the formation of selectively functionalised fused heterocyclic systems. By combining binucleophiles with the class of trifluoropyridazines synthesised in chapter 2, we hoped to show that a variety of fused systems could be produced in a regiochemically controlled manner.

All the trifluoropyridazines used proved suitable for further derivatisation with at least some binucleophilic species, although there appears to be a considerable difference in reactivity depending on the nature of the substituent already in place, with electron donating substituents causing a marked decrease in the electrophilicity of the heterocycle.

A number of asymmetrical binucleophiles have been employed, and reactions have tended to lead to a single isolated product in reasonable to good yield, demonstrating not only good selectivity between the electrophilic sites of the pyridazine, but also the nucleophilic sites of difunctional attacking species.

While the number of reactions covered in this chapter is relatively small, the principle by which we envisioned creating a library of fused systems has been demonstrated. Combination of suitable examples of trifluoropyridazines and binucleophiles will allow generation of diverse families of fused fluoroheterocycles, which may in themselves be of interest as potential drug candidates, or be amenable to further derivatisation.

3.6 References

1 G. W. Bemis and M. A. Murcko, *J. Med. Chem.*, 1996, **39**, 2887.

2 G. Sandford, R. Slater, D. S. Yufit, J. A. K. Howard, and A. Vong, *J. Org. Chem.*, 2005, **70**, 7208.

3 R. D. Chambers, J. A. H. MacBride, and W. K. R. Musgrave, *J. Chem. Soc. (C)*, 1968, 2116.

4 M. W. Cartwright, L. Convery, T. Kraynck, G. Sandford, D. S. Yufit, J. A. K. Howard, J. A. Christopher, and D. D. Miller, *Tetrahedron*, 2010, **66**, 519.

5 M. W. Cartwright, E. L. Parks, G. Pattison, R. Slater, G. Sandford, I. Wilson, D. S. Yufit, J. A. K. Howard, J. A. Christopher, and D. D. Miller, *Tetrahedron*, 2010, **66**, 3222.

Chapter 4

Reactions of Tetrabromothiophene

4.1 Background

While the previous two chapters of this thesis have been concerned with the reactions of highly halogenated pyridazines, we were also interested in applying the methodology already laid out to five-membered heterocyclic systems, particularly thiophene. In contrast to prior efforts, this chapter will focus on the chemistry of perbrominated systems, for two reasons. Firstly, perfluorinated examples of the five-membered heterocycles are either unknown, or difficult to synthesise and unstable.[1] Secondly, by moving from perfluorinated to perbrominated systems, the possibilities of performing metal-halogen exchange reactions and metal-mediated cross-couplings are introduced, widening the range of products potentially available.

A survey of the literature concerning perbrominated five-membered heterocycles reveals the paucity of published reactions. Tetrabromopyrrole has been N-methylated,[2] and the only reactions of tetrabromofuran recorded are oxidations, such as its solid-state photo-oxidation to a γ-lactone and its photo-oxidation to dibromomaleic anhydride in benzene.[3, 4]

There is a little more information about perbromothiophene and its reactions. It is synthesised in good yield by action of elemental bromine on thiophene.[5] The stability and relative ease of handling of thiophenes has meant that they have seen a variety of uses. Perbromothiophene is often encountered as a precursor of polycyclic compounds such as porphyrins,[6] dithienothiophenes,[7, 8] and TTF-type compounds.[9]

Porphyrin synthesis involves conversion of the tetrabromothiophene into 3,4-dibromothiophene, which can be arylated using a Grignard reagent, and then lithiated before undergoing a series of couplings and condensations to yield the porphyrin product, giving an indication of how this system can be used for the synthesis of polyfunctional species by sequential displacement of the four bromine atoms (Scheme 4.1).

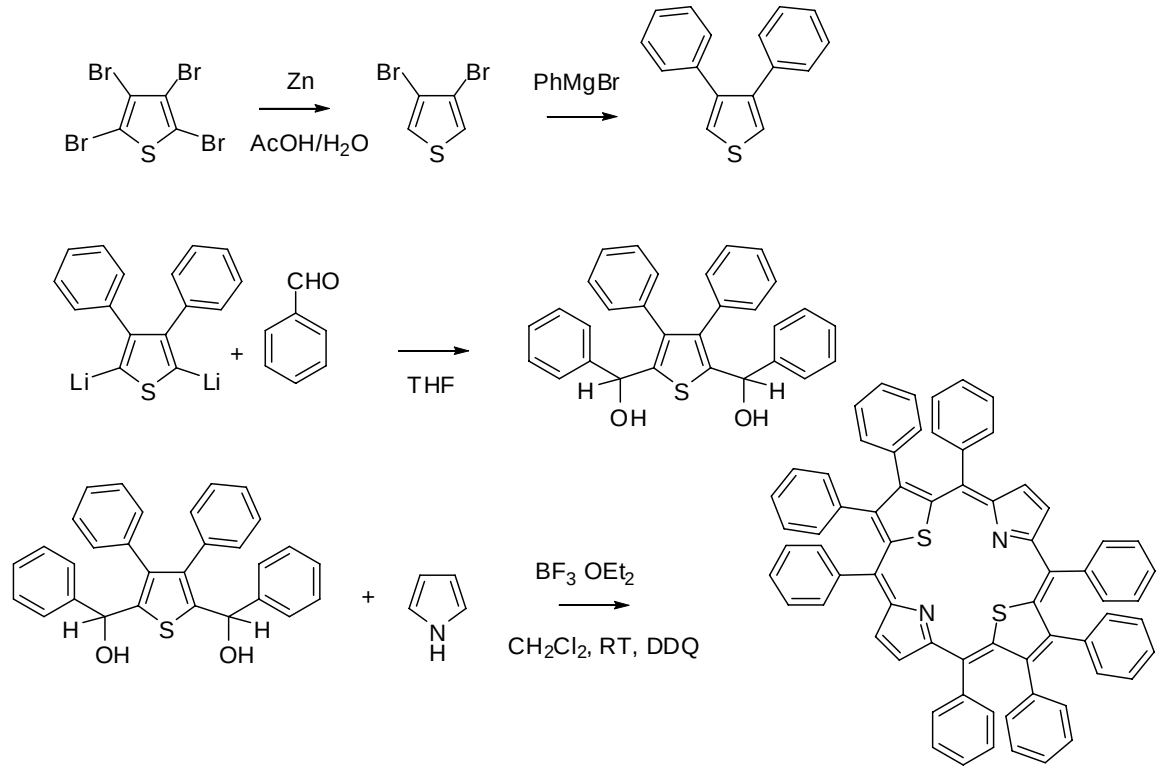

Scheme 4.1

Conceptually, syntheses of other large polycyclic molecules follow the same pattern: reaction with one reagent at the favoured 2- and 5-positions, followed by further reaction at the 3- and 4-positions, and then often some kind of condensation or ring closing reaction to generate the desired target.

Finally, tetrabromothiophene has also been used in palladium coupling reactions, both Sonogashira[10] and Suzuki-Miyaura[11] type. As in previous reactions, the 2- and 5-positions are substituted first, and the 3- and 4-positions can subsequently be functionalised with a different side group (Scheme 4.2).

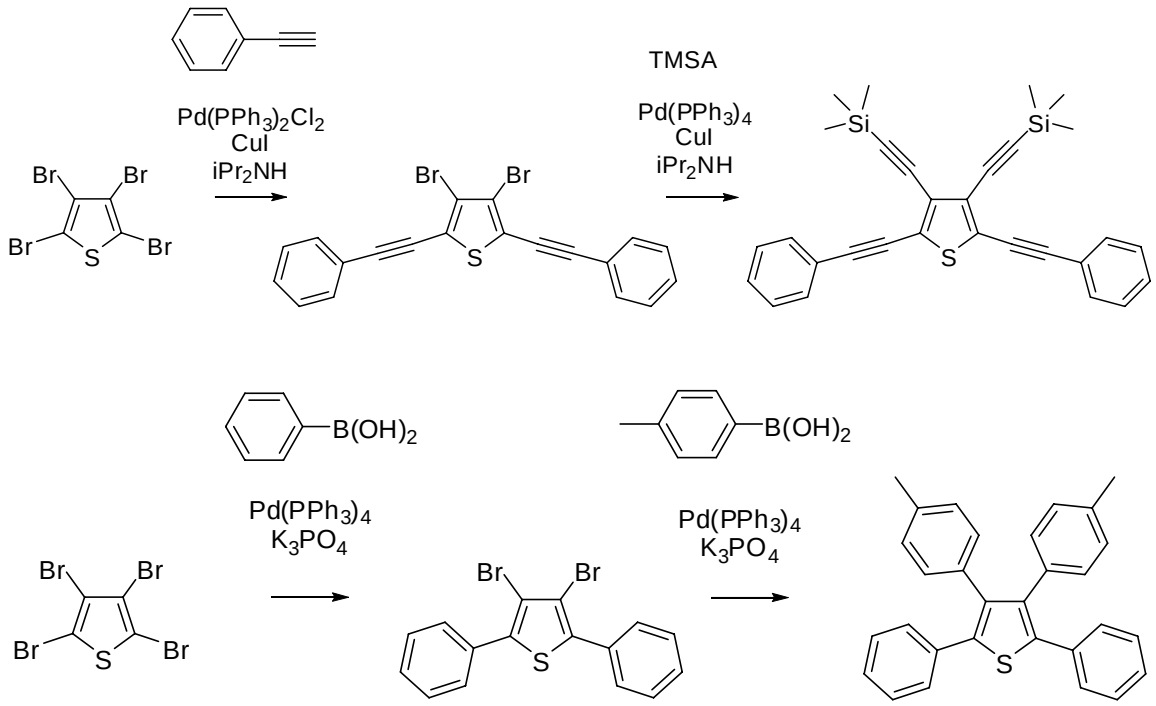

Scheme 4.2

In summary, it has been seen that tetrabromothiophene is a good substrate for metal-mediated cross-coupling reactions, although relatively few examples of its use as such appear in the literature. With the addition of lithium-halogen exchange reactions and the possibility of nucleophilic aromatic substitution chemistry, tetrabromothiophene seems a promising substrate on which to conduct investigation into sequential substitution for the purpose of synthesis of polyfunctional systems.

4.2 Aims and Approach

As discussed in previous chapters, this thesis is concerned with developing versatile, general methodology for the synthesis of a wide range of polyfunctionalised and selectively fluorinated heterocyclic systems from perhalogenated starting materials. This chapter will focus on our attempts to apply our approach to the functionalisation of the perbrominated thiophene scaffold.

By applying nucleophilic aromatic substitution conditions, as demonstrated in the preceding chapters, alongside metal-mediated coupling reactions and debromolithiations followed by trapping with suitable electrophiles, we hope to be able to gain access to diverse multi-substituted heterocycles.

For example, the scheme below (Scheme 4.3) shows a few examples of the molecules that may be prepared in this way. Included are three simple processes: nucleophilic substitution; Suzuki-Miyaura cross-coupling; and lithium-halogen exchange followed by reaction with F^+ or other suitable electrophiles.

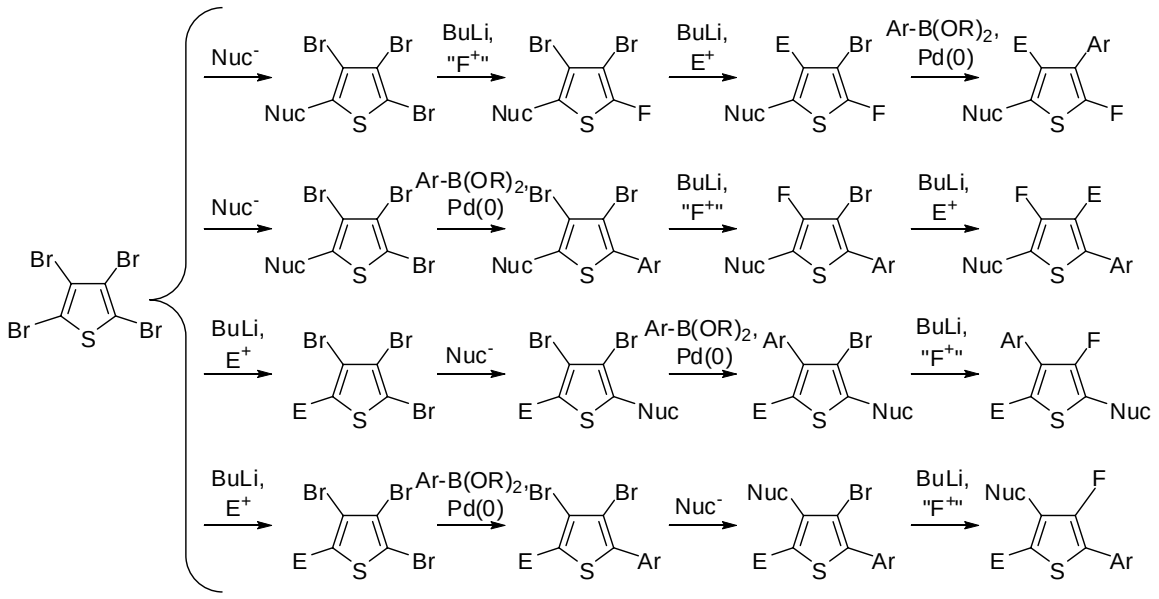

Scheme 4.3

By altering the order in which these processes are performed, it should be possible to create a range of substituted five-membered heterocycles, and also establish a mechanistic rationale for the substitution pattern.

4.3 Fluorination of Bromothiophenes

Among the processes we wanted to perform on tetrabromothiophene was the exchange of bromine for fluorine, and we envisaged this transformation taking place by way of lithium halogen exchange followed by trapping with a source of electrophilic fluorine, such as Selectfluor®.

Before performing this reaction on tetrabromothiophene, we wanted to establish its applicability, and as such we carried the process out on various mono-brominated thiophene derivatives.

Initial experiments, utilising *n*-butyllithium as the lithiating agent in THF, and Selectfluor® as the source of "F^+", proved unsuccessful, most probably due to the insolubility of the fluorinating agent in the reaction medium.

Changing the fluorinating agent to *N*-fluorobenzenesulfonimide (NFSI), which is readily soluble in THF, allowed encouraging results to be obtained (Table 4.1). Both 2- and 3-bromothiophene could be converted to the corresponding fluoroheterocycles by treatment with *n*-butyllithium and then addition of a solution of fluorinating agent in THF, followed by slow warming to room temperature from -78 °C.

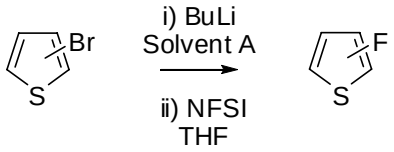

Starting material	Solvent A	Product	Yield[a] (%)
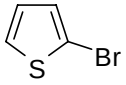	THF	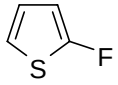 **45**	80
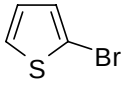	ether	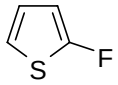 **45**	85
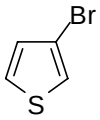	THF	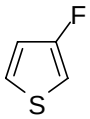 **46**	36
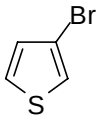	ether	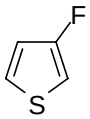 **46**	50

[a] By ^{19}F NMR spectroscopy

Table 4.1

With the entire process conducted in THF, 2-bromothiophene could be converted to the fluorothiophene **45** in 80% yield (determined by ^{19}F NMR spectroscopy of the reaction mixture with respect to an internal reference). However, isolation of the appreciably volatile fluorinated product from the reaction medium proved difficult. Similarly, 3-bromothiophene was converted to its fluorinated counterpart **46** in 36% yield. Performing

the lithiation in diethyl ether (in which NFSI is only sparingly soluble) increases the yields to 85 and 50% respectively.

With conversion from bromothiophene to fluorothiophene successfully achieved, we next turned to the investigation of the reactions of some substituted bromothiophenes. Our first substrate was 2-bromo-5-nitrothiophene, the reaction of which (Scheme 4.4) failed to produce any of the desired product, with a large volume of tarry, intractable material produced.

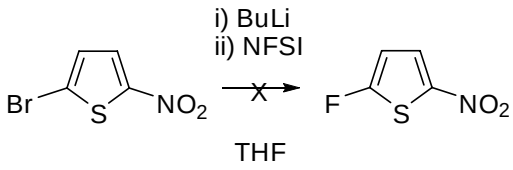

Scheme 4.4

Subsequently, a selection of substituted bromothiophenes were subjected to the fluorination conditions described above, and found to give the desired fluoroheterocycles in moderate to good yields, as shown in the table below (Table 4.2).

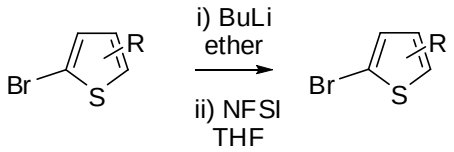

Starting material	Product	Yield[a] (%)
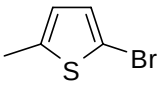	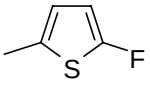 **47**	88
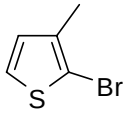	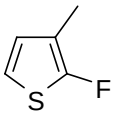 **48**	78
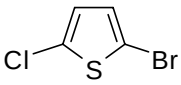	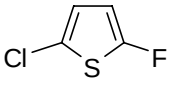 **49**	43
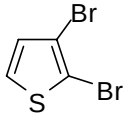	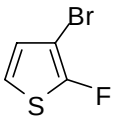 **50**	65

[a] By ^{19}F NMR spectroscopy

Table 4.2

The two methylated bromothiophene materials gave similar results to those observed for the 2-bromothiophene example. In the case of 2-bromo-5-methylthiophene, the presence of the methyl group raises the yield of fluorinated product from 80 to 88%, which may be rationalised by the increased electron density of the thienyl anion improving reactivity towards the electrophile. With the methyl group in the 3-position, the yield is slightly lower

than that observed for the unmethylated 2-bromothiophene, at 78%, most likely due to steric hindrance to reaction.

In contrast to the addition of methyl groups, the presence of electron-withdrawing halogen substituents leads to a marked decrease in yields. The fluorination of 2-bromo-5-chlorothiophene led to the formation of a single fluorinated heterocycle **49** in low yield, indicating the effect of electron-withdrawing substituents, but also demonstrating the selectivity possible when performing lithium halogen exchange on a substrate bearing different halogen atoms.

Finally, fluorination of 2,3-dibromothiophene afforded the fluorinated product **50** in 65% yield, which when compared to the yield achieved in the fluorination of 2-bromothiophene, demonstrates a reduction which may be attributed to both steric and electronic effects. Once again, only a single fluorinated thiophene product was observed, showing the excellent regioselectivity possible in these situations.

4.4 Reactions of Perbromothiophene

Having confirmed possibilities for functionalisation afforded by lithiation of bromothiophenes, we moved our focus to the chemistry of perhalogenated systems, in keeping with the theme of this thesis. Perbromothiophene **51** was readily prepared from the parent heterocycle by simple bromination, following literature procedure (Scheme 4.5).[5]

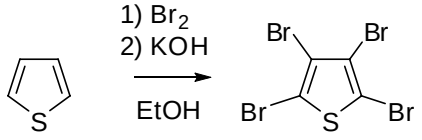

51 63%

Scheme 4.5

With our perhalogenated substrate in hand, we undertook a series of experiments aimed at establishing the viability of a number of methods for producing functionalised compounds.

4.4.1 Debromolithiations

Bearing in mind our previous results indicating the reduced yields encountered when lithiating and then fluorinating bromothiophenes bearing electron-withdrawing or sterically hindering groups, we anticipated potential problems with our perbrominated species, and as such initial experiments with the perbrominated thiophene involved trapping with H^+, as we expected the proton to be particularly readily attacked by our nucleophilic intermediate.

Lithium halogen exchange followed by the addition of dilute hydrochloric acid gave the desired 2,3,4-tribromothiophene **52** in reasonable yield (Scheme 4.6).

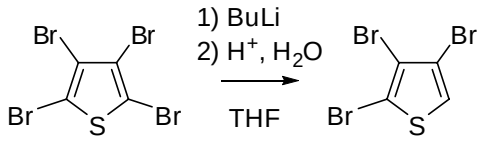

51 **52** 82%

Scheme 4.6

Encouraged by confirmation that lithiation of the perhalogenated heterocycle and subsequent trapping with an electrophile was possible in our hands, we expanded the range of electrophiles employed in order to further explore the tolerances of the process. Our results are shown in the following table (Table 4.3).

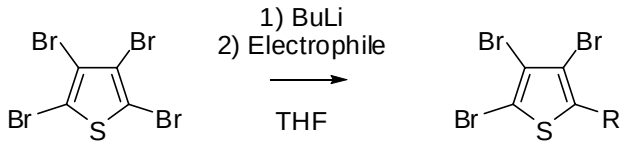

Electrophile	Product	Yield (%)
iodomethane	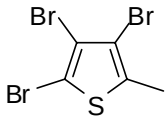 **53**	53
1-iodoheptane	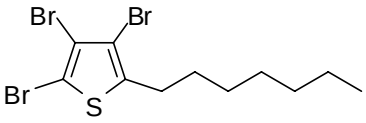	trace
benzyl bromide	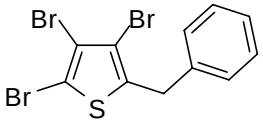	trace
NFSI	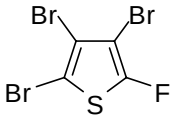	0

Table 4.3

The reaction of the thienyllithium lithium species with iodomethane gives the 2-methyl substituted tribromothiophene **53** in sufficient yield for it to be recrystallised from the organic extract of the crude reaction mixture. The structure of the product was confirmed by X-ray crystallography (Figure 4.1).

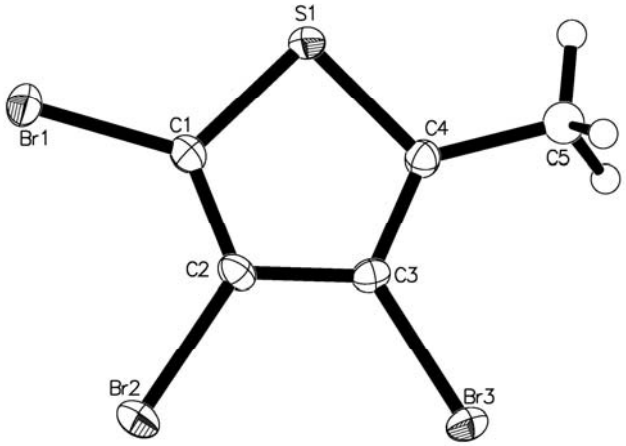

Figure 4.1

Moving from the unhindered iodomethane to the considerably bulkier 1-iodoheptane resulted in a marked decrease in the amount of product formed, and while the presence of the desired product could be surmised from GC-MS analysis of the reaction mixture, isolation of the product from the highly complex mixture was not achieved.

A similar result was observed when the electrophile employed was benzyl bromide. Once again, although GC-MS indicated that small quantities of the desired product were present, isolation of the pure compound could not be accomplished.

The final electrophile listed in the above table, NFSI, proved less reactive still. The reaction resulted in the formation of a highly complex mixture of products, within which the desired compound was not observed by either GC-MS or ^{19}F NMR spectroscopic analysis.

In conclusion, it would appear that the low yields of products arising from debromolithiation and trapping with electrophiles, coupled with the difficulties encountered during product isolation, make this approach unsuitable for, for example, parallel synthesis techniques.

4.4.2 Reactions with Nucleophiles

The next class of reactions that we wanted to explore, in keeping with the procedures described in the preceding chapters, was that involving the behaviour of tetrabromothiophene with nucleophiles. While bromothiophenes do not at first look as promising as fluoropyridazines for the purposes of functionalisation by nucleophilic aromatic substitution, there are some precedents in the literature, involving nucleophilic attack on electron deficient bromothiophenes (Scheme 4.7).[12]

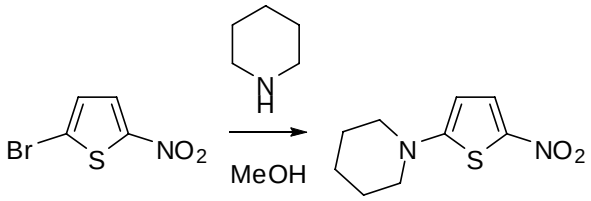

Scheme 4.7

It was envisaged that our perhalogenated substrates may act as electrophiles (Scheme 4.8), allowing the preparation of multiply substituted products by a series of nucleophilic aromatic substitutions.

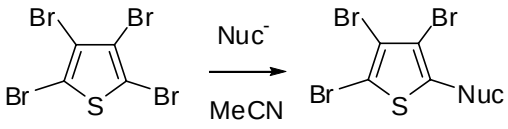

Scheme 4.8

Initial reactions were performed with sodium alkoxides, and reactions under reflux led to the formation of tribromothiophene **52**, rather than the desired ethers, most probably as a result of bromophilic attack on the substrate (Scheme 4.9).[13]

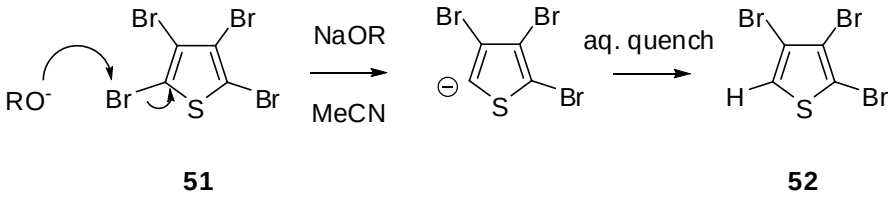

51 **52**

Scheme 4.9

Similar results were observed for the reactions of tetrabromothiophene with sodium thioethoxides, while reflux in the presence of amine nucleophiles failed to give conversion from starting materials.

It would appear that tetrabromothiophene is an unsuitable scaffold for the purposes of generating libraries of polyfunctionalised heterocyclic systems via sequential nucleophilic aromatic substitutions, and no further nucleophilic substitutions were attempted.

4.4.3 Buchwald-Hartwig and Ullmann-Type Reactions

Following the disappointing results of our investigation into the reactions of tetrabromothiophene with nucleophiles, we turned to possible alternative routes to the desired target compounds. Two obvious contenders were the Buchwald-Hartwig and Ullmann reactions, which allow the synthesis of bifunctional ethers and amines from a variety of bromo-aromatic starting materials.

The Buchwald-Hartwig amination was explored for perbromothiophene using both primary and secondary amines, and various bases, but no conversion to the desired products was observed under any of the reaction conditions (Scheme 4.10).

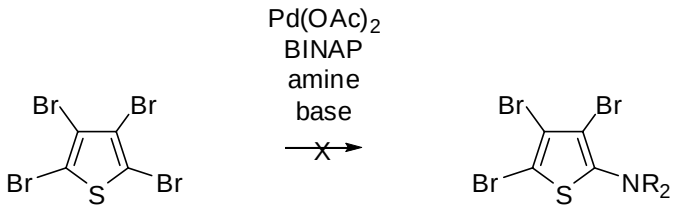

51

Scheme 4.10

The alternative approach, the copper-catalysed Ullmann reaction, was also attempted and again, we failed to observe any of the desired products in the reaction mixture (Scheme 4.11).

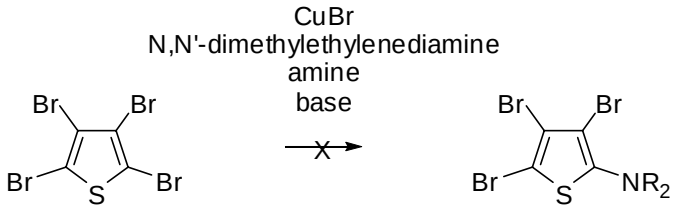

51

Scheme 4.11

With these approaches appearing unsuitable, it is apparent that the formation of thiophene-heteroatom bonds remains elusive, certainly compared to the slightly more readily achievable carbon-carbon bond forming processes.

4.4.4 Suzuki-Miyaura Reactions

Having touched upon metal-catalysed coupling reactions in the previous section, we also wanted to explore the Suzuki-Miyaura cross-coupling of tetrabromothiophene, with the intention of forming new carbon-carbon bonds for functionalisation purposes.

As outlined at the beginning of this chapter, Suzuki couplings of tetrabromothiophenes have been reported, but generally with the purpose of producing symmetrically disubstituted products. As elsewhere in this thesis, we were primarily concerned with achieving selective monosubstitution, and as such we performed the coupling reaction between tetrabromothiophene **51** and a single equivalent of phenylboronic acid in the presence of five molar % $Pd(PPh_3)_4$ and a variety of solvents and bases, in order to determine the optimum conditions for reaction. The results of this screening process, with conversion from starting material and yield of monosubstituted product **54** as determined by GC-MS analysis, are tabulated below (Table 4.4).

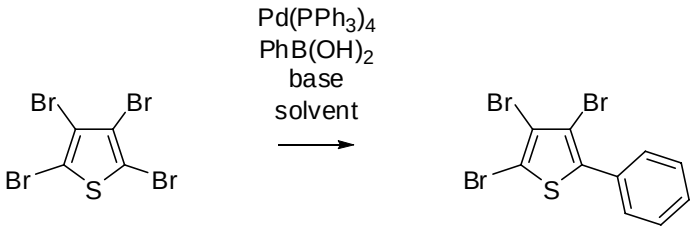

51 **54**

Base	Solvent	Conversion (%)	Yield (%)
K_2CO_3	toluene	93	81
K_2CO_3	DMF	93	72
K_2CO_3	THF	32	21
K_2CO_3	IPA	100	45
K_2CO_3	MeCN	57	57
KF	toluene	63	60
KF	DMF	81	64
KF	THF	0	0
KF	IPA	56	56
KF	MeCN	28	28
Na_3PO_4	toluene	86	74
Na_3PO_4	DMF	100	62
Na_3PO_4	THF	67	43
Na_3PO_4	IPA	84	62
Na_3PO_4	MeCN	74	74
$Ba(OH)_2$	toluene	3	3
$Ba(OH)_2$	DMF	84	54
$Ba(OH)_2$	THF	20	20
$Ba(OH)_2$	IPA	100	0
$Ba(OH)_2$	MeCN	0	0

Table 4.4

It will be noted that the best results were seen when potassium carbonate was used as the base, in a medium of toluene. Although in some cases reasonable yields were achieved, isolation of the products was arduous. The persistent presence of tetrabromothiophene and disubstituted products alongside the desired monosubstituted product, coupled with the low, and similar, affinity all three show towards stationary phases during chromatography, makes separation of the products impractical, and this approach, certainly for symmetrically halogenated thiophenes, does not seem suitable for our purposes.

4.5 Conclusions

At the start of this chapter we set out our aims in the area of the chemistry of bromothiophenes, which were to investigate the feasibility of nucleophilic substitutions, metal-catalysed cross-couplings, and debromolithiations followed by trapping with electrophiles. Despite some encouraging results, tetrabromothiophene seems a far less accommodating scaffold than tetrafluoropyridazine.

Debromolithiation of tetrabromothiophene has been demonstrated, and the thienyllithium anion has been trapped using a number of electrophiles, with varying degrees of success. While tribromothienyllithium requires the application of fairly reactive non sterically hindered electrophiles, reactions of less highly halogenated bromothiophenes have proved successful even with the comparatively unreactive NFSI, and trends in reactivity and regioselectivity of mono- and di-brominated thiophenes have been shown.

Reactions with nucleophiles have been disappointing, in contrast to our earlier studies of the reactions of perfluorinated systems, and nucleophilic aromatic substitution of tetrabromothiophene does not seem feasible due to competing bromophilic attack.

Finally, metal-mediated couplings have shown mixed results. While Buchwald-Hartwig and Ullmann-type reactions have thus far proved unsuccessful, Suzuki-Miyaura cross-couplings have allowed us to produce mono-arylated thiophenes in moderate yields.

4.6 References

1 J. Burdon, J. G. Campbell, I. W. Parsons, and J. C. Tatlow, *Chem. Commun.*, 1969, 27.

2 G. d. Varda, *Ber. Deut. Chem. Ges.*, 1888, **21**, 2871.

3 C. W. Shoppee, *J. Chem. Soc. Perk. T. 1*, 1985, 45.

4 C. W. Shoppee and W. Y. Wu, *Aust. J. Chem.*, 1987, **40**, 1137.

5 K. Araki, H. Endo, G. Masuda, and T. Ogawa, *Chem. Eur. J.*, 2004, **10**, 3331.

6 N. Agarwal, S. P. Mishra, A. Kumar, and M. Ravikanth, *Chem. Lett.*, 2003, **32**, 744.

7 J. Frey, A. D. Bond, and A. B. Holmes, *Chem. Commun.*, 2002, 2424.

8 E. Ertas and T. Ozturk, *Tetrahedron Lett.*, 2004, **45**, 3405.

9 K. Kobayashi, *Chem. Lett.*, 1985, 1423.

10 C. C. Tsou and S. S. Sun, *Org. Lett.*, 2006, **8**, 387.

11 T. T. Dang, N. Rasool, T. T. Dang, H. Reinke, and P. Langer, *Tetrahedron Lett.*, 2007, **48**, 845.

12 G. Consiglio, D. Spinelli, S. Gronowitz, A.-B. Hornfeldt, B. Maltesson, and R. Noto, *J. Chem. Soc., Perk. T. 2*, 1982, 625.

13 R. C. Mebane, K. M. Smith, D. R. Rucker, and M. P. Foster, *Tetrahedron Lett.*, 1999, **40**, 1459.

Chapter 5

Conclusions

This thesis has described the synthesis of a number of functionalised heterocyclic systems from halogenated heterocyclic precursors. As described in the introduction, versatile routes towards multiply functionalised heterocyclic cores are potentially valuable tools for the rapid exploration of new regions of chemical space, with particular emphasis on the discovery of medicinal molecules by rapid analogue synthesis of large numbers of drug-like compounds.

Tetrafluoropyridazine has been shown to be an excellent scaffold for the generation of highly functionalised species by sequential nucleophilic aromatic substitution processes. Reactions with a wide range of mononucleophiles have been demonstrated, the majority of which give good yields and high levels of regioselectivity (Scheme 5.1).

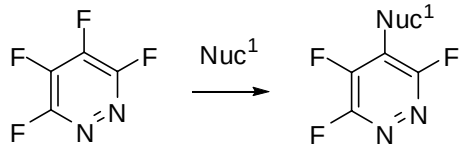

47 - 82%

Nuc^1 = amines, alcohols, ethanethiol, phenyl

Scheme 5.1

The effects directing nucleophilic aromatic substitutions in tetrafluoropyridazine have been discussed, and toleration of a number of nucleophilic species has been demonstrated.

After the first functionalisation is performed, some of the resultant trifluoropyridazine systems may be reacted again to further diversify the range of possible products. Reactions of ethylsulfanyl- substituted trifluoropyridazines with tethered difunctional nucleophiles give rise to ring-fused pyridazine systems, whose skeletal forms suggest pharmacological potential (Scheme 5.2).

Scheme 5.2

Alternatively, second substitutions may be performed using another mononucleophile to produce a difunctionalised difluoropyridazine system (Scheme 5.3). In this case, both the directing effect of the first substituent, and the character of the incoming nucleophile need to be understood to rationalise the results of reactions, with different substitution patterns being the potential result of changing the order in which nucleophiles are applied to the fluoropyridazine core. For example, to produce a pyridazine substituted at the 4- and 5-positions with ether and thioether functionalities, the various directing effects suggest that the first reaction should be with an alcohol, followed by second substitution using a thiol. The behaviour described in chapter 3 suggests that a wide range of difunctionalised difluoropyridazines should be accessible through these simple nucleophilic aromatic substitution processes.

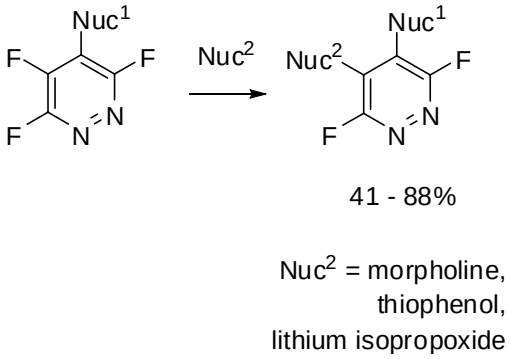

Scheme 5.3

Third substitutions of fluoropyridazines have also been demonstrated, leading to highly functionalised monofluorinated pyridazine systems. In these cases, reactions become more difficult as the less electrophilic pyridazine ring becomes decreasingly susceptible to nucleophilic attack, and the regioselectivity of the reaction suffers. Despite this, a regioselective substitution reaction of a difluoropyridazine system has been demonstrated, showing not only that tetrafluoropyridazine is amenable to at least three sequential functionalisation reactions (Scheme 5.4), but also that high regioselectivity can be carried through this process.

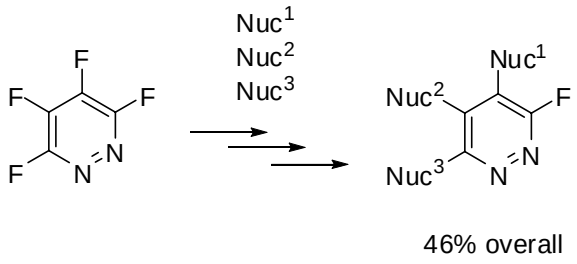

Scheme 5.4

The ready reactivity of tetrafluoropyridazine with both monofunctional and tethered bifunctional nucleophilic species suggests that it could be an excellent scaffold from which

to build libraries of highly functionalised heterocyclic compounds, which could be of particular use to the pharmaceutical industry.

We have also applied our approach to the generation of a range of highly functionalised heterocyclic compounds from a halogenated scaffold to tetrabromothiophene. As yet, our results are comparatively disappointing. The nucleophilic aromatic substitution processes which work so well for tetrafluoropyridazine do not seem applicable to tetrabromothiophene, due to the lower electrophilicity of the system, and competing bromophilic attack.

Attempts to synthesise the desired products via metal-mediated coupling chemistry have proved unsuccessful, although carbon-carbon bond forming processes proceed well. Monofunctionalisation by this route is hampered by the formation of intractable product mixtures, the result of statistical attack on a symmetrical substrate.

Finally, lithiations of bromothiophenes produce encouraging results, with mono- and di-bromo thiophenes being lithiated and trapped in good yields. Lithiation of tetrabromothiophene goes similarly smoothly, but the thienyl anion has proven resistant to trapping by electrophiles, requiring reactive, sterically undemanding species with which to react.

While the apparent obstacles to the use of tetrabromothiophene as a scaffold for the synthesis of libraries of highly functionalised heterocycles may not be insurmountable, it is clear that the possibilities offered by tetrafluoropyridazine are far more promising, having demonstrated that a multitude of heterocyclic systems of potential biological interest can be produced using simple and readily rationalised nucleophilic aromatic substitution processes.

Chapter 6

Experimental

6.1 Technical Details

All starting materials were obtained commercially (ABCR, Alfa-Aesar, Fluorochem, Lancaster, Sigma-Aldrich) or from GlaxoSmithKline's chemical stores, Stevenage. Solvents were dried using either literature procedures or via the Innovative Technology solvent purification system.

Microwave reactions were performed on a Biotage Initiator 60 EXP. Mass directed HPLC was performed on a Supelco LCABZ++ column using MicroMass MassLynx v4.0 software.

Melting points were recorded using a Gallenkamp melting point apparatus at atmospheric pressure and are uncorrected.

IR spectra were recorded using a Perkin Elmer 1600 Series FTIR using a Golden Gate attachment and analysed using GRAMS Analyst software.

NMR spectra were recorded in deuterated chloroform, unless otherwise stated, using tetramethylsilane and trichlorofluoromethane as internal references on a Varian Mercury 400, Bruker Avance 400, or Bruker DPX400 operating at 400 MHz (^{1}H NMR), 376 MHz (^{19}F NMR), and 100 MHz (^{13}C NMR), or a Varian Inova 500 operating at 500 MHz (^{1}H NMR), 470 MHz (^{19}F NMR), and 125 MHz (^{13}C NMR), or a Varian VNMRS-700 operating at 700 MHz (^{1}H NMR), 658 MHz (^{19}F NMR), and 175 MHz (^{13}C NMR). Chemical shifts are given in ppm and coupling constants are recorded in Hz.

Mass spectra were recorded on a Thermo-Finnigan Trace GCMS spectrometer, a Micromass LCT LC-MS spectrometer, a Waters Xevo QTOF spectrometer, or a Waters ZQ mass spectrometer coupled to a Waters Acquity HPLC system. Exact mass measurements were performed on a Thermo-Finnigan LTQ-FT spectrometer, a Bruker Daltonics 7T FTICR-MS or a Micromass Q-TOF hybrid quadrupole mass spectrometer.

Elemental analyses were obtained using an Exeter Analytical E-440 Elemental Analyser, or by Butterworth Laboratories Ltd. Teddington, UK.

All crystallographic data were collected on a Bruker SMART-6000 CCD (λMoKα, ω-scan, 0.3° / frame) at T = 120K. The structures were solved using direct methods and refined by full-matrix least squares on F^2 for all data using SHELXTL software. All non-hydrogen atoms were refined with anisotropic displacement parameters, H-atoms were located on the difference map and refined isotropically.

6.2 Experimental to Chapter 2

4-(3,5,6-Trifluoro-pyridazin-4-yl)morpholine **1**

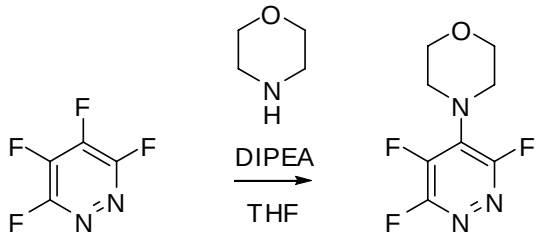

1

DIPEA (1.35 mL, 7.73 mmol) and morpholine (0.45 mL, 5.17 mmol) were added to a stirred solution of tetrafluoropyridazine (781 mg, 5.14 mmol) in THF (10 mL) at 0 °C under nitrogen, and the clear solution was stirred at 0 °C for 2 hours. The mixture was then concentrated *in vacuo*, partitioned between EtOAc and water, the phases were separated

and the aqueous phase was extracted with EtOAc. The combined organic phases were concentrated *in vacuo* to give approx. 1.4g of a light yellow oil. TLC (of the crude reaction NMR sample) showed Rf = 0.34 in 1:1 EtOAc / cyclohexane. Purification by Biotage SP4, 12+M SiO2 column (initial solvent - cyclohexane (2 column volumes), then a gradient elution over 10 CV's (cyclohexane to 80% EtOAc in cyclohexane)) gave *4-(3,5,6-trifluoro-4-pyridazinyl)morpholine* **1** (908 mg, 81%) as white crystals; mp 34.5 – 36.1 °C (Found: $[MH]^+$, 220.06923. $C_8H_8F_3N_3O$ requires: $[MH]^+$, 220.06922); ν_{max}(film)/cm^{-1} 2970.3, 2902.1, 2860.8 and 1595.1; δ_H 3.54 (4 H, br s, CH_2N), 3.80 – 3.86 (4 H, m, CH_2O); δ_C 50.12 (t, $^4J_{CF}$ 4.4, CH_2N), 66.71 (s, CH_2O), 129.29 (ddd, $^2J_{CF}$ 24.8, 3.2, $^3J_{CF}$ 3.2, C-4), 139.72 (ddd, $^1J_{CF}$ 270.8, $^2J_{CF}$ 28.8, $^3J_{CF}$ 9.6, C-5), 156.85 (dd, $^1J_{CF}$ 240.5, $^3J_{CF}$ 12.0, C-3), 157.98 (dd, $^1J_{CF}$ 240.5, $^2J_{CF}$ 3.2, C-6); δ_F -143.82 – -143.35 (1F, m, F-5), -98.62 (1 F, dd, $^3J_{FF}$ 31.0, $^5J_{FF}$ 26.4, F-6), -80.82 (1 F, dd, $^4J_{FF}$ 28.7, $^5J_{FF}$ 26.4 F-3); *m/z* (ES^+) 220 ($[MH]^+$, 100%).

N,N-diethyl-3,5,6-trifluoro-4-pyridazinamine **2**

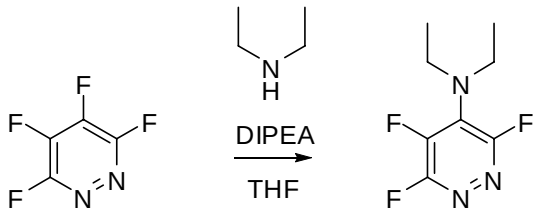

2

DIPEA (1.33 mL, 7.64 mmol) and diethylamine (0.53 mL, 5.09 mmol) were added to a stirred solution of tetrafluoropyridazine (774 mg, 5.09 mmol) in THF (10 mL) at 0 °C under nitrogen, and the clear solution was stirred at 0 °C for 4 hours. The mixture was then concentrated *in vacuo*, partitioned between EtOAc and water, the phases were separated and the aqueous phase was extracted with EtOAc. The combined organic phases were concentrated *in vacuo* to give approx. 1.2 g of a yellow oil. TLC (of the crude reaction NMR sample) showed Rf = 0.2 in 1:9 EtOAc / cyclohexane. Purification by Biotage SP4, 25+S SiO2 column (initial solvent – 3% EtOAc in cyclohexane (2 column volumes), then a

gradient elution over 10 CV's (3% EtOAc in cyclohexane to 15% EtOAc in cyclohexane), then 15% EtOAc in cyclohexane for 5 CV's) gave *N,N-diethyl-3,5,6-trifluoro-4-pyridazinamine*[1] **2** (852 mg, 82%) as a yellow oil; (Found: $[MH]^+$, 206.08973. $C_8H_8F_3N_3O$ requires: 206.08996); ν_{max}(film)/cm^{-1} 2983.8, 2940.5 and 1587.1; δ_H 1.28 (6 H, t, $^3J_{HH}$ 7.1, CH_3), 3.47 (4 H, qt, $^3J_{HH}$ 7.1, $^5J_{HF}$ 1.5, CH_2); δ_C 13.91 (s, CH_3), 46.79 (t, $^4J_{CF}$ 5.2, CH_2), 129.17 (ddd, $^2J_{CF}$ 25.6, 4.8, $^3J_{CF}$ 4.8, C-4), 137.86 (ddd, $^1J_{CF}$ 266.8, $^2J_{CF}$ 28.8, $^3J_{CF}$ 11.2, C-5), 156.97 (dd, $^1J_{CF}$ 238.1, $^3J_{CF}$ 2.4, C-3), 157.05 (dd, $^1J_{CF}$ 238.9, $^2J_{CF}$ 4.0, C-6); δ_F -146.75 (1 F, dd, $^4J_{FF}$ 28.1, $^3J_{FF}$ 24.7, F-5), -100.65 (1 F, dd, $^5J_{FF}$ 28.7, $^3J_{FF}$ 24.7, F-6), -81.44 (1 F, dd, $^5J_{FF}$ 28.7, $^4J_{FF}$ 28.1 F-3); *m/z* (ES^+) 206 ($[MH]^+$, 100%).

N-Allyl-3,5,6-trifluoro-N-methylpyridazin-4-amine **3**

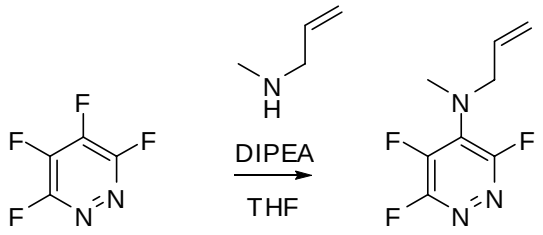

3

DIPEA (1.35 mL, 7.73 mmol) and N-methylallylamine (0.50 mL, 5.16 mmol) were added to a stirred solution of tetrafluoropyridazine (785 mg, 5.16 mmol) in THF (10 mL) at 0 °C under nitrogen, and the clear solution was stirred at 0 °C for 3.5 hours. The mixture was then concentrated *in vacuo*, partitioned between EtOAc and water, the phases were separated and the aqueous phase was extracted with EtOAc. The combined organic phases were concentrated *in vacuo* to give approx. 1.3 g of a light yellow oil. TLC (of the crude reaction NMR sample) showed Rf = 0.36 in 1:3 EtOAc / cyclohexane. Purification by Biotage SP4, 25+M SiO2 column (initial solvent – 6% EtOAc in cyclohexane (2 column volumes), then a gradient elution over 10 CV's (6% EtOAc in cyclohexane to 30% EtOAc in cyclohexane), then 30% EtOAc in cyclohexane for 5 CV's) gave *N-allyl-3,5,6-trifluoro-N-methylpyridazin-4-amine* **3** (861 mg, 82%) as a light-yellow oil; (Found: $[M]^+$,

204.07433. $C_8H_8F_3N_3O$ requires: $[M]^+$, 204.07431); ν_{max}(film)/cm^{-1} 2908.1, 1644.4 and 1593.8; δ_H 3.14 (3 H, t, $^5J_{HF}$ 3.2, CH_3), 3.97 (2 H, d, $^3J_{HH}$ 5.9, CH_2), 5.29 (1 H, dd, $^3J_{HH}$ 16.9, $^2J_{HH}$ 1.2, *H*CH), 5.32 (1 H, dd, $^3J_{HH}$ 10.3, $^2J_{HH}$ 1.2, HC*H*), 5.82 - 5.94 (1 H, m, CH); δ_C 39.60 (t, $^4J_{CF}$ 5.6, CH_3), 57.28 (t, $^4J_{CF}$ 4.8, CH_2), 119.06 (s, =CH_2), 130.09 (ddd, $^2J_{CF}$ 25.6, 4.8, $^3J_{CF}$ 4.8, C-4), 132.20 (s, CH), 138.36 (ddd, $^1J_{CF}$ 267.6, $^2J_{CF}$ 28.0, $^3J_{CF}$ 9.6, C-5), 156.94 (dd, $^1J_{CF}$ 239.7, $^3J_{CF}$ 12.8, C-3), 157.18 (dd, $^1J_{CF}$ 238.9, $^2J_{CF}$ 4.8, C-6); δ_F -145.60 (1 F, dd, $^4J_{FF}$ 28.1, $^3J_{FF}$ 26.4, F-5), -100.02 (1 F, dd, $^5J_{FF}$ 28.7, $^3J_{FF}$ 26.4, F-6), -80.87 (1 F, dd, $^5J_{FF}$ 28.7, $^4J_{FF}$ 28.1, F-3); *m/z* (ES^+) 204 ($[M]^+$, 100%).

3,5,6-Trifluoro-N-phenylpyridazin-4-amine **4**

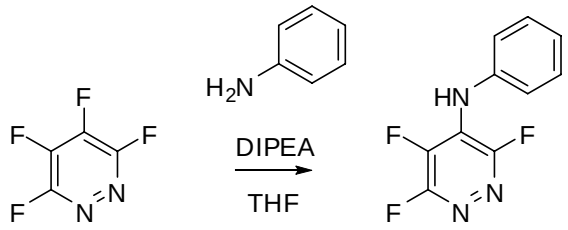

4

DIPEA (1.35 mL, 7.73 mmol) and aniline (0.46 mL, 5.10 mmol) were added to a stirred solution of tetrafluoropyridazine (776 mg, 5.10 mmol) in THF (10 mL) at 0 °C under nitrogen, and the clear solution was stirred at 0 °C for 4 hours. The mixture was then concentrated *in vacuo*, partitioned between EtOAc and water, the phases were separated and the aqueous phase was extracted with EtOAc. The combined organic phases were concentrated *in vacuo* to give approx. 1.2 g of a yellow oil. Purification by column chromatography (silica, ethyl acetate:hexane) gave *3,5,6-trifluoro-N-phenylpyridazin-4-amine* **4** (895 mg, 78%) as a white solid, mp 123.2 – 124.0 °C (Found: C, 53.61%, H, 2.81%, N, 18.74%. $C_{10}H_6F_3N_3$ requires C, 53.34%, H, 2.69%, N, 18.66%); δ_H 6.47 (1 H, br. s, NH), 7.15 – 7.40 (5 H, m, ArH); δ_C 122.7 (d, $^5J_{CF}$ 2.6, C-2'), 124.2 – 124.3 (m, C-4), 126.5 (s, C-4'), 129.4 (s, C-3'), 136.5 (ddd, $^1J_{CF}$ 272.3, $^2J_{CF}$ 29.9, $^3J_{CF}$ 6.9, C-5), 137.1 (s, C-1'), 156.8 (dd, $^1J_{CF}$ 238.2, $^2J_{CF}$ 3.3, C-6), 156.9 (d, $^1J_{CF}$ 237.7, C-3); δ_F -141.5 (1 F, dd,

$^{4}J_{FF}$ 25.4, $^{3}J_{FF}$ 24.5, F-5), -98.92 (1 F, dd, $^{5}J_{FF}$ 29.5, $^{3}J_{FF}$ 24.5, F-6), -88.96 (1 F, dd, $^{5}J_{FF}$ 29.5, $^{3}J_{FF}$ 25.4, F-3); *m/z* (ES^{+}) 224.9 ($[MH]^{+}$, 100%).

N-[(4-bromophenyl)methyl]-3,5,6-trifluoro-N-methyl-4-pyridazinamine **5**

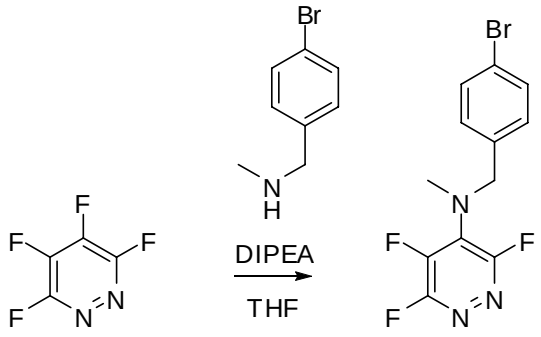

5

DIPEA (1.3 mL, 7.46 mmol) and 1-(4-bromophenyl)-N-methylmethanamine (1.05 mL, 5.26 mmol) were added to a stirred solution of tetrafluoropyridazine (786 mg, 5.17 mmol) in THF (10 mL) under nitrogen, and the solution was stirred for 24 hours. The mixture was then concentrated *in vacuo*, partitioned between EtOAc and water, the phases were separated and the aqueous phase was extracted with EtOAc. The combined organic phases were concentrated *in vacuo* to give approx. 2.3 g of a yellow oil. TLC (of the crude reaction NMR sample) showed Rf = 0.10 in 1:9 EtOAc / cyclohexane. Purification by Biotage SP4, 40+M SiO2 column (initial solvent – 3% EtOAc in cyclohexane (2 column volumes), then a gradient elution over 10 CV's (3% EtOAc in cyclohexane to 15% EtOAc in cyclohexane), then 15% EtOAc in cyclohexane for 5 CV's) gave *N-[(4-bromophenyl)methyl]-3,5,6-trifluoro-N-methyl-4-pyridazinamine* **5** (1122 mg, 65%) as white crystals, mp 77.1-78.5 °C (Found: C, 43.39%, H, 2.70%, N, 12.41%. $C_{12}H_9BrF_3N_3$ requires C, 43.40%, H, 2.73%, N, 12.65%); ν_{max}(film)/cm^{-1} 2940.9, 1601.9, 1573.9 and 1560.8; δ_H 3.09 (3 H, dd, $^{5}J_{HF}$ 3.8, 2.7, CH_3), 4.53 (2 H, s, CH_2), 7.15 (2 H, d, $^{3}J_{HH}$ 8.5, ArH), 7.49 (2 H, d, $^{3}J_{HH}$ 8.5, ArH); δ_C 39.96 (t, $^{4}J_{CF}$ 5.2, CH_3), 57.65 (t, $^{4}J_{CF}$ 4.8, CH_2), 121.90 (s, C-4'), 128.98 (s, C-2'), 130.18 (ddd, $^{2}J_{CF}$ 24.8, 4.8, $^{3}J_{CF}$ 3.2, C-4), 131.99 (s, C-3'), 134.92 (br s, C-1'), 139.00 (ddd, $^{1}J_{CF}$

270.8, $^{2}J_{CF}$ 29.6, $^{3}J_{CF}$ 10.4, C-5), 156.90 (dd, $^{1}J_{CF}$ 240.5, $^{3}J_{CF}$ 12.0, C-3), 157.43 (dd, $^{1}J_{CF}$ 239.7, $^{2}J_{CF}$ 4.0, C-6); δ_F -144.25 (1 F, dd, $^{4}J_{FF}$ 28.1, $^{3}J_{FF}$, 25.8, F-5), -99.35 (1 F, dd, $^{5}J_{FF}$ 28.7, $^{3}J_{FF}$ 25.8, F-6), -80.58 (1 F, dd, $^{5}J_{FF}$ 28.7, $^{4}J_{FF}$ 28.1, F-3); *m/z* (ES^{+}) 334.1 ($[MH]^{+}$, 100%).

Methyl N-methyl-N-(3,5,6-trifluoro-4-pyridazinyl)glycinate **6**

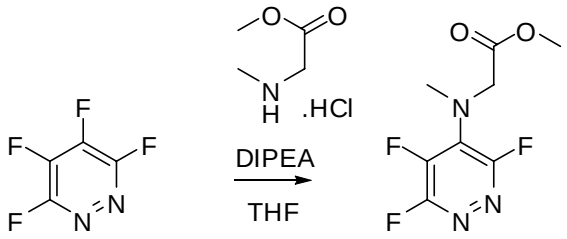

6

DIPEA (2.29 mL, 13.17 mmol) and tetrafluoropyridazine (801 mg, 5.27 mmol) were added to a stirred solution of sarcosine methyl ester hydrochloride (735 mg, 5.27 mmol) in THF (10 mL) under nitrogen, and the solution was stirred for 3 days. The mixture was then concentrated *in vacuo*, partitioned between EtOAc and water, the phases were separated and the aqueous phase was extracted with EtOAc. The combined organic phases were concentrated *in vacuo* to give approx. 0.8 g of a light yellow oil. TLC (of the crude reaction NMR sample) showed Rf = 0.24 in 1:2 EtOAc : cyclohexane. Purification by Biotage SP4, 25+M SiO2 column (initial solvent – 8% EtOAc in cyclohexane (2 column volumes), then a gradient elution over 10 CV's (8% EtOAc in cyclohexane to 40% EtOAc in cyclohexane), then 40% EtOAc in cyclohexane for 5 CV's) gave *methyl N-methyl-N-(3,5,6-trifluoro-4-pyridazinyl)glycinate* **6** (616 mg, 50%) as a light-yellow oil; (Found: C, 40.55; H, 3.34; N, 17.70. $C_8H_8F_3N_3O$ requires C, 40.86; H, 3.43; N, 17.87%); ν_{max}(film)/cm^{-1} 2958.4, 1747.1 and 1597.2; δ_H 3.27 (3 H, dd, $^{5}J_{HF}$ 3.4, 2.7, NCH_3), 3.81 (3 H, s, OCH_3), 4.14 (2 H, s, CH_2); δ_C 42.12 (t, $^{4}J_{CF}$ 5.6, NCH_3), 52.50 (s, OCH_3), 55.34 (dd, $^{4}J_{CF}$ 6.4, 4.8, CH_2), 129.62 (ddd, $^{2}J_{CF}$ 25.6, 4.8, $^{3}J_{CF}$ 3.2, C-4), 138.77 (ddd, $^{1}J_{CF}$ 269.2, $^{2}J_{CF}$ 28.8, $^{3}J_{CF}$ 9.6, C-5), 156.86 (d, $^{1}J_{CF}$ 240.0, C-3), 156.95 (dd, $^{1}J_{CF}$ 238.9, $^{2}J_{CF}$ 4.0, C-6), 169.31 (s, C=O); δ_F -144.62 (1 F, t,

$^4J_{FF}$ 27.5, $^3J_{FF}$ 25.2, F-5), -99.30 (1 F, dd, $^5J_{FF}$ 28.7, $^3J_{FF}$ 25.2, F-6), -81.00 (1 F, t, $^5J_{FF}$ 28.7, $^4J_{FF}$ 27.5, F-3); *m/z* (ES^+) 236.1 ($[MH]^+$, 100%).

3,4,6-Trifluoro-5-[(4-methylphenyl)oxy]pyridazine **7**

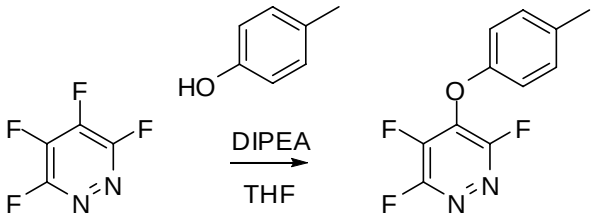

7

DIPEA (1.3 mL, 7.46 mmol) and *p*-cresol (0.53 mL, 5.07 mmol) were added to a stirred solution of tetrafluoropyridazine (768 mg, 5.05 mmol) in THF (10 mL) under nitrogen, and the solution was stirred for 26 hours. The mixture was then concentrated *in vacuo*, partitioned between EtOAc and water, the phases were separated and the aqueous phase was extracted with EtOAc. The combined organic phases were concentrated *in vacuo* to give approx. 1.1 g of a yellow oil. TLC (of the crude reaction NMR sample) showed Rf = 0.2 in cyclohexane. Purification by Biotage SP4 failed to remove traces of disubstituted product, so 90 mg of sample were removed from 899 mg of impure product and after purification by HPLC gave *3,4,6-trifluoro-5-[(4-methylphenyl)oxy]pyridazine* **7** (74 mg, 6%) as a colourless oil (Found: C, 54.93%, H, 2.86%, N, 11.40%. $C_{11}H_7F_3N_2O$ requires C, 55.01%, H, 2.94%, N, 11.66%); ν_{max}(film)/cm^{-1} 2928.0, 1614.9, 1606.0 and 1570.9; δ_H 2.38 (3 H, s, CH_3), 6.97 (2 H, d, $^3J_{HH}$ 8.7, ArH), 7.21 (2 H, dd, $^3J_{HH}$ 8.7, $^4J_{HH}$ 0.7, ArH); δ_C 20.73 (s, CH_3), 116.97 (s, C-2'), 130.56 (s, C-3'), 134.67 (ddd, $^2J_{CF}$ 27.2, 5.6, $^3J_{CF}$ 5.6, C-5), 135.75 (s, C-4'), 141.86 (ddd, $^1J_{CF}$ 282.8, $^2J_{CF}$ 28.0, $^3J_{CF}$ 7.2, C-4), 153.05 (s, C-1'), 156.77 (ddd, $^1J_{CF}$ 243.6, $^2J_{CF}$ 10.0, $^4J_{CF}$ 2.4, C-3), 159.24 (d, $^1J_{CF}$ 246.9, C-6); δ_F -140.35 (1 F, dd, $^3J_{FF}$ 24.1, $^4J_{FF}$ 24.1, F-4), -93.95 (1 F, dd, $^5J_{FF}$ 30.4, $^3J_{FF}$ 24.1, F-3), -85.54 (1 F, dd, $^5J_{FF}$ 30.4, $^4J_{FF}$ 24.1, F-6); *m/z* (ES^+) 241.2 ($[MH]^+$, 100%).

4-(Cyclohexyloxy)-3,5,6-trifluoropyridazine **8**

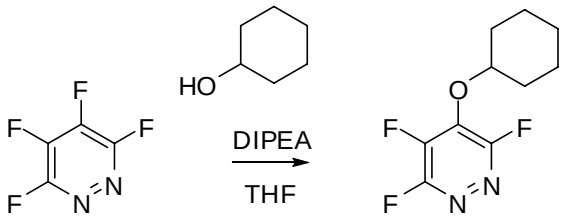

8

DIPEA (1.3 mL, 7.46 mmol) and cyclohexanol (0.55 mL, 5.29 mmol) were added to a stirred solution of tetrafluoropyridazine (777 mg, 5.11 mmol) in THF (10 mL) under nitrogen, and the clear solution was stirred for 6 days. The mixture was then concentrated *in vacuo*, partitioned between EtOAc and water, the phases were separated and the aqueous phase was extracted with EtOAc. The combined organic phases were concentrated *in vacuo* to give approx. 0.9 g of a yellow oil. TLC (of the crude reaction NMR sample) showed Rf = 0.24 in 1:49 EtOAc / cyclohexane. Purification by Biotage SP4, 25+S SiO2 column (initial solvent – 1% EtOAc in cyclohexane (2 column volumes), then a gradient elution over 10 CV's (1% EtOAc in cyclohexane to 5% EtOAc in cyclohexane), then 5% EtOAc in cyclohexane for 5 CV's) gave *4-(cyclohexyloxy)-3,5,6-trifluoropyridazine* **8** (752 mg, 63%) as a colourless oil; (Found: C, 51.70%, H, 4.54%, N, 11.77%. $C_{10}H_{11}F_3N_2O$ requires C, 51.75%, H, 4.78%, N, 12.07%); ν_{max}(film)/cm^{-1} 2940.4, 2863.4 and 1607.3; δ_H 1.02 - 2.37 (10 H, m, CH_2), 4.80 (1 H, br s, CH); δ_C 23.04 (s, C-3', C-5'), 24.93 (s, C-4'), 32.05 (s, C-2', C-6'), 83.30 (d, $^4J_{CF}$ 4.0, C-1'), 135.98 (ddd, $^2J_{CF}$ 27.2, 4.8, $^3J_{CF}$ 4.8, C-4), 140.24 (ddd, $^1J_{CF}$ 275.6, $^2J_{CF}$ 28.0, $^4J_{CF}$ 8.0, C-5), 156.73 (ddd, $^1J_{CF}$ 242.1, $^3J_{CF}$ 11.2, $^4J_{CF}$ 1.6, C-3), 159.32 (dd, $^1J_{CF}$ 244.5, $^2J_{CF}$ 2.4, C-6); δ_F -146.29 (1 F, dd, $^4J_{FF}$ 27.5, $^3J_{FF}$ 26.4, F-5), -95.77 (1 F, dd, $^5J_{FF}$ 29.3, $^3J_{FF}$ 26.4, F-6), -87.45 (1 F, dd, $^5J_{FF}$ 29.3, $^4J_{FF}$ 27.5, F-3); *m/z* (ES$^+$) 233.2 ([MH]$^+$, 100%).

3,4,6-Trifluoro-5-(2-propen-1-yloxy)pyridazine **9**

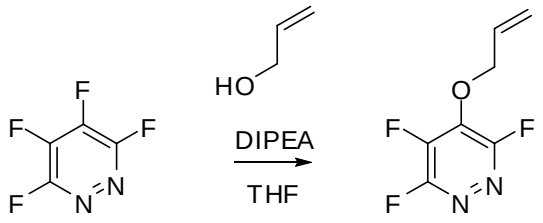

9

DIPEA (1.3 mL, 7.46 mmol) and allyl alcohol (0.36 mL, 5.26 mmol) were added to a stirred solution of tetrafluoropyridazine (780 mg, 5.13 mmol) in THF (10 mL) under nitrogen, and the solution was stirred at reflux for 24 hours. The mixture was then concentrated *in vacuo*, partitioned between EtOAc and water, the phases were separated and the aqueous phase was extracted with EtOAc. The combined organic phases were concentrated *in vacuo* to give approx. 1 g of a yellow oil. TLC (of the crude reaction NMR sample) showed Rf = 0.24 in 1:9 EtOAc / cyclohexane. Purification by Biotage SP4, 25+S SiO2 column (initial solvent – 3% EtOAc in cyclohexane (2 column volumes), then a gradient elution over 10 CV's (3% EtOAc in cyclohexane to 15% EtOAc in cyclohexane), then 15% EtOAc in cyclohexane for 5 CV's) gave *3,4,6-trifluoro-5-(2-propen-1-yloxy)pyridazine* **9** (716 mg, 73%) as a colourless oil (Found: $[MH]^+$, 191.04277. $C_7H_5F_3N_2O$ requires: $[MH]^+$, 191.04267); ν_{max}/cm^{-1} 2898.8, 1648.2 and 1611.8; δ_H 5.03 (2 H, dd, $^3J_{HH}$ 6.0, $^5J_{HF}$ 0.9, O-CH_2), 5.44 (1 H, dd, $^3J_{HH}$ 10.5, $^2J_{HH}$ 1.0, CH*H*), 5.51 (1 H, dd, $^3J_{HH}$ 16.9, $^2J_{HH}$ 1.0, C*H*H), 5.96 - 6.09 (1H, ddd, $^3J_{HH}$ 16.9, $^3J_{HH}$ 10.5, $^3J_{HH}$ 6.0, CH); δ_C 74.65 (dd, $^4J_{CF}$ 5.6, 1.6, O-CH_2), 121.37 (s, CH_2), 130.50 (s, CH), 136.18 (ddd, $^2J_{CF}$ 27.2, 4.8, $^3J_{CF}$ 4.8, C-5), 140.07 (ddd, $^1J_{CF}$ 277.2, $^2J_{CF}$ 28.8, $^3J_{CF}$ 8.0, C-4), 156.69 (ddd, $^1J_{CF}$ 242.1, $^3J_{CF}$ 11.2, $^4J_{CF}$ 1.6, C-6), 158.68 (d, $^1J_{CF}$ 242.9, C-3); δ_F -146.60 (1 F, dd, $^4J_{FF}$ 26.4, $^3J_{FF}$ 25.8, F-4), -95.79 (1 F, dd, $^5J_{FF}$ 28.7, $^3J_{FF}$ 25.8, F-3), -87.60 (1 F, dd, $^5J_{FF}$ 28.7, $^4J_{FF}$ 26.4, F-6); *m/z* (ES^+) 191.0 ($[MH]^+$, 100%).

3,4,6-Trifluoro-5-[(1-methylethyl)oxy]pyridazine **10**

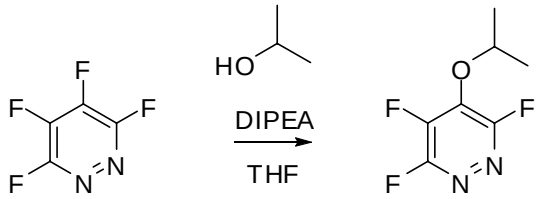

10

DIPEA (1.3 mL, 7.46 mmol) and isopropanol (0.41 mL, 5.26 mmol) were added to a stirred solution of tetrafluoropyridazine (780 mg, 5.13 mmol) in THF (10 mL) under nitrogen, and the solution was stirred at reflux for 24 hours. The mixture was then concentrated *in vacuo*, partitioned between EtOAc and water, the phases were separated and the aqueous phase was extracted with EtOAc. The combined organic phases were concentrated *in vacuo* to give approx. 0.9 g of a yellow oil. TLC (of the crude reaction NMR sample) showed Rf = 0.28 in 1:9 EtOAc / cyclohexane. Purification by Biotage SP4, 25+S SiO2 column (initial solvent – 3% EtOAc in cyclohexane (2 column volumes), then a gradient elution over 10 CV's (3% EtOAc in cyclohexane to 15% EtOAc in cyclohexane), then 15% EtOAc in cyclohexane for 5 CV's) gave *3,4,6-trifluoro-5-[(1-methylethyl)oxy]pyridazine* **10** (713 mg, 72%) as a colourless oil (Found: $[MH]^+$, 193.05830. $C_7H_7F_3N_2O$ requires: $[MH]^+$, 193.05832); ν_{max}/cm^{-1} 2990.8, 2941.6 and 1608.2; δ_H 1.47 (6 H, dd, $^3J_{HH}$ 6.1, $^6J_{HF}$ 0.8, CH_3), 5.02 - 5.14 (1 H, m, CH); δ_C 22.47 (s, CH_3), 78.85 (d, $^4J_{CF}$ 4.0, CH), 136.01 (ddd, $^2J_{CF}$ 27.1, 5.2, $^3J_{CF}$ 5.2, C-5), 140.00 (ddd, $^1J_{CF}$ 275.8, $^2J_{CF}$ 28.6, $^3J_{CF}$ 7.8, C-4), 156.76 (ddd, $^1J_{CF}$ 239.7, $^3J_{CF}$ 11.2, $^4J_{CF}$ 1.6, C-6), 159.14 (ddd, $^1J_{CF}$ 246.1, $^2J_{CF}$ 8.8, $^4J_{CF}$ 2.4, C-3); δ_F -147.01 (1 F, dd, $^4J_{FF}$ 27.0, $^3J_{FF}$ 25.8, F-4), -96.10 (1 F, dd, $^5J_{FF}$ 28.7, $^3J_{FF}$ 25.8, F-3), -87.87 (1 F, dd, $^5J_{FF}$ 28.7, $^4J_{FF}$ 27.0, F-6); *m/z* (ES^+) 193.2 ($[MH]^+$, 100%).

3,4,6-Trifluoro-5-phenylpyridazine **11**, *3,4,5-trifluoro-6-phenylpyridazine* **12**, and *3,5-difluoro-4,6-diphenylpyridazine* **13**

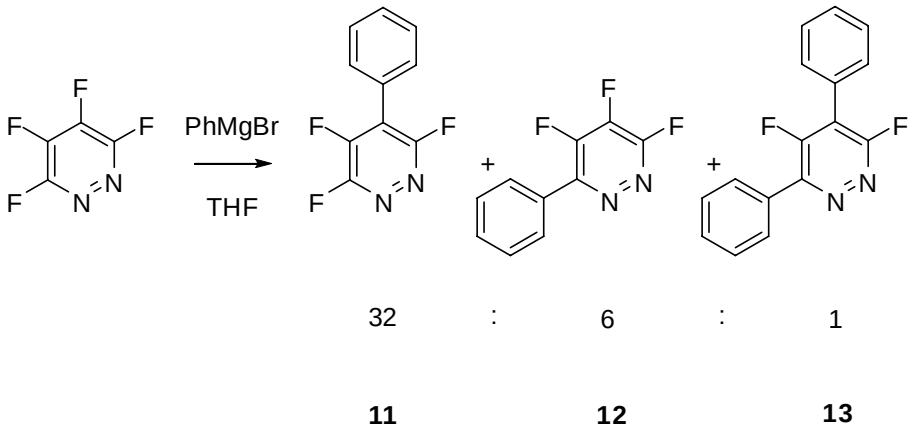

Phenylmagnesium bromide (1M solution in THF, 5.13 mL, 5.13 mmol) was added to a stirred solution of tetrafluoropyridazine (780 mg, 5.13 mmol) in THF (10 mL) under nitrogen at -78 °C. The reaction was allowed to come to RT overnight, at which point ^{19}F NMR spectroscopic analysis showed the presence of the major product, a regioisomer of the major product, and a disubstituted species. The reaction was quenched by addition of wet THF, and then concentrated, partitioned between EtOAc and water, and extracted with two further portions of EtOAc. The combined organic phases were dried and concentrated *in vacuo* to give approx. 1 g of crude product. TLC (of the crude reaction NMR sample) showed Rf = 0.25 in 1:19 EtOAc : cyclohexane. Purification by Biotage SP4, 40+M SiO2 column (gradient elution over 15 CV's (cyclohexane to 4% EtOAc in cyclohexane), then 4-20% EtOAc in cyclohexane over 5 CV's) gave 624 mg of material, recrystallisation of which (from cyclohexane) gave *3,4,6-trifluoro-5-phenylpyridazine* **11** (501 mg, 47%) as white crystals, mp 82.7-83.4 °C (Found: C, 57.15%, H, 2.41%, N, 13.22%. $C_{10}H_5F_3N_2$ requires C, 57.15%, H, 2.40%, N, 13.33%); ν_{max}/cm^{-1} 1580.6, 1558.1, 1457.9 and 1444.6; δ_H 7.56 - 7.62 (5 H, m, CH); δ_C 121.27 (ddd, $^2J_{CF}$ 31.9, 8.8, $^3J_{CF}$ 4.0, C-5), 123.65 (br s, C-4'), 129.08 (s, C-2', C-6'), 129.77 (br s, C-3', C-5'), 131.11 (s, C-1'), 147.86 (ddd, $^1J_{CF}$ 281.2, $^2J_{CF}$ 27.2, $^3J_{CF}$ 8.0, C-4), 156.58 (ddd, $^1J_{CF}$ 243.7, $^3J_{CF}$ 12.8, $^4J_{CF}$ 2.4, C-6), 162.30 (d, $^1J_{CF}$ 245.3, C-3); δ_F -129.26 (1 F, dd, $^3J_{FF}$ 26.4, $^4J_{FF}$ 21.8, F-4), -97.63 (1 F, dd, $^5J_{FF}$ 31.0,

$^{3}J_{FF}$ 26.4, F-3), -79.61 (1 F, dd, $^{5}J_{FF}$ 31.0, $^{4}J_{FF}$ 21.8, F-6); *m/z* (ES^{+}) 211.2 ($[MH]^{+}$, 100%). Minor products were identified by ^{19}F NMR spectroscopic analysis of the reaction mixture, but were not isolated: *3,4,5-trifluoro-6-phenylpyridazine* **12**; δ_F -156.68 (1 F, dd, $^{3}J_{FF}$ 25.3, $^{3}J_{FF}$ 18.7, F-4), -136.49 (1 F, dd, $^{4}J_{FF}$ 24.5, $^{3}J_{FF}$ 18.7, F-5), -96.08 (1 F, dd, $^{3}J_{FF}$ 25.3, $^{4}J_{FF}$ 24.5, F-3); *3,5-difluoro-4,6-diphenylpyridazine* **13**; δ_F -117.11 (1 F, d, $^{4}J_{FF}$ 23.4, F-5), -83.00 (1 F, d, $^{4}J_{FF}$ 23.4, F-3).

4,7-Difluoro-2-methyl-furo[2,3-d]pyridazine-3-carboxylic acid ethyl ester **14**

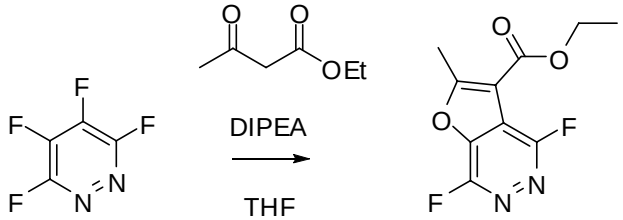

14

DIPEA (0.9 ml, 5.17 mmol) and ethyl acetoacetate (0.25 ml, 1.96 mmol) were added to a stirred solution of tetrafluoropyridazine (0.312 mg, 2.05 mmol) in THF (10 ml). After four days at room temperature, the mixture was concentrated and partitioned between DCM (3 × 10 ml) and water. The combined organic phases were dried and concentrated, giving 617 mg of crude product, and purification by column chromatography (silica, ethyl acetate:hexane) gave *4,7-difluoro-2-methyl-furo[2,3-d]pyridazine-3-carboxylic acid ethyl ester* **14** (0.192 g, 40%) as a colourless oil (Found: C, 49.6%; H, 3.4%; N, 11.9%. $C_{10}H_8F_2N_2O_3$ requires: C, 49.6%; H, 3.3%; N, 11.6%); ν_{max} / cm^{-1} 2987.8, 1719.5, 1615.1 and 1586.7; δ_H 1.44 (3H, t, $^{3}J_{HH}$ 7.1, CH_2CH_3), 2.92 (3H, s, CCH_3), 4.44 (2H, q, $^{3}J_{HH}$ 7.1, CH_2); δ_C 14.20 (s, CH_2CH_3), 14.73 (s, CCH_3), 62.05 (s, CH_2), 109.09 (d, $^{3}J_{CF}$ 3.6, C-3), 119.06 (dd, $^{2}J_{CF}$ 35.4, $^{3}J_{CF}$ 5.9, C-3a), 141.82 (dd, $^{2}J_{CF}$ 28.6, $^{3}J_{CF}$ 10.1, C-7a), 152.25 (dd, $^{1}J_{CF}$ 241.0, $^{4}J_{CF}$ 3.9, C-4), 158.73 (dd, $^{1}J_{CF}$ 247.7, $^{4}J_{CF}$ 2.3, C-7), 160.95 (s, C=O), 168.25 (s, C-2); δ_F -98.48 (1 F, d, $^{5}J_{FF}$ 33.5, F-4), -76.46 (1 F, d, $^{5}J_{FF}$ 33.5, F-7); *m/z* (EI^{+}) 242 ($[M]^{+}$, 49%), 214 (62), 197 (100), 170 (32).

3,6-Difluoro-4,5-bis(phenylthio)pyridazine **15**

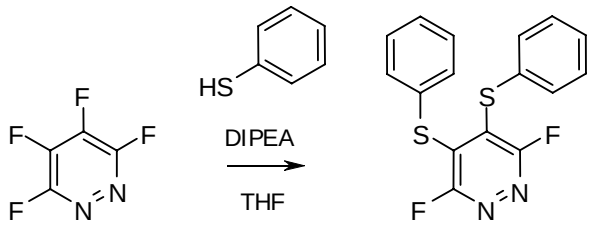

15

DIPEA (2.6 mL, 14.8 mmol) and thiophenol (1 mL, 9.7 mmol) were added to a stirred solution of tetrafluoropyridazine (780 mg, 5.13 mmol) in THF (10 mL) at 0 °C under nitrogen. Addition was performed in two separate 0.5 ml quantities. An hour after the first addition, 50% conversion to bis-substituted product was confirmed by LCMS and NMR spectroscopy, and the remaining thiophenol was added to the stirred solution. The mixture was then allowed to come to RT overnight. Aqueous sodium hydroxide was added to the flask, and the product was extracted into EtOAc. The aqueous phase was extracted with two further portions of EtOAc and the combined organic phases were combined, dried and concentrated to give approx. 1.6 g of crude product. Purification by Biotage SP4, 40+M SiO2 column (inital solvent - 1% EtOAc in cyclohexane (2 column volumes), then a gradient elution over 10 CV's (1% EtOAc in cyclohexane to 7% EtOAc in cyclohexane), then 7% EtOAc in cyclohexane for 5 CV's) gave *3,6-difluoro-4,5-bis(phenylthio)pyridazine*[1] **15** (1.31 g, 77%) as yellow crystals, mp 99.1-100.3 °C (lit. mp 97-99 °C) (Found: C, 57.73%, H, 3.00%, N, 8.34%. $C_{16}H_{10}F_2N_2S_2$ requires C, 57.82%, H, 3.03%, N, 8.43%); ν_{max}/cm^{-1} 1578.7, 1500.4 and 1377.8; δ_H 7.34 - 7.47 (10 H, m, ArH); δ_C 129.29 (s, C-4', C-4'') 129.65 (s, C-3', C-5', C-3'', C-5'') 130.26 (s, C-1', C-1'') 132.22 (s, C-2', C-6', C-2'', C-6'') 133.56 (dd, $^2J_{CF}$ 17.6, $^3J_{CF}$ 16.0, C-4, C-5) 162.59 (dd, $^1J_{CF}$ 249.3, $^4J_{CF}$ 6.4, C-3, C-6); δ_F -75.76 (2 F, br s,); *m/z* (ES^+) 333.2 ($[MH]^+$, 100%).

4-(Ethylthio)-3,5,6-trifluoropyridazine **16**

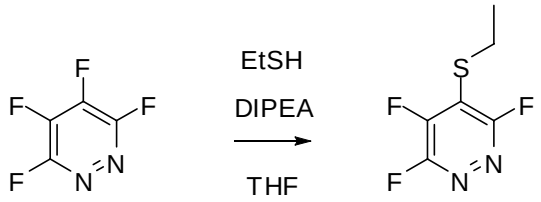

16

DIPEA (1.35 mL, 7.73 mmol) and ethanethiol (0.30 mL, 4.1 mmol) were added to a stirred solution of tetrafluoropyridazine (780 mg, 5.13 mmol) in THF (10 mL) at 0 °C under nitrogen, and the clear solution was stirred at 0 °C for 1 hour. The mixture was then concentrated *in vacuo*, partitioned between EtOAc and water, the phases were separated and the aqueous phase was extracted with EtOAc. The combined organic phases were concentrated *in vacuo* to give approx. 1.2 g of a brown oil. Purification by column chromatography (silica, hexane:ethyl acetate) gave *4-(ethylthio)-3,5,6-trifluoropyridazine* **16** (514 mg, 65%) as a colourless oil (Found: $[MH]^+$, 195.0210. $C_6H_5N_2F_3S$ requires $[MH]^+$, 195.0204); δ_H 3.27 (2 H, qt, $^3J_{HH}$ 7.4, $^5J_{HF}$ 1.1, CH_2), 1.40 (3 H, t, $^3J_{HH}$ 7.4, CH_3); δ_C 15.14 (s, CH_3), 27.37 (dd, $^4J_{CF}$ 5.5, $^4J_{CF}$ 4.0, CH_2), 121.65 (ddd, $^2J_{CF}$ 35.6, $^2J_{CF}$ 11.9, $^3J_{CF}$ 3.2, C-4), 149.29 (ddd, $^1J_{CF}$ 276.5, $^2J_{CF}$ 28.1, $^3J_{CF}$ 7.5, C-5), 155.76 (ddd, $^1J_{CF}$ 244.0, $^4J_{CF}$ 13.2, $^3J_{CF}$ 2.7, C-3), 162.65 (d, $^1J_{CF}$ 241.1, C-6); δ_F -74.55 (1F, dd, $^3J_{FF}$ 30.2, $^4J_{FF}$ 21.0, F-5), -99.36 (1 F, dd, $^3J_{FF}$ 30.2, $^5J_{FF}$ 26.4, F-6), -124.83 (1 F, dd, $^5J_{FF}$ 26.4, $^4J_{FF}$ 21.0, F-3); *m/z* (ES^+) 195.0 ($[MH]^+$, 100%).

4-(3,6-Difluoro-5-phenyl-4-pyridazinyl)morpholine **17**

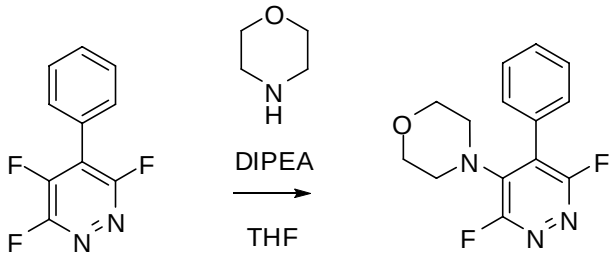

11 **17**

DIPEA (0.18 mL, 1.03 mmol) and morpholine (0.06 mL, 0.68 mmol) were added to a stirred solution of 3,4,6-trifluoro-5-phenylpyridazine **11** (143 mg, 0.680 mmol) in THF (10 mL) under nitrogen, and the solution was stirred at RT for 4 days. The mixture was then concentrated *in vacuo*, partitioned between EtOAc and water, the phases were separated and the aqueous phase was extracted with EtOAc. The combined organic phases were concentrated *in vacuo* to give approx. 0.2 g of crude product. Purification by Biotage SP4, 40+M SiO2 column (initial solvent – 5% THF in cyclohexane (2 column volumes), then a gradient elution over 10 CV's (5% THF in cyclohexane to 25% THF in cyclohexane), then 25% THF in cyclohexane for 5 CV's) gave 203 mg of product of approx. 93% purity (LCMS). 77 mg of material were further purified by RP-HPLC, and gave *4-(3,6-difluoro-5-phenyl-4-pyridazinyl)morpholine* **17** (61 mg, 32%) as white crystals, mp 180.6-182.0 °C (Found: C, 60.54%, H, 4.69%, N, 15.01%. $C_{10}H_5F_3N_2$ requires C, 60.64%, H, 4.72%, N, 15.15%); ν_{max}/cm^{-1} 2977.1, 2857.3 and 1543.8; δ_H 3.04 (4 H, td, $^3J_{HH}$ 4.7, $^5J_{HF}$ 1.6, NCH_2), 3.61 (4 H, dd, $^3J_{HH}$ 4.8, 4.6, OCH_2), 7.31 - 7.38 (2 H, m, CH), 7.42 - 7.57 (3 H, m, CH); δ_C 50.55 (d, $^4J_{CF}$ 4.8, NCH_2), 66.54 (s, OCH_2), 120.42 (dd, $^2J_{CF}$ 31.2, $^3J_{CF}$ 6.4, C-5), 128.95 (s, C-2', C-6'), 129.49 (s, C-3', C-5'), 129.53 (br s, C-4'), 129.64 (t, $^3J_{CF}$ 2.4, C-1'), 139.21 (dd, $^2J_{CF}$ 22.4, $^3J_{CF}$ 6.4, C-4), 159.38 (d, $^1J_{CF}$ 240.5, C-3), 163.36 (d, $^1J_{CF}$ 239.7, C-6); δ_F -86.89 (1 F, d, $^5J_{FF}$ 31.6, F-3), -83.96 (1 F, d, $^5J_{FF}$ 31.6, F-6); *m/z* (ES^+) 278.2 ($[MH]^+$, 100%).

4-{3,6-Difluoro-5-[(1-methylethyl)oxy]-4-pyridazinyl}morpholine **18**

Method A:

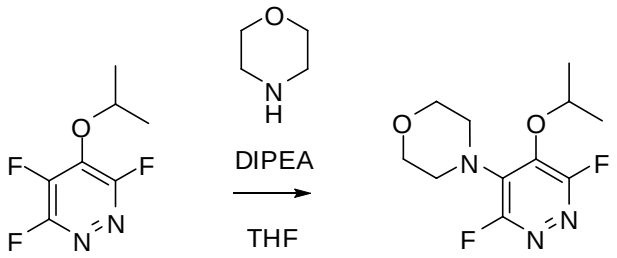

10 **18**

DIPEA (0.20 mL, 1.15 mmol) and morpholine (0.07 mL, 0.80 mmol) were added to a stirred solution of 3,4,6-trifluoro-5-[(1-methylethyl)oxy]pyridazine **10** (153 mg, 0.796 mmol) in THF (10 mL) under nitrogen, and the solution was stirred at RT for 4 days. The mixture was then concentrated *in vacuo*, partitioned between EtOAc and water, the phases were separated and the aqueous phase was extracted with EtOAc. The combined organic phases were concentrated *in vacuo* to give approx. 0.2 g of crude product. TLC (of the crude reaction NMR sample) showed Rf = 0.24 in 1:4 THF / cyclohexane. Purification by Biotage SP4, 40+M SiO2 column (initial solvent – 5% THF in cyclohexane (2 column volumes), then a gradient elution over 10 CV's (5% THF in cyclohexane to 25% THF in cyclohexane), then 25% THF in cyclohexane for 5 CV's) gave *4-{3,6-difluoro-5-[(1-methylethyl)oxy]-4-pyridazinyl}morpholine* **18** (163 mg, 79%) as white crystals, mp 73.9-75.4 °C (Found: $[MH]^+$, 260.12041. $C_{11}H_{15}F_2N_3O_2$ requires: $[MH]^+$, 260.12051); ν_{max}/cm^{-1} 2980.8, 2861.6 and 1566.9; δ_H 1.33 (6 H, d, $^3J_{HH}$ 6.2, CH_3), 3.39 (4 H, dd, $^3J_{HH}$ 4.4, $^5J_{HF}$ 3.3, NCH_2), 3.76 (4 H, t, $^3J_{HH}$ 4.4, OCH_2), 4.63 - 4.76 (1 H, m, $^3J_{HH}$ 6.2, $^5J_{HF}$ 1.4, CH); δ_C 22.37 (s, CH_3), 50.17 (d, $^4J_{CF}$ 4.8, NCH_2), 66.95 (s, OCH_2), 77.13 (d, $^4J_{CF}$ 5.6, CH), 133.26 (dd, $^2J_{CF}$ 23.2, $^3J_{CF}$ 8.0, C-4), 137.06 (dd, $^2J_{CF}$ 24.8, $^3J_{CF}$ 8.8, C-5), 159.57 (d, $^1J_{CF}$ 239.7, C-3), 160.46 (d, $^1J_{CF}$ 240.5, C-6); δ_F -93.19 (1 F, d, $^5J_{FF}$ 29.8, F-6), -86.19 (1 F, d, $^5J_{FF}$ 29.8, F-3); *m/z* (ES^+) 260.3 ($[MH]^+$, 100%).

Method B:

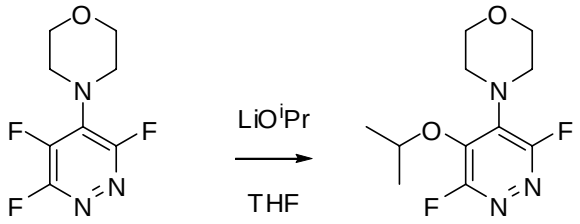

1 **18**

Lithium isopropoxide (2 M in THF, 0.45 mL, 0.90 mmol) was added to a stirred solution of 4-(3,5,6-trifluoro-4-pyridazinyl)morpholine **1** (195 mg, 0.89 mmol) in THF (10 mL) under nitrogen at -78 °C, and the solution was allowed to come to RT overnight. The reaction was quenched by the addition of wet THF, then concentrated *in vacuo*, partitioned between EtOAc and water, the phases were separated and the aqueous phase was extracted with EtOAc. The combined organic phases were concentrated *in vacuo* to give approx. 237 mg of crude product. TLC (of the crude reaction NMR sample) showed Rf = 0.16 in 1:9 EtOAc / toluene. Purification by Biotage SP4, 40+M SiO2 column (initial solvent – 2% EtOAc in toluene (2 column volumes), then a gradient elution over 10 CV's (2% EtOAc in toluene to 13% EtOAc in toluene), then 13% EtOAc in toluene for 5 CV's) gave 126 mg of product of approximately 97% purity. Further purification by RP-HPLC gave *4-{3,6-difluoro-5-[(1-methylethyl)oxy]-4-pyridazinyl}morpholine* **18** (94 mg, 41%) as white crystals, mp 73.8-75.0 °C (Found: C, 50.93%, H, 5.80%, N, 16.26%. $C_{11}H_{15}F_2N_3O_2$ requires C, 50.96%, H, 5.83%, N, 16.21%); ν_{max}/cm^{-1} 2981.6, 2861.6 and 1566.8; δ_H 1.37 (6 H, dd, $^3J_{HH}$ 6.2, $^6J_{HF}$ 0.7, CH_3), 3.43 (4 H, td, $^3J_{HH}$ 4.7, $^5J_{HF}$ 1.8, NCH_2), 3.81 (4 H, dd, $^3J_{HH}$ 4.7, 4.6, OCH_2), 4.69 - 4.80 (1 H, m, $^3J_{HH}$ 6.2, $^5J_{HF}$ 1.6, CH); δ_C 22.47 (s, CH_3), 50.28 (d, $^4J_{CF}$ 4.8, NCH_2), 67.05 (s, OCH_2), 77.21 (d, $^4J_{CF}$ 6.4, CH), 133.34 (dd, $^2J_{CF}$ 23.2, $^3J_{CF}$ 8.0, C-4), 137.18 (dd, $^2J_{CF}$ 24.8, $^3J_{CF}$ 8.8, C-5), 158.33 - 161.05 (m, $^1J_{CF}$ 240.5, C-3), 160.55 (d, $^1J_{CF}$ 239.7, C-6); δ_F -92.89 (1 F, d, $^5J_{FF}$ 30.4, F-6), -86.04 (1 F, d, $^5J_{FF}$ 30.4, F-3); *m/z* (ES^+) 260.2 ($[MH]^+$, 100%).

4-(5-(Ethylthio)-3,6-difluoropyridazin-4-yl)morpholine **19**

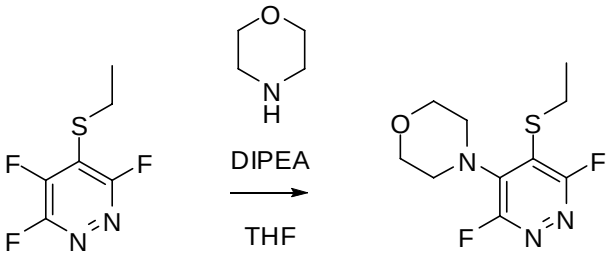

16 **19**

DIPEA (0.27 mL, 1.5 mmol) and morpholine (0.09 mL, 1.03 mmol) were added to a stirred solution of 4-(ethylthio)-3,5,6-trifluoropyridazine **16** (200 mg, 1.03 mmol) in THF (10 mL) at 0 °C under nitrogen, and the clear solution was stirred at RT overnight. The mixture was then concentrated *in vacuo*, partitioned between EtOAc and water, the phases were separated and the aqueous phase was extracted with EtOAc. The combined organic phases were concentrated *in vacuo* to give approx. 0.2 g of a light yellow oil. Purification by column chromatography gave *4-(5-(ethylthio)-3,6-difluoropyridazin-4-yl)morpholine* **19** (197 mg, 73%) as a yellow oil (Found: C, 45.63%, H, 5.06%, N, 16.16%. $C_{10}H_{13}F_2N_3OS$ requires C, 45.97%, H, 5.01%, N, 16.08%); ν_{max}/cm^{-1} 2965.9, 2853.6, 1638.7 and 1546.7; δ_H 1.29 (3 H, td, $^3J_{HH}$ 7.4, $^6J_{HF}$ 0.5, CH_3), 3.09 (2 H, qd, $^3J_{HH}$ 7.4, $^5J_{HF}$ 1.6, SCH_2), 3.41 (4 H, td, $^3J_{HH}$ 4.7, $^5J_{HF}$ 2.3, NCH_2), 3.84 (4 H, t, $^3J_{HH}$ 4.7, OCH_2); δ_C 14.91 (d, $^5J_{CF}$ 0.9, CH_3), 28.52 (d, $^4J_{CF}$ 8.9, SCH_2), 51.02 (d, $^4J_{CF}$ 4.6, NCH_2), 67.19 (d, $^5J_{CF}$ 1.5, OCH_2), 121.38 (dd, $^2J_{CF}$ 32.6, $^3J_{CF}$ 6.8, C-4), 140.97 (dd, $^2J_{CF}$ 23.4, $^3J_{CF}$ 7.1, C-5), 159.58 (dd, $^1J_{CF}$ 243.2, $^4J_{CF}$ 1.5, C-6), 164.72 (d, $^1J_{CF}$ 237.9, C-3); δ_F -88.37 (1 F, d, $^5J_{FF}$ 31.2, F-3), -78.54 (1 F, d, $^5J_{FF}$ 31.2, F-6); *m/z* (ES^+) 260.9 ($[M]^+$, 100%).

3,6-Difluoro-4-phenyl-5-(phenylthio)pyridazine **20**

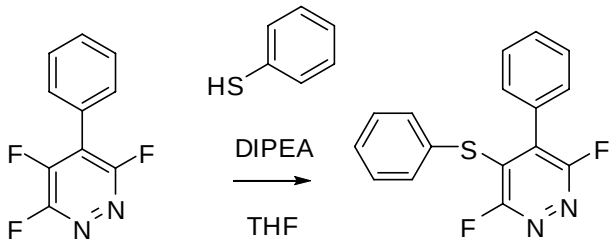

11 **20**

DIPEA (0.19 mL, 1.1 mmol) and thiophenol (0.07 mL, 0.68 mmol) were added to a stirred solution of 3,4,6-trifluoro-5-phenylpyridazine **11** (150 mg, 0.714 mmol) in THF (10 mL) at 0 °C under nitrogen, and the solution was stirred for 1 hour. Aqueous NaOH was then added to the mixture, which was partitioned with EtOAc. The aqueous phase was extracted with two further portions of EtOAc and the combined organic phases were combined, dried and concentrated to give approx. 0.3 g of crude product. Purification by Biotage SP4, 40+M SiO2 column (initial solvent - 1% THF in cyclohexane (2 column volumes), then a gradient elution over 10 CV's (1% THF in cyclohexane to 7% THF in cyclohexane), then 7% THF in cyclohexane for 5 CV's) gave *3,6-difluoro-4-phenyl-5-(phenylthio)pyridazine* **20** (188 mg, 88%) as off-white crystals, mp 78.9-80.0 °C (Found: C, 63.97%, H, 3.42%, N, 9.35%. $C_{16}H_{10}F_2N_2S_2$ requires C, 63.99%, H, 3.36%, N, 9.33%); ν_{max}/cm^{-1} 1523.7, 1443.0 and 1386.5; δ_H 7.20 - 7.31 (5 H, m), 7.33 - 7.40 (2 H, m), 7.44 - 7.55 (3 H, m); δ_C 128.65 (s, C-2', C-6'), 128.84 (d, $^3J_{CF}$ 2.4, C-1'), 128.92 (s, C-4''), 129.34 (s, C-3'', C-5''), 129.42 (s, C-3', C-5'), 130.13 (s, C-4'), 130.35 (d, $^4J_{CF}$ 2.4, C-1''), 132.09 (s, C-2'', C-6''), 132.48 (dd, $^2J_{CF}$ 29.6, $^3J_{CF}$ 4.0, C-4), 134.52 (dd, $^2J_{CF}$ 31.2, $^3J_{CF}$ 3.2, C-5), 162.18 (d, $^1J_{CF}$ 245.3, C-6), 163.36 (d, $^1J_{CF}$ 244.5, C-3); δ_F -83.29 (1 F, d, $^5J_{FF}$ 31.0, F-3), -75.29 (1 F, d, $^5J_{FF}$ 31.0, F-6); *m/z* (ES^+) 301.2 ($[MH]^+$, 100%).

3,6-Difluoro-4-[(1-methylethyl)oxy]-5-(phenylthio)pyridazine **21**

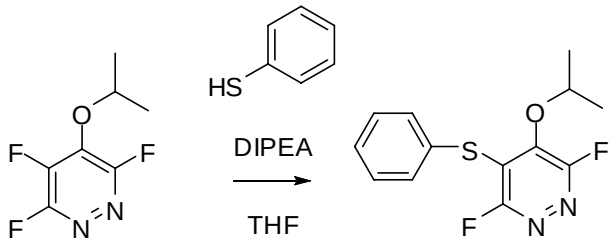

10 **21**

DIPEA (0.22 mL, 1.3 mmol) and thiophenol (0.077 mL, 0.75 mmol) were added to a stirred solution of 3,4,6-trifluoro-5-[(1-methylethyl)oxy]pyridazine **10** (160 mg, 0.833 mmol) in THF (10 mL) at 0 °C under nitrogen, and the solution was stirred for 1 hour. Aqueous NaOH was then added to the mixture, which was partitioned with EtOAc. The aqueous phase was extracted with two further portions of EtOAc and the combined organic phases were combined, dried and concentrated to give approx. 0.3 g of crude product. Purification by Biotage SP4, 40+M SiO2 column (initial solvent - 1% THF in cyclohexane (2 column volumes), then a gradient elution over 10 CV's (1% THF in cyclohexane to 7% THF in cyclohexane), then 7% THF in cyclohexane for 5 CV's) gave incomplete separation, so the mixture was recolumned on a 40+M column in toluene over 20 CV to give 205 mg of product containing ~2% disubstituted product (LCMS). 87 mg were further purified by RP-HPLC, giving *3,6-difluoro-4-[(1-methylethyl)oxy]-5-(phenylthio)pyridazine* **21** (77 mg, 33%) as pale yellow crystals, mp 45.1-46.9 °C (Found: $[MH]^+$, 283.07113. $C_{13}H_{12}F_2N_2OS$ requires: $[MH]^+$, 283.07112); ν_{max}/cm^{-1} 2985.5, 1581.1 and 1544.4; δ_H 1.26 (6 H, dd, $^3J_{HH}$ 6.1, $^6J_{HF}$ 0.9, CH_3), 4.97 - 5.08 (1 H, m, $^3J_{HH}$ 6.1, $^5J_{HF}$ 1.9, CH), 7.29 - 7.43 (5 H, m, CH); δ_C 22.40 (s, CH_3), 78.48 (d, $^5J_{CF}$ 8.0, CH), 121.17 (dd, $^2J_{CF}$ 32.0, $^3J_{CF}$ 7.2, C-5), 128.60 (s, C-4'), 129.31 (s, C-3', C-5'), 130.68 (s, C-1'), 131.86 (s, C-2', C-6'), 147.08 (dd, $^2J_{CF}$ 24.0, $^3J_{CF}$ 6.4, C-4), 157.86 (d, $^1J_{CF}$ 241.3, C-6), 163.88 (d, $^1J_{CF}$ 240.5, C-3); δ_F -92.13 (1 F, d, $^5J_{FF}$ 31.6, F-3), -76.49 (1 F, d, $^5J_{FF}$ 31.6, F-6); *m/z* (ES^+) 283.2 ($[MH]^+$, 76%).

4-[3,6-Difluoro-5-(phenylthio)-4-pyridazinyl]morpholine **22**

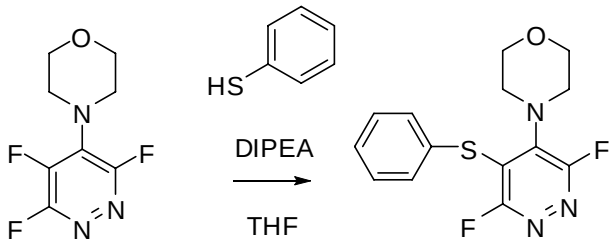

1 **22**

DIPEA (0.15 mL, 0.88 mmol) and thiophenol (0.06 mL, 0.58 mmol) were added to a stirred solution of 4-(3,5,6-trifluoro-4-pyridazinyl)morpholine **1** (129 mg, 0.589 mmol) in THF (10 mL) at 0 °C under nitrogen, and the solution was stirred for 1 hour. Aqueous NaOH was then added to the mixture, which was partitioned with EtOAc. The aqueous phase was extracted with two further portions of EtOAc and the combined organic phases were combined, dried and concentrated to give approx. 0.2 g of crude product. TLC (of the crude reaction NMR sample) showed Rf = 1.8 in 4:1 cyclohexane:EtOAc. Purification by Biotage SP4, 40+S SiO2 column (initial solvent - 5% EtOAc in cyclohexane (2 column volumes), then a gradient elution over 10 CV's (5% EtOAc in cyclohexane to 25% EtOAc in cyclohexane), then 25% EtOAc in cyclohexane for 5 CV's) gave 169 mg of product in >99% purity (LCMS and NMR spectroscopy). Further purification by RP-HPLC gave *4-[3,6-difluoro-5-(phenylthio)-4-pyridazinyl]morpholine* **22** (146 mg, 80%) as pale yellow crystals, mp 109.7-111.2 °C (Found: C, 54.13%, H, 4.19%, N, 13.60%. $C_{14}H_{13}F_2N_3OS$ requires C, 54.36%, H, 4.23%, N, 13.58%); ν_{max}/cm^{-1} 2982.7, 1581.2 and 1542.1; δ_H 3.40 (4 H, td, $^3J_{HH}$ 4.7, $^5J_{HF}$ 2.1, NCH_2), 3.70 (4 H, dd, $^3J_{HH}$ 4.7, 4.5, OCH_2), 7.21 - 7.25 (2 H, m, CH), 7.30 - 7.37 (3 H, m, CH); δ_C 50.42 (d, $^4J_{CF}$ 4.8, NCH_2), 66.83 (s, OCH_2), 116.35 (dd, $^2J_{CF}$ 32.0, $^3J_{CF}$ 5.6, C-4), 128.08 (1 C, s), 129.04 (2 C, s), 129.57 (2 C, s), 131.90 (1 C, s), 141.42 (dd, $^2J_{CF}$ 23.2, $^3J_{CF}$ 4.8, C-5), 159.07 (d, $^1J_{CF}$ 243.7, C-6), 164.90 (d, $^1J_{CF}$ 239.7, C-3); δ_F -86.16 (1 F, d, $^5J_{FF}$ 31.0, F-3), -75.95 (1 F, d, $^5J_{FF}$ 31.0, F-6); *m/z* (ES^+) 310.2 ($[MH]^+$, 100%).

4-(Ethylthio)-3,6-difluoro-5-isopropoxypyridazine **23**

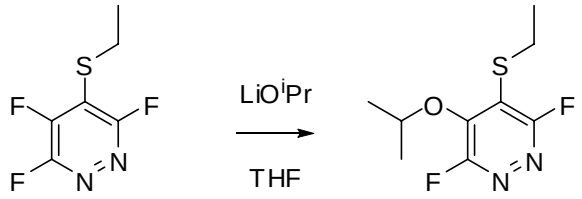

16 **23**

Lithium isopropoxide (2 M in THF, 0.58 mL, 1.16 mmol) was added to a stirred solution of 4-(ethylthio)-3,5,6-trifluoropyridazine **16** (227 mg, 1.17 mmol) in THF (10 mL) under argon at -78 °C, and the solution was allowed to come to RT overnight. The reaction was quenched by the addition of wet THF, then concentrated *in vacuo*, partitioned between EtOAc and water, the phases were separated and the aqueous phase was extracted with EtOAc. The combined organic phases were concentrated *in vacuo* to give approx. 267 mg of crude product. Purification by column chromatography (silica, 9:1 hexane:EtOAc) gave *4-(ethylthio)-3,6-difluoro-5-isopropoxypyridazine* **23** (213 mg, 78%) as a colourless oil (Found: C, 46.39%, H, 5.27%, N, 11.78%. $C_9H_{12}F_2N_2OS$ requires C, 46.14%, H, 5.16%, N, 11.96%); δ_H 1.31 (3 H, t, $^3J_{HH}$ 7.4, CH_2CH_3), 1.42 (6 H, d, $^3J_{HH}$ 5.9, $CHCH_3$), 3.16 (2 H, qd, $^3J_{HH}$ 7.4, $^5J_{HF}$ 1.3, CH_2), 4.99 (1 H, heptd, $^3J_{HH}$ 5.9, $^5J_{HF}$ 1.3, CH); δ_C 15.14 (s, CH_2CH_3), 22.82 (s, $CHCH_3$), 27.39 (d, $^4J_{CF}$ 7.1, CH_2), 78.76 (d, $^4J_{CF}$ 7.2, CH), 123.31 (dd, $^2J_{CF}$ 32.8, $^3J_{CF}$ 6.6, C-4), 146.82 (dd, $^2J_{CF}$ 24.4, $^3J_{CF}$ 7.8, C-5), 158.23 (dd, $^1J_{CF}$ 242.4, $^4J_{CF}$ 2.1, C-3), 164.04 (d, $^1J_{CF}$ 238.4, C-6); δ_F -93.80 (1 F, d, $^5J_{FF}$ 31.1, F-6), -78.72 (1 F, d, $^5J_{FF}$ 31.1, F-3); *m/z* (ES^+) 235.1 ($[MH]^+$, 100%).

3,6-Difluoro-4-isopropoxy-5-phenylpyridazine **24**

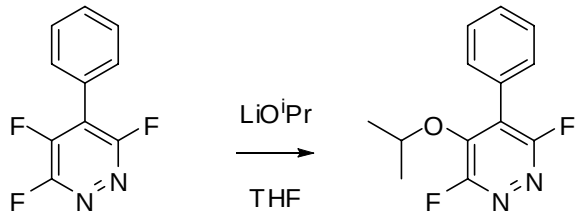

11 **24**

Lithium isopropoxide (2 M in THF, 0.40 mL, 0.80 mmol) was added to a stirred solution of 3,4,6-trifluoro-5-phenylpyridazine **11** (169 mg, 0.804 mmol) in THF (10 mL) under nitrogen at -78 °C. The mixture was allowed to come to RT overnight. The reaction was quenched by the addition of wet THF, and then concentrated, partitioned between EtOAc and water, and extracted with two further portions of EtOAc. The combined organic phases were dried and concentrated *in vacuo* to give 199 mg of crude product, Rf = 0.24 in 9:1 cyclohexane:EtOAc. Purification by Biotage SP4, 40+M SiO2 column (initial solvent - 2% EtOAc in cyclohexane (2 column volumes), then a gradient elution over 10 CV's (2% EtOAc in cyclohexane to 13% EtOAc in cyclohexane), then 13% EtOAc in cyclohexane for 5 CV's) gave *3,6-difluoro-4-isopropoxy-5-phenylpyridazine* **24** (138 mg, containing <10% of an inseparable isomer) as a colourless oil; δ_H 1.22 (6 H, dd, $^3J_{HH}$ 6.1, $^6J_{HF}$ 0.6, CH_3), 4.65 - 4.77 (1 H, m, CH), 7.49 - 7.52 (5 H, m, ArH); δ_F -92.32 (1 F, d, $^5J_{FF}$ 32.1, F-3), -83.02 (1 F, d, $^5J_{FF}$ 32.1, F-6); *m/z* (ES^+) 251.2 ($[MH]^+$, 92%).

4-(3,5-Difluoro-6-phenylpyridazin-4-yl)morpholine **25** and *4-(5,6-difluoro-3-phenylpyridazin-4-yl)morpholine* **26**

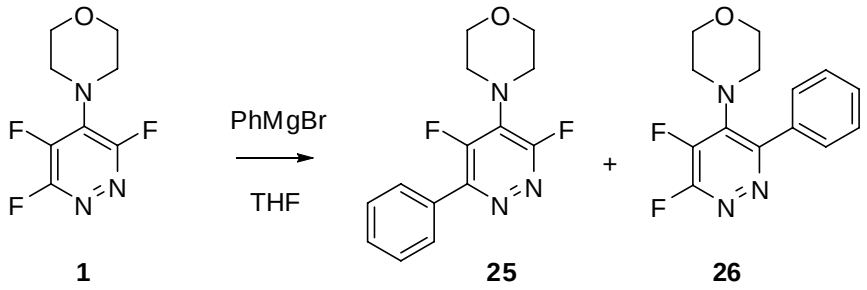

Phenylmagnesium bromide (1 M in THF, 0.85 mL, 0.85 mmol) was added to a stirred solution of 4-(3,5,6-trifluoro-4-pyridazinyl)morpholine **1** (187 mg, 0.853 mmol) in THF (10 mL) under nitrogen at -78 °C. The mixture was allowed to come to RT overnight. The reaction was quenched by the addition of wet THF, and then concentrated, partitioned between EtOAc and water, and extracted with two further portions of EtOAc. The combined organic phases were dried and concentrated *in vacuo* to give 224 mg of crude product, Rf = 0.3 in 1.5:8.5 toluene:DCM (SM Rf = 0.4). The crude product was purified by Biotage SP4, 40+S SiO2 column. Isocratic elution over 35 CV's, 5% toluene in DCM, to give 29 mg of an approximately 4:1 mixture of isomers (Minor product identified as *4-(5,6-difluoro-3-phenylpyridazin-4-yl)morpholine* **26**; δ_F -150.65 (1F, d, $^3J_{FF}$ 26.6, F-5), -102.33 (1F, d, $^3J_{FF}$ 26.6, F-6)). Further purification by MDAP gave *4-(3,5-difluoro-6-phenylpyridazin-4-yl)morpholine* **25** (15 mg, 6%) as a colourless oil (Found: $[MH]^+$, 278.10980. $C_{14}H_{14}F_2N_3O$ requires: $[MH]^+$, 278.10994); δ_H 3.49 - 3.52 (4 H, m, NCH_2), 3.83 - 3.87 (4 H, m, OCH_2), 7.50 - 7.53 (3 H, m, ArH), 7.83 - 7.87 (2 H, m, ArH); δ_C 50.5 (t, $^5J_{CF}$ 4.1, NCH_2), 67.0 (s, OCH_2), 126.5 (dd, $^2J_{CF}$ 22.8, $^2J_{CF}$ 7.9, C-4), 128.6 (s, C-3', C-5'), 128.9 (d, $^4J_{CF}$ 4.3, C-2', C-6'), 130.1 (s, C-4'), 132.1 (d, $^3J_{CF}$ 4.2, C-1'), 151.7 (dd, $^1J_{CF}$ 269.7, $^3J_{CF}$ 8.1, C-5), 152.0 (dd, $^2J_{CF}$ 8.8, $^4J_{CF}$ 2.9, C-6), 159.4 (dd, $^1J_{CF}$ 242.3, $^3J_{CF}$ 3.8, C-3); δ_F -128.2 (1 F, d, $^4J_{FF}$ 29.5, F-5), -85.0 (1 F, d, $^4J_{FF}$ 29.5, F-3), *m/z* (ES^+) 278.1 ($[MH]^+$, 100%).

3,5-Difluoro-4-isopropoxy-6-phenylpyridazine **27** *and 3,4-difluoro-5-isopropoxy-6-phenylpyridazine* **28**

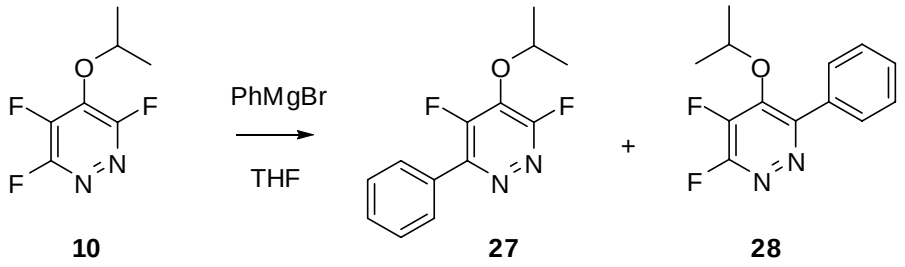

10 **27** **28**

Phenylmagnesium bromide (0.87 mL, 0.87 mmol) was added to a stirred solution of 3,4,6-trifluoro-5-[(1-methylethyl)oxy]pyridazine **10** (168 mg, 0.874 mmol) in THF (10 mL) under nitrogen at -78 °C. The mixture was allowed to come to RT overnight. The reaction was quenched by the addition of wet THF, and then concentrated, partitioned between EtOAc and water, and extracted with two further portions of EtOAc. The combined organic phases were dried and concentrated *in vacuo* to give 200 mg of crude product. Purification by Biotage SP4, 40+M SiO2 column, initial solvent - 1% EtOAc in toluene (2 column volumes), then a gradient elution over 10 CV's (1% EtOAc in toluene to 7% EtOAc in cyclohexane), then 7% EtOAc in toluene for 5 CV's gave 81 mg of impure, inseparable, product in a 3:1 ratio. *3,5-Difluoro-4-isopropoxy-6-phenylpyridazine* **27**; δ_F -133.2 (1F, m, F-5), -91.6 (1F, m, F-3); *m/z* (ES^+) 251.2 ($[MH]^+$, 100%). *3,4-Difluoro-5-isopropoxy-6-phenylpyridazine* **28**; δ_F -155.2 (1F, m, F-5), -100.3 (1F, m, F-3); *m/z* (ES^+) 251.2 ($[MH]^+$, 100%).

4-(Ethylthio)-3,5-difluoro-6-phenylpyridazine **29** and *4-(ethylthio)-3,6-difluoro-5-phenylpyridazine* **30**

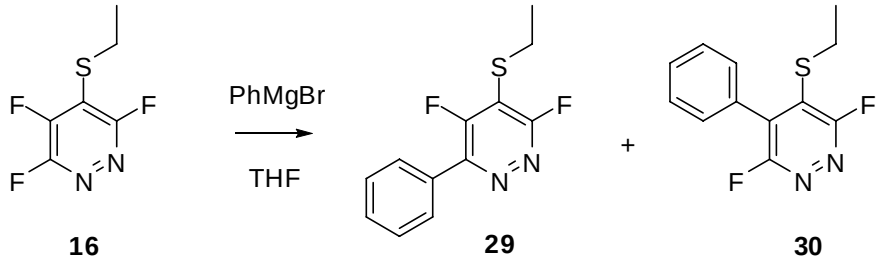

16 **29** **30**

Phenylmagnesium bromide (1 M in THF, 1.0 mL, 1.0 mmol) was added to a stirred solution of 4-(ethylthio)-3,5,6-trifluoropyridazine **16** (217 mg, 1.12 mmol) in THF (10 mL) under nitrogen at -78 °C. The mixture was allowed to come to RT overnight. The reaction was quenched by the addition of wet THF, and then concentrated, partitioned between EtOAc and water, and extracted with two further portions of EtOAc. The combined organic phases were dried and concentrated *in vacuo* to give 342 mg of crude product. Purification by column chromatography (silica, hexane:ethyl acetate, gradient elution) gave 199 mg of product as an inseparable mixture (1.8:1) of isomers. *4-(Ethylthio)-3,5-difluoro-6-phenylpyridazine* **29**; δ_F -109.6 (1F, d, $^4J_{FF}$ 22.4, F-5), -77.3 (1F, d, $^4J_{FF}$ 22.4, F-3). *4-(Ethylthio)-3,6-difluoro-5-phenylpyridazine* **30**; δ_F -85.2 (1F, d, $^5J_{FF}$ 31.2, F-3), -79.1 (1F, d, $^5J_{FF}$ 31.2, F-6).

4-(3-Fluoro-6-isopropoxy-5-(phenylthio)pyridazin-4-yl)morpholine **31** and *4-(6-fluoro-3-isopropoxy-5-(phenylthio)pyridazin-4-yl)morpholine* **32**

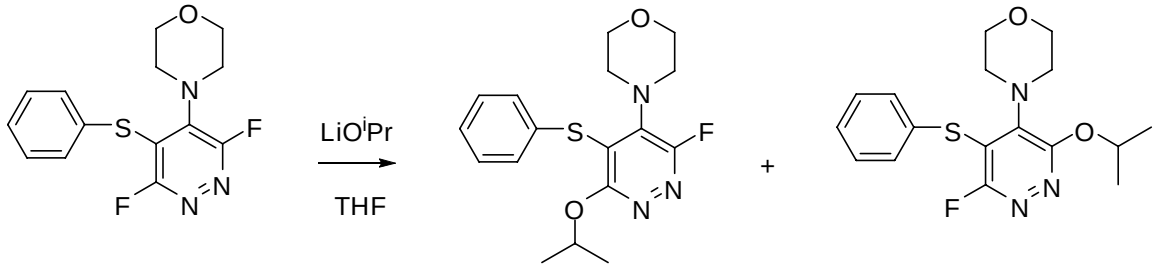

22 **31** **32**

Lithium isopropoxide (2 M in THF, 0.11 mL, 0.22 mmol) was added to a stirred solution of 4-[3,6-difluoro-5-(phenylthio)-4-pyridazinyl]morpholine **22** (68 mg, 0.22 mmol) in THF (10 ml) under nitrogen at -78 °C. The mixture was allowed to come to RT overnight. The reaction was quenched by the addition of wet THF, and then concentrated, partitioned between EtOAc and water, and extracted with two further portions of EtOAc. The combined organic phases were dried and concentrated *in vacuo* to give 89 mg of crude product. Purification by column chromatography (silica, 4:1 hexane:ethyl acetate) gave 73 mg of product as an inseparable mixture (4.5:1) of isomers.

Major isomer; δ_F -82.0 (1F, s); *m/z* (ES^+) 349.2 ($[MH]^+$, 68%).

Minor isomer; δ_F -92.1 (1F, s); *m/z* (ES^+) 349.1 ($[MH]^+$, 35%).

4,4'-(6-Fluoro-4-(phenylthio)pyridazine-3,5-diyl)dimorpholine **33**

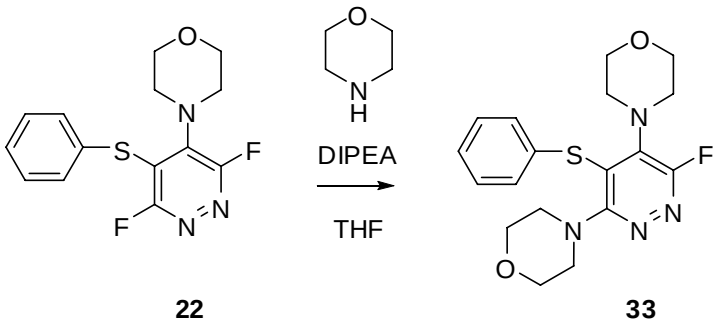

22 **33**

Morpholine (56 mg, 0.626 mmol) and DIPEA (84 mg, 1.20 mmol) were added to a stirred solution of 4-[3,6-difluoro-5-(phenylthio)-4-pyridazinyl]morpholine **22** (204 mg, 0.626 mmol) in THF (4 mL). After heating to 150 °C (mw) for 80 min, the mixture was concentrated, partitioned between EtOAc and water, and extracted with two further portions of EtOAc. The combined organic phases were dried and concentrated *in vacuo* to give 574 mg of crude product. Purification by column chromatography (silica, hexane:ethyl acetate, gradient elution) gave *4,4'-(6-fluoro-4-(phenylthio)pyridazine-3,5-diyl)dimorpholine* **33** (168 mg, 71%) as white crystals, mp 159.3-160.0 °C (Found: $[MH]^+$, 377.1436. $C_{18}H_{21}F_2N_4O_2S$ requires: $[MH]^+$, 377.1448); δ_H 3.15-3.19 (4H, m, CH_2NC-5), 3.31 (4H, t, $^3J_{HH}$ 4.7, CH_2NC-3), 3.61 (4H, t, 4.7, $^3J_{HH}$ CH_2CH_2NC-5), 3.64 (4H, t, $^3J_{HH}$ 4.7, CH_2CH_2NC-3), 7.06-7.09 (2H, m, ArH), 7.22-7.29 (3H, m, ArH); δ_C 50.51 (s, CH_2NC-3), 50.57 (d, $^4J_{CF}$ 4.2, CH_2NC-5), 66.66 (s, CH_2CH_2NC-3), 66.95 (s, CH_2CH_2NC-5), 121.48 (d, $^3J_{CF}$ 6.9, C-4), 127.65 (s, C-4'), 128.45 (s, C-3',C-5'), 129.24 (s, C-2', C-6'), 133.83 (s, C-1'), 140.26 (d, $^2J_{CF}$ 23.4, C-5), 158.71 (d, $^1J_{CF}$ 241.2, C-6), 163.91 (s, C-3); δ_F -92.57 (1F, s); *m/z* (ES^+) 377.1 ($[MH]^+$, 100%).

6.3 Experimental to Chapter 3

3-Fluoro-5,8-dimethyl-4-morpholin-4-yl-5,6,7,8-tetrahydro-pyrazino[2,3-c]pyridazine **34**

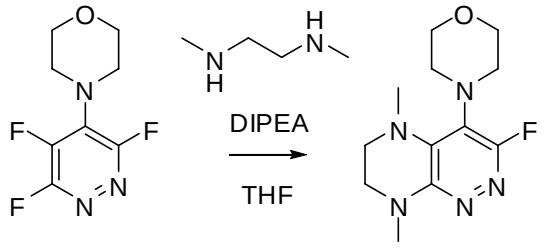

1 **34**

DIPEA (0.25 mL, 1.5 mmol) and *N*,*N*'-dimethyl-ethane-1,2-diamine (0.05 mL, 0.5 mmol) were added to a stirred solution of 4-(3,5,6-trifluoro-pyridazin-4-yl)-morpholine **1** (100 mg, 0.46 mmol) in THF (4 mL), and the mixture was stirred at room temperature for 5 days. The mixture was then concentrated, partitioned between DCM and water, the phases were separated and the aqueous phase further extracted with DCM. The organic phases were combined, dried and concentrated to give approximately 1.2 g of crude product. Purification by column chromatography (silica, 1:2 toluene:THF) gave *3-fluoro-5,8-dimethyl-4-morpholin-4-yl-5,6,7,8-tetrahydro-pyrazino[2,3-c]pyridazine* **34** (103 mg, 84%) as white crystals; mp 144.2 – 147.3 °C (Found: $[MH]^+$, 268.1574. $C_{12}H_{18}FN_5O$ requires $[MH]^+$, 268.1574); δ_H 3.08 (4H, td, $^3J_{HH}$ 4.7, $^5J_{HF}$ 1.8, CH_2NC-4), 3.14 (3H, s, CH_3N-5), 3.30 – 3.33 (2H, m, CH_2N), 3.31 (3H, s, CH_3N-8), 3.38 – 3.40 (2H, m, CH_2N), 3.76 (4H, t, $^3J_{HH}$ 4.7, CH_2O); δ_C 38.32 (s, CN-8), 41.48 (s, CN-5), 46.59 (s, C-7), 50.40 (d, $^4J_{CF}$ 4.3, *C*NC-4), 51.01 (s, C-6), 67.01 (d, $^5J_{CF}$ 0.5, CO), 119.53 (d, $^2J_{CF}$ 29.1, C-4), 134.93 (d, $^3J_{CF}$ 8.9, C-4a), 151.81 (s, C-8a), 161.23 (d, $^1J_{CF}$ 236.6, C-3); δ_F -94.54 (1F, s); *m/z* (AP^+) 267 ($[M]^+$, 100%).

3-Fluoro-4-morpholin-4-yl-9-oxa-10-thia-1,2-diaza-anthracene **35**

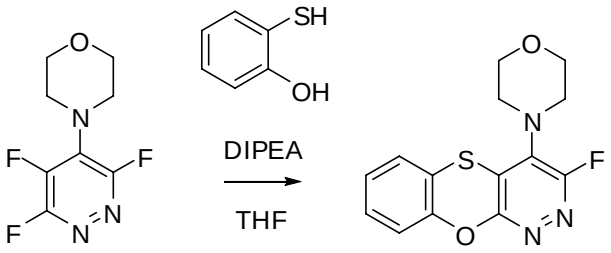

1 **35**

DIPEA (1.2 mL, 6.9 mmol) and 2-mercaptophenol (0.23 mL, 2.3 mmol) were added to a stirred solution of 4-(3,5,6-trifluoro-pyridazin-4-yl)-morpholine **1** (504 mg, 2.3 mmol) in THF (4 mL), and the mixture was stirred at room temperature overnight. The mixture was then concentrated, partitioned between DCM and water, the phases were separated and the aqueous phase further extracted with DCM. The organic phases were combined, dried and concentrated to give approximately 1.7 g of crude product. Purification by column chromatography (silica, hexane:ethyl acetate, gradient elution), followed by recrystallisation from ethanol gave *3-fluoro-4-morpholin-4-yl-9-oxa-10-thia-1,2-diaza-anthracene* **35** (476 mg, 68%) as pale yellow crystals; mp 167.7 – 169.1 °C (Found: $[MH]^+$, 306.0707. $C_{14}H_{12}FN_3O_2S$ requires $[MH]^+$, 306.0713); δ_H 3.24 (4H, td, $^3J_{HH}$ 4.7, $^5J_{HF}$ 2.1, CH_2N), 3.85 (4H, t, $^3J_{HH}$ 4.7, CH_2O), 7.07 – 7.10 (2H, m, H-6, H-8), 7.13 – 7.15 (1H, m, H-7), 7.20 – 7.22 (1H, m, H-5); δ_C 49.99 (d, $^4J_{CF}$ 3.9, CH_2N), 67.28 (d, $^5J_{CF}$ 1.3, CH_2O), 114.56 (s, C-10a), 118.94 (s, C-8), 123.54 (d, $^3J_{CF}$ 8.0, C-4a), 125.74 (s, C-6), 126.36 (s, C-7), 129.31 (s, C-5), 134.18 (d, $^2J_{CF}$ 26.3, C-4), 149.96 (d, $^4J_{CF}$ 1.0, C-9a), 159.32 (s, C-8a), 160.30 (d, $^1J_{CF}$ 243.0, C-3); δ_F -90.01 (1F, s); *m/z* (AP^+) 305 ($[M]^+$, 100%).

4-Amino-3,5,6-trifluoropyridazine **36**

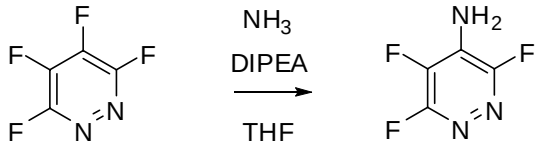

36

DIPEA (0.4 mL, 2.3 mmol) and ammonia (1 M solution in dioxane, 2.1 mL, 2.1 mmol) were added to a stirred solution of tetrafluoropyridazine (312 mg, 2.1 mmol) in THF (10 mL), and the mixture was stirred at room temperature overnight. The mixture was then concentrated, partitioned between DCM and water, the phases were separated and the aqueous phase further extracted with DCM. The organic phases were combined, dried and concentrated to give approximately 500 mg of crude product. Purification by column chromatography (silica, hexane:ethyl acetate) gave *4-amino-3,5,6-trifluoropyridazine*[1] **36** (264 mg, 86%) as a white solid; δ_H 4.70 (2H, br. s, NH_2); δ_F -153.66 (1 F, dd, $^4J_{FF}$ 30.1, $^3J_{FF}$ 25.9, F-5), -100.02 (1 F, dd, $^5J_{FF}$ 28.8, $^3J_{FF}$ 25.9, F-6), -93.30 (1 F, dd, $^4J_{FF}$ 30.1, $^5J_{FF}$ 28.8, F-3).

3-Fluoro-9-oxa-10-thia-1,2-diaza-anthracen-4-ylamine **37**

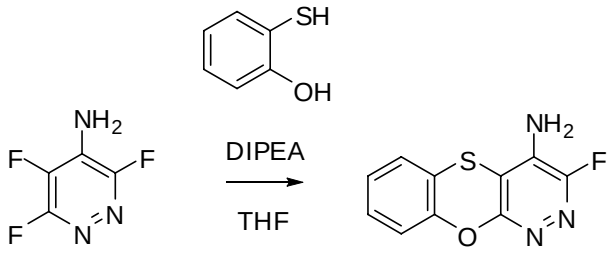

36 **37**

DIPEA (0.53 mL, 3.0 mmol) and 2-mercaptophenol (0.1 mL, 1.0 mmol) were added to a stirred solution of 3,5,6-trifluoro-pyridazin-4-ylamine **36** (150 mg, 1.0 mmol) in THF (4 mL), and the mixture was heated by microwave irradiation to a temperature of 150 °C for a

period of 10 minutes. The mixture was then concentrated, partitioned between DCM and water, the phases were separated and the aqueous phase further extracted with DCM. The organic phases were combined, dried and concentrated to give approximately 200 mg of crude product. Purification by column chromatography (silica, 1:1 hexane:ethyl acetate) followed by sublimation gave *3-fluoro-9-oxa-10-thia-1,2-diaza-anthracen-4-ylamine* **37** (29 mg, 12%) as an off-white solid; δ_H 3.34 (2H, br. s, NH_2), 7.15 – 7.22 (2H, m, H-6, H-8), 7.27 – 7.35 (2H, m, H-5, H-7), δ_C 102.97 (d, $^3J_{CF}$ 7.3, C-4a), 115.88 (s, C-8), 118.39 (s, C-10a), 125.74 (s, C-6), 126.95 (s, C-7), 129.06 (s, C-5), 133.42 (d, $^2J_{CF}$ 30.2, C-4), 150.26 (s, C-8a), 154.24 (d, $^1J_{CF}$ 233.5, C-3), 158.84 (s, C-9a); δ_F -98.415 (1F, s); *m/z* (EI^+) 235 ($[M]^+$, 100%).

4-Ethylsulfanyl-3-fluoro-5,8-dimethyl-5,6,7,8-tetrahydro-pyrazino[2,3-c]pyridazine **38**

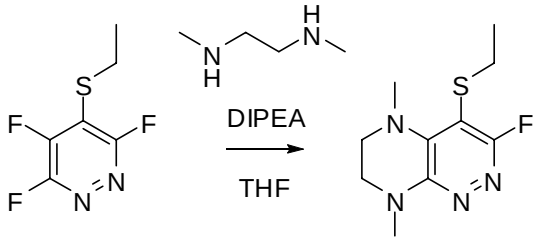

16 **38**

DIPEA (0.7 mL, 4 mmol) and *N*,*N*'-dimethyl-ethane-1,2-diamine (0.16 mL, 1.6 mmol) were added to a stirred solution of 4-ethylsulfanyl-3,5,6-trifluoro-pyridazine **16** (200 mg, 1.0 mmol) in THF (4 mL), and the mixture was stirred at room temperature overnight. The mixture was then concentrated, partitioned between DCM and water, the phases were separated and the aqueous phase further extracted with DCM. The organic phases were combined, dried and concentrated to give approximately 250 mg of crude product. Purification by column chromatography (silica, 1:9 hexane:ethyl acetate) gave *4-ethylsulfanyl-3-fluoro-5,8-dimethyl-5,6,7,8-tetrahydro-pyrazino[2,3-c]pyridazine* **38** (191 mg, 77%) as a white solid; mp 78.1 – 80.0 °C (Found: C, 49.4%; H, 6.2%; N, 23.0%. $C_{10}H_{15}FN_4S$ requires: C, 49.6%; H, 6.2%; N, 23.1%); δ_H 1.19 (3H, t, $^3J_{HH}$ 7.4, CH_3CH_2S),

2.78 (2H, q, $^{3}J_{HH}$ 7.4, CH_2S), 3.11 (3H, s, CH_3N-5), 3.31 (3H, s, CH_3N-8), 3.30 – 3.32 (2H, m, CH_2N), 3.46 – 3.49 (2H, m, CH_2N); δ_C 14.41 (s, CH_3CH_2S), 29.18 (d, $^{4}J_{CF}$ 4.4, CH_2S), 37.85 (s, CH_3N), 43.15 (s, CH_3N), 46.77 (s, CH_2N), 51.85 (s, CH_2N), 101.99 (d, $^{2}J_{CF}$ 36.1, C-4), 141.61 (d, $^{3}J_{CF}$ 5.2, C-4a), 150.82 (s, C-8a), 162.34 (d, $^{1}J_{CF}$ 227.0, C-3); δ_F -87.00 (1F, s); *m/z* (EI^+) 242 ($[M]^+$, 100%).

4-Ethylsulfanyl-3-fluoro-9-oxa-10-thia-1,2-diaza-anthracene **39**

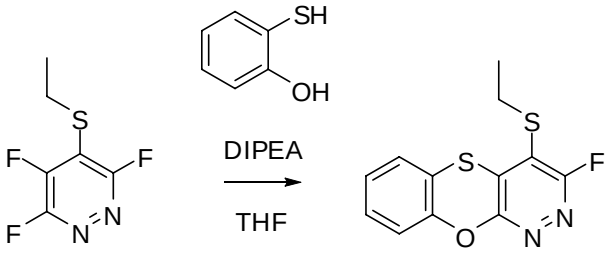

16 **39**

DIPEA (0.40 mL, 2.3 mmol) and 2-mercaptophenol (0.08 mL, 0.8 mmol) were added to a stirred solution of 4-ethylsulfanyl-3,5,6-trifluoro-pyridazine **16** (150 mg, 0.77 mmol) in THF (4 mL), and the mixture was stirred at room temperature overnight. The mixture was then concentrated, partitioned between DCM and water, the phases were separated and the aqueous phase further extracted with DCM. The organic phases were combined, dried and concentrated to give approximately 0.3 g of crude product. Purification by column chromatography (silica, 19:1 toluene:ethyl acetate) gave *4-ethylsulfanyl-3-fluoro-9-oxa-10-thia-1,2-diaza-anthracene* **39** (161 mg, 74%) as yellow crystals; mp 121.4 – 123.0 °C (Found: $[MH]^+$, 281.0220. $C_{12}H_9FN_2OS_2$ requires $[MH]^+$, 281.0219); δ_H 1.34 (3H, t, $^{3}J_{HH}$ 7.4, CH_3), 3.14 (2H, qd, $^{3}J_{HH}$ 7.4, $^{5}J_{HF}$ 1.0, CH_2), 7.07 – 7.09 (2H, m, H-6, H-8), 7.12 – 7.14 (1H, m, H-7), 7.19 – 7.23 (1H, m, H-5); δ_C 15.31 (s, CH_3), 28.82 (d, $^{4}J_{CF}$ 6.9, CH_2), 114.49 (s, C-10a), 118.83 (s, C-8), 124.04 (d, $^{2}J_{CF}$ 36.3, C-4), 125.86 (s, C-6), 126.43 (s, C-7), 129.46 (s, C-5), 133.25 (d, $^{3}J_{CF}$ 4.9, C-4a), 149.44 (s, C-8a), 157.69 (d, $^{4}J_{CF}$ 1.9, C-9a), 162.92 (d, $^{1}J_{CF}$ 238.2, C-3); δ_F -82.19 (1F, s); *m/z* (AP^+) 280 ($[M]^+$, 100%).

4-Ethylsulfanyl-3-fluoro-10H-9-oxa-1,2,10-triaza-anthracene **40**

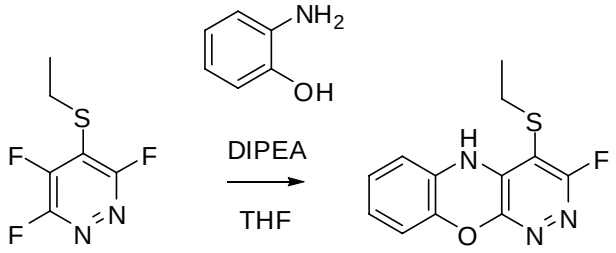

16 **40**

DIPEA (0.40 mL, 2.3 mmol) and 2-aminophenol (84 mg, 0.77 mmol) were added to a stirred solution of 4-ethylsulfanyl-3,5,6-trifluoro-pyridazine **16** (150 mg, 0.77 mmol) in THF (4 mL), and the mixture was heated by microwave irradiation to a temperature of 100 °C for a period of 5 minutes. The mixture was then concentrated, partitioned between DCM and water, the phases were separated and the aqueous phase further extracted with DCM. The organic phases were combined, dried and concentrated to give approximately 200 mg of crude product. Purification by column chromatography (silica, 5:2:3 hexane:ethyl acetate:DCM) gave *4-ethylsulfanyl-3-fluoro-10H-9-oxa-1,2,10-triaza-anthracene* **40** (153 mg, 75%) as a yellow solid; mp (with decomposition) 260 °C (Found: $[MH]^+$, 264.0597. $C_{12}H_{10}FN_3OS$ requires $[MH]^+$, 264.0607); δ_H 1.31 (3H, t, $^3J_{HH}$ 7.4, CH_3), 1.62 (1H, br. s, NH), 2.90 (2H, q, $^3J_{HH}$ 7.4, CH_2), 6.63 – 6.65 (1H, m, H-5), 6.87 – 6.94 (3H, m, H-6, H-7, H-8); δ_C 15.29 (s, CH_3), 28.91 (d, $^4J_{CF}$ 3.1, CH_2), 102.27 (d, $^2J_{CF}$ 40.1, C-4), 114.63 (s, C-5), 117.15 (s, C-8), 124.72 (s, C-7), 125.07 (s, C-6), 125.82 (s, C-10a), 137.67 (d, $^3J_{CF}$ 7.1, C-4a), 142.82 (s, C-8a), 153.49 (d, $^4J_{CF}$ 0.9, C-9a), 164.44 (d, $^1J_{CF}$ 235.1, C-3); δ_F -80.98 (1F, s); *m/z* (AP^+) 263 ($[M]^+$, 100%).

4-Ethylsulfanyl-3-fluoro-10H-9-thia-1,2,10-triaza-anthracene **41**

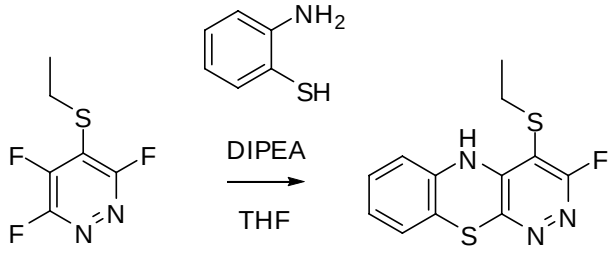

16 **41**

DIPEA (1.4 mL, 7.9 mmol) and 2-aminophenol (0.28 mL, 1.9 mmol) were added to a stirred solution of 4-ethylsulfanyl-3,5,6-trifluoro-pyridazine **16** (397 mg, 2.0 mmol) in THF (4 mL), and the mixture was heated by microwave irradiation to a temperature of 100 °C for a period of 30 minutes. The mixture was then concentrated, partitioned between DCM and water, the phases were separated and the aqueous phase further extracted with DCM. The organic phases were combined, dried and concentrated to give approximately 600 mg of crude product. Recrystallisation from chloroform gave *4-ethylsulfanyl-3-fluoro-10H-9-thia-1,2,10-triaza-anthracene* **41** (333 mg, 63%) as yellow crystals; mp 249.2 – 251.8 °C (Found: $[MH]^+$, 280.0378. $C_{12}H_{10}FN_3S_2$ requires $[MH]^+$, 280.0378); δ_H 1.35 (3H, t, $^3J_{HH}$ 7.4, CH_3), 2.48 (1H, br. s, NH), 3.11 (2H, qd, $^3J_{HH}$ 7.4, $^5J_{HF}$ 0.8, CH_2), 6.83 – 6.88 (3H, m, H-5, H-6, H-7), 7.05 – 7.07 (1H, m, H-8); δ_C 15.32 (s, CH_3), 28.87 (d, $^4J_{CF}$ 6.9, CH_2), 113.83 (s, C-8a), 117.01 (s, C-5), 122.75 (d, $^2J_{CF}$ 38.4, C-4), 124.31 (s, C-7), 126.18 (s, C-8), 129.29 (s, C-6), 135.44 (d, $^3J_{CF}$ 4.6, C-4a), 135.80 (s, C-10a), 151.74 (s, C-9a), 160.86 (d, $^1J_{CF}$ 237.5, C-3); δ_F -85.61 (1F, s); *m/z* (AP^+) 279 ($[M]^+$, 100%).

4-Ethylsulfanyl-3-fluoro-1,2,4b,9-tetraaza-fluorene **42**

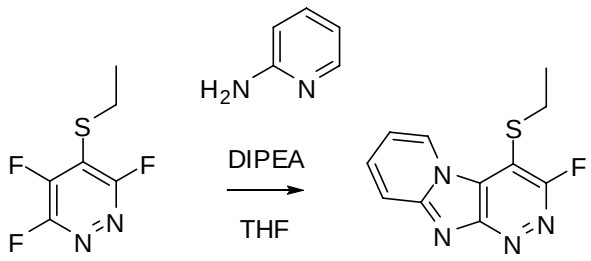

16 **42**

DIPEA (0.70 mL, 4.0 mmol) and pyridin-2-ylamine (143 mg, 1.5 mmol) were added to a stirred solution of 4-ethylsulfanyl-3,5,6-trifluoro-pyridazine **16** (199 mg, 1.03 mmol) in THF (4 mL), and the mixture was heated by microwave irradiation to a temperature of 150 °C for a period of 30 minutes. The mixture was then concentrated, partitioned between DCM and water, the phases were separated and the aqueous phase further extracted with DCM. The organic phases were combined, dried and concentrated to give approximately 300 mg of crude product. Purification by column chromatography (silica, 1:9 hexane:ethyl acetate) followed by recrystallisation from ethanol gave *4-ethylsulfanyl-3-fluoro-1,2,4b,9-tetraaza-fluorene* **42** (35 mg, 14%) as orange crystals; mp 197.8 – 199.5 °C (Found: $[MH]^+$, 249.0601. $C_{11}H_9FN_4S$ requires $[MH]^+$, 249.0610); δ_H 1.38 (3H, t, $^3J_{HH}$ 7.4, CH_3), 3.32 (2H, qd, $^3J_{HH}$ 7.4, $^5J_{HF}$ 0.7, CH_2), 6.97 (1H, td, $^3J_{HH}$ 7.2, $^3J_{HH}$ 6.8, $^4J_{HH}$ 1.1, H-6), 7.64 (1H, ddd, $^3J_{HH}$ 9.4, $^3J_{HH}$ 6.8, $^4J_{HH}$ 1.3, H-7), 7.79 (1H, dt, $^3J_{HH}$ 9.4, $^5J_{HH}$ 1.2, $^4J_{HH}$ 1.1, H-8), 9.44 (1H, dt, $^3J_{HH}$ 7.2, $^4J_{HH}$ 1.3, $^5J_{HH}$ 1.2, H-5); δ_C 15.40 (s, CH_3), 26.92 (d, $^4J_{CF}$ 7.5, CH_2), 111.12 (d, $^2J_{CF}$ 38.5, C-4), 112.07 (s, C-8), 119.14 (s, C-6), 126.41 (d, $^3J_{CF}$ 8.0, C-4a), 129.55 (s, C-7), 133.76 (s, C-5), 153.39 (d, $^4J_{CF}$ 0.9, C-9a), 158.82 (s, C-8a), 160.76 (d, $^1J_{CF}$ 229.2, C-3); δ_F -89.37 (1F, s); *m/z* (ES^+) 249 ($[MH]^+$, 100%).

4-Ethylsulfanyl-3-fluoro-8-methyl-1,2,4b,9-tetraaza-fluorene **43**

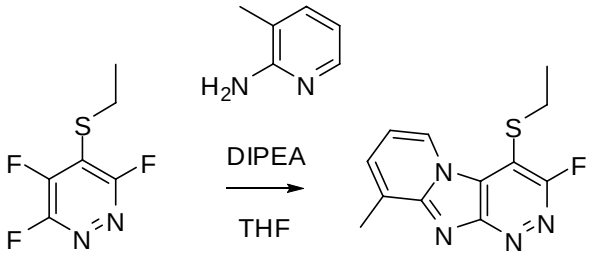

16 **43**

DIPEA (0.70 mL, 4.0 mmol) and pyridin-2-ylamine (0.15 mL, 1.29 mmol) were added to a stirred solution of 4-ethylsulfanyl-3,5,6-trifluoro-pyridazine **16** (200 mg, 1.03 mmol) in THF (4 mL), and the mixture was stirred at room temperature for seven days. The mixture was then concentrated, partitioned between DCM and water, the phases were separated and the aqueous phase further extracted with DCM. The organic phases were combined, dried and concentrated to give approximately 350 mg of crude product. Purification by column chromatography (silica, 1:9 hexane:ethyl acetate) gave *4-ethylsulfanyl-3-fluoro-8-methyl-1,2,4b,9-tetraaza-fluorene* **43** (134 mg, 50%) as orange crystals; mp 160.2 – 161.1 °C (Found: $[MH]^+$, 263.0760. $C_{12}H_{11}FN_4S$ requires $[MH]^+$, 263.0767); δ_H 1.37 (3H, t, $^3J_{HH}$ 7.3, C*H*$_3$CH$_2$S), 2.72 (3H, s, CH$_3$C-8), 3.30 (2H, qd, $^3J_{HH}$ 7.3, $^5J_{HF}$ 0.9, CH$_2$), 6.89 (1H, dd, $^3J_{HH}$ 7.0, 6.9, H-6), 7.42 (1H, d, $^3J_{HH}$ 6.9, H-7), 9.31 (1H, d, $^3J_{HH}$ 7.0, H-5); δ_C 15.39 (s, *C*H$_3$CH$_2$S), 17.69 (s, CH$_3$C-8), 29.57 (d, $^4J_{CF}$ 7.2, CH$_2$), 110.87 (d, $^2J_{CF}$ 39.4, C-4), 112.14 (s, C-7), 126.93 (s, C-5), 126.98 (d, $^3J_{CF}$ 7.9, C-4a), 129.30 (s, C-8), 131.59 (s, C-6), 154.16 (d, $^4J_{CF}$ 1.0, C-9a), 158.77 (s, C-8a), 160.78 (d, $^1J_{CF}$ 228.9, C-3), δ_F -89.55 (1F, s); *m/z* (EI^+) 262 ($[M]^+$, 100%).

4-Ethylsulfanyl-3-fluoro-6-methyl-furo[2,3-c]pyridazine-5-carboxylic acid ethyl ester **44**

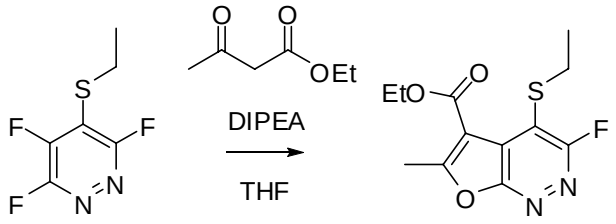

16 **44**

DIPEA (0.82 mL, 4.7 mmol) and 3-oxo-butyric acid ethyl ester (0.17 mL, 1.3 mmol) were added to a stirred solution of 4-ethylsulfanyl-3,5,6-trifluoro-pyridazine **16** (234 mg, 1.21 mmol) in THF (4 mL), and the mixture was heated by microwave irradiation to a temperature of 180 °C for a period of 90 minutes. The mixture was then concentrated, partitioned between DCM and water, the phases were separated and the aqueous phase further extracted with DCM. The organic phases were combined, dried and concentrated to give approximately 500 mg of crude product. Purification by column chromatography (silica, 2:1 hexane:ethyl acetate) gave *4-ethylsulfanyl-3-fluoro-6-methyl-furo[2,3-c]pyridazine-5-carboxylic acid ethyl ester* **44** (95 mg, 28%) as a colourless oil; (Found: $[MH]^+$, 285.0711. $C_{12}H_{13}FN_2O_3S$ requires $[MH]^+$, 285.0709); δ_H 1.29 (3H, t, $^3J_{HH}$ 7.4, SCH_2CH_3), 1.43 (3H, t, $^3J_{HH}$ 7.2, OCH_2CH_3), 2.77 (3H, s, CH_3C-6), 3.18 (2H, qd, $^3J_{HH}$ 7.4, $^5J_{HF}$ 2.3, SCH_2), 4.43 (2H, q, $^3J_{HH}$ 7.2, OCH_2); δ_C 14.37 (s, CH_3C-6), 14.98 (d, $^5J_{CF}$ 1.9, SCH_2CH_3), 15.04 (s, OCH_2CH_3), 28.68 (d, $^4J_{CF}$ 11.5, SCH_2), 61.80 (s, OCH_2), 111.04 (d, $^3J_{CF}$ 4.7, C-4a), 122.82 (d, $^2J_{CF}$ 34.8, C-4), 126.64 (d, $^4J_{CF}$ 6.6, C-7a), 161.73 (s, C-5), 162.13 (s, C-6), 162.95 (d, $^1J_{CF}$ 232.4, C-3), 168.34 (s, C=O); δ_F -84.97 (1F, s); *m/z* (ES^+) 285 ($[MH]^+$, 100%).

6.4 Experimental to Chapter 4

2-Fluorothiophene **45**

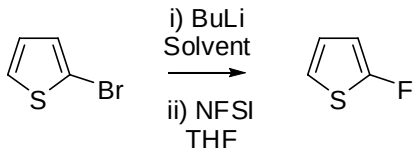

45

Method A:

2-Bromothiophene (0.82 g, 5 mmol) was dissolved in THF (30 mL) at -78 ^{o}C under argon. *n*-Butyllithium (3.8 mL, 1.6 M in hexanes) was added and the mixture left with stirring for 1h. NFSI (1.89 g, 6 mmol) in THF (15 mL) was then added and the mixture was left with stirring for a further 1h. Ammonium chloride (1 g, 19 mmol) in water (10 mL) was added and the mixture was allowed to come to room temperature. Analysis of the reaction mixture by ^{19}F NMR spectroscopy showed *2-fluorothiophene*[2] **45** (0.41 g, 80% (by comparison with a known mass of fluorobenzene)); δ_F -134.85 (br. s). No further purification was attempted due to the volatility of the product.

Method B:

As previously, but with the first step performed in diethyl ether (30 mL). *2-fluorothiophene* **45** was observed in 85% yield.

3-Fluorothiophene **46**

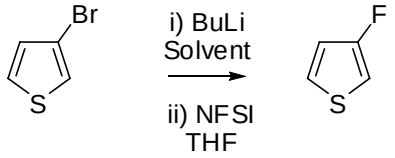

46

Method A:

3-Bromothiophene (0.82 g, 5 mmol) was dissolved in THF (30 mL) at -78 ^{o}C under argon. *n*-Butyllithium (3.8 mL, 1.6 M in hexanes) was added and the mixture left with stirring for 1h. NFSI (1.89 g, 6 mmol) in THF (15 mL) was then added and the mixture was left with stirring for a further 1h. Ammonium chloride (1 g, 19 mmol) in water (10 mL) was added and the mixture was allowed to come to room temperature. Analysis of the reaction mixture by ^{19}F NMR spectroscopy showed *3-fluorothiophene*[2] **46** (0.18 g, 36% (by comparison with a known mass of fluorobenzene)); δ_F -131.13 (d, $^{3}J_{HF}$ 3.0). No further purification was attempted due to the volatility of the product.

Method B:

As previously, but with the first step performed in diethyl ether (30 mL). *3-fluorothiophene* **46** was observed in 50% yield.

2-Fluoro-5-methylthiophene **47**

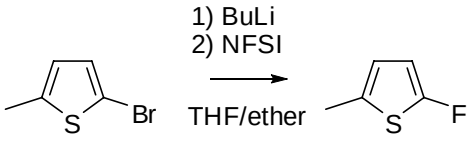

47

2-Bromo-5-methylthiophene (0.89 g, 5 mmol) was dissolved in ether (30 mL) at -78 ^{o}C under argon. *n*-Butyllithium (3.2 mL, 1.6 M in hexanes) was added and the mixture was left

with stirring for 1h. NFSI (1.58 g, 5 mmol) in THF (10 mL) was then added and the mixture was left with stirring for a further 1h. Ammonium chloride (1 g, 19 mmol) in water (10 mL) was added and the mixture was allowed to come to room temperature. Analysis of the reaction mixture by ^{19}F NMR spectroscopy showed *2-fluoro-5-methylthiophene* **47** (0.51g, 88% (by comparison with a known mass of fluorobenzene)); δ_F -133.80 (dd, $^3J_{HF}$ 4.7, $^4J_{HF}$ 2.8). No further purification was attempted due to the volatility of the product.

2-Fluoro-3-methylthiophene **48**

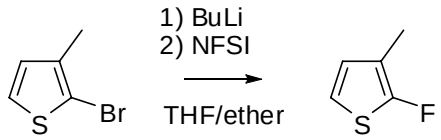

48

2-Bromo-3-methylthiophene (0.89 g, 5 mmol) was dissolved in ether (30 mL) at -78 ^oC under argon. *n*-Butyllithium (3.2 mL, 1.6 M in hexanes) was added and the mixture was left with stirring for 1h. NFSI (1.58 g, 5 mmol) in THF (10 mL) was then added and the mixture was left with stirring for a further 1h. Ammonium chloride (1 g, 19 mmol) in water (10 mL) was added and the mixture was allowed to come to room temperature. Analysis of the reaction mixture by ^{19}F NMR spectroscopy showed *2-fluoro-3-methylthiophene* **48** (0.45 g, 78% (by comparison with a known mass of fluorobenzene)); δ_F -142.14 (d, $^4J_{HF}$ 1.5). No further purification was attempted due to the volatility of the product.

2-Chloro-5-fluorothiophene **49**

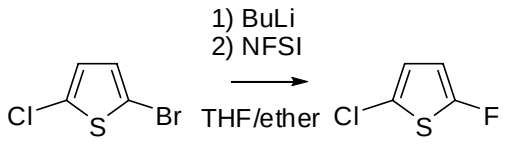

49

2-Bromo-5-chlorothiophene (0.99 g, 5 mmol) was dissolved in ether (30 mL) at -78 ^{o}C under argon. *n*-Butyllithium (3.2 mL, 1.6 M in hexanes) was added and the mixture was left with stirring for 1h. NFSI (1.58 g, 5 mmol) in THF (15 mL) was then added and the mixture was left with stirring for a further 1h. Ammonium chloride (1 g, 19 mmol) in water (10 mL) was added and the mixture was allowed to come to room temperature. Analysis of the reaction mixture by ^{19}F NMR spectroscopy showed *2-chloro-5-fluorothiophene* **49** (0.29 g, 43% (by comparison with a known mass of fluorobenzene)); δ_F -128.13 (dd, $^{3}J_{HF}$ 3.0, $^{4}J_{HF}$ 3.0). No further purification was attempted due to the volatility of the product.

3-Bromo-2-fluorothiophene **50**

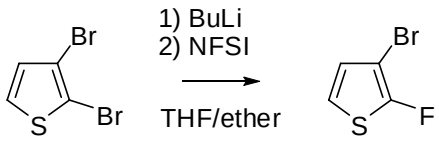

50

2,3-Dibromothiophene (1.21 g, 5 mmol) was dissolved in ether (30 mL) at -78 ^{o}C under argon. *n*-Butyllithium (3.8 mL, 1.6 M in hexanes) was added and the mixture was left with stirring for 1h. NFSI (1.89 g, 6 mmol) in THF (15 mL) was then added and the mixture was left with stirring for a further 1h. Ammonium chloride (1 g, 19 mmol) in water (10 mL) was added and the mixture was allowed to come to room temperature. Analysis of the reaction mixture by ^{19}F NMR spectroscopy showed *3-bromo-2-fluorothiophene* **50** (0.59 g, 65% (by

comparison with a known mass of fluorobenzene)); δ_F -133.53 (d, $^4J_{HF}$ 3.0). No further purification was attempted due to the volatility of the product.

Tetrabromothiophene **51**

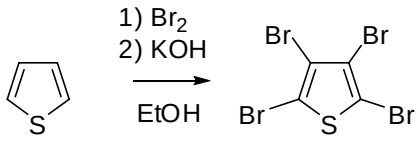

51

Thiophene (5.05 g, 0.06 mol) and chloroform (2.4 mL) were placed in a round bottomed flask and bromine (13.8 mL, 0.27 mol) was added dropwise to the stirred solution. The mixture was stirred at room temperature for 17h, then heated at reflux for 2h. The solution was cooled to room temperature, then potassium hydroxide (6.6 g, 0.12 mol) in ethanol (36 mL) was added and the mixture was heated at reflux for a further 4h, then poured into ice/water (80 mL). The product was extracted into chloroform and recrystallised from chloroform and ethanol to give *tetrabromothiophene*[3] **51** (15.09 g, 63%) as white crystals, mp 115.9 - 116.4 ^oC (lit. mp 117 - 118 °C) (Found: C, 12.03%. C_4Br_4S requires C, 12.02%); δ_C 110.3 (s, C-2, C-5), 117.0 (s, C-3, C-4); *m/z* (EI) 399.5 ($[M]^+$, 64%), 320.5 (55), 239.6 (59), 160.7 (67), 79.5 (100).

2,3,4-Tribromothiophene **52**

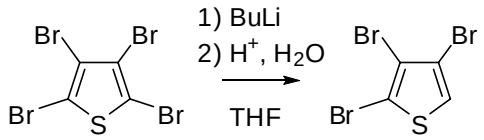

51 **52**

Tetrabromothiophene **51** (2.00 g, 5 mmol) in THF (20 mL) was added to *n*-butyllithium (3.13 mL, 1.6 M in hexanes) in THF (30 mL) under argon at -78 ^{o}C. The mixture was left with stirring for 30 min. aq. HCl (0.5 M, 10 mL) was then added, and the mixture allowed to come to room temperature. Water was added, and the product was extracted into DCM. The extracts were combined, dried and concentrated, and the crude product, after purification by column chromatography (silica, hexane) gave *2,3,4-tribromothiophene*[3] **52** (1.32 g, 82%) as white crystals, mp 42.8 - 44.6 ^{o}C (lit. mp 43 – 46 °C); δ_H 7.35 (1 H, s); δ_C 111.64 (s, C-2), 113.20 (s, C-4), 117.75 (s, C-3), 124.11(s, C-1).

2,3,4-Tribromo-5-methylthiophene **53**

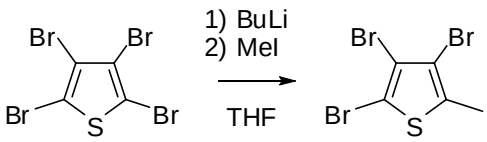

51 **53**

Tetrabromothiophene **51** (2.00 g, 5 mmol) in THF (20 mL) was added to *n*-butyllithium (3.13 mL, 1.6 M in hexanes) in THF (30 mL) under argon at -78 ^{o}C. The mixture was left with stirring for 1h. Iodomethane (0.71 g, 5 mmol) was added and the mixture was left with stirring for a further 1h. Water was added, and the product was extracted into DCM. The extracts were combined, dried and concentrated to give 1.8 g of crude product. Recrystallisation from hexane gave *2,3,4-tribromo-5-methylthiophene* **53** (0.882 g, 53%) as

white crystals, mp 86.3 - 87.0 °C (Found: C, 18.09%, H, 0.90%. $C_5H_3Br_3S$ requires C, 17.94%, H, 0.90%); δ_H 2.39 (3 H, s, C*H*$_3$); δ_C 16.7 (s, CH_3), 107.3 (s, C-2), 112.2 (s, C-4), 117.0 (s, C-3), 136.2 (s, C-5); *m/z* (EI) 333.5 ($[M]^+$, 88%), 254.7 (85), 173.6 (92), 94.5 (100).

2,3,4-Tribromo-5-phenylthiophene **54**

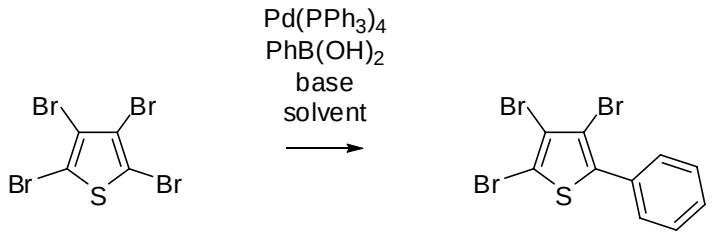

51 **54**

Tetrabromothiophene **51** (0.50 g, 1.25 mmol), phenylboronic acid (152 mg, 1.25 mmol), base (2.5 mmol), and palladium tetrakis triphenylphosphine (72 mg, 0.063 mmol) were dissolved in degassed solvent (3 mL). The mixture was stirred at reflux under an argon atmosphere for 18 h. At the end of this period the mixture was allowed to cool, and was partitioned between DCM and water. The combined organic phases were combined and concentrated, at which point analysis by GC-MS showed *2,3,4-tribromo-5-phenylthiophene* **54** (0 – 40 mg, 0 – 81% (varying with solvent and base employed)); *m/z* (EI) 397.5 ($[M]^+$, 78%), 316.6 (20), 237.7 (77), 156.6 (100).

6.5 References

1 R. D. Chambers, J. A. H. MacBride, and W. K. R. Musgrave, *J. Chem. Soc. (C)*, 1968, 2116.

2 E. Dvornikova, M. Bechcicka, K. Kamienska-Trela, and A. Krowczynski, *J. Fluorine Chem.*, 2003, **124**, 159.

3 W. Steinkopf, H. Jacob, and H. Prenz, *Liebigs Ann.*, 1934, **512**, 136.

Appendix

Crystal Structure Data Tables

A.1) 4,4'-(6-Fluoro-4-(phenylthio)pyridazine-3,5-diyl)dimorpholine 33

Table 1: Crystal data and structure refinement for 10srv173

Identification code	10srv173
Empirical formula	$C_{18}H_{21}N_4O_2FS$
Formula weight	376.45
Temperature / K	120
Crystal system	monoclinic
Space group	$P2_1$
a / Å, b / Å, c / Å	6.5813(2), 13.5706(4), 10.4143(4)
α/°, β/°, γ/°	90.00, 107.70(2), 90.00
Volume / $Å^3$	886.07(5)
Z	2
ρ_{calc} / mg mm^{-3}	1.411
μ / mm^{-1}	0.214
F(000)	396
Crystal size / mm^3	0.32 × 0.2 × 0.11
Theta range for data collection	2.05 to 59.98°
Index ranges	$-9 \leq h \leq 9$, $-18 \leq k \leq 19$, $-14 \leq l \leq 14$
Reflections collected	16499
Independent reflections	5013[R(int) = 0.0534]
Data/restraints/parameters	5013/1/319

Goodness-of-fit on F^2	1.053
Final R indexes [I>2σ (I)]	R_1 = 0.0364, wR_2 = 0.0863
Final R indexes [all data]	R_1 = 0.0385, wR_2 = 0.0885
Largest diff. peak/hole / e $Å^{-3}$	0.306/-0.250

Table 2 Fractional Atomic Coordinates ($\times 10^4$) and Equivalent Isotropic Displacement Parameters ($Å^2 \times 10^3$) for 10srv173. U_{eq} is defined as 1/3 of of the trace of the orthogonalised U_{IJ} tensor.

Atom	x	y	z	U(eq)
S1	608.2(5)	4042.3(3)	3503.9(3)	19.35(9)
F1	6231.0(16)	6141.8(7)	2210.2(10)	26.1(2)
O1	2875(2)	7497.6(9)	5456.0(14)	30.1(3)
O2	-1320(2)	1338.9(11)	-157.0(14)	33.9(3)
N1	4185(2)	3844.1(10)	1010.9(13)	20.9(3)
N2	5443(2)	4657.4(11)	1313.5(13)	21.0(3)
N3	3348(2)	5967.3(10)	3728.8(13)	19.4(3)
N4	1395(2)	2877.6(10)	1244.4(13)	18.5(2)
C1	5056(2)	5312.3(12)	2107.7(15)	19.1(3)
C2	3541(2)	5257.6(11)	2822.1(14)	16.2(3)
C3	2345(2)	4387.1(12)	2578.7(14)	16.1(3)
C4	2645(2)	3727.7(11)	1587.2(14)	17.1(3)
C5	5181(3)	6558.9(13)	4475.9(18)	23.2(3)
C6	4797(3)	6930.1(15)	5759.9(19)	28.6(4)
C7	1092(3)	6893.5(14)	4774(2)	29.3(4)
C8	1317(3)	6497.0(13)	3465.4(18)	23.8(3)
C9	-889(2)	3054.3(14)	548.3(17)	23.2(3)
C10	-2118(3)	2107.9(15)	503(2)	29.7(4)
C11	895(3)	1176.9(14)	509(2)	29.8(4)
C12	2203(3)	2101.8(12)	548.3(17)	21.6(3)
C13	2206(2)	4221.6(10)	5204.6(14)	17.8(3)
C14	1107(3)	4362.7(13)	6147.5(16)	24.3(3)
C15	2239(3)	4438.1(16)	7513.3(17)	30.9(4)
C16	4453(3)	4390.7(16)	7946.0(17)	30.3(4)
C17	5535(3)	4245.1(13)	6999.6(16)	25.0(4)
C18	4424(2)	4159.3(12)	5640.1(15)	20.5(3)

Table 3 Anisotropic Displacement Parameters ($Å^2 \times 10^3$) for 10srv173. The Anisotropic displacement factor exponent takes the form: $-2\pi^2[h^2a^{*2}U_{11}+...+2hka \times b \times U_{12}]$

Atom	U_{11}	U_{22}	U_{33}	U_{23}	U_{13}	U_{12}
S1	18.36(16)	25.39(18)	16.21(15)	-2.07(14)	8.14(12)	-4.51(16)
F1	25.4(5)	26.4(5)	29.4(5)	0.6(4)	12.8(4)	-7.0(4)
O1	34.6(7)	22.5(6)	38.1(7)	-9.9(5)	18.6(6)	-5.7(5)
O2	26.2(6)	37.1(7)	40.2(7)	-20.4(6)	12.7(6)	-9.5(6)
N1	20.1(6)	26.7(7)	17.4(6)	-0.7(5)	7.7(5)	-0.9(5)
N2	19.6(6)	26.1(7)	19.0(6)	1.4(5)	8.4(5)	-1.5(6)
N3	17.9(6)	19.9(6)	20.4(6)	-4.1(5)	6.1(5)	-0.9(5)
N4	16.6(6)	21.4(6)	17.8(6)	-4.4(5)	5.7(5)	-1.1(5)
C1	16.0(6)	21.8(7)	19.8(6)	2.9(6)	6.1(5)	-1.2(6)
C2	15.1(6)	18.8(7)	15.1(6)	2.0(5)	5.0(5)	1.3(6)
C3	14.8(6)	19.6(6)	14.1(6)	1.0(5)	4.8(5)	0.0(5)
C4	15.7(6)	20.4(7)	14.5(6)	0.7(5)	3.6(5)	1.1(5)
C5	19.9(7)	21.8(8)	26.9(8)	-6.7(6)	5.6(6)	-4.6(6)
C6	35.1(9)	26.0(9)	24.6(8)	-6.9(7)	9.1(7)	-5.9(8)
C7	30.9(9)	22.0(8)	41.7(10)	-7.5(7)	20.8(8)	-4.2(7)
C8	20.2(7)	23.2(8)	28.3(8)	-2.4(7)	7.5(6)	2.7(7)
C9	15.3(7)	32.1(9)	20.8(7)	-4.9(6)	3.6(6)	1.4(6)
C10	23.1(8)	37.4(10)	30.4(9)	-14.1(8)	10.8(7)	-6.8(8)
C11	29.8(9)	24.5(8)	37.6(10)	-9.1(7)	13.8(7)	-4.7(7)
C12	20.9(7)	23.5(8)	21.8(7)	-5.9(6)	8.7(6)	0.3(6)
C13	22.9(7)	16.6(8)	15.8(6)	0.2(5)	8.9(5)	0.3(5)
C14	23.6(7)	32.4(9)	20.7(7)	-1.1(6)	12.3(6)	0.2(7)
C15	33.9(9)	42.5(10)	20.6(8)	-1.9(7)	15.0(7)	-1.3(8)
C16	34.5(9)	41.2(10)	15.7(7)	0.5(7)	8.5(7)	0.1(8)
C17	26.1(7)	30.3(10)	18.8(7)	3.0(6)	7.1(6)	1.2(7)
C18	22.2(7)	21.5(8)	19.6(6)	1.6(6)	8.8(5)	2.3(6)

Table 4 Bond Lengths for 10srv173.

Atom	Atom	Length/Å	Atom	Atom	Length/Å
S1	C3	1.7674(14)	N4	C12	1.467(2)
S1	C13	1.7802(16)	C1	C2	1.416(2)
F1	C1	1.3515(19)	C2	C3	1.399(2)
O1	C6	1.431(2)	C3	C4	1.425(2)
O1	C7	1.431(2)	C5	C6	1.520(2)
O2	C10	1.434(2)	C7	C8	1.514(2)
O2	C11	1.429(2)	C9	C10	1.511(3)
N1	N2	1.3581(19)	C11	C12	1.515(3)
N1	C4	1.3351(18)	C13	C14	1.3987(19)
N2	C1	1.291(2)	C13	C18	1.393(2)
N3	C2	1.3813(19)	C14	C15	1.394(2)
N3	C5	1.461(2)	C15	C16	1.390(3)
N3	C8	1.468(2)	C16	C17	1.394(2)
N4	C4	1.399(2)	C17	C18	1.387(2)
N4	C9	1.476(2)			

Table 5 Bond Angles for 10srv173.

Atom	Atom	Atom	Angle/°	Atom	Atom	Atom	Angle/°
F1	C1	C2	118.67(14)	C2	C3	C4	117.86(13)
O1	C6	C5	110.84(16)	C3	S1	C13	102.82(7)
O1	C7	C8	111.10(14)	C3	C2	C1	113.34(13)
O2	C10	C9	111.30(14)	C4	N1	N2	118.98(13)
O2	C11	C12	111.89(16)	C4	N4	C9	115.05(13)
N1	C4	N4	116.80(13)	C4	N4	C12	116.40(12)
N1	C4	C3	122.89(14)	C4	C3	S1	118.95(11)
N2	C1	F1	113.83(13)	C5	N3	C8	112.81(13)
N2	C1	C2	127.48(15)	C7	O1	C6	109.74(14)
N3	C2	C1	123.26(14)	C11	O2	C10	110.33(14)
N3	C2	C3	123.30(13)	C12	N4	C9	109.99(13)
N3	C5	C6	108.63(13)	C14	C13	S1	116.24(12)
N3	C8	C7	109.80(15)	C15	C14	C13	119.77(15)
N4	C4	C3	120.17(13)	C15	C16	C17	119.19(16)
N4	C9	C10	109.44(15)	C16	C15	C14	120.63(15)
N4	C12	C11	108.62(13)	C17	C18	C13	120.14(13)
C1	N2	N1	118.86(12)	C18	C13	S1	123.99(11)
C2	N3	C5	120.98(13)	C18	C13	C14	119.61(14)
C2	N3	C8	118.77(13)	C18	C17	C16	120.65(15)
C2	C3	S1	123.10(11)				

Table 6 Hydrogen Atom Coordinates ($Å \times 10^4$) and Isotropic Displacement Parameters ($Å^2 \times 10^3$) for 10srv173.

Atom	x	y	z	U(eq)
H5B	5390.0(3)	7104(17)	3950.0(2)	27(5)
H5A	6470.0(4)	6140(18)	4670.0(2)	33(6)
H6A	4730.0(3)	6401(16)	6360.0(2)	22(5)
H6B	6050.0(4)	7363(17)	6260.0(2)	27(5)
H7A	1000.0(3)	6319(16)	5360.0(2)	29(6)
H7B	-210.0(4)	7311(19)	4610.0(2)	35(6)
H8A	120.0(3)	6065(17)	3030.0(2)	23(5)
H8B	1290.0(4)	7048(19)	2860.0(2)	32(6)
H9A	-1120.0(3)	3293(16)	-420.0(2)	28(5)
H9B	-1460.0(4)	3639(19)	980.0(3)	40(7)
H10B	-3750.0(4)	2151(19)	-70.0(3)	37(6)
H10A	-1990.0(4)	1860(18)	1440.0(2)	37(6)
H11B	1170.0(3)	938(17)	1410.0(2)	26(5)
H11A	1330.0(4)	690.0(2)	-70.0(3)	46(7)
H12A	2120.0(4)	2305(19)	-380.0(2)	36(6)
H12B	3660.0(3)	1971(17)	1060.0(2)	25(5)
H14	-430.0(3)	4438(16)	5830.0(2)	22(5)
H15	1440.0(3)	4545(17)	8150.0(2)	30(6)
H16	5180.0(4)	4471(19)	8880.0(3)	40(6)
H17	7150.0(4)	4175(19)	7270.0(2)	36(6)
H18	5300.0(3)	3983(17)	4990.0(2)	25(5)

A.2) 4-Ethylsulfanyl-3-fluoro-9-oxa-10-thia-1,2-diaza-anthracene 39

Table 1 Crystal data and structure refinement for 09srv149

Identification code	s149
Empirical formula	$C_{12}H_9N_2OFS_2$
Formula weight	280.33
Temperature	120(2)
Crystal system	Monoclinic
Space group	$P2_1/n$
a/Å, b/Å, c/Å	10.6924(5), 9.8670(4), 11.0623(5)
α/°, β/°, γ/°,	90.00, 92.444(10), 90.00
Volume/Å^3	1166.03(9)
Z	4
ρ_{calc}mg/mm^3	1.597
m/mm^{-1}	0.457
F(000)	576
Crystal size	0.42 × 0.21 × 0.04
Theta range for data collection	2.59 to 29.50°
Index ranges	$-14 \leq h \leq 14$, $-13 \leq k \leq 13$, $-15 \leq l \leq 15$
Reflections collected	10747
Independent reflections	3249[R(int) = 0.0657]
Data/restraints/parameters	3249/0/199
Goodness-of-fit on F^2	1.008
Final R indexes [I>2σ (I)]	R_1 = 0.0429, wR_2 = 0.1035
Final R indexes [all data]	R_1 = 0.0637, wR_2 = 0.1129

Largest diff. peak/hole	0.609/-0.354

Table 2 Atomic Coordinates ($Å \times 10^4$) and Equivalent Isotropic Displacement Parameters ($Å^2 \times 10^3$) for 09srv149. U_{eq} is defined as 1/3 of of the trace of the orthogonalised U_{IJ} tensor.

Atom	x	y	z	U(eq)
S1	8239.2(5)	6351.8(5)	4028.4(4)	21.63(14)
S2	8039.8(5)	4398.8(5)	6125.4(4)	23.13(14)
F1	8568.5(13)	1401.9(12)	5237.8(11)	32(3)
O1	9090.9(14)	4916.1(14)	1677.3(11)	25.5(3)
N1	9236.7(16)	2863.1(17)	2481.6(14)	22.4(4)
N2	9068(16)	1953.6(17)	3382.6(15)	23.8(4)
C1	9064(18)	8474.4(19)	2731.7(17)	19.4(4)
C2	9546.3(19)	9104(2)	1734.6(18)	21.6(4)
C3	9869.4(19)	8325(2)	743.9(17)	22.2(4)
C4	9714.2(19)	6931(2)	753.8(16)	21.4(4)
C5	9230.1(18)	6316.2(19)	1755.6(16)	19(4)
C6	8893.7(17)	7077.4(19)	2748.3(16)	17.9(4)
C7	8988.8(18)	4135(2)	2692.2(17)	19.1(4)
C8	8604.5(17)	4658.2(18)	3804.2(16)	18.2(4)
C9	8464.6(17)	3737.1(19)	4735.9(16)	18(4)
C10	8709.2(19)	2389(2)	4415.9(18)	22.8(4)
C11	7560(2)	3013(2)	7083.8(18)	24.9(4)
C12	7171(2)	3679(3)	8252(19)	29.9(5)

Table 3 Anisotropic Displacement Parameters ($Å^2 \times 10^3$) for 09srv149. The Anisotropic displacement factor exponent takes the form: $-2\pi^2[h^2a^{*2}U_{11}+...+2hka \times b \times U_{12}]$

Atom	U_{11}	U_{22}	U_{33}	U_{23}	U_{13}	U_{12}
S1	30.3(3)	17.1(2)	18.1(2)	-0.41(17)	7.76(19)	2.31(19)
S2	31.4(3)	21(3)	17.3(2)	1.07(17)	4.92(19)	-0.7(2)
F1	49.3(8)	18.7(6)	28.1(6)	6(5)	4.1(6)	2.8(6)
O1	41.3(9)	17.7(7)	18(6)	-2.4(5)	8.7(6)	-3.7(6)
N1	24.6(9)	18.3(8)	24.5(8)	-1.4(6)	3.7(7)	-1(7)
N2	26.2(9)	18.6(8)	26.8(8)	-0.2(7)	1.5(7)	0.8(7)
C1	20.7(9)	20.1(10)	17.5(8)	-1.4(7)	0.5(7)	2.4(7)
C2	23.3(10)	19.7(10)	21.8(9)	1.6(7)	-0.4(8)	0.2(8)
C3	22.2(10)	25.6(10)	19.1(9)	5.5(7)	2.8(8)	0.7(8)
C4	23.9(10)	23.7(10)	16.8(8)	-0.5(7)	3.6(8)	2.1(8)
C5	21.5(9)	17.5(9)	18.1(8)	-0.9(7)	1.7(7)	-0.8(7)
C6	19(9)	18.4(9)	16.5(8)	1.1(7)	3.2(7)	-1.1(7)
C7	17.5(9)	19.5(9)	20.3(9)	-0.7(7)	2.7(7)	-2.1(7)

C8	19.1(9)	15.6(9)	19.8(8)	-0.1(7)	0.6(7)	-0.5(7)
C9	15(9)	19.8(9)	19.2(8)	-0.7(7)	0.4(7)	-1.2(7)
C10	24.3(10)	19.5(10)	24.6(9)	2.1(7)	0.5(8)	-0.4(8)
C11	26.7(11)	25.7(11)	22.6(9)	6.6(8)	4(8)	-1.3(9)
C12	27.2(11)	40(13)	23(10)	9.7(9)	6.3(9)	4.1(10)

Table 4 Bond Lengths for 09srv149.

Atom	Atom	Length/Å	Atom	Atom	Length/Å
S1	C8	1.7363(19)	C1	C2	1.385(3)
S1	C6	1.7584(18)	C1	C6	1.391(3)
S2	C9	1.7478(19)	C2	C3	1.394(3)
S2	C11	1.818(2)	C3	C4	1.386(3)
F1	C10	1.345(2)	C4	C5	1.383(3)
O1	C7	1.370(2)	C5	C6	1.390(3)
O1	C5	1.392(2)	C7	C8	1.411(3)
N1	C7	1.305(3)	C8	C9	1.387(3)
N1	N2	1.359(2)	C9	C10	1.404(3)
N2	C10	1.295(3)	C11	C12	1.523(3)

Table 5 Bond Angles for 09srv149.

Atom	Atom	Atom	Angle/°	Atom	Atom	Atom	Angle/°
C8	S1	C6	100.21(9)	C1	C6	S1	118.11(14)
C9	S2	C11	108.81(9)	N1	C7	O1	111.76(16)
C7	O1	C5	121.31(14)	N1	C7	C8	125.19(18)
C7	N1	N2	118.00(16)	O1	C7	C8	122.99(17)
C10	N2	N1	118.81(17)	C9	C8	C7	116.91(17)
C2	C1	C6	120.59(18)	C9	C8	S1	119.50(14)
C1	C2	C3	119.48(18)	C7	C8	S1	123.53(14)
C4	C3	C2	120.48(17)	C8	C9	C10	113.97(17)
C5	C4	C3	119.39(17)	C8	C9	S2	116.68(14)
C4	C5	C6	120.94(17)	C10	C9	S2	129.34(15)
C4	C5	O1	115.35(16)	N2	C10	F1	113.70(17)
C6	C5	O1	123.70(16)	N2	C10	C9	127.07(19)
C5	C6	C1	119.11(17)	F1	C10	C9	119.23(17)
C5	C6	S1	122.77(14)	C12	C11	S2	105.34(15)

Table 6 Hydrogen Atom Coordinates ($Å \times 10^4$) and Isotropic Displacement Parameters ($Å^2 \times 10^3$) for 09srv149.

Atom	x	y	z	U(eq)
H1	8900(2)	9000(2)	3374(19)	22(6)
H2	9651(19)	10030(2)	1684(18)	21(5)
H3	10210(2)	8730(2)	70(2)	26(6)
H4	9940(2)	6410(2)	130(2)	33(6)
H111	6850(2)	2530(3)	6700(2)	38(7)
H112	8260(2)	2410(2)	7230(19)	29(6)
H121	6450(2)	4300(2)	8120(2)	32(6)
H122	6960(2)	3030(3)	8780(2)	33(7)
H123	7870(2)	4250(2)	8660(2)	34(7)

A.3) 4-Ethylsulfanyl-3-fluoro-10H-9-oxa-1,2,10-triaza-anthracene 40

Table 1 Crystal data and structure refinement for 09srv155

Identification code	s155ncs
Empirical formula	$C_{12}H_{10}N_3SFO$
Formula weight	263.29
Temperature	120(2)
Crystal system	Orthorhombic
Space group	$Pca2_1$
a/Å, b/Å, c/Å	12.566(9), 5.2062(4), 35.081(3)
α/°, β/°, γ/°,	90.00, 90.00, 90.00
Volume/$Å^3$	2295.0(17)
Z	8
$\rho_{calc}mg/mm^3$	1.524
m/mm^{-1}	0.286
F(000)	1088
Crystal size	0.48 × 0.1 × 0.04
Theta range for data collection	3.24 to 27.30°
Index ranges	$-15 \leq h \leq 15$, $-6 \leq k \leq 6$, $-35 \leq l \leq 44$
Reflections collected	13348
Independent reflections	4103[R(int) = 0.0642]
Data/restraints/parameters	4103/1/336
Goodness-of-fit on F^2	1.014
Final R indexes [$I>2\sigma(I)$]	$R_1 = 0.0490$, $wR_2 = 0.0989$
Final R indexes [all data]	$R_1 = 0.0833$, $wR_2 = 0.1088$

Largest diff. peak/hole	0.241/-0.294

Table 2 Atomic Coordinates ($Å \times 10^4$) and Equivalent Isotropic Displacement Parameters ($Å^2 \times 10^3$) for 09srv155. U_{eq} is defined as 1/3 of of the trace of the orthogonalised U_{IJ} tensor.

Atom	x	y	z	U(eq)
S1	6624.7(7)	12446(2)	4062.6(4)	29.1(3)
F1	4546(4)	15220(6)	4167.7(16)	42.5(13)
O1	4069(2)	7973(6)	3115.3(10)	31.6(8)
N2	3439(3)	11148(8)	3480.7(12)	32.4(9)
N1	6076(3)	8337(7)	3455(11)	23.3(9)
N3	3554(3)	13040(7)	3747.5(12)	33.9(10)
C1	4481(3)	13300(9)	3907.6(14)	27.4(11)
C2	5392(3)	11845(9)	3835.9(13)	25(10)
C3	5297(5)	9951(7)	3569(2)	19(2)
C4	4266(5)	9741(9)	3407(2)	21.8(16)
C5	6695(5)	4723(10)	3058(2)	24.3(18)
C6	6450(3)	2873(9)	2797.8(14)	29.7(11)
C7	5451(4)	2754(10)	2629.8(13)	32.9(11)
C8	4670(5)	4470(12)	2740(2)	29.8(14)
C9	4882(3)	6282(9)	3010.9(14)	23.4(10)
C10	5887(3)	6484(9)	3177.1(13)	22.2(10)
C11	6647(7)	9734(11)	4398(3)	44(2)
C12	5773(8)	9864(13)	4700(3)	66(3)
S2	4103.8(7)	2537(2)	5640.1(4)	29(2)
F2	2012(4)	-230(6)	5549.7(15)	37.6(12)
O2	1546(2)	7024(5)	6588.7(9)	29.8(7)
N21	3551(3)	6681(7)	6250.1(11)	23.5(9)
N22	923(2)	3867(8)	6215.9(12)	30.4(9)
N23	1022(3)	1978(8)	5952.1(12)	34.6(10)
C21	1961(3)	1679(9)	5800.8(14)	27.9(11)
C22	2878(3)	3162(8)	5865.2(13)	22.1(10)
C23	2756(5)	5071(8)	6141(3)	23(2)
C24	1734(4)	5313(10)	6320(2)	23.3(16)
C25	4119(5)	10276(10)	6623(2)	21.2(16)
C26	3929(3)	12153(9)	6904(13)	27.7(10)
C27	2929(4)	12272(10)	7071.8(14)	31.3(11)
C28	2145(5)	10520(12)	6966(2)	30.9(15)
C29	2368(3)	8706(8)	6696.6(13)	22.5(10)
C30	3377(3)	8532(8)	6524.4(13)	19.1(9)
C31	4159(6)	5206(9)	5319(3)	30.2(19)
C32	3331(6)	5164(10)	5016(3)	39(2)

Table 3 Anisotropic Displacement Parameters ($Å^2 \times 10^3$) for 09srv155. The Anisotropic displacement factor exponent takes the form: $-2\pi^2[h^2a^{*2}U_{11}+...+2hka \times b \times U_{12}]$

Atom	U_{11}	U_{22}	U_{33}	U_{23}	U_{13}	U_{12}
S1	24(4)	25.9(6)	37.3(7)	-3.8(6)	1.5(4)	-4.7(5)
F1	32(2)	39(3)	56(3)	-11.4(16)	11(2)	9.8(12)
O1	14(12)	30(2)	50(2)	3.1(16)	-6.8(14)	2.5(12)
N2	19.7(18)	30(3)	47(3)	11(2)	3.5(18)	2.1(18)
N1	12.7(15)	25(2)	32(2)	-6(18)	-3.6(16)	1.8(14)
N3	24.5(19)	32(3)	45(3)	7(2)	10.2(18)	8.2(16)
C1	28(2)	25(3)	29(3)	1(2)	10.8(19)	5(18)
C2	25(2)	26(3)	24(3)	4(2)	7.1(18)	-2.3(17)
C3	16(3)	23(6)	17(4)	8.2(18)	2(3)	-0.2(14)
C4	26(3)	16(3)	24(4)	10(2)	2(3)	1.4(18)
C5	17(3)	22(3)	34(4)	-4(2)	7(2)	8.4(17)
C6	28(2)	32(3)	29(3)	-8(2)	8(2)	-0.8(19)
C7	40(3)	39(3)	20(2)	-4(2)	2(2)	-12(2)
C8	21(3)	35(3)	34(4)	10(3)	-6(2)	-3(3)
C9	17.7(19)	26(3)	27(3)	7(2)	0(19)	1(17)
C10	16.6(19)	24(3)	26(3)	2(2)	0.7(17)	-1.7(16)
C11	47(4)	39(5)	46(6)	5(3)	-20(4)	-7(3)
C12	82(6)	86(8)	30(6)	13(3)	11(5)	-21(3)
S2	24.1(5)	25.1(6)	37.7(6)	-5(6)	-1.1(4)	3.7(5)
F2	45(2)	31(2)	36(3)	-4.9(14)	-10(2)	-8.3(12)
O2	15.3(13)	28.7(18)	45(2)	-0.8(16)	8.1(13)	2.9(12)
N21	12.7(16)	23(2)	35(3)	-1.1(19)	3.8(16)	-2.8(13)
N22	12.6(16)	34(3)	44(3)	8(2)	-3.3(17)	-5.1(17)
N23	23.5(19)	39(3)	41(3)	2(2)	-7.1(18)	-8.2(17)
C21	29(2)	19(3)	36(3)	5(2)	-10(2)	-1.9(18)
C22	13.4(17)	22(3)	31(3)	7(2)	-3.7(17)	-1.6(16)
C23	10(3)	16(5)	43(6)	4.9(19)	1(3)	0(14)
C24	6(2)	27(3)	37(4)	-1(3)	-1(3)	2(17)
C25	18(3)	30(3)	16(3)	5(2)	0(2)	6.9(18)
C26	31(2)	25(3)	27(3)	3(2)	-2.7(19)	1(19)
C27	37(2)	26(3)	31(3)	-5(2)	1(2)	10(2)
C28	26(3)	36(3)	31(4)	-2(3)	9(3)	15(3)
C29	16.2(19)	19(3)	32(3)	4(2)	0.4(19)	0.4(17)
C30	19(2)	17(2)	21(3)	2(2)	2.4(17)	7.6(15)
C31	28(3)	23(4)	39(5)	-5(2)	8(3)	-1.3(17)
C32	42(4)	41(5)	36(5)	7(2)	11(4)	0(2)

Table 4 Bond Lengths for 09srv155.

Atom	Atom	Length/Å	Atom	Atom	Length/Å
S1	C2	1.769(4)	S2	C22	1.761(4)
S1	C11	1.837(9)	S2	C31	1.791(8)
F1	C1	1.356(6)	F2	C21	1.330(6)
O1	C9	1.397(5)	O2	C24	1.319(7)
O1	C4	1.398(7)	O2	C29	1.406(5)
N2	C4	1.298(7)	N21	C23	1.360(7)
N2	N3	1.367(6)	N21	C30	1.379(6)
N1	C3	1.351(7)	N22	C24	1.318(7)
N1	C10	1.392(6)	N22	N23	1.356(6)
N3	C1	1.300(6)	N23	C21	1.303(6)
C1	C2	1.396(6)	C21	C22	1.406(6)
C2	C3	1.365(8)	C22	C23	1.395(8)
C3	C4	1.420(9)	C23	C24	1.434(9)
C5	C6	1.363(8)	C25	C30	1.347(7)
C5	C10	1.430(7)	C25	C26	1.407(8)
C6	C7	1.388(6)	C26	C27	1.389(6)
C7	C8	1.383(8)	C27	C28	1.392(8)
C8	C9	1.366(8)	C28	C29	1.365(8)
C9	C10	1.395(6)	C29	C30	1.407(6)
C11	C12	1.529(14)	C31	C32	1.487(13)

Table 5 Bond Angles for 09srv155.

Atom	Atom	Atom	Angle/°	Atom	Atom	Atom	Angle/°
C2	S1	C11	99.5(3)	C22	S2	C31	100.0(3)
C9	O1	C4	118.5(4)	C24	O2	C29	118.8(4)
C4	N2	N3	117.3(4)	C23	N21	C30	120.7(4)
C3	N1	C10	121.0(4)	C24	N22	N23	122.1(4)
C1	N3	N2	117.8(4)	C21	N23	N22	116.6(4)
N3	C1	F1	114.9(4)	N23	C21	F2	113.8(4)
N3	C1	C2	126.9(5)	N23	C21	C22	127.7(5)
F1	C1	C2	118.2(4)	F2	C21	C22	118.5(5)
C3	C2	C1	116.3(5)	C23	C22	C21	114.3(4)
C3	C2	S1	120.9(4)	C23	C22	S2	122.6(4)
C1	C2	S1	122.8(4)	C21	C22	S2	122.9(4)
N1	C3	C2	126.1(6)	N21	C23	C22	123.6(6)
N1	C3	C4	119.6(6)	N21	C23	C24	118.7(6)
C2	C3	C4	114.3(5)	C22	C23	C24	117.7(5)
N2	C4	O1	112.1(5)	N22	C24	O2	116.5(5)
N2	C4	C3	127.4(6)	N22	C24	C23	121.4(6)
O1	C4	C3	120.4(5)	O2	C24	C23	122.2(5)
C6	C5	C10	119.2(5)	C30	C25	C26	122.0(5)
C5	C6	C7	121.3(5)	C27	C26	C25	118.7(5)
C8	C7	C6	119.7(5)	C26	C27	C28	119.8(5)
C9	C8	C7	120.2(5)	C29	C28	C27	119.5(5)
C8	C9	C10	121.3(4)	C28	C29	O2	117.8(4)
C8	C9	O1	118.3(4)	C28	C29	C30	121.8(4)

C10	C9	O1	120.3(4)	O2	C29	C30	120.4(4)
N1	C10	C9	119.9(4)	C25	C30	N21	122.7(4)
N1	C10	C5	121.8(4)	C25	C30	C29	118.0(5)
C9	C10	C5	118.2(5)	N21	C30	C29	119.2(4)
C12	C11	S1	113.5(5)	C32	C31	S2	114.3(4)

Table 6 Hydrogen Bonds for 09srv155.

D	H	A	d(D-H)/Å	d(H-A)/Å	d(D-A)/Å	D-H-A/°
N1	H1N	N2	0.86(4)	2.15(4)	2.983(5)	163(4)
N21	H2N	N22	0.78(5)	2.25(5)	2.997(5)	158(6)

Table 7 Hydrogen Atom Coordinates ($Å \times 10^4$) and Isotropic Displacement Parameters ($Å^2 \times 10^3$) for 09srv155.

Atom	x	y	z	U(eq)
H5A	7394	4841	3160	29
H6A	6974	1639	2730	36
H7A	5305	1500	2440	40
H8A	3984	4389	2627	36
H11A	6569	8115	4252	53
H11B	7348	9690	4526	53
H12A	5075	9777	4576	99
H12B	5833	11481	4841	99
H12C	5850	8417	4877	99
H1N	6730(3)	8740(9)	3496(13)	21(11)
H25A	4792	10238	6500	25
H26A	4475	13315	6977	33
H27A	2780	13547	7258	38
H28A	1461	10586	7081	37
H31A	4083	6813	5467	36
H31B	4869	5236	5196	36
H32B	3419	6665	4850	59
H32C	2624	5207	5133	59
H32A	3405	3593	4864	59
H2N	4140(4)	6400(11)	6184(16)	48(16)

A.4) 4-Ethylsulfanyl-3-fluoro-8-methyl-1,2,4b,9-tetraaza-fluorene 43

Table 1 Crystal data and structure refinement for s125

Identification code	s125
Empirical formula	$C_{12}H_{11}N_4SF$
Formula weight	262.31
Temperature	120(2)
Crystal system	Monoclinic
Space group	$P2_1/c$
a/Å, b/Å, c/Å	3.91740(10), 16.8084(2), 17.1269(2)
α/°, β/°, γ/°,	90.00, 92.580(10), 90.00
Volume/Å^3	1126.58(3)
Z	4
ρ_{calc}mg/mm^3	1.547
m/mm^{-1}	0.286
F(000)	544
Crystal size	0.42 × 0.22 × 0.16
Theta range for data collection	1.70 to 29.49°
Index ranges	$-5 \leq h \leq 5$, $-23 \leq k \leq 23$, $-23 \leq l \leq 23$
Reflections collected	15223
Independent reflections	3149[R(int) = 0.0487]
Data/restraints/parameters	3149/0/207
Goodness-of-fit on F^2	1.069
Final R indexes [I>2σ (I)]	$R_1 = 0.0340$, $wR_2 = 0.1121$
Final R indexes [all data]	$R_1 = 0.0372$, $wR_2 = 0.1154$

Largest diff. peak/hole	0.473/-0.271

Table 2 Atomic Coordinates ($Å \times 10^4$) and Equivalent Isotropic Displacement Parameters ($Å^2 \times 10^3$) for s125. U_{eq} is defined as 1/3 of of the trace of the orthogonalised U_{IJ} tensor.

Atom	x	y	z	U(eq)
S1	4800.4(7)	9260.61(15)	1188.52(14)	18.33(11)
F1	3010.7(19)	9186.9(4)	2892.2(4)	23.84(18)
N1	5038(3)	7981.5(6)	3202.9(5)	20.9(2)
N2	6493(3)	7282.2(6)	3041.4(5)	20.8(2)
N3	9018(2)	6511(6)	2041.9(5)	18.5(2)
N4	8539(2)	7444.6(5)	1070.8(5)	15.13(19)
C1	7473(3)	7185.3(6)	2311.2(6)	17.2(2)
C2	7108(3)	7776.8(6)	1717.5(6)	15.4(2)
C3	5591(3)	8502.2(6)	1876.2(6)	16(2)
C4	4615(3)	8527.2(6)	2654.2(6)	18.1(2)
C5	9633(3)	6679.6(6)	1303.7(6)	16(2)
C6	11249(3)	6188.8(6)	749.5(6)	17.4(2)
C7	11702(3)	6499.7(6)	22.1(6)	18.7(2)
C8	10610(3)	7284(7)	-187.4(6)	19.5(2)
C9	9025(3)	7748.4(6)	331.6(6)	17.4(2)
C10	12374(3)	5373.3(7)	1003.7(7)	22(2)
C11	6482(3)	10150.9(6)	1689.9(6)	19.8(2)
C12	7578(3)	10735.4(7)	1074.6(7)	23.3(2)

Table 3 Anisotropic Displacement Parameters ($Å^2 \times 10^3$) for s125. The Anisotropic displacement factor exponent takes the form: $-2\pi^2[h^2a^{*2}U_{11}+...+2hka \times b \times U_{12}]$

Atom	U_{11}	U_{22}	U_{33}	U_{23}	U_{13}	U_{12}
S1	21.8(17)	15.88(17)	17.09(16)	-1.03(8)	-1.51(11)	1.85(9)
F1	26.7(4)	22.6(3)	22.7(3)	-5.2(2)	7(3)	3.9(3)
N1	23.4(5)	22.3(5)	17.2(4)	-0.8(3)	4.4(3)	-1.7(4)
N2	25(5)	20.2(4)	17.4(4)	0.2(3)	3.4(3)	-0.7(4)
N3	21(4)	17.4(4)	17.2(4)	1.2(3)	1.6(3)	-0.6(3)
N4	16.8(4)	14.4(4)	14.2(4)	-0.6(3)	1(3)	-0.2(3)
C1	18.3(5)	16.9(5)	16.3(5)	1.3(4)	0.3(4)	-2.9(4)
C2	15.5(4)	16.8(5)	14.1(4)	-0.7(3)	1.1(3)	-2.2(4)
C3	16.4(4)	16.2(5)	15.6(4)	-1.2(3)	0.9(3)	-1.3(4)
C4	18.6(5)	18(5)	17.9(5)	-3.4(4)	3.1(4)	-1.1(4)
C5	16.3(4)	14.3(4)	17.3(4)	1.2(3)	-0.6(4)	-1(3)
C6	17.7(5)	15.7(4)	18.8(5)	-0.8(4)	1.7(4)	-0.3(4)
C7	20.1(5)	17.9(5)	18.3(5)	-2.2(4)	3.2(4)	0.3(4)

C8	23.2(5)	19.5(5)	16.1(4)	0.3(4)	3(4)	-0.4(4)
C9	20.6(5)	17.5(5)	14.2(4)	1.6(3)	1.4(4)	0.4(4)
C10	25(5)	16.3(5)	25(5)	1.4(4)	4.4(4)	4(4)
C11	24.2(5)	16.2(5)	19(5)	-1.8(4)	0.4(4)	-0.2(4)
C12	27.3(6)	18.2(5)	24.4(5)	2.1(4)	0.6(5)	-0.1(4)

Table 4 Bond Lengths for s125.

Atom	Atom	Length/Å	Atom	Atom	Length/Å
S1	C3	1.7536(11)	N4	C5	1.4073(13)
S1	C11	1.8330(11)	C1	C2	1.4247(14)
F1	C4	1.3467(12)	C2	C3	1.3887(14)
N1	C4	1.3184(14)	C3	C4	1.4033(14)
N1	N2	1.3408(13)	C5	C6	1.4270(14)
N2	C1	1.3346(13)	C6	C7	1.3698(15)
N3	C5	1.3284(13)	C6	C10	1.4985(15)
N3	C1	1.3742(14)	C7	C8	1.4268(15)
N4	C2	1.3815(12)	C8	C9	1.3545(15)
N4	C9	1.3861(12)	C11	C12	1.5169(16)

Table 5 Bond Angles for s125.

Atom	Atom	Atom	Angle/°	Atom	Atom	Atom	Angle/°
C3	S1	C11	103.29(5)	C4	C3	S1	124.64(8)
C4	N1	N2	120.26(9)	N1	C4	F1	113.73(9)
C1	N2	N1	116.31(9)	N1	C4	C3	128.70(10)
C5	N3	C1	104.18(9)	F1	C4	C3	117.58(9)
C2	N4	C9	131.35(9)	N3	C5	N4	113.50(9)
C2	N4	C5	105.74(8)	N3	C5	C6	127.93(10)
C9	N4	C5	122.88(8)	N4	C5	C6	118.57(9)
N2	C1	N3	124.38(10)	C7	C6	C5	117.64(9)
N2	C1	C2	124.05(10)	C7	C6	C10	124.38(10)
N3	C1	C2	111.57(9)	C5	C6	C10	117.98(9)
N4	C2	C3	134.78(9)	C6	C7	C8	122.11(10)
N4	C2	C1	105.01(9)	C9	C8	C7	120.56(10)

C3	C2	C1	120.21(9)	C8	C9	N4	118.23(10)
C2	C3	C4	110.45(9)	C12	C11	S1	108.07(8)
C2	C3	S1	124.83(8)				

Table 6 Hydrogen Atom Coordinates ($Å \times 10^4$) and Isotropic Displacement Parameters ($Å^2 \times 10^3$) for s125.

Atom	x	y	z	U(eq)
H7	12810(4)	6177(9)	-359(8)	24(4)
H8	10950(4)	7474(9)	-705(8)	18(3)
H9	8210(3)	8272(9)	247(8)	16(3)
H101	14240(5)	5429(11)	1422(11)	39(4)
H102	10420(4)	5052(10)	1181(9)	27(4)
H103	13240(6)	5081(12)	585(13)	51(5)
H111	4620(4)	10356(9)	2018(8)	19(3)
H112	8350(4)	9997(9)	2010(9)	22(4)
H121	8650(5)	11215(10)	1329(10)	38(4)
H122	5530(6)	10958(11)	747(12)	48(5)
H123	9140(4)	10486(11)	719(10)	31(4)

A.5) 2,3,4-Tribromo-5-methylthiophene 53

Table 1: Crystal data and structure refinement for 10srv123

Identification code	10srv123
Empirical formula	$C_5H_3SBr_3$
Formula weight	334.86
Temperature / K	120
Crystal system	Monoclinic
Space group	$P2_1/c$
a / Å, b / Å, c / Å	15.5475(5), 3.97300(10), 13.8532(5)
α/°, β/°, γ/°	90.00, 111.420(10), 90.00
Volume / $Å^3$	796.61(4)
Z	4
ρ_{calc} / mg mm^{-3}	2.792
μ / mm^{-1}	15.361
F(000)	616
Crystal size / mm^3	0.37 × 0.12 × 0.05
Theta range for data collection	1.41 to 30.48°
Index ranges	$-22 \leq h \leq 22$, $-5 \leq k \leq 5$, $-19 \leq l \leq 19$
Reflections collected	10157
Independent reflections	2430[R(int) = 0.0332]
Data/restraints/parameters	2430/2/90
Goodness-of-fit on F^2	1.066
Final R indexes [I>2σ (I)]	$R_1 = 0.0226$, $wR_2 = 0.0468$
Final R indexes [all data]	$R_1 = 0.0313$, $wR_2 = 0.0493$

Largest diff. peak/hole / e $Å^{-3}$	0.540/-0.628

Table 2 Atomic Coordinates ($Å \times 10^4$) and Equivalent Isotropic Displacement Parameters ($Å^2 \times 10^3$) for 10srv123. U_{eq} is defined as 1/3 of of the trace of the orthogonalised U_{IJ} tensor.

Atom	x	y	z	U(eq)
Br1	1116.5(8)	1848(4)	98.0(7)	21.11(19)
Br1A	4775.2(3)	1196.1(19)	3634.1(5)	18.54(11)
Br2	880.92(16)	-2020.1(6)	2285.99(19)	19.29(7)
Br3	3016.47(16)	-2486.7(5)	4327.78(17)	17.62(6)
S1	3161.4(4)	2221.1(14)	1537.9(4)	15.27(11)
C1	2038.2(15)	1048(5)	1331.1(17)	15.8(4)
C2	1987.2(15)	-419(5)	2192.6(17)	15.5(4)
C3	2854.4(15)	-612(5)	3030.5(16)	14.1(4)
C4	3555.7(15)	726(5)	2795.0(17)	15.4(4)
C5	4577(6)	1110.0(4)	3509(11)	20
C5A	1260(6)	1760.0(2)	284(6)	20

Table 3 Anisotropic Displacement Parameters ($Å^2 \times 10^3$) for 10srv123. The Anisotropic displacement factor exponent takes the form: $-2\pi^2[h^2a^{*2}U_{11}+...+2hka \times b \times U_{12}]$

Atom	U_{11}	U_{22}	U_{33}	U_{23}	U_{13}	U_{12}
Br1	17.2(5)	27.2(3)	16.1(5)	2.4(4)	2.7(3)	1.5(4)
Br1A	13.2(2)	25.2(2)	15.8(2)	0.21(18)	3.6(2)	-1.5(2)
Br2	15.21(12)	20.91(11)	24.51(13)	-0.19(9)	10.52(10)	-1.74(8)
Br3	22.02(13)	18.88(11)	14.10(11)	1.58(8)	9.12(10)	-0.51(9)
S1	15.6(3)	17.7(3)	13.8(3)	0.7(2)	6.9(2)	-1.5(2)
C1	13.4(10)	16.4(10)	18.1(11)	-0.4(9)	6.3(9)	-0.1(8)
C2	13.6(10)	17.3(10)	17.6(11)	-3.1(8)	8.0(9)	-1.8(8)
C3	18.3(11)	12.7(9)	13(1)	-1.2(8)	7.8(9)	-0.2(8)
C4	15.0(11)	16.7(10)	14.1(10)	-0.5(8)	5.0(9)	0.5(8)

Table 4 Bond Lengths for 10srv123.

Atom	Atom	Length/Å	Atom	Atom	Length/Å
Br1	C1	1.812(2)	C1	C2	1.356(3)
Br1A	C4	1.836(2)	C1	C5A	1.538(7)
Br2	C2	1.882(2)	C2	C3	1.424(3)
Br3	C3	1.876(2)	C3	C4	1.356(3)
S1	C1	1.727(2)	C4	C5	1.542(9)
S1	C4	1.727(2)			

Table 5 Bond Angles for 10srv123.

Atom	Atom	Atom	Angle/°	Atom	Atom	Atom	Angle/°
S1	C1	Br1	120.83(13)	C3	C4	S1	110.92(17)
S1	C4	Br1A	120.51(13)	C3	C4	C5	128.0(6)
C1	C2	Br2	123.66(18)	C4	S1	C1	92.27(11)
C1	C2	C3	113.5(2)	C4	C3	Br3	123.23(17)
C2	C1	Br1	128.65(18)	C4	C3	C2	112.84(19)
C2	C1	S1	110.51(17)	C5	C4	Br1A	0.6(6)
C2	C1	C5A	129.0(4)	C5	C4	S1	121.1(6)
C2	C3	Br3	123.94(16)	C5A	C1	Br1	0.5(4)
C3	C2	Br2	122.88(16)	C5A	C1	S1	120.4(4)
C3	C4	Br1A	128.53(18)				

Table 6 Hydrogen Atom Coordinates ($Å \times 10^4$) and Isotropic Displacement Parameters ($Å^2 \times 10^3$) for 10srv123.

Atom	x	y	z	U(eq)
H5C	4800	-1015	3875	30
H5B	4635	2902	4014	30
H5A	4947	1678	3091	30
H5AA	759	2980	401	30
H5AB	1022	-377	-67	30
H5AC	1502	3119	-150	30